Multi-agent modelling of seismic crisis

Julius Bangate

▶ **To cite this version:**

Julius Bangate. Multi-agent modelling of seismic crisis. Computers and Society [cs.CY]. Université Grenoble Alpes, 2019. English. NNT : 2019GREAM057 . tel-02613082

HAL Id: tel-02613082
https://theses.hal.science/tel-02613082

Submitted on 19 May 2020

HAL is a multi-disciplinary open access archive for the deposit and dissemination of scientific research documents, whether they are published or not. The documents may come from teaching and research institutions in France or abroad, or from public or private research centers.

L'archive ouverte pluridisciplinaire **HAL**, est destinée au dépôt et à la diffusion de documents scientifiques de niveau recherche, publiés ou non, émanant des établissements d'enseignement et de recherche français ou étrangers, des laboratoires publics ou privés.

Communauté
UNIVERSITÉ Grenoble Alpes

THÈSE

Pour obtenir le grade de

DOCTEUR DE LA COMMUNAUTÉ UNIVERSITÉ GRENOBLE ALPES

Spécialité : **Informatique**

Arrêté ministériel : 25 mai 2016

Présentée par

Julius BAÑGATE

Thèse dirigée par **Julie DUGDALE,** HDR, MCF, LIG, Université Grenoble Alpes, et codirigée par **Elise BECK,** MCF, PACTE, Université Grenoble Alpes

préparée au sein du **Laboratoire d'informatique de Grenoble (LIG) et Laboratoire de sciences sociales (PACTE)**
dans **l'École Doctorale Mathématiques, Sciences et technologies de l'information, Informatique**

Modélisation multi-agents d'une crise sismique

Multi-agent modelling of seismic crisis

Thèse soutenue publiquement le **18 décembre 2019**,
devant le jury composé de :

Madame Julie DUGDALE
HDR, MCF, LIG, Université Grenoble Alpes, Directrice de thèse
Madame Elise BECK
MCF, PACTE, Université Grenoble Alpes, Co-Encadrante, Examinatrice
Madame Carole ADAM
MCF, LIG, Université Grenoble Alpes, Co-Encadrante, Invitée
Monsieur Frédéric AMBLARD
Professeur, Université Toulouse-1 Capitole, IRIT, Examinateur
Madame Sandrine ANQUETIN
Directrice de Recherche, IGE, Grenoble, Examinatrice, Présidente
Monsieur Alexis DROGOUL
Directeur de Recherche, IRD UMI UMMISCO-Vietnam, Rapporteur
Monsieur Éric DAUDÉ
Chargé de Recherche, HDR, CNRS, UMR IDEES, Université de Rouen, Rapporteur

MULTI AGENT MODELLING OF SEISMIC CRISIS

By

Julius Bañgate

Université Grenoble Alpes

PHD THESIS

December 18, 2019

Abstract

Evacuations are necessary during earthquake crisis to mitigate and avoid risks of exposure to hazards that can cause injury or death. Evacuation are social in nature. This is mainly because the main agents in evacuations are people who possess highly evolved social strategies for coping with danger. Social attachment theory posits that proximity seeking behaviours are activated during danger. In this situation people seek attachment figures. Attachment figures include familiar people, places, object, etc. The presence of attachment figures promotes the feeling of calm and safety. Conversely, their absence result in anxiety and flight. This means for example that during disasters individuals may seek family members, before evacuating. Also, this explains the behaviour why people gather personal property before heading to familiar exits and places, or follow groups/crowds, etc.

In this framework, a multidisciplinary approach – based on social, geoscience, spatial and computer sciences – is proposed to simulate individuals' behaviours after an earthquake in the city of Grenoble, France. For this purpose, SOLACE, a multi agent model on crisis evacuations was developed to answer eight key questions (Q1 to Q8) that can explain the nature and impact of human evacuation behaviour modulated by social attachment. The effect of several parameters on the number of arrivals in safe areas was observed: social attachment (Q1); knowledge (Q2); number of close bonds (Q3); time of day (Q4); presence of disability (Q5); presence of casualties (Q6); earthquake intensity (Q7); and radius of danger zones around buildings (Q8).

The results of the experiments point to the importance of social interactions during evacuations. The behaviours of individuals are significantly affected by their social environment that responds to the challenges imposed by the physical environment produced by earthquake disasters. The capacity and tendency for social interaction are inherent in humans and need to be considered in evacuations. It was shown that social attachment is important because it can facilitate saving more lives during earthquake disasters.

The first and main contribution of the research is to add to arguments stressing the importance of human behaviour and the social dynamics that emerge during crisis evacuations. The second major contribution of the study is SOLACE, the multi agent-based model for earthquake evacuation implemented using social attachment. The third major contribution is that the research supports the benefit of using accurate spatial data in dynamic multi agent-based models.

Résumé

L’évacuation des populations est nécessaire pendant les crises sismiques afin d'atténuer et d'éviter l'exposition à des dangers qui peuvent causer des blessures ou la mort. Tout comme le risque, l’évacuation est de nature sociale. Cela s'explique principalement par le fait que les personnes qui évacuent possèdent des stratégies sociales très évoluées pour faire face au danger. La théorie de l'attachement social suppose que la recherche de personnes ou de lieux familiers est réalisée en situation de danger. Dans cette situation, les gens recherchent des figures d'attachement. Les figures d'attachement comprennent des personnes, des lieux, des objets familiers, etc. La présence de figures d'attachement favorise le sentiment de calme et de sécurité. Inversement, leur absence entraîne l'anxiété et la fuite. Cela signifie, par exemple, qu'en cas de catastrophe, les personnes peuvent chercher des membres de leur famille avant d'évacuer. Cela explique aussi pourquoi les gens recueillent des biens personnels avant de se diriger vers des sorties et des endroits familiers, ou de suivre des groupes ou des foules, etc.

Dans ce contexte, une recherche pluridisciplinaire a été menée, basée sur les apports des sciences sociales, de la terre, de l’information spatiale et de l’informatique, pour simuler les comportements des individus à la suite d’un séisme dans la ville de Grenoble (France). Dans cette optique, SOLACE, un modèle multi-agents sur les évacuations de crise, a nous avons développé pour répondre à huit questions clés (Q1 à Q8) qui peuvent expliquer la nature et l'impact des comportements d'évacuation humaine modulés par les liens sociaux. L'effet de plusieurs paramètres sur le nombre d'arrivées dans les zones sûres a nous avons observé: il s’agit de l'attachement social (Q1), des connaissances (Q2), du nombre de liens étroits (Q3), de l'heure de la journée (Q4), de la présence d'un handicap (Q5), de la présence de victimes (Q6), de l'intensité du séisme (Q7) et du rayon des zones dangereuses autour des bâtiments (Q8).

Les résultats des expériences montrent l'importance des interactions sociales pendant les évacuations. Les comportements des individus sont fortement influencés par leur environnement social qui répond aux défis imposés par l'environnement physique produit par les catastrophes sismiques. La capacité et la tendance à l'interaction sociale sont inhérentes aux humains et doivent être prises en compte dans les évacuations. Nous avons démontré que l'attachement social est important parce qu'il peut faciliter le sauvetage d'un plus grand nombre de vies lors de catastrophes sismiques.

La première et principale contribution de la recherche est d’appuyer les arguments soulignant l'importance du comportement humain et des dynamiques sociales qui émergent lors des évacuations de crise. La deuxième contribution majeure de l'étude est SOLACE, le modèle multi-agents d'évacuation en cas de tremblements de terre mis en œuvre en utilisant l'attachement social. La troisième contribution majeure est que la recherche confirme l'avantage d'utiliser des données spatiales précises dans des modèles dynamiques multi-agents.

Table of Contents

Abstract 3

Résumé 4

List of Tables 10

List of Figures 11

List of Equations 14

List of Code 15

Acknowlegements 17

CHAPTER 1. INTRODUCTION 18

1.1 General description of the problem 18

1.2 Significance of the problem 24

1.3 Problem statement 25

1.3.1 Need for a realistic behavioural model 26

1.3.2 Need for a multi-disciplinary approach 26

1.3.3 Need for models that are easily understood by stakeholders 28

1.4 Research questions and hypotheses 28

1.5 Contributions 30

1.6 Structure of the thesis 30

CHAPTER 2. SEISMIC RISK & CRISIS CONTEXT 31

2.1 Disaster, crisis, risk and related concepts 31

2.2 Physical elements of seismic crisis 32

2.2.1 Seismology and buildings 33

2.2.2 State of the art in seismic vulnerability assessment of buildings at urban scale 35

2.3 Human and social aspects of seismic risk 36

2.3.1 Earthquakes and people 36

2.3.2 Evacuation and human behaviour 36

2.3.3 State of the art in the study of evacuation and human behaviour 39

2.3.4 Social theories that explain crisis and evacuation behaviours 41

2.3.4.1 Popular notions 41

2.3.4.2 Attachment behaviours 42

2.3.4.3 Group formation and behaviours 44

2.4 Summary of the chapter 46

CHAPTER 3. STATE OF THE ART 47

3.1 Pedestrian evacuation models 47

3.2 Geographic information and spatial models of crisis environments 49

3.2.1 Geoinformation, GIScience, GISystems (GIS) 49

3.2.2 Utility of geoinformation and GIS for risk and crisis research 50

3.2.3 Limitations of GIS 52
3.3 Agent based models 53
3.3.1 Agent based modelling, social simulation, pedestrian simulation 53
3.3.2 Social simulation of evacuations 53
3.3.2.1 Social force model 54
3.3.2.2 Roan's model 55
3.3.2.3 Earthquake Pedestrian Evacuation Simulation (EPES) 55
3.3.2.4. Evacuation Simulation with Children, Authorities, Parents, Emotions and Social Comparison (ESCAPES) 56
3.3.2.5 Exitus 56
3.3.2.6 Multi-Agent Simulation for Egress Analysis (MASSEgress) 56
3.3.2.7 Social Agents for Egress (SAFEgress – 2014) 57
3.3.2.8 Social Agents for Egress (SAFEgress – 2015) 57
3.3.2.9 Social Identity Model Application (SIMA) 57
3.3.2.10 Okaya and Takahashi's Robocup Rescue 58
3.3.2.11 Liu et al.'s model 58
3.3.2.12 Lou et al.'s model 58
3.3.2.13 Simulation of Transient Evacuation and Pedestrian Movements (STEPS) 59
3.3.2.14 Ta et. al.'s Model 59
3.3.2.15 Wang et al.'s Model 59
3.3.2.16 Zia et al.'s Model 59
3.3.2.17 Adam et al.'s Model 59
3.3.2.18 Agent-based Model for Earthquake Evacuation in Lebanon (AMEL) 60
3.4 Summary of the chapter 63

CHAPTER 4. DESCRIPTION OF THE METHODOLOGY 69
4.1 Multi-disciplinary approach 69
4.2 Description of the methodology 71
4.3 Study area 75
4.4 Sources of data 80
4.5 Summary of the chapter 81

CHAPTER 5. AGENT BASED MODEL OF SOCIAL ATTACHMENT 83
5.1 Model of the individual and social attachment 83
5.1.1 Social distance and strength of bonds 84
5.1.2 Visual familiarity and limits to perception imposed by distance 85
5.1.3 Voice familiarity and the limits to perception imposed by distance 89
5.1.4 Affective Perception Distance 92
5.2 Individual motion and navigation in free space 95
5.3 Model of spatial environment 96

5.4 Model of seismic crisis environment 99
5.5 SOLACE multi-agent model and UML diagram 101
5.6 Software application model and system architecture 106
5.7 Summary of the chapter 107

CHAPTER 6. IMPLEMENTATION, CALIBRATION & VALIDATION OF THE SOCIAL ATTACHMENT MODEL 108
6.1 Spatial data processing workflows 108
6.1.1 Deriving safe areas and danger zones 109
6.1.2 Scaling macroseismic damage and vulnerability data to the building level 111
6.1.3 Spatial data subsets 112
6.1.4 Vector data modification (adding doors, carving out doorways and simplify layers) 114
6.2 Agent based modelling workflow 115
6.2.1 GAMA simulation user interface 115
6.2.2 Use of probabilities in generating agent populations 117
6.2.2.1 Use of probabilities in generating agent populations and assigning vulnerability and damage to every building (GAML Code) 117
119
6.2.2.2 Debris creation 122
6.2.2.3 Spatially distributed heterogeneous human agent populations 124
6.2.2.4 Creating non-human agents 127
6.2.3 Complex multi-agent dynamics 128
6.2.2.1 Interactions with barriers 129
6.2.2.2 Interactions with debris in the environment (avoidance, injury, death) 129
6.2.2.3 Defining social relationships 130
6.2.2.4 Social attachment implemented with BDI 131
6.2.4 Versions of running the simulation 133
6.2.5 SOLACE data visualisation user interface 134
6.2.6 Simulation data 135
6.2.7 Dynamic time series charts 137
6.3 Hardware considerations 138
6.4 Calibration, simulation and validation 139
6.4.1 Calibrating population data 139
6.4.2 Checking disaster video footage 139
6.4.2.1 Indoor video – pre-evacuation behaviours 139
6.4.2.2 Outdoor video – pedestrian evacuation behaviours outdoors 140
6.4.3 Consultation with experts to validate the model 142
6.5 Summary of the chapter 143

CHAPTER 7. DESIGN OF EXPERIMENTS 144
7.1 Experiment scenarios 144
7.1.1 Question 1. Role of social attachment 144
7.1.2 Question 2. Role of knowledge 145
7.1.2.1 SET 1. Nearby safe area 145
7.1.2.2 SET 2. Single safe area far from population initial location – free space navigation 145
7.1.2.3 SET 3. Single safe area located in a distant location from the population initial location, with shortest path navigation, percentage of the population with knowledge of safe area 146
7.1.3 Question 3. Role of the number of close bonds 148
7.1.4 Question 4. Effect of time of day 149
7.1.5 Question 5. Effect of the presence of disability 149
7.1.6 Question 6. Effect of the presence of casualties 149
7.1.7 Question 7. Effect of intensity 150
7.1.8 Question 8. Effect of the radius of danger zones and availability of safe areas 150
7.2 General description of experiments and simulation with the model 151
7.2.1 Time 152
7.2.2 Spatial extents 152
7.2.3 Parameters 153
7.3 Summary of the chapter 154

CHAPTER 8. RESULTS 155
8.1 Introduction 155
8.2 Description of charts used 155
8.3 Answers to research questions 155
8.3.1 Question 1: Does social attachment affect the number of arrivals in safe areas? 155
8.3.2 Question 2: Does the knowledge of nearby safe areas affect the number of arrivals in safe areas? 161
8.3.2.1 Set 1. Nearby safe areas 161
8.3.2.2 Set 2. Single safe area far from population initial location – free space navigation 162
8.3.2.3 Set 3. Single safe area located in a distant location from the population initial location, with shortest path navigation, percentage of the population with knowledge of safe area 163
8.3.2.4 Short conclusion from 3 sets of experiments 165
8.3.3 Question 3: How does the number of close bonds affect evacuation? 166
8.3.4 Question 4: How does the time of day affect evacuation? 167
8.3.5 Question 5: How does disability affect the number of arrivals in safe areas? 170
8.3.6 Question 6: Does the presence of casualties on the route affect the number and time of arrivals in safe areas? 172
8.3.7 Question 7: Does intensity affect the number of arrivals in safe areas? 177
8.3.8 Question 8: How does the radius of the danger zone around buildings affect the number of arrivals in safe areas? 181
8.4 Summary of the chapter 183

CHAPTER 9. CONCLUSION 187
9.1 Synthesis and conclusions 187
9.2 Contributions 189
9.3 Future work 190
9.3.1 Improving the model 190
9.3.2 Possible applications in different domains 192
9.3.2.1 Geospatial science 192
9.3.2.2 Social sciences 194
9.3.2.3 Geoscience 195
9.3.2.4 Computer science 195
9.4 Concluding remarks 196
Bibliography 197
APPENDIX 210
Appendix 1.0 GAMA Code 210

List of Tables

Table 1. Intensity and effects on People and Objects, EMS-98 (Grünthal, European Macroseismic Scale 1998, 1998) 21
Table 2 Magnitude and intensity comparison near epicentre (USGS_a, 2019) 22
Table 3 Comparison of casualties and building damage with respect to building codes (Nienhuys, 2015) 23
Table 4 World's most earthquake prone cities (Smith J. P., 2019) 24
Table 5 2015 Population and Built-up surface potentially exposed to earthquake by region, 475 years Return Period (Pesaresi, et al., 2017) 24
Table 6 Differentiation of structures into vulnerability classes, EMS-98 (Grünthal, European Macroseismic Scale 1998, 1998) 33
Table 7 Damage grades for masonry and reinforced concrete structures, EMS-98 (Grünthal, European Macroseismic Scale 1998, 1998) 34
Table 8 Classification of damage, EMS-98 (Grünthal, European Macroseismic Scale 1998, 1998) 34
Table 9 Evacuation speeds 38
Table 10 Evacuation behaviour 40
Table 11 Attachment figures and possible behaviours during evacuations 43
Table 12 Affiliative reactions to threat (Mawson, 2005) 44
Table 13 Social theories 45
Table 14 Variations in scale in modelling pedestrian evacuation simulations 48
Table 15 Behaviour and time studies (Delay) 49
Table 16 ABM implementing social theories for evacuations 60
Table 17 Model Implementation 64
Table 18 Model Implementation - Continued 65
Table 19 Attachment figures in the models 66
Table 20 Behaviours in models 67
Table 21 Other features of models 68
Table 22 Historical earthquakes from intensity IV felt in Grenoble (www.sisfrance.net, 2018). Please note that the intensity values I_{Origin} and $I_{Grenoble}$ are expressed as real numbers and not in their roman numeral equivalents. 77
Table 23 Description of data used for model development, initialisation of parameters and validation of results 80
Table 24 Social distance (SD) and strength of bond (SB) from a reference adult parent 85
Table 25 Distances related to perception, fixation and recognition of people 87
Table 26 Voice levels with respect to distance from source 90
Table 27 Mean strength of emotional bonds for France (Suvilehto, et al., 2015) 93
Table 28 Pre-evacuation behaviours in the SOLACE model 103
Table 29 Examples of BDI implemented with social attachment in SOLACE 104
Table 30 Evacuation behaviours modelled/implemented taking into account BDI 105
Table 31 Data layers in Figure 37 and Figure 38 110
Table 32 Building data with IRIS attributes 111
Table 33 Number of vector elements for the model for each layer 113
Table 34 Attributes for doors 114
Table 35 Evaluating probabilities for building typology typeVC with the flip() function. The assigned value to typeVC is contained within the braces (i.e. "a", "b", "c", "d", or "e"). 118
Table 36 Evaluating probabilities for building damage typeDCV during an intensity V earthquake scenario with the flip() function. The assigned value is contained within the braces (i.e. 0, 1, 2, 3, 4, or 5). 118
Table 37 Building Vulnerability Class in the order of decreasing vulnerability 120
Table 38 Building Damage Grade in the order of increasing damage 121
Table 39 Intensity related parameters in the calculation of debris values are 0, 1, 2, 3, 4 and 5. 124
Table 40 Human agents in SOLACE 127
Table 41 Non-human agents in SOLACE 128
Table 42 Perception lines available for the model – adult agents perceiving others/objects 132
Table 43 Ways of running SOLACE 134
Table 44 Tables available in the Python UI 136
Table 45Time series charts available in the Python UI 138
Table 46 Hardware Platforms used for developing and running SOLACE simulations 138
Table 47 Themes for the research questions 144
Table 48 Parameters and values for question 1 experiments 145

Table 49 Parameters and values for question 2 experiments....145
Table 50 Parameters and values for question 2 experiments – set 3....148
Table 51 Parameters and values for question 3 experiments....149
Table 52 Parameters and values for question 4 experiments....149
Table 53 Parameters and values for question 5 experiments....149
Table 54 Parameters and values for question 6 experiments....150
Table 55 Parameters and values for question 8 experiments....150
Table 56 Size of danger zones, safe areas and barriers (in square meters and percent)....151
Table 57 Initial simulation parameters....153
Table 58 Difference in percentage arrivals in the With Attachment and No Attachment scenarios....158
Table 59 Difference in percentage arrivals in the with attachment and no-attachment scenarios for Intensity IV and VIII....161
Table 60 Effect of knowledge of safe areas on adult arrivals....162
Table 61 Simple experiment. Number of arrivals after 5400 cycles (1 hour 30 minutes)....162
Table 62 Number of arrivals after 6000 cycles....164
Table 63 Summary of results for experiment on evacuation with knowledge....165
Table 64 Effect of social bonds on the number of arrivals in safe areas....167
Table 65 Difference in percentage arrivals with respect to time of day at the 900th cycle....169
Table 66 Difference in percentage arrivals with respect to presence of disabled at the 900th cycle....171
Table 67 Percentage arrivals and interaction with casualties at the 900th cycle, Day, With Attachment....175
Table 68 Estimated injury distributions at building collapse, % of trapped occupants (Coburn_1, Spence, & Pomonis, 1992; Coburn & Spence, 2002)....176
Table 69 Debris production with respect to intensities....177
Table 70 Number of buildings with different levels of damage for each intensity scenario (Probabilistic)....179
Table 71 Percentage of buildings with different levels of damage for each intensity scenario (Probabilistic)....179
Table 72 Available areas for IRIS extents with danger zone at half the height of adjacent buildings....182
Table 73 Summary of results....183
Table 74 Summary of answers to research questions....187

List of Figures

Figure 1. Worldwide frequency of earthquakes (IRIS_b, 2019)....21
Figure 2 Percentage of deaths per disaster type, 1996 – 2015 (CRED, 2016)....23
Figure 3 Top ten urban centres population exposed to seismic magnitude greater than class 5 in MMI scale. Data shown is for 2015, and showing the change since 1990 (EC-JRC, 2018)....25
Figure 4 Population change by age-group, world and OECD countries, 1950 to 2090. OECD calculations are based on United Nations Department of Economic and Social Affairs, Population Division (2010), World Population Prospects: The 2010 Revision, United Nations (OECD, 2015)....25
Figure 5 Relevant domains for modelling human behaviour in a seismic crisis context....27
Figure 6 Temporal context of events and actions for earthquake evacuations (Alexander D. , 1990)....37
Figure 7 Multi-disciplinary approach carried out to develop a simulation of earthquake crisis....69
Figure 8 Detailed methodology carried out to develop a simulation of earthquake crisis....71
Figure 9 Location of Grenoble with respect to Metropolitan France. Map by Julius Bañgate, 2019 with data from (BRGM, 2019; Google, 2018). BRGM was the source of the Department boundaries. Google is the source of the terrain basemap....75
Figure 10 Grenoble city boundary map by Julius Bañgate, 2019 with data from: (Riedel_a, et al., 2015; OpenStreetMap & Contributors, 2018; BRGM, 2019). The IRIS boundary data is from Rieldel et a.l; the Commune boundary is from BRGM; the basemap is from OpenStreetMap.....75
Figure 11 Seismic zones for metropolitan France May 1, 2011, article D.563-8-1 du code de l'environnement, Ministère de l'Ecologie, du Développement durable, des Transports et du Logement. Map is created by Julius Bañgate, 2019 with data from published GIS Data Source: (BRGM, 2019)....76
Figure 12 Seismicity of Grenoble and in the Belledonne fault area (ISTerre, 2019; Thouvenot, Fréchet, Jenatton, & Gamond, 2003). The grey broken line is the fault. The left image shows more recent earthquakes indicating magnitudes. The right image shows historic earthquakes.....77
Figure 13 Location of historical earthquakes in the nearby region. Earthquakes have intensities greater than 5 around Grenoble. Earthquake data from www.sisfrance.net (www.sisfrance.net, 2018). Map by Julius Bañgate,

2019 with data on Seismic zones and boundaries from planseisme.fr (www.planseisme.fr, 2018). Topographic data from OpenTopo (OpenTopogaphy, 2018) 78
Figure 14 Grenoble zone amplification increments, zone boundaries are estimated and digitized based on a figure from Dunand & Guéguen, 2012. Map by Julius Bañgate, 2019. 79
Figure 15 SOLACE Attachment Model 84
Figure 16 Regression analysis results comparing visual acuity and age in three study groups (Salthouse, Hancock, Meinz, & Hambrick, 1996) 88
Figure 17 Visual acuity with respect to distance from object 88
Figure 18 Visual acuity and normal vision 20/20 vs 20/200 (www.allaboutvision.com, 2018) 89
Figure 19 Voice levels at a distance from source calculated using the Inverse Square Law. As reference 0 dB, threshold for hearing; 20 dB, sound of rustling leaves or a mosquito; 40 dB, quiet room, home, bird call; 60 dB normal conversation where individuals are 1 meter apart; 80 dB is a road with busy traffic; 100 dB, motor horns 7 meters away; 120 dB, siren 30 meters away; 140 dB, is the threshold for pain. (Engineering Toolbox, 2018).91
Figure 20 Example visualisation of distances from a noise point source outside the LIG Building on the UGA Campus. The left image is the LIG building. The image on the right is the open space in front of the University Science Library. The normal conversation distance is 1 to 4 meters. Beyond 4 meters individuals need to talk louder or at much higher decibels to be heard by other individuals. To be heard at the level of a normal conversation at 50 meters, in ideal situations, from the origin, the voice level has to be at 105 dB (Shout_5 in Table 26). 91
Figure 21 PD_{Normal} values with respect to values with respect to Age based on Salthouse et al.'s Snellen Visual Acuity Ratio and 50 meters visual perception distance (Salthouse, Hancock, Meinz, & Hambrick, 1996) 93
Figure 22 Perception distance influenced by social bond strength 94
Figure 23 Movement and navigation of the individual in the SOLACE model 95
Figure 24 Example of agent movement in SOLACE model 96
Figure 25 SOLACE Spatial data model 97
Figure 26 Study area features that act allow agent movement or as barriers 97
Figure 27 Extracting free space by subtracting barrier layers from extents 98
Figure 28 SOLACE danger zones 98
Figure 29 SOLACE Safe Areas extracted by the subtracting building footprint and danger zone from free space 99
Figure 30 SOLACE earthquake modelling 100
Figure 31 SOLACE simplified UMLClass diagram 102
Figure 32 Model for building egress 104
Figure 33 Human agent decision making 105
Figure 34 SOLACE System Architecture 106
Figure 35 Spatial data processing workflows 108
Figure 36 Geoprocessing workflow for the creation of danger zones and safe areas 109
Figure 37 Spatial layers used in the model at the scale of the city of Grenoble 109
Figure 38 Safe areas and danger zones in the city center of Grenoble. Danger zones are the red areas around buildings. The width of the zone or the distance from the building is half the height of the structure. The safe areas are the green coloured spaces. Large open spaces suitable for evacaution in the figure are (1) Place Victor Hugo, (2) Parc Jardin de Ville, (3) Verdun, (4) Parc du Département de l'Isere, (5) Parc Jadin des Plantes, (6) Parc Paul Mistral, and (7) Parc Jardin Hoche. 110
Figure 39 Assigning building with IRIS damage and vulnerability data 111
Figure 40 Building data with IRIS layer attributes 112
Figure 41 2-IRIS Subset (Left), 9-IRIS Subset 113
Figure 42 Doors and buildings in SOLACE. Human agents are generated inside door polygons at the start of the simulations. 114
Figure 43 SOLACE Code Modules 115
Figure 44 SOLACE user interface using GAMA (2D) 116
Figure 45 SOLACE user interface using GAMA (3D) 116
Figure 46 Left: Building Vulnerability – Typology (A to E); Damage: Building Damage (0 to 5) for Intensity VIII Scenario. 119
Figure 47 Building vulnerability classes from left to right are from A to E in the order of decreasing vulnerability. 121
Figure 48 Building damage at Intensity VIII scenario. Values are from from left to right are from 1 to 5 in the order of increasing damage. 122
Figure 49 Violet squares are debris created by damaged buildings during the duration of the earthquake in the simulation. Debris are generated within danger zones. Snapshot of a simulation for intensity.. 124
Figure 50 Creating non-human agents from shapefiles 128

Figure 51 Effect of debris on human agents. Healthy adult and child agents have black and green heads respectively. Injured agents have red heads. Dead agents have white heads and do not have perception areas. (a) Top view.(b) Side view. ……..130
Figure 52 SOLACE data view user interface 134
Figure 53 Python code creating the SOLACE menu items for creating charts displaying information for evacuation, perception and location.....135
Figure 54 Python code for displaying data as a chart or a table in the browser. An html file is created using python. In the code, D3 is used to embed the data using javascript.....135
Figure 55 Evacuation progress file in percent. Dynamic D3 browser-based tables to monitor and inspect generated tables compare evacuation progress in real time.....136
Figure 56 Evacuation progress file in percent viewed from a web browser. Dynamic D3 browser based tables to monitor and inspect generateted compare evacuation progress in real time.....136
Figure 57 GOTO file viewed from a web browser. Dynamic D3 browser-based tables to monitor and inspect generated compare evacuation progress in real time. 137
Figure 58 Dynamic D3 browser-based charts to monitor and compare evacuation progress in real time.....137
Figure 59 SOLACE Server Configuration 139
Figure 60 Validating social dynamics in the simulation by comparing with video from indoor scenes. (a) Nepal, May 12, 2015 earthquake. (b) March 11, 2011 Sendai, Japan earthquake. 140
Figure 61 Emergent spatial patterns of social dynamics in the simulation by comparing with video from outdoor scenes. (a) Asan, Nepal, April 25, 2015 earthquake (b) simulation showing agent dynamics.....141
Figure 62 Emergent spatial patterns of social dynamics in the simulation by comparing with video from outdoor scenes. (a) Zocalo Square, Mexico City during the Sept. 19, 2017 earthquake (b) clusters of agents in Place Victor Hugo, Grenoble. 141
Figure 63 Emergent spatial patterns of social dynamics in relation to presence of debris, injuries and deaths. (a) pedestrian scene from Mexico earthquake on Sept. 19, 2017 (b) simulation showing agent interaction width debris and other agents. In the figure, injured agents have red head and dead agents have white heads. Healthy agents have black (adult) and green heads (child). (c) pedestrian scene, Christchurch, New Zealand 142
Figure 64 Consultation with experts.....142
Figure 65 Simple experiment on individual navigation through urban pathways.....146
Figure 66 Catchment radius of the safe area defined by the black circle drawn with thick broken lines. 146
Figure 67 Agent navigation towards safe area using the shortest path. Agents (small yellow triangles on roads) move from initial building locations (dark grey and light grey polygons) towards the safe area (green circle) by way of shortest paths defined from road centrelines (white-orange vector lines). The intensity simulated is Intensity IV, which explains the absence of debris damage and therefore blocked pathways.....147
Figure 68 Agent navigation around blocked pathways. The agent with the long and green perception line has perceived a road segment which is part of the shortest route (white with thin red centreline). In its current location, the agent is able to travel freely in space as it navigates towards the portion of the shortest path towards safe zones. Buildings without damage are shown as grey polygons. Damaged buildings are yellow-orange polygons. Debris blocking roadways are shown as violet squares. Red polygons surrounding damaged buildings are danger zone.....148
Figure 69 Map of available safe areas (a) > Half the height of buildings (b) uniform 6 meters around buildings 151
Figure 70 Available safe areas (a) > Half the height of buildings (b) uniform 6 meters around buildings 151
Figure 71 Workflow for the experiments.....152
Figure 72 Adult arrivals in safe areas, Intensity IV – Day (a) histogram, (b) timeseries 156
Figure 73 Adult arrivals in safe areas, Intensity IV - Night (a) histogram, (b) timeseries.....156
Figure 74 Adult arrivals, Intensity V – Daytime (a) histogram, (b) timeseries; 156
Figure 75 Adult arrivals, Intensity VI – Daytime (a) histogram, (b) timeseries 157
Figure 76 Adult arrivals, Intensity VIII – Day (a) histogram, (b) timeseries 157
Figure 77 Adult arrivals, Intensity VIII – Night (a) histogram, (b) timeseries 157
Figure 78 Comparison across different intensities – (a) Daytime only for Intensity IV, 5, 6 and 8, (b) Extreme values Intensity IV vs Intensity VIII for Day and night time scenarios 159
Figure 79 Perceiving Goals: (a) no social attachment, (b) with social attachment 159
Figure 80 Creation of Social Groups facilitated by social attachment 160
Figure 81 Effect of knowledge of safe areas on adult arrivals, Intensity IV – Night (a) histogram, (b) timeseries 162
Figure 82 Results of evacuation with knowledge 164
Figure 83 Possible configurations of safe areas to improve evacuation. (a) Open areas far from the boundary. (b) Open areas closer to the boundary. (c) A mix of boundaries outside and inside the boundary. (d) Safe areas away from buildings inside the boundary. 165

Figure 84 Effect of the number of social bonds on adult arrivals in safe areas, ...166
Figure 85 Effect of the number of social bonds compared with No-Attachment Intensity IV – Night (a) histogram, (b) timeseries....167
Figure 86 Effect of the time of day on evacuation, Intensity IV: (a) histogram, (b) timeseries....168
Figure 87 Effect of the time of day on evacuation, Intensity VI: (a) histogram, (b) timeseries....168
Figure 88 Effect of the time of day on evacuation,Intensity VIII: (a) histogram, (b) timeseries; 168
Figure 89 Comparison of day vs night time evacuation arrivals with respect to intensity at the 900th cycle 169
Figure 90 Effect of the presence of disabled, Intensity VI – With Attachment: (a) histogram, (b) timeseries; ..171
Figure 91 Effect of the presence of disabled, Intensity VI – No Attachment: (a) histogram, (b) timeseries 171
Figure 92 Casualties on the route, (a) active agents, (b) deceased, and (c) active injured adult agents 172
Figure 93 Casualties on the route, Intensity VIII, (a) number of active, (b) deceased, and (c) injured....173
Figure 94 Adult agents interacting with deceased adult agents along the route (a) histogram, (b) time series...173
Figure 95 Adult agents interacting with injured adult agents along the route (a) histogram, (b) time series....174
Figure 96 Percent arrivals in safe areas – With Attachment, Day (a) histogram, (b) timeseries....175
Figure 97 Percent arrivals and non-arrivals in safe areas – With Attachment, Day (a) Intensity IV, (b) Intensity V, (c) Intensity VI, (d) Intensity VII....175
Figure 98 Number of Debris and Intensity –(a) histogram at 14th Cycle, (b) timeseries 0 to 20th Cycle....177
Figure 99 Debris damage during the August 24, 2016 Amatrice, Italy earthquake (Mag. 6, Int X) (Legi il Firenzepost, 2016; Quest, et al., 2016) 178
Figure 100 Damage during the August 24, 2016 Amatrice, Italy earthquake (Mag. 6, Int X) (Mesa, 2016; Quest, et al., 2016) 178
Figure 101 Buildings with damage for Intensity VIII within the 2-IRIS coverage area 179
Figure 102 Buildings with damage for Intensity VIII within the 9-IRIS coverage area 180
Figure 103 Buildings with damage for Intensity VIII within the 69-IRIS coverage area....180
Figure 104 Effect of radius of the danger zone on evacuation – With Attachment (a) histogram, (b) timeseries 181
Figure 105 Safe areas with respect to extents (IRIS 2, IRIS 9 and IRIS 69)....182
Figure 106 Danger zones, safe areas, and barriers (a) IRIS 2, (b) IRIS 9, (c) IRIS 69 182
Figure 107 Effect of increased coverage and availability of safe area (a) histogram, (b) timeseries 183
Figure 108 Evacuation arrivals of adults in safe areas at cycle 900 (15 minutes) for all scenarios. 185
Figure 109 Evacuation arrivals of adults in safe areas at cycle 900 (15 minutes) for all scenarios. 186
Figure 110 Indoor evacuation in a hospital floor with complex layout (Bañgate, 2016) 193
Figure 111 Egress from building (Bañgate, 2016)....193
Figure 112 Floor layout of LIG Building....194

List of Equations

Equation 1 Risk Equation 1.... 31
Equation 2 Risk Equation 2.... 31
Equation 3.... 92
Equation 4.... 92
Equation 5.... 92
Equation 6.... 93
Equation 7.... 94
Equation 8.... 94
Equation 9....100
Equation 10....100
Equation 11....101
Equation 12....101
Equation 13....101
Equation 14....102
Equation 15....102
Equation 16....102
Equation 17....104
Equation 18....104

List of Code

Code 1....117
Code 2....117
Code 3....118
Code 4....118
Code 5....119
Code 6....119
Code 7....119
Code 8....120
Code 9....122
Code 10....123
Code 11....123
Code 12....124
Code 13....125
Code 14....125
Code 15....126
Code 16....126
Code 17....126
Code 18....127
Code 19....129
Code 20....129
Code 21....129
Code 22....130
Code 23....130
Code 24....131
Code 25....131
Code 26....131
Code 27....132
Code 28....132
Code 29....152
Code 30 Getting the shapefile with damage and vulnerability data. (Equivalent to Code 1) 210
Code 31 Getting the values from fields of type float. (Equivalent to Code 2)....210
Code 32 Assigning building typology (vulnerability class) using the flip() function. (Equivalent to Code 3)...210
Code 33 Assigning building damage for intensity scenarios using the flip() function. (Equivalent to Code 4) .210
Code 34 Saving building data to shapefile (Equivalent to Code 5) 210
Code 35 Load the building shapefile for intensity VI scenario (Equivalent to Code 6)....210
Code 36 Initialise building agent from building shapefile (Equivalet to Code 7)....210
Code 37 Building species (Equivalent to Code 8)....211
Code 38 Creating debris at every timestep within the duration of the simulated earthquake. Equivalent to Code 9 211
Code 39 Amount of debris created based on typology (Equivalent to Code 10)....211
Code 40 Debris created at each time step (Equivalent to Code 11)....211
Code 41 Building collapse (Equivalent to Code 12)....211
Code 42 General parameters. Equivalent to Code 13. 212
Code 43 List of IRIS units. Equivalent to Code 14....212
Code 44.Generating night time population. Equivalent to Code 15....212
Code 45 Generating day time population. Equivalent to Code 16....212
Code 46 List of the population of Adults (30 -59 y.o.) for each IRIS. Equivalent to Code 17....212
Code 47 Generating human agent population. Equivalent to Code 18....213
Code 48 Agent avoiding buildings. Equivalent to Code 19. 213
Code 49 Generating casualties. Equivalent to Code 20. 213
Code 50 Agents avoiding debris. Equivalent to Code 21....213
Code 51 Defining social relationships. Equivalent to Code 22. 214
Code 52 Assigning kin and friend IDs. Equivalent to Code 23....214
Code 53 Predicates for adult agents. Equivalent to Code 24....214
Code 54 Predicates for child agents. Equivalent to Code 25....214
Code 55 Reflex when detecting earthquakes. Equivalent to Code 26....215
Code 56 Perception distances. Equivalent to Code 27....215

Code 57. Perceiving other agents. Equivalent to Code 28 215
Code 58 End simulation. Equivalent to Code 29.....215

Acknowlegements

We would like to thank and acknowledge the Arc 7, Rhône Alpes Region for providing the funding for this research and the IXXI/ISH for supporting its dissemination in conferences.

We also like to thank and acknowledge the members of the jury, Sandrine Anquetin, Frédéric Amblard, Alexis Drogoul and Eric Daudé for accepting the invitation to be in the panel.

I personally would like to thank my supervisors Julie Dugdale, Elise Beck and Carole Adam for providing the guidance in the completion of this work. Also great thanks to all the colleagues at Magma/HawAI at LIG and the Environment team at PACTE for all their support. Also, for the other colleagues at LIG and PACTE.

This work is also especially dedicated to my wife Ion, my daughter Abelita and my family.

CHAPTER 1. INTRODUCTION

1.1 General description of the problem

The innate individual human response when faced with danger is geared towards survival or self-preservation (Mobbs, Hagan, Dalgleish, Silston, & Prévost, 2015). Traditionally, individual responses to danger were more popularly viewed with respect to the fear response and on purely egoistic[1] terms. These responses include freeze, fight, flight, fright, or faint (Schmidth, Richey, Zvolensky, & Maner, 2008; Bracha, 2004). Panic, which refers to irrational, groundless, hysterical flight with the complete disregard for others, has also been used to describe the "chaotic behaviour" of escaping crowds (Heide, 2004). Escape panic in particular has be identified as the cause of highly competitive behaviours, during escapes from disasters in mass gatherings, that resulted in stampedes, causing injuries and deaths (Ngai, Burkle, Hsu, & Hsu, 2009; Khan & Noji, 2016). Experts however consider mass panic occurring in emergencies to be rare, a myth, unsupported by evidence, and do not accurately describe human behaviour during emergencies (Cocking, Drury, & Reicher, 2009; Heide, 2004).

Human behaviour however during disasters are numerous, varied, dynamic and complex. The egoistic perspective is not sufficient to describe human behaviour in crisis scenarios. This is evidenced by behaviours during disasters which are non-egoistic, such as collective action (cooperation) and altruism[2] (Cocking, Drury, & Reicher, 2009; Ma H. K., 2017; Heide, 2004). Humans are intrinsically social, and behaviours during disasters are social in nature (Dunbar, 2019). People are embedded in social structures, institutions and relationships where interactions are governed by social and cultural norms (Burns, Roszkowska, Johansson, & Corte, 2018; Misyak, Melkonyan, Zeitoun, & Charter, 2014; Bianchi & Squazzoni, 2015). People utilise highly evolved social strategies at their disposal, but are modulated by learned cultural norms when individually or collectively handling threat (Alexander_a, 2012). Social constraints and role obligations do not suddenly dissolve, but are actually amplified in emergency situations (Goltz, 2017). According to Mawson, people do not flee danger, but seek the proximity of familiar people and places during threat situations (Mawson_a, 2005). The reason according to Mawson is that separation from attachment figures is a much greater stressor than the threat itself. This social attachment view, which extends to the domain of disasters the pioneering work on attachment by Bowlby and Ainsworth (Bowlby_a, 1982; Ainsworth, 1989), may provide the key to the deeper understanding of social and collective behaviours when responding to threats (e.g. seeking others, following leaders, herding, moving as a group, etc.). This may also explain risky behaviours, such as remaining with others in danger zones, or heading towards danger to be with loved ones.

The benefits of social and collective response to threat has been developed through evolution (Gavrilets, 2015). People are less anxious when in a group, therefore reducing the risk of panic (Moussaïd & Trauernicht, 2016). When part of a group, it less demanding cognitively, and less stressful when minding threat. This is so because at the very basic level of seeking safety, more pairs of eyes are able to scan and identify threat when dangers present themselves. The proper identification and assessment of hazards and the threats posed, with knowledge, can in theory, bring forth the appropriate response. Individuals also have different sensitivities or personalities, which can affect their situational awareness and assessment of risk (Slovic & Weber, 2002). The notion of being safe also is relative and may be different with respect to each person. Strategies employed by people therefore, when coping with life threatening situations, can be different from others. Also, adopted actions to implement survival strategies may be facilitated by individual capabilities, or hampered by physical and mental limitations (e.g. mobility impairments, disability, decreased sensory awareness). A mixture of individuals with different personality traits within groups can facilitate survival in disasters (Ein-Dor_b, 2014). When in

[1] Egoistic or egocentric, taken only from the perspective of the individual's self without taking cognisance of others

[2] Altruism, meaning disinterested and self-less concern for the well-being of others

social groups, individuals needing help can be provided aid by others. Individuals can either act as sentinels, follow, lead, mimic or help others when escaping threat (Ein-Dor_b, 2014).

Evacuation is the strategy used to safeguard human lives during disasters. Paramount to ensuring general safety of populations is having people evacuate to safe areas as fast as possible. During evacuations complex social interactions may be influenced by different attachment styles triggering variations in individual behaviour (Ein-Dor_a, 2014; Ein-Dor T. , Mikulincer, Doron, & Shaver, 2010).

Given the inevitability of encounters with different disasters in the future (albeit with random and unpredictable occurrence), it is highly justified to study evacuations, to increase the number of survivors. Understanding the impact of social behaviours on evacuations is paramount, as social interaction is central during evacuations. This will require bottom-up microscopic modelling and simulation of individual humans as cognitive social agents and their social behaviours during crisis scenarios. Simulation can provide a way of visualising possible futures with the interplay of space and time processes from multiple factors simultaneously considered in evacuation scenarios (Bianchi & Squazzoni, 2015).

Agent-based modelling (ABM) has been used to study complex social interactions between heterogeneous agents via computer simulations (Bianchi & Squazzoni, 2015). The ABM of evacuation of large heterogeneous populations during disasters is a complex task. This requires the integration of social interactions into the model to replicate the complexity inherent in reality. The ABM approach can facilitate the understanding and highlight the importance of social contexts by looking at individual behaviours during disasters in a micro-oriented perspective (Bianchi & Squazzoni, 2015). Experts agree, that to achieve more realism in models, the physical, social and psychological aspects of human behaviour need to be implemented in models (Chu, Pan, & Law, 2011). However, human social behaviours are only recently being integrated into evacuation models (Zhou, et al., 2010). This is the outstanding challenge to improve evacuation models which lack social interactions.

ABM and social simulations of evacuations have been developed to study crisis events. The objectives of these models vary, and can include (1) forensic analysis of past events, (2) evaluation of building floor or city layouts for optimal evacuation design, (3) definition of evacuation strategies, and (4) visualisation for more effective risk awareness campaigns (Ronchi, Kuligowski, Reneke, Peacock, & Nilsson, 2013; Bulumulla, Padgham, Singh, & Chan, 2017). Most of the models are for fire, flood and large crowd events. There are very few models for earthquakes. Of the models for earthquakes, most model only the evacuation towards safe areas in distant locations and travelling by car. In these models the effect of exposure of people to building damage such as injuries or death are not considered. Also, blockage of pathways from debris damage are not considered. In particular models, for pedestrian level evacuations during the onset and few seconds just after earthquakes, are few. The scale of implementation of the models vary. Most of the simulations deal with egress from indoor locations such as from rooms, buildings, stadiums or other large venues. Micro-level pedestrian evacuation simulations of outdoor city scale environments are rare and less common.

Accuracy in modelling also demands the precise spatial and temporal representation of the object/entity crisis environment that defines the context of crisis environments. Modelling the physical environment, the phenomena, and hazards has received much focus in risk and disaster sciences and related domains. The concentrations has been on prediction, dynamics of phenomena, etc. and the has been the forte of most risk modelling. Data from these studies are represented in their correct locations and dimensions as geospatial data. Developments in ABM platforms, such as GAMA, make it possible to integrate geospatial data with dynamic models (Drogoul, et al., 2013). In the GAMA simulation platform everything is an agent. Geospatial objects are easily integrated into models. For evacuations, faithful representation of buildings, open spaces, pathways, and safe areas, in their correct locations, dimensions, and distances locations makes for realistic estimates of evacuation times.

The particular focus of this work is the modelling and simulation of social evacuation behaviours of heterogeneous human populations during earthquake disasters using ABM. Surviving strong earthquakes requires evacuating structures and seeking safety by heading towards safe areas. Regardless of the absence or presence of damage, vulnerable buildings must be emptied immediately to ensure safety of occupants, especially from damage from possible after-shocks[3].

Earthquakes are natural phenomena that are sudden, occur without warning, random, and currently remain unpredictable (Geller, 1997). Earthquakes are caused by a sudden slip on a fault to release the build-up of tectonic stresses (USGS_b, 2019). The measure of energy released by the earthquake at the source (or hypocentre of focus[4]) is called *magnitude*. It is based on measurement of the maximum motion recoded by a seismograph (USGS_c, 2019). The larger the magnitude, the higher the energy released, the greater the potential for damage (IRIS_b, 2019). The frequency of worldwide earthquake occurrence (per year) is shown in Figure 1. According to IRIS[5] (2019), earthquakes are always happening somewhere on the planet. From IRIS, globally: (a) magnitude 2 earthquakes are generally not felt, but occur several hundred times a day; (b) major earthquakes (greater than magnitude 7), happen more than once per month; and (c) great earthquakes (greater than magnitude 8), occur once a year (IRIS_b, 2019).

Some areas such as those in active tectonic regions such as the Pacific Ring of Fire, account for 80% of the occurrence of very strong earthquakes, and 90% or all earthquakes. Areas with active faults zones are also very prone to earthquakes. Earthquakes can also re-occur in the same general area. Earthquakes can occur in swarms for a long period, especially after a very strong earthquake. Return periods describe the repeat occurrence of earthquakes. For some areas a damaging earthquake can happen every 50 years, 100 years, or 400 years, etc. Comparing this to the span of average human lifetimes, one can consider experiencing a highly destructive earthquake to be very rare. Establishing return periods of earthquakes is also challenging, as geologic record of earthquakes do not go back very far into the past. Also, new active faults are also being discovered. Some are revealed usually after an unexpected earthquake. Increased coverage from new seismic sensors deployments in the field make possible the discovery of new active regions.

[3] Succeeding quakes may be stronger or weaker. In both cases possible damage can result from weakened structures.

[4] The hypocentre or focus is a point on the fault plane where the rupture starts. The depth is taken at the hypocentre. The epicenter is the location on the earth's surface vertically above the hypocentre (Seismology Research Centre, 2019)

[5] IRIS (Integrated Research Institutions for Seismology)

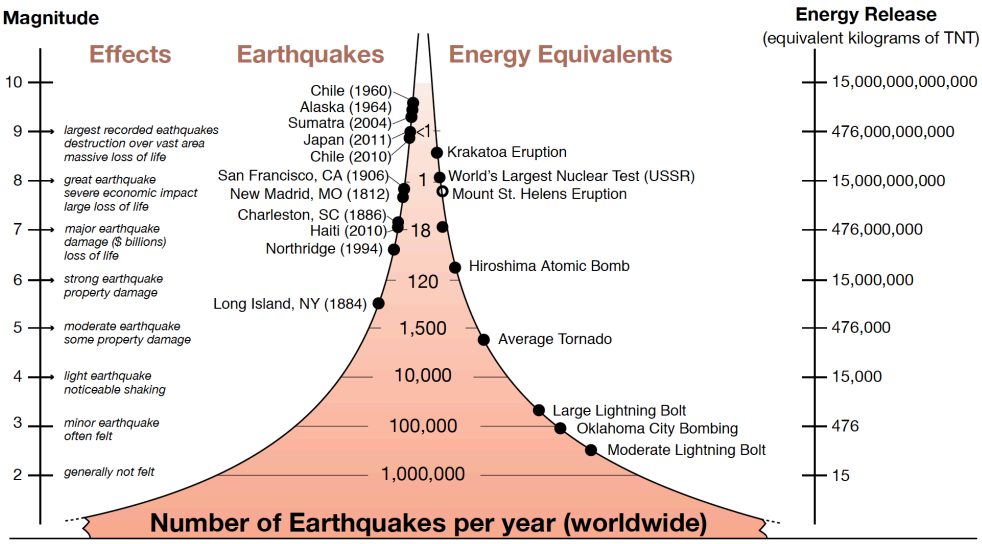

Figure 1. Worldwide frequency of earthquakes (IRIS_b, 2019)

The measure used to describe the effect of earthquakes on humans, structures (buildings) and other objects on the surface is called *intensity* (USGS_a, 2019). The higher the intensity value, the greater the effect of the shaking. The effect of the earthquake decreases as the distance from the source increases. The effects of intensity on people and objects are described in Table 1. A more detailed review of the effects on structures is presented in Chapter 2.

Table 1. Intensity and effects on People and Objects, EMS-98 (Grünthal, European Macroseismic Scale 1998, 1998)

Intensity	Description	Observed effects on people	Observed effect on objects
I	Not felt	Not felt, even under the most favourable circumstance.	No effect.
II	Scarcely felt	Tremor is felt only at isolated instances (>1%).	No effect.
III	Weak	Felt indoors by a few; people at rest feel a swaying or light trembling.	Hanging objects swing slightly.
IV	Largely observed	Felt indoors by many; felt outdoors by a few; few are awakened; level of vibration is not frightening; vibration is moderate; observers feel a slight trembling or swaying of the building, room or bed, chair, etc.	China, glasses, windows, and doors rattle; hanging objects swing; light furniture shakes visibly in a few cases; woodwork creaks in a few cases.
V	Strong	Felt indoors by most, outdoors by few; a few people are frightened and run outdoors; many sleeping people are awakened; observers feel a strong shaking or rocking of the whole building, room or furniture.	Hanging objects swing considerably; china and glasses clatter together; small top-heavy and/or precariously supported objects may be lifted or fall down; doors and windows swing open or shut; in a few cases window panes break; liquids oscillate and may spill from well-filled containers; animals indoors may become uneasy.
VI	Slightly damaging	Felt by most indoors and by many outdoors; few persons lose their balance; many people are frightened and run outdoors.	Small objects of ordinary stability may fall and furniture may be shifted; in a few instances glasses and dishware may break; farm animals (even outdoors) may be frightened.
VII	Damaging	Most people are frightened and try to run outdoors; many find it difficult to stand, especially on upper floors.	Furniture is shifted and top-heavy furniture may be overturned; objects fall from shelves in large numbers; water splashes from containers, tanks and pools.
VIII	Heavily Damaging	Many find it difficult to stand, even outdoors.	Furniture may be overturned; objects like TV sets, typewriters, etc., fall to the ground; tombstones may occasionally be displaced,

			twisted or overturned; waves may be seen on soft ground.
IX	Destructive	General panic; people may be forcibly thrown to the ground.	Many monuments and columns fall or are twisted; waves are seen on soft ground.
X	Very Destructive		
XI	Devastating		
XII	Completely devastating		

Few: 0 – 20%; Many: 10 – 60 %; Most: 50 – 100 %

The possible range of intensities near the epicentres of earthquakes produced with respect to magnitudes are shown in Table 2. The effects of earthquakes can be felt over large geographical regions. Increasing distance from the source however decreases the effect. Other factors that can result in the variation of effects and can be due to different physical factors such as elevation, soil type, typology of building (i.e. construction, materials, design, number of floors), etc.

Earthquakes with high magnitude, long duration and shallow depth, become destructive when they occur very close to highly populated areas. High intensities can result in many deaths, injuries and property damage. Poorly built structures (i.e. those that do not comply with local building codes) are more prone to collapse during strong earthquakes. The longer the duration of building shaking, the greater the damage (IRIS_a, 2019). Building codes define regulations for design, construction, alteration and maintenance of structures (FEMA, 2019). According to FEMA, these codes specify the minimum requirements to ensure the health, safety and welfare of building occupants. Eurocode 8 is used in Europe for the design of structures for earthquake resistance (JRC-EC, 2018). The purpose of Eurocode 8 is that, in the event of earthquakes, (a) human lives are protected, (b) damage is limited, and (c) structures important for civil protection remain operational. Building codes are regularly updated to (a) address shortcomings of the current code (e.g. insufficient design for minimum intensity parameter); (b) include improvements in technology (e.g. better construction practices, retrofits), (c) address newly discovered threats (e.g. occurrence of higher intensity quake in the area; discovery of new faults; possibility of future higher magnitude/intensity earthquakes) (Vaughan & Turner, 2013; FEMA, 2019).

Table 2 Magnitude and intensity comparison near epicentre (USGS_a, 2019)

Magnitude	Typical Maximum Modified Mercalli Intensity
1.0 – 3.0	I
3.0 – 3.9	II – III
4.0 – 4.9	IV – V
5.0 – 5.9	VI – VII
6.0 – 6.9	VII - IX
7.0 and higher	VIII or higher

Large loss of life during earthquakes has been reported in countries where enforcement of building and seismic codes is poor, such as Haiti, Pakistan, China and Nepal. (Nienhuys, 2015). Table 3 presents notable earthquake events in these countries with the number of deaths, damaged buildings and evidence of the application of seismic codes. Chile is an example of a country which has benefitted from the strict implementation of building codes (Franklin, 2015). Chile's buildings are required to withstand 9.0 magnitude earthquakes. With earthquake resistant structures, Chile withstood a very strong 8.4 magnitude earthquake in September 2015 with few casualties and very minimal number of damaged buildings. It can be seen from Table 1 that even with higher magnitude earthquakes, Chile's building damage and loss of life is very much lower than the aforementioned countries.

Table 3 Comparison of casualties and building damage with respect to building codes (Nienhuys, 2015)

Year	Country	M_w[6]	Max PGA g	Deaths	Damaged Buildings	Deaths per 1000 collapsed buildings	Date Code Published	Evidence of seismic code applied
2005	Pakistan, Kashmir	7.6	0.23	88,000	?400,000	?220.0	1986	No
2008	China, Sichuan	7.9	0.23	87,150	?1,000,000	?87.0	1959	No
2010	Chile	8.8	0.65	525	81,000	6.5	1972	Yes
2010	Haiti, Léogâne	7.0	0.44	222,570	105,000	2,120.0	Not available	-
2015	Nepal	7.8	≈0.25	8,790	605,253	14.5	1994	No
2015	Chile, Illapel	8.3	0.25	15	270	-	1972	Yes

? Data is not adequately verifiable especially for Low Income Countries (LIC); - not sure; ≈ approximately

Compared to other natural calamities, deadly earthquake disasters occur with rarity. However, the number of casualties from earthquake disasters from 1996 to 2015, at 55.6% (Figure 2), has been the largest compared to other disasters (CRED, 2016). The majority of deaths during earthquakes are from damaged structures (Kenny, 2009). In particular 75% are caused by building collapse (Coburn, Spence, & Pomonis, 1992).

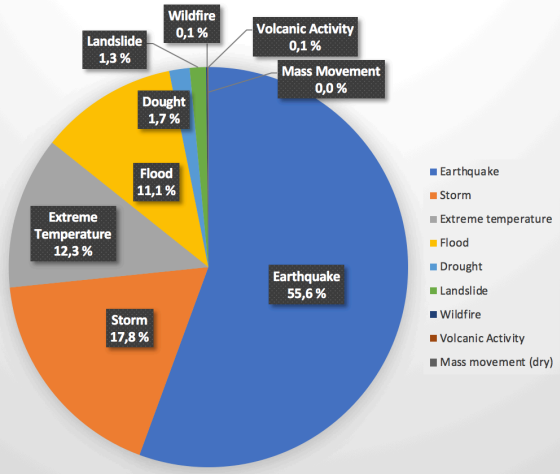

Figure 2 Percentage of deaths per disaster type, 1996 – 2015 (CRED, 2016)

Earthquake prediction is currently an impossible task (Geller, 1997). However, recurrence interval (return periods) of earthquakes can be established from statistical analysis of past earthquake data. Recurrence intervals are useful for risk mitigation efforts. Earthquake "Big One" scenarios have been developed for many major cities that are earthquake prone. These scenarios are used to prepare populations for projected future damaging earthquakes. Experts agree that these strong earthquakes will happen, however the time of occurrence is not known. The "Big One" earthquake scenarios for major cities most prone to earthquakes are shown in Table 4. "Big One" scenarios are used to prepare populations for large earthquakes by way of earthquake drills. Citizens are taught proper evacuation behaviours and directed to nearest safe areas. Authorities test institutional readiness in implementing community evacuation plans and in deploying personnel and resources for rescue work and managing cascade effects like fires.

[6] M_w, Moment magnitude

Table 4 World's most earthquake prone cities (Smith J. P., 2019)

City	Population	Last Major Strong Quake	Big One Magnitude	Return Period	Deaths	Injuries
Tokyo, Japan **(Tokyo Metro. Govt., 2019; Hurst, 2019)**	37 M	1923 (M_w 7.9)	M 7.3	100 years (Due)	9,700	150,000
Jakarta, Indonesia	17.7 M		M 8.7			
Manila, Philippines **(Sabillo, 2015; JICA, 2004)**	12 M	1658 (M_s 7.5)	M 7.2	400 - 500 years (Overdue)	34,000	114,000
Los-Angeles, USA	10 M	1857	M 7.8	100 years (Overdue)	1,800	50,000
Osaka, Japan	19.2 M			100-150 years		

1.2 Significance of the problem

Disastrous earthquakes are sure to happen in the future. The only uncertainty is the time when these will occur. Strong earthquakes are anticipated where large stresses build up, especially in active fault zones where expected earthquakes have exceeded their known recurrence intervals (earthquakes are overdue)[7].

These future earthquakes pose dangers to large populations, especially in the large. The exposure of the general population to earthquake is most significant compared to other hazards (Pesaresi, et al., 2017). The most current estimate in 2015 of the number of people potentially exposed to earthquake is 2.72 billion or 37% of the global population (GEO-JRC, 2017). More than 170 million people in Europe are potentially exposed to earthquakes (Pesaresi, et al., 2017). The breakdown for exposure of populations different global regions is shown in Table 5. For cities, globally, 700 million people living in urban centres are exposed (EC-JRC, 2018). Top ten big cities (shown in Figure 3) exposed to earthquakes include, Jakarta (Indonesia), Tokyo (Japan), Dhaka (Bangladesh), Mumbai (India), Cairo (Egypt), Mexico City (Mexico), Beijing (China), Osaka (Japan), Istanbul (Turkey) and Karachi (Pakistan). The combined population of these the top 10 cities is 200 million people.

Table 5 2015 Population and Built-up surface potentially exposed to earthquake by region, 475 years Return Period (Pesaresi, et al., 2017)

Category	Africa	Asia	Europe	Latin America	North America	Oceania	N/A	Total
Exposed Population-Inhabitants (unit in Million)	233.3	1,912.2	173.5	304.4	73.9	20.0	0.4	2,717.8
Exposed built-up (unit in Km^2)	11,102	121,814	46,257	25,167	27,895	5,888	83	238,207

Demographic changes especially ageing societies point to challenges, especially to the mobility of individuals to successfully carry out speedy evacuations. Figure 4 shows the increasing trend in the number of 60 years and older exceeding the number or younger (>60) by 2050 for the world population, and around 2020 for OECD countries. Most of these populations will also be concentrated in cities. This means that evacuation plans must be studied and adopted for this future older population. The problem with current evacuation plans and simulations is that are based mostly on the mobility of healthy adults. Future plans must be developed to be more inclusive especially for those with mobility limitations.

[7] With time, stresses accumulate in active fault zones. The release of these stresses, result in large earthquakes.

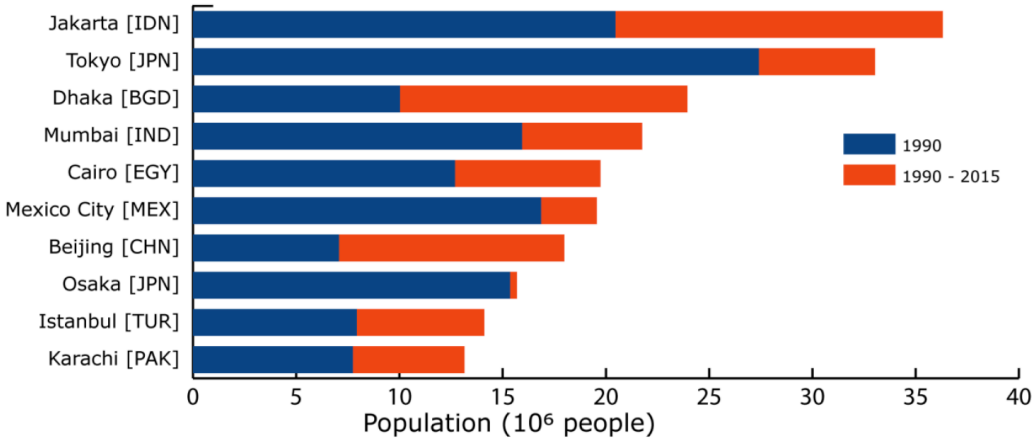

Figure 3 Top ten urban centres population exposed to seismic magnitude greater than class 5 in MMI scale. Data shown is for 2015, and showing the change since 1990 (EC-JRC, 2018)

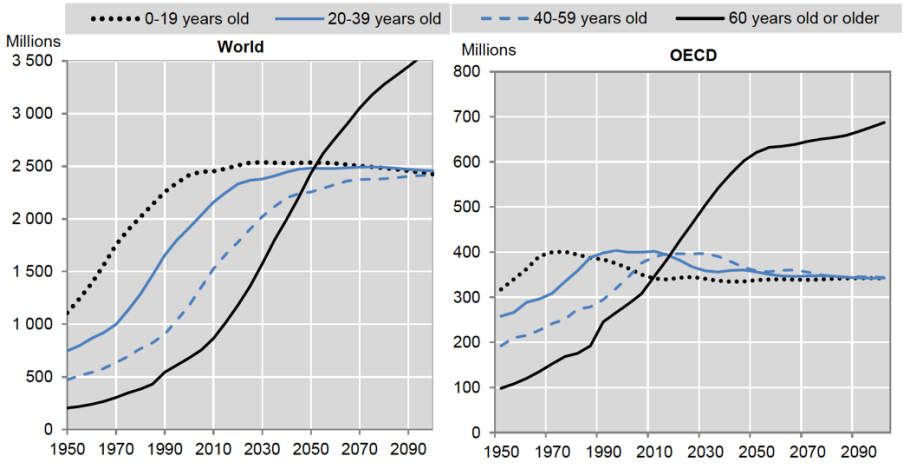

Figure 4 Population change by age-group, world and OECD countries, 1950 to 2090. OECD calculations are based on United Nations Department of Economic and Social Affairs, Population Division (2010), World Population Prospects: The 2010 Revision, United Nations (OECD, 2015)

1.3 Problem statement

The certainty of future earthquakes, especially in large populated areas, points to the need and urgency of developing solutions to minimise impacts of disasters. Ideally, universal compliance to building codes could help ensure that structures are earthquake resilient (UNCRD, 2008). According to UNCRD, this is currently not the case especially for poor and developing countries. Governments have obligations to implement building codes. However countries do not become completely building compliant overnight. Improvements and strict implementations of building codes may also be too slow, even for developed countries, and this may not be able to keep up with impending disasters. Enforcement will be challenging for old cities with historic city centres and heritage sites, as there will be structures that pre-date modern building codes. Compliance also will entail huge costs and requires a long time to achieve. In this context, impacts of disasters and can only be minimised but not totally eliminated (Lacasse, 2016). The ultimate test of compliance or non-compliance to building codes, or even the effectiveness of current building codes, unfortunately can be seen only after major earthquake events (Nienhuys, 2015).

Evacuations will always be necessary as people will need to seek safe areas to survive earthquake disasters. This is especially true when individuals think that they are vulnerable and perceive the risk of building damage or collapse. Solutions focusing on human behaviours can be less costly and maybe much faster to implement, compared to cost and speed of making structural improvements. The social

and behavioural approach can likewise be beneficial in developing awareness and proactive attitudes towards earthquake risk into local cultures and communities (Shapira, Aharonson-Daniel, & Bar-Dayan, 2018). A well ingrained culture on earthquake risk can be strategic to maintain vigilance both in the short term and for the future (Ibrion_b, Mokhtari, & Nadim, 2015; Ibrion_a & Paltrinieri, 2018; Ibrion_c, 2017). This is especially needed because of the possible long intervals between destructive earthquakes which can skip several human generations.

Social attachment theory is used in this research as the guiding framework for individual behaviour and social interactions during earthquake evacuations. Social attachment refers to the activation of affiliation or proximity seeking behaviours towards attachment figures during threat situations (Mawson, 2005). Attachment figures refer to individuals for whom a person shares a social bond such as family members and friends. Social bonds can likewise be formed with strangers when situations imposed by shared identity is present (such as a dangerous situation or common activity) (Tajfel & Turner, 1986; Drury, Cocking, & Reicher, 2009). Social attachment is extended in this work to include attachment to objects (e.g. phone, wallet, computer), places (e.g. home, familiar routes, safe areas), tasks (e.g. routine, work), and pets.

1.3.1 Need for a realistic behavioural model

Realistic ABM and microscopic pedestrian social evacuation simulations are needed to study the impact of human behaviour in different earthquake crisis scenarios. The complexity of the problem of modelling social interactions during evacuations in the context of an earthquake disaster is immense and may be solved using ABM. Bottom-up and microscopic scale modelling of pedestrian social behaviours with interactions with objects in correct geographic space has the potential to create possible evacuation scenarios of crisis environments.

Realistic models of earthquake crisis evacuations can be beneficial in identifying the critical factors that would make evacuations successful, resulting to more saved lives. Social interactions during the expected crisis will be inevitable especially in cities with high concentrations of people. The impact of behaviours needs to be tested to define advice on proper behaviours. Resilience to earthquakes of current and planned infrastructures needs to be tested using simulations to ensure that: (a) evacuation plans are updated and assure inclusivity; (b) more safe areas are identified or designed; (c) bottlenecks that limit the mobility and the flow of people are eliminated.

Agent based models may prove to be good tools to deliver formalisations of social behaviours during earthquakes. These formalisations have the potential to encapsulate and transmit to future generation the knowledge on earthquakes evacuations and their impact. Long recurrence intervals between earthquakes result in the threat of earthquakes being forgotten leading to lowering of risk perceptions. The current stock of vulnerability data (people and structures) from different domains is rich and can be integrated into social geospatial ABMs to develop realistic dynamic models and simulations. Developing a social and geographic ABM for earthquake evacuation will help addressing the lack of realistic geographically referenced social simulations for crisis scenarios.

1.3.2 Need for a multi-disciplinary approach

The complexity inherent in crisis situations provides huge challenges for modellers and requires inputs from different domains; therefore a multi-disciplinary approach in necessary. Replicating this complexity requires the integration of the social and physical elements of seismic risk with spatial and temporal dynamics in developing a basic multi agent model. The domains relevant to this work are geographic information science, geoscience, social science and computer science. The intersection of these domain would lead to the objective of this. The tight coupling of insights, methods, techniques and data from the domains are necessary in building the realistic pedestrian evacuation models.

Figure 5 shows the four core areas with the dominant themes and example keywords. The diagram in the figure can be viewed in several ways. From each quadrant, one can see the domain, the dominant theme, and key topics or keywords respectively. In a clockwise direction, the upper left quadrant is on social science and deals with human aspects such as behaviour and human factors. The upper right quadrant is for computer science, with the focus on artificial intelligence in particular agent-based modelling. The lower right quadrant shows geographic information science, which concentrates on accurate geospatial representations of data. The lower left quadrant is for geoscience, which deals with environment or context of the crisis such as the hazards and vulnerable structures.

Pairings of the domains also have some significance. The left half of the figure, composed of social science and geoscience, describes the context of the seismic crisis. The right half of the figure, composed of computer science and geographic information science, defines methods, tools and implementation tasks to build and implement the computer model. The upper half pairs of social science and computer science deal with salient and dynamic aspects of social behaviours. The lower half pairs geoscience and geoinformation science defines the static, physical and spatial aspects of risk and other components of the model.

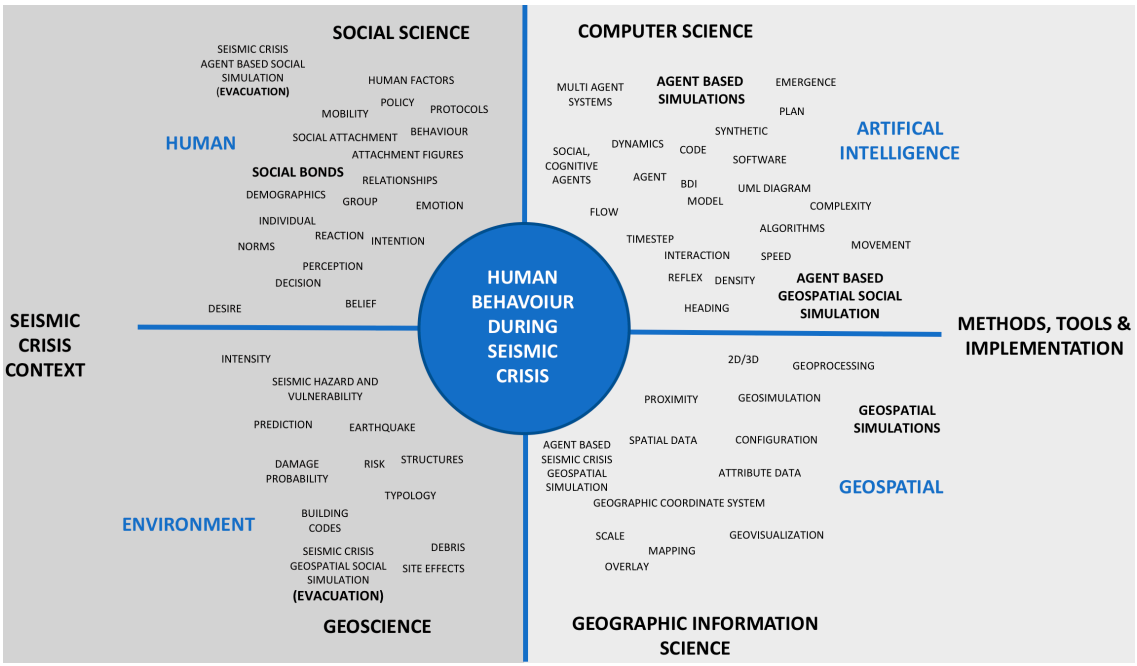

Figure 5 Relevant domains for modelling human behaviour in a seismic crisis context

Basic parameters of time, distance and speed are crucial parameters for evacuations. These parameters are important to accurately quantify arrival times in safe areas. In particular, these refer to individual speeds, distances, and amount of time needed to reach safe zones. To realistically simulate movement and behaviours in their correct spatial contexts, the crisis environment needs to be constructed with correct spatial configurations. This can be done using real geographic data. Geographic information science provides the tools and techniques to develop the spatial model of the crisis environment. Related attribute information can likewise be linked to location and integrated to the spatial model.

The characterisation of the effects of shaking on structures and people is explained by the geosciences. Different earthquake intensities, define unique damage scenarios to vulnerable structures. Distribution of debris damage can be generated around different building typologies. Delays in evacuations are also caused by debris blocking pathways or trapping individuals. Debris can also cause injuries or death. Exposure to damage, injuries and death can impact behaviours and social interactions.

Observed behaviours during evacuations can be explained by theories from the social sciences, that provide the strong foundation needed for developing the models. In the definition of heterogeneous populations, the level of detail needs to be representative of the real population being modelled. For the population of human agents, it needs to be reflective of existing demographics. Basic attributes should at least include age and disability. These basic profiles can be used to define the structure of the population. Social roles, membership in groups, social and economic activities, daily mobility, and possible behaviours can be generated from the demographic data.

Computer science through agent-based modelling and simulation can integrate the inputs from the aforementioned domains to design and implement a model and run multiple simulations. Algorithms can be used to define how agents move around space, interact socially, and respond to the physical elements of the synthetic crisis environment. Data processing and visualisation techniques are useful for the analysis of results and the generation of conclusions.

1.3.3 Need for models that are easily understood by stakeholders

This body of work falls into the general category of disasters, risk and public safety research. Therefore, the primary stakeholders of this study are the general public, authorities and interested experts from different domains dealing with pedestrian earthquake evacuations. Results are expected to help enhance people's current perception of seismic risk. The hope is to inspire concrete actions to mitigate this risk. Examples of concrete actions are (a) the development of optimum evacuation strategies that are inclusive of all mobility types, (b) the modification of space to facilitate fast evacuations, and (c) addressing seismic structural vulnerabilities. For the model to be useful and have impact, it has to be easily understood.

The multi-disciplinary nature of the problem requires that elements or components used in developing the model are readily understandable by experts and the general public. These components include data, theories, techniques, algorithms and software code. Simulation results should also be communicated in a form that is easy to understand. The output should likewise be very visual and can be in easy formats such as graphs, maps, videos, and dynamic real time displays. The model interface should also be easy to use where tools to modify parameter setting are accessible. This will allow users to define their own scenarios to test and run in simulations. Advanced users of the model can modify the data (attributes and spatial data) to update the model. The model can also be configured to expand coverage or completely change the study area.

1.4 Research questions and hypotheses

The objective of evacuations is to save human lives during disasters. The measure of success for evacuation used in the research is the number of arrivals in safe areas. Evacuations are social in nature and therefore, the interactions between individuals as they interact with the crisis environment can have effects on their evacuation. To establish the significance of several parameters on evacuation, eight research questions were developed focused on the determining the impact success of evacuations. The research questions and accompanying hypothesis are presented as follows:

- Question 1 (Q1): Does social attachment affect the number of arrivals in safe areas

  Hypothesis: **Yes, social attachment can affect the number of arrivals.** Social attachment triggers affiliation or proximity seeking behaviours that result in emergent social interactions. Social attachment is expressed in pre-evacuation behaviours and social interactions during evacuations. These behaviours and interactions can take away or shave off precious seconds from actually heading towards safe areas. With all these emergent social interactions accounted for, over-all, social attachment can delay evacuations leading to lesser number of arrivals in safe areas.

- Question 2 (Q2): Does the knowledge of nearby safe areas affect the number of arrivals in safe areas?

  Hypothesis: **Yes, knowledge of the location of nearby safe areas increases the number of arrivals in safe areas.** Knowing where to go defines precise navigation goals or targets. This can help speed up the evacuation of individuals. A result of this is the greater number of arrivals in safe areas compared to the case when knowledge is not available.

- Question 3 (Q3): How does the number of close bonds affect evacuation?

  Hypothesis: **A larger number of closely bonded individuals during evacuation can delay evacuations.** The number and type of social interactions during evacuations can slow down individuals. The presence of many closely bonded individuals in an area can result in individuals moving towards and staying with the groups rather than proceeding to safe areas. This can result in lesser number of arrivals in safe areas.

- Question 4 (Q4): How does the time of day affect evacuation?

  Hypothesis: **Daytime evacuations allow for a greater number of agents to arrive in safe areas. Night time evacuations will result in lesser arrivals in safe areas.** This is due to the difference in perception distances. Perception distances allow individuals to see in the forward or gaze directions. Perception distances are much longer during daytime than night time. Longer perception distances allow individuals to see other people, objects and safe places, which are much further. The overall effect is more people arriving in safe areas.

- Question 5 (Q5): How does disability affect the number of arrivals in safe areas?

  Hypothesis: **Presence of disabled individuals in the population will result in a lower number of arrivals in safe areas.** The disabled are relatively slower than able individuals during evacuations. Social interactions between persons with disability and able individuals can also effectively slow down evacuations.

- Question 6 (Q6): Does the presence of casualties on the route affect the number and time of arrivals in safe areas?

  Hypothesis: **Presence of casualties in the route can trigger evacuations and result in more arrivals in safe areas.** Presence of casualties (i.e. injured and dead) in the routes can modify behaviour and trigger evacuation. The presence of deaths and injuries provide the cue or confirmation of a dangerous or life-threatening situation. This cue forces individuals to immediately consider moving to safe zones.

- Question 7 (Q7): Does intensity affect the number of arrivals in safe areas?

  Hypothesis: **High intensities will result in a lesser number of arrivals in safe areas.** There is an inverse relationship between intensity and the number of arrivals in safe areas. High intensities create more damage, blocking routes towards safe areas. Being hit by debris can cause deaths and injuries.

- Question 8 (Q8): How does the radius of the danger zone around buildings affect the number of arrivals?

  Hypothesis: **Large radius of danger zones around buildings decreases the number of arrivals in safe areas.** Danger zones are areas around structures where the probability of individuals being trapped, hurt or killed by debris is high. A larger radius for danger zones conversely decreases the effective area allotted for safe zones. A larger danger zone radius

likewise increases the evacuation travel distance from buildings to safe zones. Blocked pathways within danger zones force individuals to take longer routes toward safe areas.

1.5 Contributions

The main contribution of this thesis is a social geographic microscopic pedestrian evacuation model of seismic crisis. The name of the model is **SOLACE** for SOciaL Attachment and Crisis Evacuations. SOLACE implements social attachment theory (Mawson_a, 2005) as the core framework that governs social interactions during disasters. The model is specific to the City of Grenoble, France and implemented at the scale of the census blocks comprising the city. This model uses spatial data (e.g. buildings, roads), behaviours, demographics, probabilities and macro-seismic assessments data. Human agents in this model are social, cognitive and spatially aware. They are capable of socially interacting with each other. The interactions are within the context provided by spatially distributed physical effects of earthquake shaking and damage. The crisis context (i.e. intensity scenarios) is guided by the work of Riedel, et al. which used a macro scale seismic risk assessment method to define structural vulnerability and damage (Riedel_a, et al., 2015).

The model is envisioned to be useful as a platform to test different scenarios where social attachment is relevant or not during evacuations. The model also accounts for human factors, demographic distribution, mobility of populations during different times of day/week, social interactions, cultural predispositions or norms of behaviours, configurations of the built environment, presence or absence of evacuation plans and seismic vulnerability of structures. With the model's use of geospatial information, which is commonly used by urban planners, SOLACE has the potential to aid in the development policies related to public safety.

SOLACE may be used to model evacuations in different places. Data layers appropriate to new study areas however would need to be acquired. For France, since data exist and are available, minor modifications can easily be done. SOLACE also has possibility to be applied outside of France, provided that the data is available. Use of the model may help the exploration of different scenarios to prepare for future disasters.

The thesis also contributes to the long-standing problem in geographic information science, which is integrating static spatial geometry and data with dynamic social processes. GIS is traditionally static. Computer science through agent-based modelling makes this integration of static and dynamic spatiotemporal processes possible. Several insights from this integration are presented at the conclusion of this research.

1.6 Structure of the thesis

The succeeding chapters of the thesis are organized as follows: Chapter 2 presents a concise review of the literature on seismic risk and the crisis context. Chapter 3 presents a state of the art on pedestrian evacuation models. Chapter 4 details the adopted methodology. Chapter 5 discussed SOLACE, the agent-based model for social attachment. Chapter 6 describes the implementation of the model. Chapter 7 describes the design of the experiments. Chapter 8 presents the results of the experiments. Chapter 9 discusses the results of the study, future work and closes with a conclusion.

CHAPTER 2. SEISMIC RISK & CRISIS CONTEXT

This chapter elaborates on risk and crisis during earthquake disasters. The objective is to provide the proper context, rationale, and firm foundation for the development of the agent-based model for earthquake evacuations. The chapter is divided into four parts. The first section presents a global context of the work within the concepts and terminologies related to risk. The second section is on the physical aspects of seismic risk from the viewpoint of geoscience. Discussions revolve around the concept of hazard and the impact on structures and people. The third section is on the social aspects of the crisis from the perspective of social science. This section focuses on the human and social response to earthquakes. A rich discussion on the relevant theories to explain these behaviours is also presented. This is consistent with this work's focus on human factors and behaviour of individuals and groups during disaster evacuations. The physical environment provides the setting where all these social interactions take place. The fourth part provides a small discussion and summary of the chapter.

2.1 Disaster, crisis, risk and related concepts

Within the focus of this study, the following definitions of crisis, disaster, risk, hazard, exposure, vulnerability and capacity are presented. The definitions are used and viewed in the context of an individual, social group and buildings effected by earthquakes.

Crisis can be defined as an unexpected and unwanted hazardous event that can lead to an unstable or dangerous situation that can severely interrupt and pose a serious threat to the fundamental values, norms, and normal functioning of exposed individuals, groups, communities or the whole society (Poal, 1990; Stern, 2003; Boin, 2005). The focus of this work is seismic crisis. The scenarios considered are developing crisis conditions triggered by an earthquake. The time frame considered for the scenarios is the first thirty minutes of the event (during and immediately after). This covers the moment of the start of shaking and the resulting evacuation. The effect of the crisis on people is the primary focus. In particular, individual behaviours and dynamic social interactions during earthquake evacuations.

A ***disaster*** is defined as a serious disruption of the functioning of a community at any scale due to hazardous events interacting with conditions of exposure, vulnerability and capacity. It leads to one or more of the following: human, material, economic and environmental losses and impacts (UNISDR_a, 2019). Disasters happen not only because of the causing natural events, but also due to the social, political and economic environments that influence how people live (Wisner, Blaikie, Cannon, & Davis, 2003).

Disaster risk refers to the potential of loss of life, injury, or destroyed or damage assets that can occur in a system, society, or a community during a specific period of time (UNISDR_a, 2019). The general model used to calculate risk is shown in Equation 1 (Alexander_a, 2012; UNISDR_a, 2019). This, according to UNISDR is determined probabilistically as a function of hazard, exposure and vulnerability. A second equation (Equation 2) includes capacity.

Equation 1 Risk Equation 1

$$Risk = Hazard \times Exposure \times Vulnerability$$

The other version of the risk equation that includes capacity as a parameter is shown in Equation 2.

Equation 2 Risk Equation 2

$$Risk = \frac{Hazard \times Exposure \times Vulnerability}{Capacity}$$

Hazard is defined as possible future occurrence of a natural process, phenomenon or human activity that may cause loss of life, injury or other health impacts, property damage, social and economic disruption or environmental degradation (UNISDR_a, 2019; Cardona, et al., 2012). Most of the previous studies on risk especially before the 1990s focused on the hazard aspect (Cardona, et al., 2012). In this work, earthquake is the natural hazard in focus. Increasing degree or intensity of earthquakes cause widespread damage in the affected area. Debris and damage structures from earthquake shaking are hazards that can injure or cause loss of life (Johnston, et al., 2014).

Exposure is defined as the situation of people, infrastructure, housing, production capacities, and other tangible human assets located in hazard-prone areas (UNISDR_a, 2019). From Equation 1, it can be seen that, when there is no exposure to a hazard, there is also no associated risk. For extreme disasters, exposure, is the more dominant parameter that defines the degree of disaster risk (UNISDR_b, 2019). Extreme disasters affect all, regardless of the degree of vulnerability. Exposure changes with time and location (Cardona, et al., 2012). The continued growth of cities concentrates populations and assets in very few places. When these cities are located in hazard prone areas, or when hit by natural hazards, exposure is very high (Brecht, Deichmann, & Wang, 2013). Earthquakes are felt over very large areas and can occur within the interval of a few seconds. Areas closer to the epicentre generally incur more damage. The resulting damage can be extensive over affected regions. Debris or collapsed structures expose large populations of individuals to danger. Building inventories are therefore important to determine the level of exposure of structures and facilities (Bevington, et al., 2012). Studies of historical earthquakes point to the distribution of vulnerable structures and their level of occupancy during earthquakes to be the main factors controlling the severity of human loss (Jaiswal_1 & Wald, 2008). As people spend more time indoors (almost up to 90% inside buildings) than outdoors, the exposure of populations to building related damage will be high (Klepeis, et al., 2001; WHO-Europe, 2013). The area nearest to vulnerable structures, defined from the building edge, defines the deposition zone for debris. Immediate exposure of individuals to debris in this deposition zone can pose dangers and can result in injuries or loss of life. Longer term effects can be displacement or coping with loss (ACAPS, 2013; Bengtsson_a, Lu, Thorson, Garfield, & Schreeb, 2011; Lu, Bengtsson, & Holme, 2012).

Vulnerability refers to the conditions determined by physical, social, economic and environmental factors or processes which increase the susceptibility of an individual, a community, assets or systems to the impacts of hazards (UNISDR_a, 2019). Vulnerability is inherent and unique in the case of individuals, social groups, objects, or situations. Many parameters however define vulnerability, making it difficult to be precisely assessed (Weichsekgartner, 2016). Furthermore, vulnerability changes depending on parameters used for scale, time and space (Cardona, et al., 2012). Also, the influencing variables and characteristics of vulnerability change over time. The focus on vulnerability has increased in more recent risk research, and is has now gained the same level of emphasis as the study of hazards (Cardona, et al., 2012). According to Cardona et. al., vulnerability strengthens the contribution of the human and social dimensions in the risk equation.

Capacity refers to the combination of all the strengths, attributes and resources available to manage and reduce disaster risk and strengthen resilience, like evacuation plans, preventive information, emergency services, etc. (UNISDR_a, 2019). Coping capacity is the usual term used in disaster literature. As can be deduced from Equation 2, when the capacity to cope with a disaster is high, the risk posed by a disaster becomes low. Capacity includes the social structure that can help individuals cope and deal with the effects of disasters.

2.2 Physical elements of seismic crisis

The physical elements of seismic risk are discussed in this section. In particular, the impact of earthquakes on buildings, people and environment objects. This provides the detailed description of the environmental cues that can possibly be perceived by individuals, at the moment of shaking. Then, a state of the art of the seismic vulnerability of buildings is presented.

2.2.1 Seismology and buildings

Here the semantic framework of seismic risk is covered.

Intensity can be defined as a classification of the strength of shaking in terms of its locally observed effects during an earthquake (Musson R. M., 2012). Intensity is descriptive rather than analytical, but capable of being used for analysis and interpretation (Grünthal, European Macroseismic Scale 1998, 1998). Also, intensity scales consist of a series of descriptions of the different degrees of earthquake shaking on people, objects, nature, and damage to various building typologies (Grünthal, European Macroseismic Scale 1998, 1998). Different countries use macroseismic intensity scales fitted to local conditions and experience. Examples are the European Macroseismic Scale of 1998 (EMS-98), Japan Meteorological Agency (JMA) Seismic Intensity Scale and the Modified Mercalli Intensity (MMI) Scale of the United States (Grünthal, European Macroseismic Scale 1998, 1998; JMA, 2018; USGS, 2018). The scale assignments however are not equivalent. Musson et al. devised a conversion from different scales to EMS-98 (Musson, Grünthal, & Stucchi, 2009). The awareness of differences in intensity scales is important especially when interpreting compiled observations and reports from different countries.

Variation in felt intensities have been observed from tall buildings. Stronger earthquake vibrations are felt in upper storeys than from lower storeys (Grünthal, European Macroseismic Scale 1998, 1998). Also, from Grünthal, the severity of the vibrations can also depend on the behaviour of buildings according to the frequency of the shaking, and variations in elevation. More symmetric and regular building designs are also able to withstand earthquake shaking.

Variation in intensities can also be influenced by soil amplification or topographical conditions. Sites with alluvial soil deposits, and basin type topographies normally report higher intensities. Examples of these areas include Mexico City, and Grenoble, France (Dunand & Guéguen, 2012).

Table 6 Differentiation of structures into vulnerability classes, EMS-98 (Grünthal, European Macroseismic Scale 1998, 1998)

Type of Structure		Vulnerability Class					
		A	**B**	**C**	**D**	**E**	**F**
MASONRY	Rubble stone, fieldstone	○					
	Adobe (earth brick)	○——					
	Simple stone	⊢- - -○					
	Massive stone		⊢——○- - -				
	Unreinforced, with manufactured stone units	⊢- - -○- - -					
	Unreinforced, with RC floors		⊢——○- - -				
	Reinforced or confined			⊢- - -○——			
REINFORCED CONCRETE (RC)	Frame without earthquake-resistant design (ERD)	⊢- - - ——	○- - -				
	Frame with moderate level of ERD		⊢- - - ——	○	——		
	Frame with high level of ERD			⊢- - - ——	○	——	
	Walls without ERD		⊢- - - ——	○	——		
	Walls with moderate level of ERD			⊢- - - ——	○	——	
	Walls with high level of ERD				⊢- - - ——	○	——
STEEL	Steel structures			⊢- - - ——		○	——
WOOD	Timber structures		⊢- - - ——		○	——	

Legend: ○ most likely vulnerability class; —— probable range;
- - - - Range of less probable, exceptional cases

Vulnerability is used in EMS-98 to express differences in the way buildings respond to earthquake shaking. Buildings are classified into different typologies. The typologies include masonry, reinforced concrete, steel and wood. These are further grouped to vulnerability classes, A to F. Typologies and

vulnerability assignments are shown in Table 6. Damage, with respect to typology is classified from Grades 1 to 5, in the order of increasing damage. For each intensity, EMS-98 provides the damage grade with respect to the vulnerability class. Deformation of buildings under earthquake loading depends on building type. Damage grades specific for masonry and reinforced concrete structures are detailed in Table 7.

The impact of shaking on buildings at different intensities is detailed in Table 8. It details the EMS-98 intensity scale (Grünthal, European Macroseismic Scale 1998, 1998). The tables include the intensity category, general description, and the effect on buildings. Quantities are described by overlapping probability ranges namely: Few, 0 to 20%; Many, 10 to 60%; and Most, 50 to 100%. From the table it can be seen that no buildings are damaged at earthquake intensities less than V. Starting from intensity V, with increasing intensities, more damage is observed from the different building typologies. The quality and level of detail of building typologies and the description of degrees of damage in EMS-98 makes it a very useful tool for investigating vulnerability, seismic hazard and seismic risk (Musson R. M., 2012; Giovinazzi & Lagomarsino, 2004)

Table 7 Damage grades for masonry and reinforced concrete structures, EMS-98 (Grünthal, European Macroseismic Scale 1998, 1998)

Grade	Description	Masonry	Reinforced Concrete
1	Negligible to slight damage (no structural damage, slight non-structural damage)	Hair-line cracks in very few walls; fall of small pieces of plaster only; fall of loose stones from upper parts of buildings in very few cases.	Fine cracks in plaster over frame members or in wall base; fine cracks in partitions and infills.
2	Moderate damage (slight structural damage, moderate non-structural damage)	Cracks in many walls; fall of fairly large pieces of plaster; partial collapse of chimneys.	Cracks in columns and beams of frames and in structural walls; cracks in partition and infill walls; fall of brittle cladding and plaster; fall of mortar from the joints of wall panels.
3	Substantial to heavy damage (moderate structural damage, heavy non-structural damage	Large and extensive cracks on most walls; Roof tiles detach; Chimneys fracture at the roof line; Failure of individual non-structural elements (partitions, gable walls)	Cracks in columns and beam column joints of coupled walls; spalling of concrete cover; buckling of reinforced rods; large cracks in partition and infill walls; failure of individual infill panels.
4	Very heavy damage (heavy structural damage, very heavy non-structural damage)	Serious failure of walls; partial structural failure of roofs and floors.	Large cracks in structural elements with compression failure of concrete and fracture rebars; bond failure of beam reinforced bars; tilting of columns; Collapse of a few columns or of a single upper floor
5	Destruction (very heavy structural damage)	Total or near collapse	Collapse of ground floor or parts (e.g. wings) of buildings.

Table 8 Classification of damage, EMS-98 (Grünthal, European Macroseismic Scale 1998, 1998)

Intensity	Description	Effect on buildings
I	Not felt	No damage.
II	Scarcely felt	No damage.
III	Weak	No damage.
IV	Largely observed	No damage.
V	Strong	Damage of grade 1 to a few buildings or vulnerability class A and B.
VI	Slightly damaging	Damage of grade 1 is sustained by many buildings of vulnerability class A and B; a few of class A and B suffer damages of grade 2; a few of class C suffer damage of grade 1
VII	Damaging	Many buildings of vulnerability class A suffer damage of grade 3, a few of grade 4; many buildings of vulnerability class B suffer damage of grade 2, a few of grade 3; a few buildings of vulnerability class C sustain damage of grade 2; a few buildings of vulnerability class D sustain damage of grade 1.
VIII	Heavily damaging	Many buildings of vulnerability class A suffer damage of grade 4, a few of grade 5; many buildings of vulnerability class B suffer damage of grade 3, a few of grade 4; many buildings of vulnerability class C suffer damage of grade 2, a few of grade 3; a few buildings of vulnerability class D sustain damage of grade 2.
IX	Destructive	Many buildings of vulnerability class A sustain damage of grade 5; many buildings of vulnerability class B suffer damage of grade 4, a few of grade 5; many buildings of vulnerability class C suffer damage of damage of grade 3, a few of grade 4; many

		buildings of vulnerability class D suffer damage of grade 2, a few of grade 3; a few buildings of vulnerability class E sustain damage of grade 2.
X	Very Destructive	Most buildings of vulnerability class A sustain damage of grade 5; many buildings of class B sustain damage of grade 5; many buildings of vulnerability class C suffer damage of grade 4, a few of grade 5; many buildings of vulnerability class D suffer damage of grade 3, a few of grade 4; many buildings of vulnerability class E suffer damage of grade 2, a few of grade 3; a few buildings of vulnerability class F sustain damage of grade 2.
XI	Devastating	Most buildings of vulnerability class B sustain damage of grade 5; most buildings of vulnerability class C suffer damage of grade 4, many of grade 5; many buildings of vulnerability class D suffer damage of grade 4, a few of grade 5; many buildings of vulnerability class E suffer damage of grade 3, a few of grade 4; many buildings of class F suffer damage of grade 2, a few of grade 3.
XII	Completely Devastating	All buildings for class A, B and practically all of vulnerability class C are destroyed; Most buildings of vulnerability class D, E and F are destroyed; the earthquake effects have reached maximum conceivable effects.

Few: 0 – 20%, Many: 10 – 60%, Most: 50 – 100%

2.2.2 State of the art in seismic vulnerability assessment of buildings at urban scale

The large exposure of people and buildings in urban areas to earthquake makes seismic risk assessments necessary and urgent. To establish an appraisal of the risk, conducting very detailed risk assessment of buildings is ideal. Estimating the vulnerability of buildings at the urban and regional scales however, requires a large number of samples (Giovinazzi & Lagomarsino, 2004). This is expensive, time consuming and complicated (Riedel_a, et al., 2015; Giovinazzi & Lagomarsino, 2004). Many studies on vulnerability to seismic risk of large urban areas similarly faced this difficulty in a lack of data (Senouci, Bard, Farsi, & Beck, 2013; Guettiche, Guéguen, & Mimoune, 2017). In particular, detailed and extensive building stock inventories with the necessary structural and constructional parameters, are lacking. To overcome this limitation of data, macro scale seismic analysis methods have been proposed by several authors (Giovinazzi & Lagomarsino, 2004; Riedel_a, et al., 2015). Macro scale methods when adapted as a strategy result in reduced cost of building surveys at the urban scale (Guettiche, Guéguen, & Mimoune, 2017). Because of the low cost and relative simplicity compared to other methods, macro-seismic scale method may have greater possibility of being implemented especially for developing countries and cities with moderate risk.

The macro scale methodology of Giovinazzi and Lagomarsino developed vulnerability curves for buildings consistent with the EMS98 macroseismic scale, building typologies, vulnerability classes and damage scale (Giovinazzi & Lagomarsino, 2004). Their vulnerability calculations likewise include the effect of soil amplification. Classical probability theory and fuzzy set theory to develop the method. Their method was proposed to be used for vulnerability and damage scenario assessment of European towns under the RiskUE project.

Riedel et al., 2015 developed a macro scale methodology for seismic vulnerability assessment of urban environments using readily available data. Their method used association rule learning and support vector machines (Riedel_a, et al., 2015). They proposed two vulnerability proxies that create a relationship between building characteristics present in the French national census database, and the most probable EMS98 vulnerability class. The authors claim that the method can be applied anywhere provided basic information on buildings are available. The information on the buildings included date of construction, number of floors ranked by category, roof shape, construction material, qualitative description of plan and elevation and position in the block. The data used to develop the proxies was from Grenoble, France. It was tested for Nice using the more sophisticated RiskUE method and produced similar results.

A novel urban scale risk assessment method was developed by Salameh et al., 2017. They investigated the relationship between site and building frequencies using ambient vibration measurements (Salameh,

et al., 2017). Sets of numerical simulations were analysed using neural networks that yielded easy-to-use mathematical relationships. Interpolated maps for damage increments to buildings in test sites in Beirut, Lebanon were calculated using a neural network approach. From an older study, and still using ambient vibration measurements, Salameh, et al., 2016, found that only the height of a building has a significant influence in the determination of the fundamental period for a structure (Salameh, et al., 2016). They also concluded that the fundamental period depends on the soil type the building is constructed on.

Scenarios of the debris created in outdoor urban environments from the damaged buildings have been studied in more recent earthquake events (Rojo, Beck, & Lutoff, 2017; Santarelli, Bernardini, & Quagliarini, 2018). Deposition of debris along streets relate to building vulnerability, earthquake severity and width of the street with respect to building height and width (Santarelli, Bernardini, & Quagliarini, 2018). The debris from building damage that fall into pathways highly expose individuals to risk and influence pedestrian evacuation mobility. Debris can (1) completely block pathways, (2) act as obstacles, (3) trap or entomb individuals, or (4) cause injuries and deaths (Ramirez & Peek-Asa, 2005).

2.3 Human and social aspects of seismic risk

2.3.1 Earthquakes and people

A person's perception of shaking during earthquakes can depend on several factors. It can include (a) intensity of the shaking, (b) response of the structure, (c) presence of visual and auditory cues from surroundings, and (d) individual sensitivity to the event.

Human behaviours and psychological conditions are strongly correlated to seismic intensities (Ohta & Omote, 1977; Kuwata & Tanaka, 2002). People's responses range from bad to worse with increasing intensity (Ohta & Omote, 1977). The EMS-98 intensity scale (Table 1) is used to describe the effects and response of individuals' and environment objects to earthquakes (Grünthal, European Macroseismic Scale 1998, 1998). The scale provides a very general description of individual sensitivities, responses, and encountered difficulties, due to shaking. In the scale, evacuation is described as egress from indoor locations as running outdoors. The succeeding section provides a richer discussion on crisis evacuations and human behaviour.

2.3.2 Evacuation and human behaviour

Evacuation is the temporary mass physical movement of people that collectively emerge from coping with threats, damages or disruptions (Aguirre B. , 1983). The objective is to move as many people as possible from areas of danger or possible harm to locations that are safe. This must be done with the least amount of time possible before the destructive effects of the hazard are felt (Averill, et al., 2005; Kuligowski & Hoskings, 2010). Immediate evacuations are needed for sudden onset events that can create extensive damage and result in large numbers of injuries and deaths. Sudden onset events occur without warning and lasts a few seconds (Norton, Schreet, Aitken, Herard, & Lajolo, 2013). People are generally caught unaware and unprepared during these events. Earthquakes are sudden onset events that can likewise directly trigger other hazards. The resulting hazards include tsunamis, landslides, ground subsidence, liquefaction, fires, and failures in major transportation, industrial and nuclear infrastructures. These secondary hazards may occur just a bit after the shaking. These possibilities add to the anxiety of people and fuel more the urgency to evacuate. Longer duration events such as typhoons and floods normally can be anticipated due to warnings. In these situations, people are able to prepare before proceeding to evacuate.

Delayed evacuation has been seen as cause of many deaths in past disasters. Examples are the September 11, 2001 terrorist attack on the World Trade Centre (WTC) in the United States, and the 2011 Great

East Japan earthquake and tsunami (Averill, et al., 2005; Fraser_a, Leonard, Matsuo, & Murakami, 2012). Delays in evacuation are due to pre-movement actions individuals perform before actually heading to safety (Vistnes, Grubits, & He, 2005). Iwanaga and Matsuura, found that delays in evacuation during the 2011 Great East Japan earthquake and tsunami were generally caused by psychological conditions of normality bias, "sympathy behaviour" (or imitation, contagion), and altruism (or helping) behaviour (Iwanaga & Matsuura, 2014).

Emotional reactions to crisis are triggered with the perception of cues from the physical and/or social environment. This perception can shape an individual's resulting behaviour. The reactions can include fear, anxiety, confusion, anger, bewilderment, frustration, etc. These emotions can either start, hasten, stall or even completely stop evacuations. When people are within a group, emotional cues are quickly detected by members, thereby affecting the behaviour of the group (Papelis, et al., 2011). Without appropriate cues, and individual knowledge of evacuation protocols, people may ignore/disregard, wait, or evacuate improperly (Johnson, Johnson, & Sutherland, 2011).

Figure 6 details the possible sequence of events/actions with their temporal duration in an earthquake event. Shaking lasts only for a few short seconds. Individuals need to evacuate to safe areas within minutes. Return to homes can be within a few hours. This is only possible when the danger has subsided (no threat of aftershocks) and building evaluation/inspections show no serious visible structural damage (Bazzuro, Cornell, Menun, & Motahari, 2004). The return however can be after a longer period, such as several days, if there is damage, and repairs are possible. Longer term accommodation may need to be secured when return is impossible, as in the case of total structural collapse.

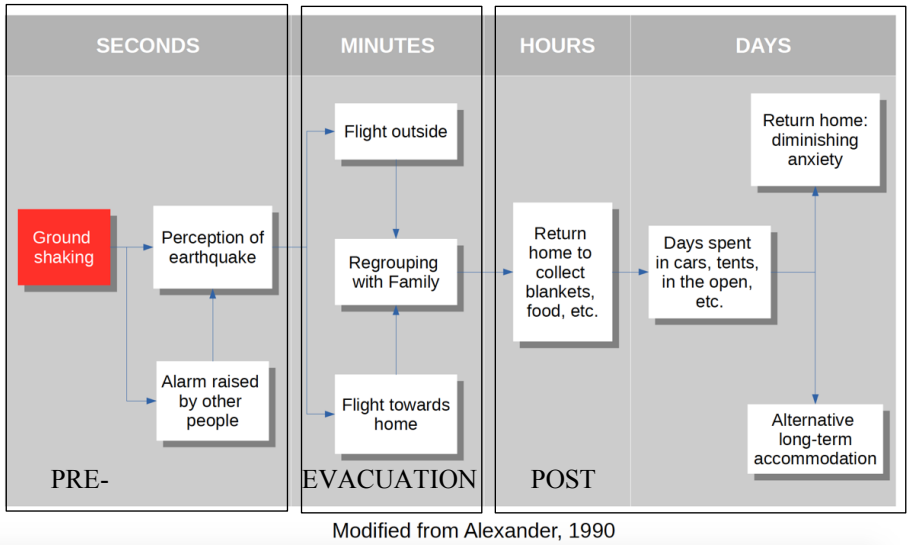

Figure 6 Temporal context of events and actions for earthquake evacuations (Alexander D. , 1990)

Evacuations can be divided into different stages namely pre-evacuation, evacuation and post-evacuation. In all of these stages, people have been reported to perform actions that deviate from immediately heading to, or remaining in, safe areas. During shaking, individuals are advised to protect selves by doing the officially prescribed set of actions: duck, cover, and hold-on (ECA, 2019; OSHA, 2019).

Pre-evacuation is the stage where the critical decision to evacuate is made. Most of the delays occur during the pre-evacuation stage. In this stage, an individual perceives the ground-shaking, evaluates the situation, defines options and plan, decides on the option to take, and executes chosen plan into actions. The decision to evacuate for example can be facilitated by: (1) observations of the threat, (2) clear instructions to evacuate given during the event, (3) level of fear, (4) adopting similar actions/evacuation of friends and co-worker, and (5) previous evacuation experience (Averill, et al., 2005). Also, people

tend to adjust behaviour with respect to the severity of the threat, and generally do not evacuate at the same time (Sorensen, 1991).

During the pre-evacuation stage, individuals seek information to confirm the experienced hazard and solicit advice on the proper things to do. Information is derived from face to face conversations, by phone, announcements, checking the internet, social media and radio for news, looking outside (windows/doors) or simply milling around. Family members or other close relations are sought to be gathered in one place or called by phone to confirm if safe. Some individuals manage objects or property. Examples of this include getting belongings, shutting down computers or turning off the power or the gas. Some individuals simply freeze or are unable to move and stay immobile (Prati, Catufi, & Pietrantoni, 2012). Other individuals maintain their current activity/task and disregard the hazard completely (Lindell_a, et al., 2016; Prati, Catufi, & Pietrantoni, 2012). When inside a car for example, individuals may continue driving (Lindell_a, et al., 2016; Ohta & Omote, 1977). Some seek protection from under sturdy tables. Others are able to help other individuals requiring aid.

The actual evacuation stage is when an individual decides to evacuate. At this stage, egress from the danger zone is made, and the individual heads toward known safe areas. Individuals employ different strategies to move towards safe areas. Depending on the intensity the hazard and an individual's mobility, people either crawl, walk, run or are assisted to evacuate. Typical evacuation speeds found in current studies are presented in Table 9.

Table 9 Evacuation speeds

Mode	Category	Individual (meters/sec)	Group (meters/sec)	Source
Crawl	All body types	0.65 – 0.90		(Kady & Davis, 2009)
Walk	Children Adult Elderly	0.56 – 0.84 0.91 – 1.73 0.70 – 1.11	- 0.88 0.75	(Adams & R., 2011; Kady & Davis, 2009; Fraser, et al., 2014)
Run	Children Adult Elderly	1.14 – 2.23 1.78 – 3.83 -		(Adams & R., 2011; Wood & C, 2012)
Disabled	All types	0.10 – 1.77	0.21 – 1.98	(Shi, Xie, Cheng, Zhou, & Zhang, 2009; Boyce, Shields, & Silcock, 1999)
Rescue device	All types		0.55 – 1.5	(Adams & R., 2011)
Stairs	Children Adult Elderly	0.25 – 1.4 0.056 – 1.7 0.21		(Larusdottir & Diderichs, 2011; Peacock, Hoskins, & Kuligowski, 2011; Fraser, et al., 2014)

Following behaviour, such as following leaders, or groups, has been observed. This results in emergent macro-level herding and flocking towards exits and safe areas (D'Orazio, Spallazzi, Quagliarini, & Bernardini, 2014a). Providing help to others is common, especially to those with mobility impairments (Averill, et al., 2005). This however introduces some delays. Groups with mobility impaired members, particularly the disabled, tend to remain together, adopting the speed of the slowest member. Large groups effectively constrict pathways, slows down evacuations, and delays egress especially of non-group members (Samuelson, 2011).

During the post-evacuation stage, together with personal safety, regrouping with close family members, friends and colleagues become the main motivations (Alexander D. , 1990). When all members are accounted for, individuals or groups settle down to rest and recover from their evacuation. However, when some members are missing, some return to danger areas to rescue or provide help (Iwanaga & Matsuura, 2014). When the danger has passed, some return home to recover property or supplies (Prati, Catufi, & Pietrantoni, 2012; Alexander D. , 1990).

2.3.3 State of the art in the study of evacuation and human behaviour

General observations of crisis behaviour from earthquakes and other disaster studies are presented in this section. Each case provides examples of individual or group behaviours in different social contexts such as with family members, friends, colleagues or strangers. The cases also present different locational contexts such as the home and workplace. The influence of location on evacuation is of interest. The level of familiarity and attachment to one's home for example is greater than other places. Also, in general, homes are considered as safe havens and provide protection from the elements. The pull of the home on the individual can delay evacuations when inside homes. For workplaces, presence of formal evacuation protocols can be in place to facilitate faster egress from structures. Familiarity with office layouts and exits likewise can hasten egress (Iliyas & Mani, 2018). The much lesser personal bonds shared by individuals with people at work may make evacuation more focused on personal and individual safety. This relative lack of attachment, or pull of the workplace and people at work, in theory, can lead to faster evacuations.

Close family relationships are highlighted in Jon et al.'s study of behaviours during the Christchurch, New Zealand and Hitachi, Japan earthquakes (Jon, et al., 2016). Notable behaviours included (1) contacting family members, (2) protecting children, (3) going home, (4) going to the home of a relative or friend. This agrees with the findings of Mikami and Ikeda and reported by Iwanaga and Matsuura who found that people during disasters tend to get together with family members (Mikami_a & Ikeda, 1985; Iwanaga & Matsuura, 2014). This is done to ensure the safety of all members so that they may eventually evacuate together. These behaviours were also reported by survivors of the 2011 Great East Japan Earthquake and Tsunami. In this disaster, many people died unnecessarily due to delayed evacuation or non-evacuation. The delays resulted from fulfilling social and family responsibilities (to children and elderly parents). Interestingly this is in direct contrast to the findings of Heath et al. In their study of the household evacuation during the California floods of 1997, they found that households with children more successfully evacuated than households without children (Heath S. E., Kass, Beck, & Glickman, 2001). This may be explained by the protective actions of parents prioritising children and prompting the urgent evacuations. Heath however found a delay in the evacuation of households with pets. Some households treat pets as family members and owners prefer to stay with pets at home due to logistical difficulties of capturing or transporting pets.

Flight behaviour is one of the strongest features of mass behaviours in Italian earthquakes (Alexander D. , 1990). This anxious behaviour can be traced back to previous hazard experiences such as the eruptions of Mount Vesuvius, known existence of other hazards and knowledge of the poor structural integrity of old buildings. During tremors, residents generally seek family members, run outdoors and regroup with other members. Those away from home however, return to check for the safety of family members and the resulting damage to their dwellings.

Group interaction was observed by D'Orazio et. al. from the analysis of earthquake evacuation video data (D'Orazio, Spallazzi, Quagliarini, & Bernardini, 2014a). The observed groups: exchanged information, moved closer together, and evacuated away from danger. Individuals either followed other individuals (leader-follower behaviour) or formed groups (herding or flocking behaviour) (D'Orazio, Spallazzi, Quagliarini, & Bernardini, 2014a).

Selfish behaviours are rare during disasters (Cocking, Drury, & Reicher, 2009). What has been observed to be common is the prevalence of altruism. Increased levels of altruism results in people helping each other. In the intensively studied Sept. 11, 2001 terrorist attack at the World Trade Centre (WTC event) in the US, many survivors reported providing and receiving help during evacuation (Averill, et al., 2005). In the study, it was found that occupants helped others even when aware of the heightened risk, before proceeding with their own evacuation. Twenty percent reported being helped by someone and thirty percent helped others. Individuals helped others with mobility impairments induced by injury, disability, health condition, pregnancy and old age. Sources of help included co-workers,

superiors (manager/supervisor), floor warden, police officer, fire fighter and strangers. Evacuation delays can be deadly as it should be noted that many who helped other people also perished from being caught in the structural collapse of the WTC towers 1 and 2. Other notable behaviours in the WTC during pre-evacuation which included: (1) talking to others, (2) gathering personal items, (3) helping other people, (4) searching for others, (5) talking on the phone and moving between floors.

The abovementioned examples demonstrate the social nature of human behaviour during crisis evacuations. These are governed by social bonds that are either strong and fixed such as within family members or weak and dynamic with friends or colleagues or strangers. These ties strongly influence behaviour when people evacuate as families, groups of friends or strangers in large crowds. To differentiate altruism with respect to the cost-associated with helping, between kin and non-kin relationships, a questionnaire-based study was conducted by Stewart-Williams, 2007 (Stewart-Williams, 2007). In the study it was found that as cost of helping increase, kin received a larger share of the given help than non-kin. For low-cost help, people helped friends more than siblings. For medium-cost, siblings are friends are helped equally. For very high-cost help, a greater willingness to help sibling than friends. The work of Bode et al. reproduces in an experiment the same idea of the relationship between increased cost and frequency or strength of helping behaviour (Bode, Miller, O'Gorman, & Codling, 2015). Their experiment used a virtual environment to simulate pedestrian evacuation from a building. Their results showed that the reduction in the frequency in helping behaviour is gradual rather than having sharp transitions. Moussaïd and Trauernicht developed a conceptual "Help-or-Escape" game to test helping behaviour during disaster evacuation (Moussaïd & Trauernicht, 2016). They found that people may maintain or increase the same helping intention but are able to help less in an emergency condition due to the mechanical restriction imposed by limited time. They concluded that emergencies seem to amplify people's natural cooperation tendency. A summary of observed evacuation behaviours, mentioned in this section are summarised in Table 10 with respect to the different stages of evacuation.

Table 10 Evacuation behaviour

Stage	Behaviour	Actions	Source
Pre-evacuation	Seeking information	Milling, talking to others (by phone, face to face)	(Averill, et al., 2005; Bernardini, D'Orazio, & Quagliarini, 2016; Kuligowski & Hoskings, 2010; Jon, et al., 2016; Zhou_a, et al., 2018; Beck, Dugdale, Truong, Adam, & Colbeau-Justin, 2014)
	Seeking family members/other people	Calling, searching	(Mikami_b & Ikeda, 1985; Jon, et al., 2016; Fraser, et al., 2014; Alexander D. , 1990; Johnston, et al., 2014; Zhou_a, et al., 2018)
	Manage objects/property	Get belongings, shut down computers, turn off power/gas	(Averill, et al., 2005; Jon, et al., 2016; Zhou_a, et al., 2018; Beck, Dugdale, Truong, Adam, & Colbeau-Justin, 2014)
	Freeze	Stay in place	(Prati, Catufi, & Pietrantoni, 2012; Lindell_b, et al., 2016; Jon, et al., 2016; Beck, Dugdale, Truong, Adam, & Colbeau-Justin, 2014)
	Maintain activity	Continue working, driving	(Averill, et al., 2005; Jon, et al., 2016; Lindell_b, et al., 2016; Zhou_a, et al., 2018; Beck, Dugdale, Truong, Adam, & Colbeau-Justin, 2014)
	Seek protection	Drop-cover-and hold on	(Wood & Glik, 2013; D'Orazio, Spallazzi, Quagliarini, & Bernardini, 2014a; Lindell_b, et al., 2016; Zhou_a, et al., 2018)
	Helping	Protect others, assist mobility impaired (children, pregnant women, elderly, disabled, injured)	(Urata & Hato, 2012; Kuligowski & Hoskings, 2010; Johnston, et al., 2014; Zhou_a, et al., 2018)
Evacuation	Flight	Move (walk, run, crawl), use stairs, elevator, head towards home, go to nearest exit or safe area	(Fraser, et al., 2014; Kady & Davis, 2009; Kuligowski, et al., 2015; Alexander D. , 1990)

	Following	Follow leader, herding, flocking	(Beck, Dugdale, Truong, Adam, & Colbeau-Justin, 2014; D'Orazio M. , Quagliarini, Bernardini, & Spalazzi, 2014b)
	Helping others	Assist mobility impaired	(Averill, et al., 2005)
Post-evacuation	Regrouping	Regrouping with family members, friends, colleagues	(Prati, Catufi, & Pietrantoni, 2012)
	Helping/rescue	Returning to danger areas to rescue family member, friend, colleague	(Fraser_b, Leonard, Matsuo, & Murakami, 2012; D'Orazio M. , Quagliarini, Bernardini, & Spalazzi, 2014b)
	Recover objects	Return home to get supplies	(Prati, Catufi, & Pietrantoni, 2012)

2.3.4 Social theories that explain crisis and evacuation behaviours

Social theories that explain the complex behaviour of people during evacuations can be divided into three categories: (1) based on popular notions, (2) attachment, and (3) group behaviour. Several theories are necessary to account for the complexity of social behaviours. Each theory has its own focus, strengths and weaknesses in explaining behaviour. Each theory complements the other theories to provide the broader explanation of behaviours.

2.3.4.1 Popular notions

The first category presents popular notions derived from observations of individual behaviour. This includes Normative, Emergent Norm and Panic Theories.

Normative theory states that everyday social roles and rules that govern daily life applies and can be observed in emergency situations (Chu, Pan, & Law, 2011). Examples of this include respecting and helping elders, caring for and prioritising children, aiding the disabled, following traffic rules, obeying instructions of authority figures, and maintaining social order and organisation. This theory assumes that human behaviour is predictable during disasters. Expected proper behaviours during disasters are prescribed in manuals and evacuation plans and practiced during drills. Social norms however, are likely to be followed during slow onset disasters, where there is longer time available to allow for social norms to take hold during lengthy evacuations (Frey, Savage, & Torgler, 2011).

Unexpected or illogical behaviours however are observed during disasters, which cannot seem to be explained by the assumptions of normative theory. For example, individuals may follow only the familiar routes to an exit, even if these are not the designated/fastest evacuation pathways (Ma, Wang, & Larrañaga, 2011). During indoor evacuations, people normally head towards the familiar front door, usually missing or not using nearby exits (Rai & Wong, 2009). Taking another example from aircraft evacuations, people have been observed to take the time in retrieving luggage before proceeding to evacuate from a burning aircraft (FSF, 2004). These illogical behaviours can be due to the differences in how individuals handle stress imposed by crises. Stress can make individuals more prone to cognitive biases that distort judgement and decision-making (Comes, 2016; Johnston & S., 2009; Murata, Nakamura, & Karwowski, 2015).

Emergent Norm Theory posits that crisis destroys traditional normative guidelines defining appropriate behaviour. Because of the context and urgency demanded by crisis situations, people are forced to interact and create new meanings or norms to guide behaviour (Aguirre & Wenger, 1998). Once a dominant norm is defined, group members with differing opinions may remain silent for fear of group censure. Aguirre et al. add that enduring social relationships determines the social interactions associated with the emergence of a dominant norm (Aguirre & Wenger, 1998). This can be the result of an instance of collective behaviour such as risk taking, use of common resources or cooperation.

Panic refers to inappropriate or excessive fear and/or flight and is where instinct overwhelms socialisation and dissolves collective bonds (Mawson_a, 2005). Survival becomes the primary objective of the individual resulting in competitive behaviours within the crowd (Strauss, 1944; Drury, Cocking, & Reicher, 2008). Panic can be viewed on two levels: (1) individual panic as disorganisation due to fear; and (2) mass panic as disorderly flight leading to disastrous results for crowds (Ma, Wang, & Larrañaga, 2011). Crowd stampedes for example are attributed to panic leading to fatalities where people are crushed or trampled by the crowd (Helbing, Farkas, & Vicsek, Simulating Dynamical Features of Escape Panic, 2000; Riboldi, 2014).

Mawson's review of literature on panic yielded the following interesting findings (Mawson_b, 2007). (1) Firstly, the behaviours can be described as panic: manic or hyperactive behaviour, flight, aggression, desperate attacks on people, emotional explosion, agitation and motor restlessness, and immobility or freezing; (2) Secondly, individuals experiencing panic are susceptible to social influence, such as being infected with fear, or mimicking the behaviour of others (looking when other run, escaping through the same exits as other people). (3) Lastly, individuals may experience the deterioration of cognitive function and personality. These can include temporary impairments in perception, cognition, and control of motor impulses, difficulties in thinking, feelings of bewilderment, puzzlement and confusion.

Many experts however believe that mass panic is rare in disasters and that it is largely a myth and unsupported by evidence (Cocking, Drury, & Reicher, 2007). Ma et al. however support the existence of panic for crowd disasters (Ma, Wang, & Larrañaga, 2011). An individual's panic reaction can be helpful in triggering flight, allowing individuals to immediately seek shelter, go to the nearest exit, and head towards a safe area. Alternatively, panic can be deadly, for example when individuals freeze, or are unable to move, this will delay their evacuation. According to Ma et al., panic prone individuals include children, females, the elderly, the mobility impaired, those with strong beliefs, those having poor knowledge, and those experiencing fatigue and weakened perception (Ma, Wang, & Larrañaga, 2011). From the same authors, the necessary conditions for panic to occur include (1) a confined space caused by a structure, a dark environment, or being in a crowd, (2) beliefs on the potential danger, and (3) presence of triggers such as an earthquake or fire.

2.3.4.2 Attachment behaviours

The second category presents the social theories explaining the observation that individuals tend to seek the family members and other close relations and during threat situations. This category includes Attachment, Social Attachment and Social Baseline theories.

Human beings have innate attachment behavioural systems (Bowlby_a, 1982). This motivates individuals to seek the proximity of significant others (attachment figures) during times of need or threat (Bowlby_a, 1982; Ainsworth, 1989). Attachment figures include family members, friends, pets, colleagues, authorities and even strangers. Objects, places, and information present within the sphere of social interaction are also considered as attachment figures. Non-human attachment figures evoke familiarity and are usually linked to a person or a fond memory. During threat, affiliation to attachment figures is activated. The presence of attachment figures results in providing an individual with a sense of security, thereby reducing stress and anxiety. Attachment therefore can regulate other emotions such as fear and panic by allowing individuals to focus on attachment figures. Such attachments can influence an individual's decisions, destinations (goals), social interactions, and speed/direction of movement. This can lead to pre-evacuation behaviours that seek, protect and defend attachment figures (Adam C. , Danet, Thanagarjah, & Dugdale, 2016b). Attachment to a place, such as the home, invokes memories of safety and warmth provided, and may influence the decision to stay or evacuate during dangerous situations. Other examples include seeking family members, milling, herding, protecting property, seeking pets, helping others/strangers, etc. Table 11 presents attachment figures and possible behaviours during evacuations.

Humans fundamentally desire and maintain interpersonal attachments. However, the strength of bonds varies depending on the attachment figure. A person may be more strongly attached to their pet than their mother. The strength of emotional bonds for different relationships may also vary across cultures. Strong bonds are a natural result of high familiarity, which is strengthened with frequent social interaction (Suvilehto, Glerean, Dunba, Hari, & Nummenmaa, 2015). This familiarity facilitates faster perception (recognition) of attachment figures, especially from a distance, when affiliation or proximity seeking behaviours are activated during disasters (Liccione, et al., 2014; Mawson, 2005; Kok, Taubert, Burg, Rhodes, & Alais, 2017; O'Toole, et al., 2011; Barton & Corrow, 2016). Perceiving the familiars at some distance, or perception distance, can be through sight such as seeing facial expression, body language, posture, gesture, actions, signals/signs. This can also be through hearing such as voice, sound, calling by name, cry for help, screams or warnings. Perception is also influenced by cognitive representations resident in memory or acquired through knowledge (Liccione, et al., 2014).

Table 11 Attachment figures and possible behaviours during evacuations

Attachment figure	Examples	Example behaviour	Source
Person	Child, spouse, parent, sibling, kin, friend, colleague, leader, mobility impaired, stranger	Seeking, calling, checking on the whereabouts, following, leading, helping, rescuing	(Jon, et al., 2016; Averill, et al., 2005; Drury, Cocking, & Reicher, 2009)
Group	Family, relatives, friends, colleague	Reuniting with members, following group (decision, direction/heading), relocating to group's home, herding, flocking	(Averill, et al., 2005; Prati, Catufi, & Pietrantoni, 2012; Daamen W. , et al., 2014a; D'Orazio M. , Quagliarini, Bernardini, & Spalazzi, 2014b)
Object	Personal property	Recovering personal property	(Averill, et al., 2005; Flight Safety Foundation, 2004; Prati, Catufi, & Pietrantoni, 2012; Lindell_b, et al., 2016)
Place	Home, exits, entrance, pathways, routes, designated safe area, elevator	Returning home, take familiar routes, head towards entrance, known exits/safe areas	(Jon, et al., 2016; Prati, Catufi, & Pietrantoni, 2012; Averill, et al., 2005; D'Orazio M. , Quagliarini, Bernardini, & Spalazzi, 2014b)
Animals	Pets, farm animals	Staying home with pets, evacuating with pets	(Heath S. E., Kass, Beck, & Glickman, 2001)
Task	Work, routine, driving, sleeping	Continuing with current task, getting luggage before evacuating aircraft during emergency	(Wood & Glik, 2013; D'Orazio, Spallazzi, Quagliarini, & Bernardini, 2014a)
Information	News, announcements	Seek from conversations, radio, email, social media, etc.	(Averill, et al., 2005)

Social attachment theory is based on Bowlby's attachment theory and is used to explain behaviours specifically in disaster situations. According to Mawson, the response to a variety of threats and disasters is not to flee or attack but affiliation. Affiliation refers to seeking the proximity of familiar persons and places, even if it involves approaching or remaining in a situation of danger (Mawson, 2005). Mawson also states that separation from attachment figures is a greater stressor than the physical danger itself. Whereas the presence of familiar persons and places have a calming effect. Mawson argues that this may provide an explanation of several evacuation behaviours. Examples include the (1) slow reaction of individuals within groups to warning, (2) delay in leaving work areas, (3) waiting for social group members before evacuating and (4) seeking family members.

The central ideas of the theory are: (1) the dominant motive in disasters is to maintain proximity to familiars, (2) flight involves the movement away from danger and towards people and places viewed as familiar, (3) flight-and-affiliation depends on perceived danger and social context (i. e. the location and activities of familiars, (4) fear is diminished by proximity to attachment figures, (5) when an individual is close to attachment figures, in the presence of threat, intense affiliation is triggered, and does not cause flight, (6) moving as a group maintains proximity during flight, (7) mild threats can induce flight-and-affiliation behaviours when individuals are alone or with strangers.

According to Mawson, there are four possible outcomes of individual and collective reaction to threat and disaster. As presented in Table 12, (1) Top left: when attachment figures are present and the perceived degree of danger produces mild anxiety, affiliation is triggered producing increased attachment. Individuals tend to seek the proximity of familiar people and locations. (2) Bottom left: when attachment figures are present and the perceived danger is severe producing fear or terror, occasional or low-to-intense flight and affiliation is triggered resulting in orderly evacuations. (3) Top right: when attachment figures are absent, and the perceived danger is mild, this triggers low intensity flight-and-affiliation, resulting in orderly evacuation away from danger and towards the familiar, and (4) Bottom right: when the attachment figure is absent, and the perceived danger is high, intense flight-and-affiliation is triggered resulting in mass panic.

Table 12 Affiliative reactions to threat (Mawson, 2005)

		Attachment Figures (Predisposing Conditions)	
		Present	**Absent**
Perceived Degree of Danger (Precipitating conditions object)	**Mild Anxiety**	Affiliation (Increased attachment), seek the proximity of familiar people and locations	Low intensity flight-and-affiliation, orderly evacuation away from the danger and towards the familiar
	Severe Fear/Terror	Occasional low-to-intense flight and affiliation; orderly evacuation	Intense flight-and-affiliation; mass panic

Evacuation behaviours that can be explained by social attachment theory include: (1) individuals with close ties seeking each other and evacuating as a group, (2) movement to familiar exits and doorways (entrance), (3) delayed evacuation start (departure), (4) slow evacuation speeds, (5) slow reaction to warnings and waiting for primary group members, (6) reluctance to leave one's home, (7) preservation of social organisation, (8) mutual aid and cooperation, (9) calmness during evacuations, (10) heading home, (11) seeking other survivors (formation of groups), and (12) reuniting with familiar people and surroundings (Mawson, 2005; Iliyas & Mani, 2018).

Social baseline theory provides the neuro-scientific explanation as to why humans form social ties and seek proximity (Coan, 2008). Beckes and Coan believe that human brains prefer proximity to predictable social environments. When proximity is maintained, or re-established, the brain is less vigilant in detecting potential threats (Beckes & Coan, 2011). From the same authors, humans utilise social resources or social proximity to conserve costly cognitive resources through social regulation of emotion. This includes the distributing the task of detecting environmental risks across individuals within groups. This also results to inter-dependence in achieving goals and providing help during times of need.

2.3.4.3 Group formation and behaviours

Formation of groups have been observed during evacuations. If one is to follow the previously discussed theories on attachment, one would expect clustering or only of individuals with close relationships such as families or friends. It is however a common observation that groups can be composed of individuals with varying degrees of strength of social bond. It is even possible to have a group composed of complete strangers. This is inevitable especially for large disasters. Disasters therefore can facilitate the formation of new bonds and new attachments. This section discusses the social theories to explain the formation of social groups and the resulting behaviours. Group behaviour during disaster may be explained by social defence, self-categorisation and social identity theories. These theories extend social attachment theory to the level of social groups.

Social defence theory extends Bowlby's and Mawson's attachment theories. Ein-dor et al. claim that having a mix of secure, anxious and avoidant members in a group provides unique survival advantages (Ein-Dor T. , Mikulincer, Doron, & Shaver, 2010). Secure individuals are good leaders and are best at coordinating tasks. They are however slower to react to dangers because of proximity seeking behaviours. Anxious individuals are fast in detecting and reacting to danger and can act as sentinels of groups. Avoidant individuals are accustomed to looking out for their own interests and more likely to

rely on self-protective flight-or-fight reactions in times of danger. Primarily motivated to save themselves, they are first to open exits, break windows and can find routes for other group members to follow. This theory may help to explain the different behaviours found in a in group of individuals.

Self-categorisation theory refers to the process when a person categorises himself or herself as an individual or a group member. This involves the process of de-personalisation where the individual stereotypes themselves in line with the group. This process of self-categorisation as a group member makes crowd behaviour possible (Turner & Killian, 1987). This results to two types of crowds. A physical crowd of individuals that shares only physical location, and a psychological crowd where people act together. Social behaviour observed in emergencies is a consequence of emergent self-categorisation rather than a function of pre-existing bonds, prior interpersonal relationships or interactions (Daamen W. , et al., 2014b; Drury, Cocking, & Reicher, 2008). From the same study, this makes individuals transition and adapt to become part of a psychological crowd useful in surviving mass emergencies and disasters. This differs from social-defence theory in that self-categorisation theory focuses on a person identifying with a group rather than characteristics of individuals in a group.

Social identity theory corrects the limitation of social attachment theory in explaining the behaviour with unfamiliar people, objects and strangers. Social attachment theory suggests that people may display panic behaviour when with strangers. This is contrary to the observed helping behaviour among strangers during disasters (Drury, Cocking, & Reicher, 2009). Social identity theory accounts for the development of bonds between strangers in unfamiliar places precipitated by events. Shared social identity increases supportive behaviour and coordination during emergency situations. Helping behaviour towards strangers, such as aiding the elderly and injured individuals or rescuing people under rubble can be explained by social identity theory.

A summary table of the theories is presented in Table 13. It can be concluded in this section that social interactions facilitated by attachment can influence evacuation behaviour during disasters and crisis events. Cocking et al. identify that the strength of social attachment theory over the panic model is its emphasis on the maintenance of social bonds and the co-operative nature of groups during disasters (Cocking, Drury, & Reicher, 2007). Cocking and colleagues however identified two main drawbacks: (1) the pessimistic implications for large groups as it is more difficult to ensure safe evacuation of all group members; and (2) it discounts the possibility of developing attachment bonds and eventual co-operation between strangers.

Table 13 Social theories

Category	Theory	Idea	Behaviour	Source
Popular Notions	Normative	Social norms and bonds persist during disasters, social structure is retained	Normal, helping, cooperation	(Chu, Pan, & Law, 2011)
	Emergent Norm	Dissolution or suspension of existing norms, creation of new norms (non-traditional) from social interaction	Non-traditional/Illogical	(Aguirre & Wenger, 1998)
	Panic	Breakdown of existing bonds and norms (social and cultural)	Herding, irrational, selfish, disorderly and competitive	(Mawson, 2005; Ma, Wang, & Larrañaga, 2011; Helbing & Johansson, 2013; Strauss, 1944; Drury, Cocking, & Reicher, 2008)
Attachment Behaviour	Attachment	Bond formation from childhood developed towards adult life	Proximity seeking	(Bowlby, 1982; Mikulincer & Shaver, 2007)
	Social attachment	Activation of attachment bonds during threat	Proximity seeking, cooperation	(Mawson, 2005)

	Social baseline	Instinctive development of social bonds to maximise social resources and distribution of risk	Proximity seeking, cooperation, sentinel	(Sivers I. v., et al., 2016; Tajfel & Turner, 1986)
Group Behaviour	Social defence	Variation in attachment styles between groups is optimal to ensure survival during disaster	Leadership, cooperation, sentinel, anxious	(Ein-Dor T. , Mikulincer, Doron, & Shaver, 2010)
	Self - categorisation	Individuals transition to become members of the psychological crowd, shared fate	Cooperation	(Turner & M, 1987)
	Social identity	Development of bonds between strangers in unfamiliar locations and disaster situations	Helping	(Sivers I. v., et al., 2016; Tajfel & Turner, 1986; Drury, Cocking, & Reicher, 2009)

2.4 Summary of the chapter

This chapter described the seismic crisis environment with respect to the physical environment and social aspects. The physical aspect presented earthquakes as a hazard and how it affects exposed structures and individuals. Risk is described by the intensity of the earthquake hazard, exposure and vulnerability. The social aspect described how people are affected and behave during crisis. Social theories were presented to explain these behaviours. Social attachment theory was described as the underlying framework that govern social interactions during disasters.

As a final analysis, the underlying behaviour for social interactions can be attributed to social attachment theory. Feeling of safety when with attachment figures and therefore the activation of proximity seeking behaviours is towards familiars is core to the theory. Familiarity is driven by strong social bonds present in existing relationships or weak social bonds that are formed dynamically and in-situ by the disaster context (through the formation of new social identities via self-categorisation). New attachment figures can be formed on-the-fly with non-familiars and this can accommodate strangers. The motivations for the behaviours of seeking safety are explained by social baseline and social defence theories. Individual conduct during disasters such as observance or existing norms are explained by normative theories, or through new norms of behaviour as explained by emergent norm theory.

The main benefit of using social attachment is its possible usefulness in modelling. The emphasis on attachment figures, highlights the social nature of evacuation behaviours as reported from literature. The theory provides the answers to the question why people evacuate. It lays out the main motivations for crisis behaviour. These include actions or goals. Individuals moving or heading towards goals points to the sensitivity of evacuation to spatial elements present in the crisis environment. With these explanatory elements, social attachment theory is suitable for modelling pedestrian evacuation behaviour especially on large spatial scales such as large communities like cities. The next chapter is about the state of the art of modelling evacuation behaviour.

CHAPTER 3. STATE OF THE ART

Pedestrian evacuation models require accurate representations of crisis environments and realistic social interactions. This chapter presents a state of the art in the realistic modelling of pedestrian evacuation during earthquake crisis scenarios. The chapter is divided into four sections. The first is a brief note and introduction on pedestrian models. The second section focuses on the use of geoinformation in the development of realistic spatial models of earthquake crisis environments. This section focuses on the strengths of GIS in creating synthetic spatial environments and populations. The section also identifies the weaknesses of GIS particularly the handling of time, which is an outstanding area of concern for improvement in the context of dynamic crisis modelling. The third section presents the developments in realistic multi agent-based modelling of human behaviour during crisis evacuations. This section presents models and social simulations applied to evacuations. The chapter ends in the fourth section with a short conclusion.

3.1 Pedestrian evacuation models

Pedestrian evacuation is the situation where individuals or groups travel on foot, by walking or running from areas of danger to safer areas. This has been main mode of evacuation especially during the start and the first few minutes of sudden onset events such as earthquakes. Movement is usually from indoor locations towards outdoor open areas considered safe from debris and damage. Pedestrians have more flexibility in moving to different locations, especially when travelling by car is not feasible (FHWA, 2018). The study of pedestrian models is critical in the development of evacuation scenarios. Determining the fastest routes, or the nearest safe areas for people to seek shelter, is important to everyone, especially to decision makers and planners. Lessening the amount of time needed for individuals to reach safe areas is the desired outcome of evacuation plans. The more lives saved, within the least time possible, the more effective the plan. Plans can focus on enhancing mobility of populations in urban spaces by ensuring accessibility of evacuation routes and safe areas. Pedestrian evacuation models can also be useful in preparing for actual evacuations by anticipating challenges learned from models (Gaire, Song, Christensen, Sharifi, & Chen, 2018).

Making evacuations faster and efficient is the focus of evacuation studies. Understanding the causes of delays is crucial. In the context of crowd dynamics in pedestrian evacuations, this requires the appreciation of the complementary interplay between the natural and social environments (Sieben, Schumann, & Seyfried, 2017). Physically based models consider pedestrians as particles. Social models consider pedestrians as individuals with cognitive and social abilities.

To quantify evacuation delays, current evacuation strategies concentrate on the physical and spatial aspects of natural environments such as (1) evacuation time, (2) evacuation routes (best, fastest, shortest), (3) effectiveness of building layouts, (4) availability and placement of exits, (5) placement of guidance or information aids or alarms, and (6) effects of barriers, etc.

Social aspects studied in evacuation models include the effect of egress speeds and behaviour of people, as individuals or groups. The speed adopted for movement in current models however is usually the speed of able-bodied individuals. Movement speed depends on individual characteristics when a person is alone. When embedded in a group, individuals adjust their speeds with respect to group members, especially when in the company of mobility challenged individuals (Frydenlund, Elzie, Collins, & Robinson, 2014). A decrease in walking speed is also observed with increasing group size (Moussaid, Perozo, Garnier, Helbing, & Theraulaz, 2010). Also, from Moussaid et al. (2010), dynamic social interactions, when present, also affect the physical organisation or configuration of groups or crowds. This can likewise affect the speed of evacuations. Increases in the size of social groups in a crowd likewise lengthens egress time (Bode, Holl, Mehner, & Seyfried, 2015). Bode et al. in their crowd egress experiments that presence of social groups increased the average egress time of individuals (Bode, Holl, Mehner, & Seyfried, 2015). Other findings in Bode et al.'s study are: (a) individuals in social groups

took longer to show movement response, (b) groups took longer to move towards exit zone, and (c) social groups followed longer paths towards exits. Krüchten and Shadschneider also had a similar finding and concluded that even with the initial benefit of order and compactness in movement, groups with cooperative behaviour are slower to evacuate (Krüchten & Schadschneider, 2017). Lastly Bode et al. conclude that social groups can affect the pre-movement time and movement time of evacuating individuals (Bode, Holl, Mehner, & Seyfried, 2015).

The realistic modelling of pedestrian crowds requires the considerations imposed by different scales (Kneidl, Hartmann, & Borrman, 2012). According to Kneidl et al. (2012), in addition to behavioural aspects, movement on the short-scale and human navigation on the large-scale also needs to be modelled properly. Different scales define different levels of analysis. The scales are categorised as micro, meso, and macro scales. For pedestrian evacuation simulations, the relevance of scale in different contexts are presented in Table 14.

Table 14 Variations in scale in modelling pedestrian evacuation simulations

Domain	**Micro**	**Meso**	**Macro**	**Source**
Perspective	Local		Global	(Nasi, 2013)
Pedestrian simulation	Individual pedestrian and Interactions	Individual pedestrian, simplified dynamics and flow	Pedestrian flow	(Kormanova, 2013)
Pedestrian simulation problems	Consider each individual, can control different parameters related to dynamics (e.g. velocity)	Consider individuals but not individual interactions b/w them	Focus on problem of space allocation for individuals (e.g. mean velocity, linear momentum, density, flow, kinetic energy)	(Martinez-Gil, Lozano, Garcia-Fernandez, & Fernandez, 2017)
Evacuation	Each individual at risk, detailed representation of evacuation routes	Between micro and macro; lumped parameters; evacuation time based on capacity of evacuation routes, geographical basis	Estimate evacuation times based on key parameters (e.g. lumped population groups, distance to nearest shelter or higher ground, evacuation route, average evacuation speed.	(Lumbroso, et al., 2010)
Evacuation	Detailed evacuation planning	Detailed evacuation planning	First order estimates of evacuation times for relatively large areas.	(Lumbroso, et al., 2010)
Models	Cellular automata, social force, velocity-based, discrete choice, lattice gas		Hughes model, Jiang et al.	(Martinez-Gil, Lozano, Garcia-Fernandez, & Fernandez, 2017; Liu, Zeng, Chen, & Wu, 2017)
Models	Every pedestrian is considered as an individual.	Aggregation of several pedestrians in a region (e.g. room, hall, railway platform)	See crowd as a continuum medium characterised by averaged quantities (velocity, mean velocity)	(Twarogowska, Goatin, & Duvigneau, 2014; Teknomo, Takeyama, & Inamura, 2010; Teknomo & Gerilla, 2008)

The model scale used in simulations depends on the domain or parameter investigated. *Microscopic models* describe individuals and interactions (Kormanova, 2013). *Macroscopic models* produce pedestrian flows, and human interaction is not closely studied (Kormanova, 2013). In macroscopic models, crowds are seen as a continuum characterized by averaged quantities (e.g. density, mean velocity) (Twarogowska, Goatin, & Duvigneau, 2014). Macroscopic models are concerned with emergent phenomena, such as the emergence of crowds. *Mesoscopic models* combine aspects of microscopic and macroscopic models and therefore, (a) can handle individuals, (b) includes simplifications of dynamics and, (c) requires less data (Kormanova, 2013). Microscopic models have high granularity or detail and require longer computation times. The benefit of macroscopic models, according to Kormanova, is the speed of the simulations, which require less computation time. Several studies have proposed hybrid methods, which enable transitions between scales to produce more realism in models.

Being built from the ground up, the microscopic scale is ideal for observing emergent properties of complex systems. The benefit of having a microscopic model at the scale of an individual is having the ability to precisely define and specify characteristics of the primary actors, who are the human individuals, in pedestrian evacuations. Also, having the crisis environment modelled from the perspective of an individual, or how one will possibly see or experience it in reality, provides the benefit of being able to test spatial and social configuration that are familiar to planners and stakeholders. The results or emerging dynamics from the models would likewise be relatable, easy to understand, or surprising results easier to accept. Aggregation is also possible from the micro to the meso and macro scales (Crooks, Castle, & Batty, 2007). The reverse, or disaggregation, from the macro, to meso, then to micro however is not possible.

In this work, we consider spatial, social and temporal aspects. Simulations using agent-based models benefit from the dynamic transitioning between scales. Agents can be developed at the micro scale, but agent interactions happen in at the meso and micro scales. Emergent properties manifest at the aggregation of scales. Emergence is the set of unexpected behaviours that result from the interaction between different components of the environment (Johnson C. W., 2006).

Detailed empirical observations of pedestrian evacuations have been reported in several studies. The studies included the pre-evacuation behaviours, and the associated delay time for each action, and modes of movement (e. g. walk, run, assisted). They can be used in the calibration of models and development of scenarios. Example are for indoor and outdoor scenarios. These studies are detailed in Table 15.

Table 15 Behaviour and time studies (Delay)

Domain	Collection method	Behaviours	Delay time	Modes of Movement	Source
Earthquake	Annotated video tapes	Yes	Yes	Yes	(Zhou b, et al., 2018)
Earthquake	Annotated video tapes	Yes			(D'Orazio M. , Quagliarini, Bernardini, & Spallazi, 2014b)
Fire	Fire investigation, unannounced drill, experiments	Yes	Yes	Yes	(Shi, Xie, Cheng, Zhou, & Zhang, 2009)
Fire, Drill, WTC	Derived from other studies,	Yes	Yes	Yes	(Fahy & Proulx, 2001)
Various Contexts	Experiments, drills, compiled from other studies	Yes	Yes	Yes	(Peacock, Kuligowski, & Averill, 2011)

The study of pedestrian evacuation and its dynamics is a young and a growing field. In 2011, Averill outlined five grand challenges for the field. These include (1) developing and validating a comprehensive theory that can predict human behaviour during pedestrian evacuations, (2) building a comprehensive database of actual emergency data, (3) accept and embrace variance due the inherent stochasticity of pedestrian movement and evacuations, (4) integrate results of indoor evacuation models with fire models for more accuracy and reliable design of models, and (5) accept and embrace technology that improve people's movement, situational awareness, and egress pathways in evacuations (Averill J. D., 2011).

The spatial aspects of crisis environments are discussed in the next section.

3.2 Geographic information and spatial models of crisis environments

3.2.1 Geoinformation, GIScience, GISystems (GIS)

Geographical information or geoinformation refers to the information on the surface or near the surface of the earth. At the core of geoinformation is location. Location can be the common attribute

that can be used to link seemingly unrelated objects or information. To illustrate, a building for example can have data on coordinates, address, land use, property valuation, soil type, risk zonation (e.g. earthquake, crime, health risk, pollution), service area (e.g. for utilities, delivery service, cellular service, transportation routes), distance and travel times to (e.g. road, school, hospital, work, safe zone), etc. An individual can likewise be linked to the location of this building based on activity (e.g. residence, work, etc.).

Popular geoinformation technologies used in daily life, especially for navigation, are maps, global positioning system (GPS) receivers, geographic information systems (GIS), and remote sensing. Goodchild defines geographic information science, or *GIScience,* as "that branch of information science that deals with the geographical domain" (Goodchild M. F., 2011). He further clarifies the definition by stating that, it deals with "the set of fundamental scientific questions raised by geographic information and the technologies that collect, manipulate and communicate it." Also, Goodchild, defines geographic information systems as the computer system that performs operations on geographical data. This includes acquisition, compilation, display, analysis and modelling, sharing and archiving.

3.2.2 Utility of geoinformation and GIS for risk and crisis research

Precision and faithful representations or modelling of crisis environments is a requisite to gaining optimum appraisals of risk. For pedestrian evacuation models in particular, with the focus on human life, the required degree of precision and detail is high. The elements of risk need to be in the correct spatial and temporal contexts. These contexts include spatial configurations or dimensions, shapes, heights, distances, elevations, temporal variations, and other characteristics of elements of the environment. Building the accurate contexts into risk or disaster models however requires a multitude of data from across several domains (van Westen & Geordiadou, 2001).

Use of geospatial technologies for disaster management is increasing (Abdalla & Li, 2010). According to Abdalla and Li, this is due to the following reasons: (1) increasing accessibility of data and technology, (2) reliability and effectiveness in providing accurate models or real-world phenomena, (3) ability to embed information from different sources, (4) effectiveness in generating knowledge and (5) decision aid support.

GIS has been used in several studies to define accurate spatial models of seismic crisis environment scenarios using real geographic data (Hori, et al., 2018 ; Abdalla & Li, 2010; Saputra, et al., 2017). A clear analytical definition of vulnerability is crucial (Section 2.1), as this allows for the easy implementation in a GIS environment (Giovinazzi & Lagomarsino, 2004). Hazard and vulnerability data can be used for the (1) development of damage scenarios, (2) consequences on buildings and people, and (3) evaluation of economic loss. Damage and loss scenarios are powerful tools in the design of efficient seismic mitigation policies, GIS also becomes a useful policy instrument (Senouci, Bard, Farsi, & Beck, 2013). Applications of GIS, related to large scale (urban) earthquakes include (1) seismic microzonation[8] and site effects, (2) macrozonation[9], (3) macroseismic[10] vulnerability assessments, (4)

[8] Seismic microzonation is sub dividing a region into smaller areas having different potential for hazardous effects (Gupta & Zafar, 2016). Further from Gupta and Zafar, the effects of earthquakes depend on ground geomorphological attributes, which consist of geological, geomorphology and geotechnical information. According to Stéphane Cartier, "the scientific characterization of seismic micro-zones enables the definition of more precise rules for building and urban planning" (Cartier, 2007). Seismic microzonation requires input from civil engineering and engineering geology, in particular, from the field of geotechnical engineering (Mihalic, Ostric, & Krkac, 2011). Micro zonation is usually carried out or cities and urban centres (Anbazhagan, 2013).

[9] Macrozonation is carried out considering seismicity, geology without considering geotechnical aspects (Anbazhagan, 2013). Seismic macrozonation maps are based on regional characterisation of earthquake hazards at smaller scales (Mihalic, Ostric, & Krkac, 2011). Generally done, at the scale of a large region such as a district, state or country.

[10] Macroseismic, in this context, is the adjective used to describe methodologies that identify with the European Macroseismic Scale (Bernardini, Giovinazzi, Lagomarsino, & Parodi, 2007).

damage assessments, (5) design of evacuation plans, and (6) shelter location-allocation problems (Riedel, Guéguen, & Dunand, 2014; Riedel I. , et al., 2014; Coutinho-Rodrigues, Natividade-Jesus, & Sousa, 2015; Glatron & Beck, 2008; Zhao, Coates, & Xu, 2017; Nwe & Tun, 2016; Saputra, et al., 2017 ; Hori, et al., 2018 ; Nath & Thingbaijam, 2009; Zhao, et al., 2017) (Rezaie & Panahi, 2015).

A very good example of spatial modelling with GIS for seismic crisis in the urban context is the work of Hori et al., 2018. They developed the integrated earthquake simulation (IES) to analyse processes related to earthquake hazard and disaster for a Tokyo Metropolis test site (Hori, et al., 2018). Fragility or vulnerability curves and finite element methods were used to define and generate hazard scenarios using GIS buildings and soils data. Use of high-performance computing facilities was necessary to run the simulation for a 10 km x 10 km test area. The K computer, Japan's supercomputer was used in the calculations. The authors plan to extend IES as a base for generating social simulations of evacuations.

For pedestrian city scale evacuation with GIS, a very good example is the work of Shimura and Yamamoto, 2014. The authors used multi-objective genetic algorithms to optimize the determination of optimal evacuation routes during earthquake disasters (Shimura & Yamamoto, 2014). Evacuation is evaluated over road network vectors polyline shapefiles. Destination evacuation sites are polygons. Other layers in the model are building footprints and parks. Daytime and night time populations in roads were considered. Population data was generated from several census statistics. Also considered in their study are dynamic conditions that can affect evacuations. The events considered are debris blocking streets and fire. The adopted methodology was an attempt for a quantitative, objective and more realistic approach in the determination of evacuation routes in earthquake evacuation plans.

GIS has also been utilized in the study of affected populations of earthquake disasters. One area is the visualisation and analysis of patterns of post disaster displacements. Tracking displaced individuals has been done using (1) anonymized geo-located mobile phone records and (2) cell tower mobile traffic data (ACAPS, 2013; Bengtsson, Lu, Thorson, Garfield, & Scheeb, 2011; Wilson, et al., 2016; Sekimoto, 2013). Movement data collected from SIM cards and GPS coordinates from mobile devices can be used to estimate the magnitude, distribution and trends in population displacement (Bengtsson, Lu, Thorson, Garfield, & Scheeb, 2011; Kawahata, Mizuno, & Ishii, 2017; Song, Zhang, Sekimoto, & Horanont, 2013).

Mobility of populations in built and open spaces during earthquake disasters can define exposure to risk posed by damage. GIS has been used in modelling population exposure to risk with respect to daily and seasonal variations in building occupancy (Robinson, et al., 2018). Daytime and night time indoor populations of residential and non-residential buildings differ and this was found to affect projections of population loss during possible earthquakes (Robinson, et al., 2018; Ara S. , 2013; Wood, Ratliff, Schelling, & Weaver, 2014; Ara S. , 2014). For disaster research, the representation of the population at any point in time of a day is very important (Harland, Birkin, & Martin, 2014). Exposure of populations to earthquakes, especially for outdoor environments, can be potentially derived from origin-destination, household-travel, or activity surveys (Chapleau & Morency, 2005; Singh, 2005). The very fine temporal resolution or time slices in these surveys are normally hourly intervals for an entire day. This is very useful in establishing the location of populations with high precision at very specific periods within the day. This allows for the creation very fine population exposure and loss models. Different scenarios can be defined based on hourly mobility and therefore account for time related variations in population densities. This can complement the limitation of population census survey data, which normally feature only a static snapshot of household populations. They can only be used to represent night time estimates of residential populations indoors (Harland, Birkin, & Martin, 2014; Batista e Silva & Poelman, 2016).

Synthetic populations are usually generated for use in microscopic models and microsimulations of urban areas (Farooq, Bierlaire, Hurbubia, & Flötteöd, 2013; Philips, Clarke, & Watling, 2017). Synthetic populations are necessary to address data limitations especially due to privacy restrictions. Populations are based on data from census, activity surveys or household travel surveys. GIS has been used to define

the spatial distribution and locations with respect to daily activity and linked land use (McBride, Davis, Lee, & Goulias, 2016). A toolkit has been developed by Kevin et al. for generating spatially explicit synthetic populations (Chapuis, Taillandier, Renaud, & Drogoul, 2018). It works directly with GIS data and can produce synthetic populations at varying spatial scales with acceptable realism. The tool is promising and can be very useful for fine grained pedestrian evacuation microsimulations.

3.2.3 Limitations of GIS

The power of GIS is its ability to create accurate representation of the real world (Goodchild M. , 2005). However, GIS is traditionally static. Spatial information has been collected and processed as snapshots of phenomena. Much of the focus of development and use in GIS has been on the spatial aspect at the expense of the temporal dimension (Brown, Riolo, Robinson, North, & Rand, 2005). It is not fully capable of handling time or complex dynamic temporal information. One strategy that can be adopted to address this limitation has been to include time as an additional attribute to layers. This makes spatio-temporal visualisations possible, and to some extent, geosimulations[11] of complex phenomena (Marceau & Beneson, 2011). The issue about handling time in GIS can be resolved as the technology progresses.

Gahegan, in his critique of GIS, said that the research focused on GIS and time has revolved around providing temporality for objects (Gahegan, 2017). Further he stressed that current GIScience ontology favoured the primacy of objects rather than process. He pointed out that when GIS is able to represent processes that give rise to objects, or simulate processes acting on objects, GIS will be a more powerful modelling environment for complex and dynamic systems. An example of an ideal GIS, according to Gahegan, is one that integrates physically based and socially based models.

Another limitation of GIS, also owing to its static heritage, is that it lacks operators that explicitly describe the movement of features (Brown, Riolo, Robinson, North, & Rand, 2005). This is a problem especially for dynamic microscopic pedestrian evacuation models, where navigation of space is important in the realistic evaluation (Hussein, 2016). When fine scales are used in modelling, where streets, buildings, and parcels of property, questions on local dynamics of movement become more significant than location (Batty, 2003). In this context, according to Batty, geometry becomes key, and together with dynamics, this poses important challenges for GIS. This is a concern as the way geometry is handled with movement has not been a focus of spatial analysis. Dynamics is the Achilles heel of geography and GIS (Batty, 2003).

Another great issue is the apparent lack of GIS data. For example, generally there is insufficient data related to seismic vulnerability at the urban scale (Senouci, Beck, Farsi, & Cartier, 2018). There are many issues on GIS data that are becoming part of general public concern. Issues include: (a) availability, (c) quality, (d) completeness, (e) reliability, (f) rights, and (g) privacy. On the technical side, these are (a) collection, (b) models, (c) methodologies, (d) algorithms, (e) technical infrastructures. In the context of crisis, the issues in GIS are: (a) immediacy, (b) relevancy, and (c) sharing (Cai, Sharma, MacEachren, & Brewer, 2006). Many of these issues are being addressed and some progress is being made as technologies and policies on data improve. The efforts to share geospatial data in open formats and the use of open platforms can help resolving this problem of data for disasters (Poorazizi, Hunter, & Steiniger, 2015; Goetz & Zipf, 2012).

[11] Geosimulation is a simulation methodology with explicit attention to space and geography (Benenson & Torrens, 2004). According to Benenson and Torrens, with geosimulations, urban systems are considered as aggregations of spatially non-modifiable elements, or objects at atomic resolutions (i.e. people as individuals, buildings, etc.). Directly quoting the same authors "geosimulation models concentrate on the collective outcomes of interactive behavior, treating observed patterns and phenomena at above-individual levels of urban hierarchy as emergent".

There is however an inherent problem in how GIS data is collected, still, with respect to time. Most collection campaigns or activities record or collect snapshots of phenomena. What still remains to be seen, especially in the context of disasters, are full recordings or continuous collections of data about phenomena, as they happen, and during the entirety of a phenomena's occurrence. In particular, data with high fidelity and fine temporal and spatial resolutions are needed for disaster events. Availability of this data, impacts modelling and most importantly the validation of results from dynamic models. Data points from current geographic data might be not be enough to fully develop and validate models and evaluate results of dynamic simulations.

Agent based modelling and pedestrian simulations are discussed in the next section.

3.3 Agent based models

3.3.1 Agent based modelling, social simulation, pedestrian simulation

A computational *agent* is a discrete entity defined in terms of its attributes and behaviours. Wooldridge and Jennings describe agents to be autonomous, operating without direct human intervention, having social ability (i.e. interacts with other agents), able to perceive and respond to their environment, and exhibiting goal directed behaviour (Wooldridge & Jennings, 1995). Gilbert and Troitzsch add that agents can be constructed to simulate some simplified aspects of human intentions which can include beliefs, desires, motives and emotions (Gilbert & Troitzsch, 2005). Multi-agent systems (MAS) allow heterogeneous agents to cooperate according to complex modes of interaction (Ferber, 2007). MAS have been used to investigate several phenomena and have proven to be a powerful tool for modelling in the social sciences and other related fields (Kravari & Bassiliades, 2015).

Agent based models are good examples of process models which make use of sophisticated representations of time and behaviour (Brown, Riolo, Robinson, North, & Rand, 2005). However, according to Brown et al., process models have traditionally been implemented at the expense of sophisticated representations of space and spatial relationships. Current developments show agent-based models and tools are now being been integrated with GIS (Drogoul, et al., 2013; Taillandier, Amoroux, & Drogoul, 2010; Amoroux, Chu, Boucher, & Drogoul, 2007; Daudé, et al., 2019). This integration gives modellers the ability to link agents to actual geographic locations (Crooks A. T., 2006). According to Brown et al., the "rich temporal representations of agent-based models complement the spatial data representations of GIS" (Brown, Riolo, Robinson, North, & Rand, 2005). However, on the integration of GIS, Crooks and Castle noted the following issues: (1) quoting Gilbert, the integration is still a difficult process (Gilbert N. , 2007); (2) many considerations on data in particular the type, how to use, and how agents would interact with the data, and (3) large computational overhead when dealing with thousands of agents interacting with vector and raster features (Crooks & Castle, 2012).

Among the MAS architectures, a belief, desire, and intention (BDI) approach is ideal for modelling people (Adam & Gaudou, 2016). From Adam and Gaudou, BDI attempts to capture the common understanding of how humans reason with: beliefs which represent knowledge of the environment and the agent's self or internal state, desires or the goals the individual decides to achieve, and the intentions which describe a set or sequence of steps needed to achieve the determined goals. Still from the same authors, BDI architecture allows an agent to *err*. BDI enables agents to have subjective representations of the environment in terms of beliefs that can be incomplete, flawed or different from other agents. Also, agents can communicate and reason with other agents, have the ability to explain behaviours, exhibit emotion, able to internalise norms, and capable of making independent decisions.

3.3.2 Social simulation of evacuations

Agent based modelling has been useful in modelling complex and dynamic systems. According to Crooks et al., ABM is fast becoming a dominant paradigm in social simulation (Crooks, Castle, & Batty,

2007). Social simulations deal with the modelling of large populations of synthetic agents that represent humans or groups of humans. The entities that are modelled are ideally equipped with attributes and behaviours that representative real humans in the scenarios being modelled (Balke & Gilbert, 2014). In order to increase the accuracy of social simulations, models need to be as close as possible to reality (Bourgais, Taillandier, & Vercouter, 2018). This requires giving the agents social features.

Agent based models have been implemented to simulate human social behaviour during evacuations. Some of the models are implemented guided by data from observations and surveys. Social theories are often not explicitly stated. The succeeding paragraphs describe different models and the social theories used to model agent evacuation behaviour. The models are likewise evaluated with respect their level of use of attachment and social attachment theory either explicitly or implicitly. To do this the following indicators are sought: (1) mention of social relationships, (2) existence of social groups, (3) affiliation and proximity seeking behaviours towards familiars or attachment figures during danger.

3.3.2.1 Social force model

The social force model (SFM) from Helbing et al. is a very popular model for pedestrian behaviour during panic and normal situations (Helbing D. , Farkas, Molnar, & Vicsek, 2002). In the social force model, pedestrians are modelled as particles, with motion governed by laws akin to and conforming to Newtonian laws of physics. Helbing et al. define social forces which can be repulsive or attractive forces, similar to relationships between human agents and human with their environment. Notable parameters in the model for normal situation include: (1) a "territorial effect" which is a repulsive force that maintains the distance between pedestrians. This territorial effect is defined by the strength of interaction and repulsive interactions which are culture dependent. (2) A social force for attractive interactions towards objects such as window displays, and a (3) social force for joining behaviour, such as for families, friends or tourist groups. This parameter makes sure that individuals in a social group re-join the group when separated by other pedestrians. This parameter can be seen as analogous to the close bonds between family members, friends or the pull of a safe area. The panic situation is governed by another equation. Social forces for panic situations include the (1) physical interaction forces which are defined by a body force and sliding friction force, and (2) repulsion to boundaries or walls and other obstacles.

The model is commonly used for indoor scenarios especially along narrow pathways and bottlenecks. It is often used as a base model and modified to suit the objectives of other studies. Simulation results of Helbing et al. replicated several empirical observations of scenarios. For normal situations, they were able to replicate (1) lane formation, (2) oscillations at bottlenecks, (3) dynamics at intersections. For panic situations, the model replicated (1) freezing by heating effect, (2) transitioning to incoordination due to clogging, (3) faster is slower effect due to impatience, (3) phantom panics, and (4) ignorance of available exits. Simulation results according to the authors suggest that the optimal behaviour during escape situations is a suitable mixture of individualistic and herding behaviour.

With respect to social attachment theory, SFM has provision for social bonds of social groups in the joining behaviour parameter. However, the discussion on the social force parameters is very general, and needs further clarification. Some examples of points to be clarified are (1) the definition of bond strength with respect to social relationships, (2) the social contexts in which attraction or repulsion is activated, or (3) how to quantify parameters such as the effect of culture. Also, the SFM is not able to explain the social factors and motivations for movement. Other than panic, the attraction forces were not supported with other social theories. The pedestrian agents are also non-cognitive with only the binary choices of attraction or repulsion. The modelled moment is during evacuation or egress, no pre-evacuation behaviours are defined. The social forces however, as used in the paper are applied to explain behaviours and flow of individuals in indoor, narrow passageways and bottle necks. It is not stated how the model will be applied with respect to evacuation in large open spaces.

3.3.2.2 Roan's model

Roan developed an agent-based simulation model based on the study of human behaviour from fire investigation reports (Roan, 2013). The work demonstrated panic and to some extent emergent norm theories by simulating trampling during stampedes. The simulation is a grid-based agent base model. For agent navigation it used A* shortest path search and the Primary Queue Flood fill algorithms. Pedestrian were only categorised based on age as child, adult and elderly. No social relationships were defined to avoid complexity of behaviour and modelling methods. Other agents are door and fire/smoke. The model was used to recreate and test indoor fire scenarios from previous deadly fire events. These are the (1) Gothenburg dance hall, (2) Rhode Island nightclub and (3) Helmet chicken processing plant. Strategies of agents tested included (1) evacuating through main exits, (2) communicating with others after noticing fire; panic behaviour starts in some agents, (3) evacuating through windows, (4) finding shelter, (5) search for alternative routes, and (6) escape from fire or smoke. To validate the results, casualty statistics from the model were compared with the casualty reports from the fires and a visualisation of the location of deaths in the simulated spaces. Some level of agreement was achieved between model results and fire report with respect to the number of deaths, injuries and location of deaths (e.g. main exit, hallways).

Roan's model is a good example of the application of panic for fire events that occur in enclosed and unfamiliar locations. In these events, panic is usually used to describe people's reactions. The main strategy to survive is to head for the nearest exit, which unfortunately, causes more deaths due to stampedes and trapping. People usually seek to exit through the door from which they entered. Not considering to include social groups, in the model, may seem appropriate, in the context of considering only panic as the main influence of behaviour. Panic implies the breakdown of social structure or social norms. Also, in considering the chaotic physical environment of occupants during fires, it might be difficult to identify and seek others due to the dark environment or presence of smoke. However, for social gatherings and venues, people of the same social groups normally stay in one location. Adding social attachment in the model can make it more realistic.

3.3.2.3 Earthquake Pedestrian Evacuation Simulation (EPES)

Earthquake Pedestrian Evacuation Simulation (EPES) model pedestrian (children, adult and disabled) behaviour during an earthquake (D'Orazio M. , Quagliarini, Bernardini, & Spallazi, 2014b). The model implements a modified version of Helbing's social force model to include the behaviours derived by the authors from the study of evacuation video tapes. The social force model is modified by the authors to reflect panic and evacuation conditions during an earthquake. Herding and collision avoidance are replicated in the model. The combination of ABM architecture and social force approach is seen to produce more realistic simulations. Social attachment is implemented through the bonds that maintain cohesion in pedestrian groups (clans), and the attraction to safe areas. Social attachment theory here is not directly or fully implemented but can be considered as implied.

Pedestrian motion decisions are based on (1) avoiding obstacles and other people, (2) necessity to follow group behaviour, (3) maintenance of own desired speed, and (4) a drive-to-target term. The benefit of the model is its specificity to the earthquake scenario. It includes pre-evacuation and evacuation behaviours, as well as algorithms to calculate paths towards safe areas. Pre-evacuation behaviour are connected to the EMS98 intensity scales, with percentages defined per intensity values. Modified parameters from the social force model are: (1) drive-to-target force which defines (a) attraction to safe areas, (b) herd behaviour (c) influence of collective velocity, and (d) formation of groups; (2) Attractive forces which define (a) attraction for group bonds, formation of evacuation groups; (3) Repulsive force, which is a mechanism used to (a) avoid contact and maintain safe distance from hazards such as buildings, debris, or conversely (b) maintain safe distance to safe areas, shelters. The model also defines the criteria for the formation of damage in the area called mean damaged grade based on the vulnerability and ductility index of the building combined with the EMS magnitude. The software implementation of

EPES features a GIS environment built in the TAJ development environment, using Java IDE-Eclipse translated in the Alan language.

Similar to the Helbing's social force model, EPES, provides a general but very technical framework and gives equations for agent attraction and repulsion to elements in the crisis environment. EPES is appropriate for the seismic crisis scenario. Further elaboration on the social aspects particularly attachment expressed in the clan bond and attraction parameter are needed to explain further pedestrian motivations for movement. Social attachment theory, when used as the analysis framework to explain evacuation behaviour can further add to explaining pedestrian motivations for proximity seeking actions.

3.3.2.4. Evacuation Simulation with Children, Authorities, Parents, Emotions and Social Comparison (ESCAPES)

Evacuation Simulation with Children, Authorities, Parents, Emotions and Social Comparison (ESCAPES) is an airport evacuation tool focused on the spread of knowledge, emotional contagion and social comparison (Tsai, et al., 2011). The main social theory implemented is Social Comparison Theory (SCT). SCT explains the tendency of people who face uncertainty to copy the actions of other people who are in close proximity. Notions of connectivity and neighbourhood are introduced by the authors in ESCAPES. The focus of the simulations are families composed of parents and children. Social attachment and social attachment theory are expressed in the seeking behaviours of family members during evacuations. Agents in ESCAPES include travellers, families and authorities. Emotional, informational and behavioural interactions are implemented with the Belief Desire and Intention architecture. Agent in the model have access to 14 available behaviours. The interaction between agents include: (1) spread of knowledge, which includes the knowledge of an exit locations and knowledge of the event (2) emotional contagion and (3) social comparison. During evacuations, parents immediately seek children before proceeding to an exit. Children, while travelling slower, exclusively follow parents (Tsai, et al., 2011). ESCAPES also feature the calming effect of the presence of authorities during dangerous situations.

3.3.2.5 Exitus

Exitus focuses on the evacuation of individuals with mobility impairments (Manley, 2012). Agents include no-disabled, motorised and non-motorised wheelchair users, visually impaired, hearing impaired and stamina impaired. This model addresses a need for more models on the evacuation of the mobility impaired. Exitus implements Helbing's Social Force Model and Hall's Proxemics theory (Hall, 1990). Social attachment is expressed through seeking and helping behaviours in assisting the mobility impaired. Attachment is also expressed in the interpersonal distances defined in proxemic theory. Experiments with different dimensions of wheelchairs were conducted to investigate (1) clogging effect in hallways and stairwells, and (2) use of elevators. Model evacuation time was likewise tested with Exitus in different scenarios such as airport and sports arena evacuation scenarios.

3.3.2.6 Multi-Agent Simulation for Egress Analysis (MASSEgress)

Multi-Agent Simulation for Egress Analysis (MASSEgress) simulates individual behaviour through sensing, decision making, behaviour selection and motor control. Interaction between agents define social behaviour. Panic and emergent norm theories are implemented. This results in queuing, competition, herding, and leader following behaviours (Pan, 2006). MASSEgress provides a realistic way of perceiving other agents and obstacles in the environment using the concept of a view volume, which consist of a view angle and a perception range. A person is visible when inside the view volume and not occluded by any obstacle. The decision-making process is described by (1) familiarity, (2) decision making type, (3) urge to exit, (4) stress threshold type, and (5) herd factor. Behaviour selection is governed by decision rules. Different decision rules and styles are constructed for different personality types. Steering behaviours in MASSEgress includes: (1) random walk; (2) collision avoidance, (3) seek,

(4) negotiation or exchanging information, and agreement, and (5) target following. Social behaviours in MASSEgress are sensitive to (1) individual behaviour, (2) group size, (3) individual behaviour within a crowd, and (4) effects of geometric constraints.

MASSEgress has been used to simulate egress from small indoor to large venues. This includes evacuation simulations for (1) a small room, (2) department store, (3) night club fire, and (4) a university building. The model was envisioned to incorporate characteristics of social and organisational interaction to extend its ability in modelling human behaviour.

3.3.2.7 Social Agents for Egress (SAFEgress – 2014)

Social Agents for Egress (SAFEgess-2014) simulates evacuation behaviours of occupants affiliated to social groups, defined by a unique structure and group norm (Chu, Parigi, Law, & Latombe, 2014). Agents are defined by static and dynamic profiles. Static profiles include (1) physical characteristics (e.g. age, gender, body size, speed, personal space), (2) familiarity with the environment, (3) knowledge of exits, (4) group affiliation, (5) social order and, (6) assigned roles. Dynamic profiles include: (1) location, (2) urge, (3) knowledge, (4) visible group member, and (5) neighbouring agents. Factors implemented include group intimacy, leadership and separation distance. High intimacy groups include couples or families. Lower intimacy groups can represent co-workers. SAFEGress has been use in indoor evacuation experiments. The authors observed interesting results and egress patterns when visual and cognitive abilities were provided to agents. Although not directly stated in the paper, social attachment is applied in the model evidenced by the existence of social groups, and use of familiarity, and intimacy in agent profiles.

3.3.2.8 Social Agents for Egress (SAFEgress – 2015)

Social Agents for Egress (SAFEgess-2015) implements the modelling evacuation of social groups and emulates human capabilities of perception and navigation (Chu M. L., 2015). Different agent behaviours modelled include: (1) following perception to evacuate; (2) following knowledge to evacuate; (3) navigating with group members; (4) navigating with entire social group; (5) following the crowd to evacuate; and (6) following authority's instructions. In a simulation step, agents perceive the environment, interprets the urge to evacuate, and decides a behaviour through a tiered reasoning process, and interpret the action. Agents, when with a social group, tend to adopt longer routes and take more time to exit. SAFEGress allows the testing of different behavioural models to decouple the effects of individual and social factors related to egress performance. Strength of affiliation to social group is defined by an agent's group compliance attribute. Group influence and intimacy level is the parameter that describes the social group. Simulations results with SAFEegress showed that group size and type, affect how fast consensus to evacuate is achieved. Larger group sizes take longer to decide. Groups with high intimacy likewise arrive at decisions faster. With respect to the urge to evacuate, individual members of a group adopt the highest urge among visible group members. This makes agents evacuate sooner that when alone. SAFEGress has been tested for indoor scenarios like a museum and a stadium. Social attachment is embedded in SAFEGress and is evident from the use of social groups and the concept of intimate groups. Social attachment theory likewise has been mentioned by the author with respect to people attaching to familiar places and people during disasters. This likely helped in the development of the theoretical framework of the SOLACE model.

3.3.2.9 Social Identity Model Application (SIMA)

Social Identity Model Application (SIMA) implements the social categorisation and social identity theories with a focus on helping behaviour. In particular, the focus is helping others or strangers. It has two main components implemented in sequence: establishing social identity then helping behaviour. Pedestrians who do not share a social identity with a group heads straight for safety without caring for others (Sivers I. v., et al., 2016). From Drury et al., "social identity could operate as a function of the (shared) threat when people experience and emergency" (Drury J. , et al., 2009). Also, from Drury et al.

shared identities promote supportive behaviours during emergencies. SIMA was used to recreate the scenario of a London Underground bombing event. The results showed helping behaviour and agents formed orderly queues to evacuate. The simulation produced similar results matching survivor accounts. This is relevant, as this further validates the role of social attachment theory. As strangers are able to form a new social group triggered by the shared identity from a disaster, the newly formed social group, and its members become new attachment figures. Closely bonded groups are known to help each other, and likewise, produce orderly queues during egress.

3.3.2.10 Okaya and Takahashi's Robocup Rescue

Okaya and Takahashi's RoboCup Rescue simulation is an evacuation model based on the BDI architecture and Helbing's Social Force Model. The model developed revolved around the role human relationships and its effects on (1) states of BDI at each timestep, (2) agent intentions such as altruism are integrated in the social force model and (3) other physical factors. This was developed using the RoboCup Rescue Simulation v. 1 (RCRS) platform (Okaya & Takahashi, 2011). Agents in the model are adults, parents and children. Agents are able to establish the belief, of risk to themselves, or with respect to the family; have the desire to avoid the risk, perform the intention to evacuate or seek refuge or hear guidance. The intention of parents, in the family context, is to seek and evacuate with their child. Child agents always have the intention of following parents. Results showed delayed evacuation times for parents who take care of their children. The results of evacuation simulations reveal (1) family members evacuate together; (2) guidance during evacuation affects crowd behaviours; and (3) evacuation takes more time when congestion occurs. This model implements the social attachment from the presence of family agents and seeking behaviours.

3.3.2.11 Liu et al.'s model

Liu et al. presented a framework coupling building and human behaviour in an earthquake scenario (Liu, et al., 2016). The model tries to extend ABM research by integrating engineering models of structural hazards. Physical modelling of the crisis environment employed finite element methods. Social group formation and strong social relationships are defined by agents sharing the same home base. The strength of relationship to neighbour agents is lesser. Group formation is facilitated by the agent's willingness to form groups and is defined by a function. Agents are also able to switch groups, when a group that it shares a stronger connection with is encountered. Group behaviour includes grouping and travelling. Herding behaviour is done by individuals or groups not familiar with a building. Rescuing behaviour is the expression of an agent's altruism. Social algorithms included in the egress model are grouping, herding, rescuing and information sharing. Results showed that for all damaged scenarios, social behaviours produced significant delays in evacuation. Results of simulation found that grouping behaviours increase evacuation time. The authors noted from their results, that the mean evacuation time can be underestimated by as much as 20%, if social behaviours are not included. Attachment and social attachment are implemented implicitly in the model.

3.3.2.12 Lou et al.'s model

Lou et al. developed a simulation for normal and emergency scenarios for a Singapore train station (Lou, et al., 2008). Social group and crowd related behaviours are modelled from social psychology, such as social attachment theory. The authors consider a two-stage cognitive process in decision making. This includes (1) situational awareness grounded on expectations about people, social roles and events, and triggered by external stimulus, (2) consequent changes in internal attributes influence feelings, social states and physical condition. Individual agents are categorised into (1) roles, namely staff, civilian or tourist; (2) age groups, as child, adult, and elderly; (3) strength of social relationship as normal tie, strong tie, or individual, (4) personalities: altruist, common person, or avoidantist. Modelled behaviours include: wander, flock, evade, lead, follow, seek, individual escape, group escape, idle, help, and run aimlessly. In the normal situation, people wander individually or as a group.

3.3.2.13 Simulation of Transient Evacuation and Pedestrian Movements (STEPS)

Simulation of Transient Evacuation and Pedestrian movements (STEPS) by Mott MacDonald Ltd is a microsimulation tool for pedestrian movement (Waterson & Pelliser, 2010). This can be used for normal and emergency conditions (evacuation mode). Agent attributes include free walking speed, awareness, patience, association to other members (a 'family' group), and pre-movement time. This model implements attachment and social attachment theory.

3.3.2.14 Ta et. al.'s Model

Ta, et al. presented an excellent and very detailed formalisation of group behaviours and actions during emergency situations based on social theory (Ta, Gaudou, Longin, Ho, & Nguyen, 2017). The model accounts for social relations in the defining of people as a group, attributes of groups, the their behaviours and actions according to group type. Effects of emotion and group behaviour on evacuation decision making were considered. Agent behaviours within social and physical groups were formalised. Also, included in the model, are the influence of communication, knowledge and guidance provided by authorities (leaders, security agents). This model implements the attachment and social attachment theory.

3.3.2.15 Wang et al.'s Model

Wang et al. developed an optimisation method for emergency evacuation and considered social bond effects (Wang, Luh, Chang, & Marsh, 2009). They considered the disorder and blocking effects caused by social bonds during evacuations. According to them, close bonds such as with family members and familiar colleagues help maintain order in evacuations. This is demonstrated by queuing behaviours that make evacuations smooth and efficient. Loose bonds between unfamiliar individuals can increase competitiveness resulting in pushing and shoving behaviours. This triggers disorder, blocking of exits and eventual delays in evacuation. The model implements social attachment theory.

3.3.2.16 Zia et al.'s Model

Zia et al.'s model is implemented as a city scale evacuation simulation using the leader-follower strategy (Zia, Farrahi, Riener, & Ferscha, 2013). Proximity and the level of knowledge of a leader influences the following behaviour of the agents. Running the model on a high-performance environment ensured success in simulating a large population of agents. The model used a cellular automata or a grid-based model of the city to facilitate processing. The authors conclude that scale becomes a real issue when the population of agents includes billions of space agent and millions of mobile agents. An additional advice is to minimise interactions of moving agents to tolerable limits to ensure completion of simulations. This however will constrain the success of large-scale evacuation social simulation with cognitive and social agents implemented with BDI.

3.3.2.17 Adam et al.'s Model

Adam et al. implemented the BDI architecture with the Tactics Development Framework (TDF) to model evacuation and protective behaviours of residents during bushfires (Adam C. , Danet, Thangarajah, & Dugdale, 2016). Behaviours implemented in the model can be categorized as attachment behaviours are (1) defend property (stay and defend it), (2) stay alive (protect self and family). Also, place attachment can be seen in the actions of a civilian agent which are shelter at home, defend property, monitor house, prepare property and fight fire.

3.3.2.18 Agent-based Model for Earthquake Evacuation in Lebanon (AMEL)

Agent-based Model for Earthquake Evacuation in Lebanon (AMEL) is a model and prototype of a simulator showing pedestrian movements following different human behaviours after an earthquake (Truong, Beck, Dugdale, & Adam, 2013; Beck, Dugdale, Truong, Adam, & Colbeau-Justin, 2014). The behaviours were synthesised from survey results and focused on people's mobility. Leader-follower behaviour was implemented. Agents are able to perceive other agents, move to safe areas and follow leaders.

A summary of the reviewed models is shown in Table 16. The table details the model, dominant social theory used, types of the social agents, and the implemented behaviours. Summaries of technical details for each model are shown in Table 17, Table 18, Table 19, Table 20 and Table 21. The legend used in the table includes: (Y) for implemented, (*Y), for mimicked or simulated, (-) for not implemented, and () blank for not specified.

Table 16 ABM implementing social theories for evacuations

Model	Theory	Agents	Behaviour
EPES (D'Orazio et al., 2014b)	Panic, Social Attachment	Pedestrian (child, adult, disabled), clan	Herding
ESCAPES (Tsai et al., 2011)	Social Comparison, Attachment, Social Attachment	Family members, travellers, authorities	Follow parent, drag into shop, find child, find the other parent
EXITUS (Manley, 2012)	Social Force Model, Proxemics Theory, Attachment, Social Attachment	Non-disabled, motorised wheelchair users, non-motorised wheelchair users, visually impaired, hearing impaired, stamina impaired	Helping
(Liu et al., 2016)	Social Attachment	Adult, elderly	Grouping, herding, rescuing, and information sharing
(Luo et al., 2008)	Social Attachment	Staff, civilian, tourist, child, adult, elderly	Wander, flock, evade, lead, follow, seek, escape (individual, group), idle, help, run aimlessly
MASSEgress (Pan, 2006)	Panic, Emergent Norm, Attachment, Social Attachment	Individuals	Competition, queuing, herding, leader-follower
Robocup Rescue (Okaya and Tokahashi, 2011)	Panic, Social Force, Social Attachment	Adult, parent, child	Group evacuation, guidance
SAFEgress-2014 (Chu et al., 2014), (Chu and Law, 2013)	Social Attachment	Family, couple, co-worker	Group evacuation
SAFEgress-2015(Chu, 2015)	Social attachment	Building occupants	Navigating with group, following (crowd, authority)
SIMA (Sivers et al., 2016)	Social Identity, Self-Categorisation, Attachment, Social Attachment	Pedestrians	Helping
Social Force (Helbing et al., 2002; Helbing and Johansson, 2013)	Panic, Social Force, attachment, Normative	Pedestrian, family	Panic, herding, queuing, cooperation, self-organisation
(Roan, 2013)	Panic, Emergent Norm	Individuals	Panic, trampling, queuing, self-organisation
STEPS (Waterson and Pelliser, 2010), (Caliendo et al., 2012)	Normative, Social Attachment	Family, friends	Walking, association, evacuating together
(Ta et al., 2017)	Panic, Social attachment	Customers, leaders, family, friends, colleagues	Leader-follower, seek members, maintain group, share information
(Wang et al., 2009)	Social attachment	Family	Queuing, pushing and shoving
(Zia et al., 2013)	Social attachment	Pedestrian	Leader-follower, seek leader

(Adam et al., 2016)	Social attachment	Civilian, family, property	Stay alive (protect self and family), stay and defend (property), take cover in shelter
AMEL (Truong et al., 2013; Beck et al., 2014)	Social attachment	Pedestrians	Imitate others (Leader-follower), seek, same activity (move, stay in place), change activity (move to safe area, unsafe area), stay in place)

Table 17 details several implementation parameters related to the models. Fields in the table describe: the parameter used to facilitate social interaction, Social Bonds; type of disaster or crisis or Hazard; if the model concerns indoor Occupants or Pedestrians; the number of agents tested, Population; use of BDI or Decision tree; use of spatial data, GIS, or generic vector data, CAD; the spatial extent, if within building, city block or city, Scale; if implemented in Vector, or Grid formats; implements or results as Individual, Group or Crowd; sets up the risk environment such as fire, earthquake or flood, in the Hazard field; and the simulation Platform used. Table 18 is a continuation of Table 17.

From Table 17 to Table 18 it can be seen that: (a) social bond is assigned using parameters usually defined by group ID, (b) generic models of evacuation are common, (c) fire is more commonly modelled than earthquakes, (d) most model indoor occupants and few outdoor pedestrians, (e) small population of agents are modelled, very few model large populations, (f) BDI is used by some models, most use decision trees, (g) generic vector and CAD data are used for indoor evacuations, while GIS for district to city scale implementations, (h) most employ a grid, (i) individual agent behaviours are mostly modelled with some having attributes for group and crowd behaviours, (j) most hazards are not modelled as dynamic environment objects but indicated by alarms or cues, and (k) most platforms used require specialised computer science skills.

Table 19 presents the type of agents in the models. The types of agents are attachment figures in social contexts and presented as individuals, groups, and non-human entities. Human agents include adult, elderly, disabled, injured, child, spouse, parent, sibling, kin, pet, friend, colleague, authority, and stranger. Social groups include: family, friends, colleagues, authorities, and strangers. Non-human agents include place, object, task and information. This table shows that most models have attachment figures that (1) are individual: adults, children, elderly and the disabled. (2) within groups of families, friends and colleagues, (3) evacuate to safe places (exits, designated safe areas). Seldomly modelled are objects (e.g. phones, bags, property), and tasks (e.g. chores, work, driving).

Table 20 shows the different types of behaviours implemented. In models, agents are able to Lead, Follow, Seek, Help, Freeze, Wait, Manage property, Ignore, Mill around, Regroup, Flee, Protect, Seek cover, Stay in place, Continue task, Grab objects, Inform, Go to exit/safe area, Rescue, be Altruistic/cooperative, Do not know what to do, Wander, Herd, Compete, Queue, Panic, or have Normal behaviour. Most of the models implement the lead, follow, seek, helping and herd behaviours. Detailed pre-evacuation behaviours are seldom implemented in models. These include: freeze, wait, manage property, ignore event, mill around, protect others, seek cover, stay in place, continue tasks and grab objects

Table 21 shows other complex concepts implemented. These include: emotion, contagion, communication, decision making, norms, trust, inclusion of transport network, rescue, institutional response, physical modelling of earthquake effects, use of guidance (such as for alerts/alarms, and wayfinding e.g. signage), stress, patience, knowledge, and experience, and cascading Effects: tsunami, fire, and other cascading effects.

The reviewed models reveal several observations. The first observation is that most of the models implement, attachment and social attachment, in an implicit manner. This can be seen from the use of

social groups, relationships between agents, and the seeking behaviours of agents. It is only the model of Lou et al., 2008, which explicitly stated their implementing social attachment theory.

The second observation is that Helbing's social force model is often used to implement attraction and repulsion between agents especially when social bonds are difficult to quantify. The equations and parameters in the social force model are generic and have been applied in many models. Having being based on the kinetic energy equations in physics, it has been successfully used to define the motion of agents in models and simulations (Wang P. , 2016). Using the equation and parameters need to be clarified, or contextualised to the type of force being defined. For example, models, such as EPES, Exitus and that of Okaya and Takahashi, actually modify and refine the definitions of the social force model parameters to meet the needs of the models. The main critique to the social force model is the particle like behaviour of agents, and the lack of cognitive abilities of agents. In reality, people can stop motion, and change direction. To add cognitive features to the particle-like (or particle only) features of the social force model, BDI has been integrated in Okaya and Takahashi's RoboCup Rescue model.

The third observation is that several of the models do not account for the fine differences in individual characteristics such as age, roles (e.g. parent, child), membership in groups, mobility and impairments/disability, in defining heterogeneous populations. EXITUS is the only model that focused on disability. EPES also had disabled agents as part of the population. SIMA included agents with injuries. Elderly agents are included in EPES, Liu et al., SAFEgress, and Roan' model. Parental roles are featured in ESCAPES, Lou et al., and RoboCup Rescue.

The fourth observation is that most models only address indoor evacuations, at the scale of a room, building floor, or large venues such as stadiums and concert halls. This can be due to the limits imposed by computing resources. Also, this can be due to the focus of most of the models, which evaluate and investigate past disaster events such as fires, stampedes and terrorist attacks that occur in indoor environments. Knowledge and data accumulated in these areas, particularly in fire disasters, support the development of models.

The fifth observation is that pre-movement or pre-evacuation behaviours are not considered in the models. Detailed pre-evacuation and evacuation behaviours need to be considered to have a better estimate of total evacuation time. This observation is particularly true for egress models modelling panic situations. Examples are social force, EPES, ESCAPES, SAFEGress, MASSEgress. This can be due to the focus of the models on egress speeds or movement towards exits. Adding cognitive features to egress models, such as with BDI, can provide agents with the menu of actions that can define pre-evacuation actions.

The sixth observation is that most interactions are only with other human agents. Behaviours should also account for interactions with non-human attachment figures such as places, objects, tasks and information. These interactions improve models as it can explain actions such as retrieving objects, preferring to stay in place, etc.

The seventh observation is that most of the models are implemented using grids (cellular automata) and are very mathematical using complex equations.

The eight observation is that real geographic data for modelling large areas are seldom used.

The ninth observation is that the BDI architecture can be used to model more complex dynamics and behaviours.

Lastly the tenth observation is that the models focused more on human agents. There was a lack of discussions on how the risk scenario and environment agent (e.g. building vulnerability, spread of fire) were set in the models.

3.4 Summary of the chapter

The chapter presented the efforts in developing realistic microscopic pedestrian evacuation simulations during crisis. Achieving realism requires the integration of geographic information and agent based social simulation and modelling. The two domains complement each other in creating the spatial and temporal fidelity and resolutions needed to recreate the dynamic social processes in crisis evacuations. Agent based modelling facilitates the creation of cognitive and social agents that interact with space.

Social attachment is presented as the underlying social theory used in the presented evacuation social simulations and models. In the models, social attachment was implicit with respect to the existence of social groups defined by bonds such as family, friends, colleagues and strangers. The mechanism for social interactions however are governed by other more dominant social theories such as social force, panic, social identity theories etc.

SOLACE advances the state of the art by explicitly focusing on social attachment, which facilitates the microscopic social interactions during pedestrian evacuations. The SOLACE cognitive/social agents are situated in an earthquake crisis environment modelled using geographic data. The effect of social attachment on evacuation will be tested with SOLACE using different scenarios.

Table 17 Model Implementation

Model	Social Bond	Hazard	Occupant	Pedestrian	Population	BDI	Decision- tree	GIS	CAD/vector	Scale	Vector	Grid	Individual	Group	Crowd	Hazards	Platform
EPES (D'Orazio et al., 2014b)	Cohesion ($C_{ij,b}$), clan bond, shared evacuation target bond	Earthquake	Y	Y	1000	-	Y	Y	-	City Sector	-	Y	Y	Y	-	Y	IDE-Eclipse, Alan Plug-in
ESCAPES (Tsai et al., 2011)	Family bond, contagion, mimic others (social comparison)	Generic	Y	-	100	Y	-	-	Y	Building (airport)	Y	-	Y	Y	-	-	OpenSteer (C++), Massive Software
EXITUS (Manley, 2012)	Social force, proxemic threshold	Generic	Y	-	71; 400; 15000	-		-	Y	Building (school, office, airport stadium)	-	Y	Y	Y			C++, MFC library (Windows)
(Liu et al., 2016)	Shared home base defines strong bond	Earthquake	Y	-	259; 450	-		-	Y	Building			Y	Y		Y	NetLogo
(Luo et al., 2008)	Attraction tendency, relationship type, group id	Explosion	Y	-	64	-	Y			Building (train station)			Y	Y			Java 2D and 3D
MASSEgress (Pan, 2006)	Bond to leader, herding factor	Generic	Y	-	980; 350; 420; 2524; 600	-	Y	-	Y	Building, department store, nightclub	-	Y	Y	Y	Y	-	C++, Visual LISP, OpenGL
Robocup Rescue (Okaya and Tokahashi, 2011)	Kin Relationship, altruism (f_{alt})	Generic	Y	Y	550	Y	-	Y	-	Building (hall), Block			Y	Y		-	RoboCup Rescue Simulation v.1 (RCRS)
SAFEgress 2014 (Chu et al., 2014), (Chu and Law, 2013	Predefined social group (default leader, intimacy, influence, seeking-property), crowd (social order, roles)	Generic, Fire	Y	-	2002	-	Y	-	Y	Building	-	Y	Y	Y	Y	-	OpenGL
SAFEgress 2015, (Chu, 2015)	Pre-defined social group, social group index, group (compliance, influence, consensus, separation tolerance, intimacy), crowd compliance	Generic	Y	-	100; 1000;350;550;1320	-	Y	-	Y	Building (museum, stadium)	-	Y	Y	Y	Y	-	C++

Legend: (Y) - implemented, (*Y) - mimicked, (-) - not implemented, and ( ) blank – not specified.

Table 18 Model Implementation - Continued

Model	Social Bond	Hazard	Occupant	Pedestrian	Population	BDI	Decision- tree	GIS	CAD/vector	Scale	Vector	Grid	Individual	Group	Crowd	Hazards	Platform
SIMA (Sivers et al., 2016), (Seitz, 2016)	Person sharing social identity parameter $perc_{sharingSI}$, proximity	Bomb attack	Y	-	192; 60	-	Y	-	Y	Train station	Y	-	Y	Y	Y	-	Optimal Steps Model (OSM), Vadere
Social Force (Helbing et al., 2002; Helbing and Johansson, 2013)	Attracting forces $f_{ik}^{att}(t)$, joining behaviour	Generic	Y	Y	200; 90	-		-	Y	Multiscale			Y	Y	Y	-	Java
(Roan, 2013)	Common destination, situation/context	Fire	Y	-	500; 400; 458; 90	-	Y	-	-	Floor (nightclub, dance hall, factory)	-	Y	Y	-	-	Y	Repast
STEPS (Caliendo et al., 2012; Waterson and Pelliser, 2010; Kuligowski et al., 2010)	Association to a 'family group'	Generic, fire	Y	Y	156	-		-	Y	Building, airport, stadium, stations, road tunnel	-	Y	Y	Y	-	-	
(Wang et al., 2009),(Wang et al., 2008)	Social bond (α)	Fire	Y	-	110	-		-		Building	-	Y	Y	Y	Y	Y	FDS+Evac 5.20
(Ta et al., 2017), (Ta et al., 2015)	Group ID (social, physical), roles (leader, follower), knowledge	Fire	Y	-	50	-	Y	-		Building (market)			Y	Y	Y	Y	GAMA
(Zia et al., 2013)	Proximity, leader-follower, knowledge	Generic, flood	-	Y		-	Y	Y	-	City sector, city		Y	Y				Repast HPC
(Adam et al., 2016)	Family, property ownership	Bushfire	-	Y	125 00; 200 K	Y	-	-	-		-	Y	Y	-	-	Y	GAMA
AMEL(Truong et al., 2013), (Beck et al., 2014)	Leader-follower, knowledge	Earthquake	-	Y	100 0	-	Y	Y	-	City district	Y	-	Y	Y	-	Y	GAMA

Legend: (Y) - implemented, (*Y) - mimicked, (-) - not implemented, and ( ) blank – not specified.

Table 19 Attachment figures in the models

Model	Adult	Elderly	Disabled	Injured	Child	Spouse	Parent	Sibling	Kin	Pet	Colleague	Authority	Stranger	Family	Friends	Colleagues	Authorities	Strangers	Place	Object	Tasks	Information
EPES (D'Orazio et al., 2014b)	Y	Y	Y	-	Y	-	-	-	-	-	-	-	-	-	-	-	-	-	Y	-	-	-
ESCAPES (Tsai et al., 2011)	Y	-	-	-	Y	-	Y	-	-	-	-	Y	-	Y	-	-	Y	-	Y	-	-	-
EXITUS (Manley, 2012)	Y	-	Y	-	-	-	-	-	-	-	-	-	-	-	-	-	-	-	Y	-	-	-
(Liu et al., 2016)	Y	Y	-	-	-	-	-	-	-	-	-	-	-	-	-	-	-	-	Y	-	-	-
(Luo et al., 2008)	Y	-	-	-	Y	Y	Y	Y	Y	-	-	-	-	-	-	-	-	-	Y	-	-	Y
MASSEgress (Pan, 2006)	Y	-	-	-	-	-	-	-	-	-	-	-	-	-	-	-	-	-	Y	-	-	-
Robocup Rescue (Okaya and Tokahashi, 2011)	Y	-	-	-	Y	-	Y	-	-	-	-	Y	-	Y	-	-	-	-	Y	-	-	Y
SAFEgress (2014) (Chu et al., 2014), (Chu and Law, 2013)	Y	-	-	-	-	Y	-	-	-	-	-	-	-	Y	-	Y	-	-	Y	-	-	-
SAFEgress (2015)(Chu, 2015)	Y	Y	-	-	Y	-	-	-	-	-	-	Y	-	Y	Y	-	Y	-	Y	Y	-	-
SIMA (Sivers et al., 2016), (Seitz, 2016)	Y	-		Y	-	-	-	-	-	-	-	-	-	-	-	-	-	Y	Y	-	-	-
Social Force (Helbing et al., 2002; Helbing and Johansson, 2013)	Y	-	-	-	-	-	-	-	-	-	-	-	-	Y	Y	-	-	Y	Y	Y	-	-
(Roan, 2013)	Y	Y	-	-	Y	-	-	-	-	-	-	-	-	-	-	-	-	-	Y	-	-	Y
STEPS (Caliendo et al., 2012; Waterson and Pelliser, 2010; Kuligowski et al., 2010)	Y	-	-	-	-	-	-	-	-	-	-	-	-	Y	Y	-	-	-	Y	-	-	-
(Wang et al., 2009),(Wang et al., 2008)	Y	-	-	-	-	-	-	-	-	-	-	-	-	-	-	-	-	-	Y	-	-	-
(Ta et al., 2017), (Ta et al., 2015)	Y	-	-	-	-	-	-	-	-	-	-	Y	Y	Y	Y	Y	Y	Y	Y	-	-	Y
(Zia et al., 2013)	Y	-	-	-	-	-	-	-	-	-	-	-	-	-	-	-	-	-	Y	-	-	Y
(Adam et al., 2016)	Y	-	-	-	-	-	-	-	-	-	-	-	-	-	-	-	-	-	Y	-	-	-
AMEL(Truong et al., 2013), (Beck et al., 2014)	Y	Y	-	-	Y	-	-	-	-	-	-	Y	-	-	-	-	-	-	Y	-	Y	-

Legend: (Y) - implemented, (*Y) - mimicked, (-) - not implemented, and ( ) blank – not specified.

Table 20 Behaviours in models

Model	Lead	Follow	Seek	Help	Freeze	Wait	Manage property	Ignore event	Mill around	Regroup	Flee	Protect others	Seek cover	Stay in place	Continue task	Grab objects	Inform	Go to exit/safe area	Rescue	altruistic	Do not know	Wander	Herd	Compete	Queue	Panic	Normal
EPES (D'Orazio et al., 2014b)	Y	Y	-	-	-	-	-	-	-	Y	-	-	-	-	-	-	-	Y	-	-	-	-	Y	-	-	Y	-
ESCAPES (Tsai et al., 2011)	Y	Y	Y	-	-	-	-	-	-	-	-	-	-	-	-	-	-	Y	-	-	-	Y	-	-	-	-	-
EXITUS (Manley, 2012)	-	-	-	Y	-	-	-	-	-	-	-	-	-	-	-	-	-	Y	-	-	-	-	-	-	-	-	-
(Liu et al., 2016)	-	-	-	-	-	-	-	-	-	Y	-	-	-	-	-	-	Y	Y	Y	-	-	-	Y	-	-	-	-
(Luo et al., 2008)	-	Y	Y	Y	Y	-	-	-	-	-	-	-	-	-	-	-	-	Y	-	-	-	Y	-	-	-	-	-
MASSEgress (Pan, 2006)	Y	Y	Y	-	-	-	-	-	-	-	-	-	-	-	-	-	-	Y	-	Y	-	Y	Y	Y	Y	-	-
Robocup Rescue (Okaya and Tokahashi, 2011)	Y	Y	Y	-	-	-	-	-	-	-	-	-	-	-	-	-	-	Y	-	-	-	-	-	-	-	-	-
SAFEgress (2014) (Chu et al., 2014), (Chu and Law, 2013)	-	Y	Y	-	-	-	-	-	-	-	-	-	-	-	-	-	-	Y	-	-	-	-	-	-	-	-	-
SAFEgress (2015)(Chu, 2015)	Y	Y	Y	-	-	Y	-	-	-	Y	-	-	-	-	-	-	-	Y	-	-	-	Y	-	-	-	-	-
SIMA (Sivers et al., 2016), (Seitz, 2016)	-	-	Y	Y	-	-	-	-	-	-	-	-	-	-	-	-	-	Y	-	-	-	-	-	-	Y	-	-
Social Force (Helbing et al., 2002; Helbing and Johansson, 2013)	-	-	-	-	-	-	-	-	-	-	-	-	-	-	-	-	-	Y	-	-	-	-	-	-	-	Y	Y
(Roan, 2013)	-	-	Y	-	-	Y	-	-	-	-	-	-	Y	-	-	-	-	Y	-	-	-	-	-	Y	Y	Y	-
STEPS (Caliendo et al., 2012; Waterson and Pelliser, 2010; Kuligowski et al., 2010)	-	-	-	-	-	-	-	-	-	Y	-	-	-	-	-	-	-	Y	-	-	-	-	-	-	Y	-	-
(Wang et al., 2009),(Wang et al., 2008)	-	-	-	-	-	-	-	-	-	-	-	-	-	-	-	-	Y	Y	-	-	-	-	-	Y	Y	-	-
(Ta et al., 2017), (Ta et al., 2015)	Y	Y	Y	Y	-	Y	-	-	Y	Y	-	-	-	-	-	-	-	Y	-	-	-	-	Y	-	-	Y	-
(Zia et al., 2013)	Y	Y	Y	-	-	-	-	-	-	-	-	-	-	-	-	-	-	Y	-	-	-	-	-	-	-	-	-
(Adam et al., 2016)	-	-	-	-	-	-	Y	-	-	-	-	-	-	Y	-	-	-	Y	-	-	-	-	-	-	-	-	-
AMEL(Truong et al., 2013), (Beck et al., 2014)	Y	Y	Y	-	-	-	-	-	-	-	-	-	Y	Y	Y	Y	-	Y	-	-	-	Y	-	-	-	-	-

Legend: (Y) - implemented, (*Y) - mimicked, (-) - not implemented, and ( ) blank – not specified.

Table 21 Other features of models

Model	Emotion	Contagion	Trust	Norms	Culture	Group decision making	Communication/negotiation	Guidance (direction signs)	Alarms	Stress	Patience	Knowledge	Experience	Learning	Memory	Physical model (damage)	Transport network	Institutions (firemen)	Tsunami	Fire	Other cascade (eg. stampede)	HPC (Grid/cluster/GPU)	TDF (Tactics Devt. Framework)
EPES (D'Orazio et al., 2014b)	-	-	-	-	-	-	-	-	-	-	-	-	-	-	-	Y	-	-	-	-	-	-	-
ESCAPES (Tsai et al., 2011)	Y	Y	-	-	-	-	Y	-	-	-	-	Y	-	-	-	-	-	-	-	-	-	-	-
EXITUS (Manley, 2012)	-	-	-	-	-	-	-	-	-	-	-	-	-	-	-	-	-	-	-	-	-	-	-
(Liu et al., 2016)	-	-	-	-	-	-	-	-	-	-	-	-	-	-	-	Y	-	-	-	-	-	-	-
(Luo et al., 2008)	-	-	-	-	-	-	-	-	-	-	-	-	-	-	-	-	-	-	-	-	-	-	-
MASSEgress (Pan, 2006)	-	-	-	-	-	-	Y	Y	-	Y	-	-	-	-	Y	-	-	-	-	-	-	-	-
Robocup Rescue (Okaya and Tokahashi, 2011)	-	-	-	-	-	-	Y	Y	-	-	-	Y	-	-	-	-	-	-	-	-	-	-	-
SAFEgress (2014) (Chu et al., 2014), (Chu and Law, 2013)	-	-	-	-	-	-	-	-	-	-	-	Y	-	-	Y	-	-	-	-	-	-	-	-
SAFEgress (2015)(Chu, 2015)	-	-	-	-	-	Y	-	Y	Y	-	-	Y	-	-	Y	-	-	-	-	-	-	-	-
SIMA (Sivers et al., 2016), (Seitz, 2016)	-	-	-	-	-	-	-	-	-	-	-	-	-	-	-	-	-	-	-	-	-	-	-
Social Force (Helbing et al., 2002; Helbing and Johansson, 2013)	-	-	-	-	-	-	-	-	-	-	-	-	-	-	-	-	-	-	-	-	-	-	-
(Roan, 2013)	-	Y	-	-	-	-	Y	-	Y	-	Y	-	-	-	-	-	-	-	-	-	Y	-	-
STEPS (Caliendo et al., 2012; Waterson and Pelliser, 2010; Kuligowski et al., 2010)	-	-	-	-	-	-	-	-	Y	-	Y	-	-	-	-	-	-	-	-	Y	-	-	-
(Wang et al., 2009), (Wang et al., 2008)	-	-	-	-	-	-	-	Y	-	Y	Y	-	-	-	-	-	-	-	-	-	-	-	-
(Ta et al., 2017), (Ta et al., 2015)	Y	Y	-	Y	-	Y	Y	-	Y	-	-	Y	-	-	-	-	-	-	-	-	-	-	-
(Zia et al., 2013)	-	-	-	-	-	-	-	-	-	-	-	Y	-	-	-	-	-	-	-	-	-	Y	-
(Adam et al., 2016)	-	-	-	-	-	-	-	-	-	-	-	-	-	-	-	-	-	-	-	-	-	-	Y
AMEL (Truong et al., 2013), (Beck et al., 2014)	-	-	-	-	-	-	-	-	-	-	-	-	Y	-	Y	-	-	-	-	-	-	-	-

Legend: (Y) - implemented, (*Y) - mimicked, (-) - not implemented, and ( ) blank – not specified

CHAPTER 4. DESCRIPTION OF THE METHODOLOGY

This chapter details the methodology used in the study. The chapter is divided into five sections. The first section discusses the multi-disciplinary approach. The second section describes the detailed methodology. The third section presents the study area. The fourth section describes the general sources of data. The fifth section presents a short conclusion.

4.1 Multi-disciplinary approach

The first task of this work is to determine the influence of social factors, specifically social attachment, on pedestrian evacuations during earthquake crisis. The accomplishment of this task requires a realistic and very detailed agent based pedestrian evacuation model for seismic crisis that is geospatial, microscopic, cognitive and social. These descriptions come from very different fields. Earthquakes are from the domain of the geosciences, geospatial from geographic information science (*GIScience*), social from social science, and microscopic and cognitive pertains to agent simulations from computer science.

The multi-disciplinary approach combines the four domains. Each of the domains (1) contributes to building the necessary seismic context, (2) provides the theories, methods and tools to develop and implement a geographic agent-based model, and (3) ensures that social attachment is implemented as the framework for interaction. This integration is illustrated in Figure 7. In the figure, each circle defines the relevant features represented by the keywords considered from each domain. The quadrants, where each of the circles falls defines the theme. The themes are geospatial, environment, human and artificial intelligence. The intersections refer to integrations of the domains. The left and right halves define roles of the domains in the model.

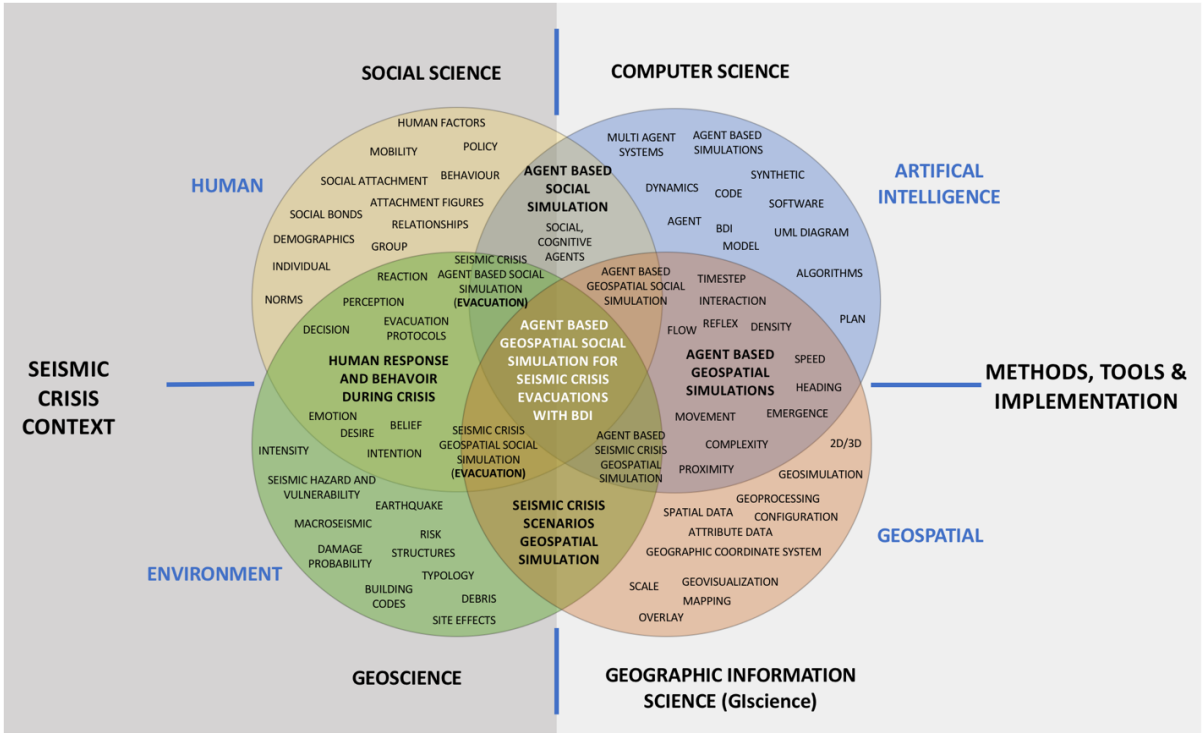

Figure 7 Multi-disciplinary approach carried out to develop a simulation of earthquake crisis

The domains in the left half portion of the figure, are used to define the seismic crisis context. These are geoscience and social science. Geoscience describes the physical aspects of the environment. This includes the physical elements of risk which are the earthquake hazard, vulnerable structures, damage or debris, and danger zones. Social science describes the human element. This focuses on the primary actor of evacuations, the human individual. Considered in this domain are individual and group behaviour, human factors, social dynamics, and social attachment.

The domains in the right half portion of the figure provide the methods and tools that facilitate the implementation of the model and simulations. These are provided by *GIScience* and computer science. *GIScience* defines the geospatial context of the crisis. It ensures that model elements are in the correct geographic locations, scale, distances, dimensions and configurations. Computer science, through multi agent modelling, transforms all these crisis elements into dynamically interacting agents. It glues together all the inputs from the three other domains to implement the multi-agent model and simulation.

The intersections of the domains give rise to interesting combinations. These combinations are presented in the following paragraphs. The purpose of the discussion is to look into the contribution of the synergies of the domains in more detail. The other objective is to stress the necessity of the integration of the domains to achieve the goal of the research.

The crisis context is described first with geoscience and social science. (1) The combination of geoscience and social science appropriately defines the context of the crisis with respect to the physical and social aspects. This combination defines the *response and behaviours of individuals* during seismic crisis events. An example of this is the description or observations of the response of the individuals provided by the EMS98 scale. These observations are from field surveys and used as inputs in the creating evacuation protocols or procedures based on earthquake intensity measures. This combination however is not enough to define a realistic model needed by this study. The combination lacks the spatial representation of both the risk and implementation of dynamic agent social interactions.

(2) When geoscience is combined with *GIScience*, it can produce *geospatial simulations* of the crisis. In these simulations, geographically correct representation of the crisis environment, such as spatial distribution of vulnerable and damaged structures, can be achieved. Examples of results from this integration are risk maps, evacuation routes and plans, dynamic geospatial simulations and 3D visualisations of the risk environment. This combination however also lacks the human and dynamic cognitive and social elements.

(3) When geoscience is combined with computer science, it can be used to develop computational models for or determining patterns or earthquake return periods and forecasting earthquakes. Examples of this are mathematical formalisations and related graphs of earthquake phenomena. This can include calculations of return periods, magnitude-intensity determination, building integrity calculations, etc.

The combinations of the other domains are discussed next starting with social science. (4) Considering only social science and computer science produces agent based social simulations, with cognitive agents. However, missing elements would be the earthquake crisis context and explicit geographic representation or dynamic visualisation.

(5) When only social science and *GIScience* are considered, the result would be a geovisualisation or geosimulation of population distributions and daily mobility without the crisis context. Implementing agent social interaction with social rules of behaviour is also not possible. Good examples of these are demographic distribution maps during different times (day, year, past, present, future projections).

(6) When only computer science and *GIScience* are considered, it can produce agent based geospatial simulations, however only of geographic objects and without the seismic crisis and related social context. An example of this is are 3D maps of physical features of or urban areas which includes buildings, street networks and open spaces.

From the points considered in the preceding paragraphs, it is clear that achieving the objective of the study requires the multi-disciplinary approach. Integrating all the four domains with respect to the themes, namely geospatial, environment, human, and artificial intelligence, makes possible the development of an agent based geospatial social simulation for seismic crisis evacuations using cognitive agent architectures.

4.2 Description of the methodology

The methodology adopted consists of nine major components or nodes. These are: (1) inputs, (2) conceptual modelling, (3) software implementation, (4) software code verification, (5) instantiation, (6) calibration, (7) sensitivity analysis, (8) simulation experimentation, and (9) validation. The methodology, with these major nodes, is illustrated in Figure 8. A discussion or each node is presented in the following paragraphs. The numbered steps are discussed thereafter.

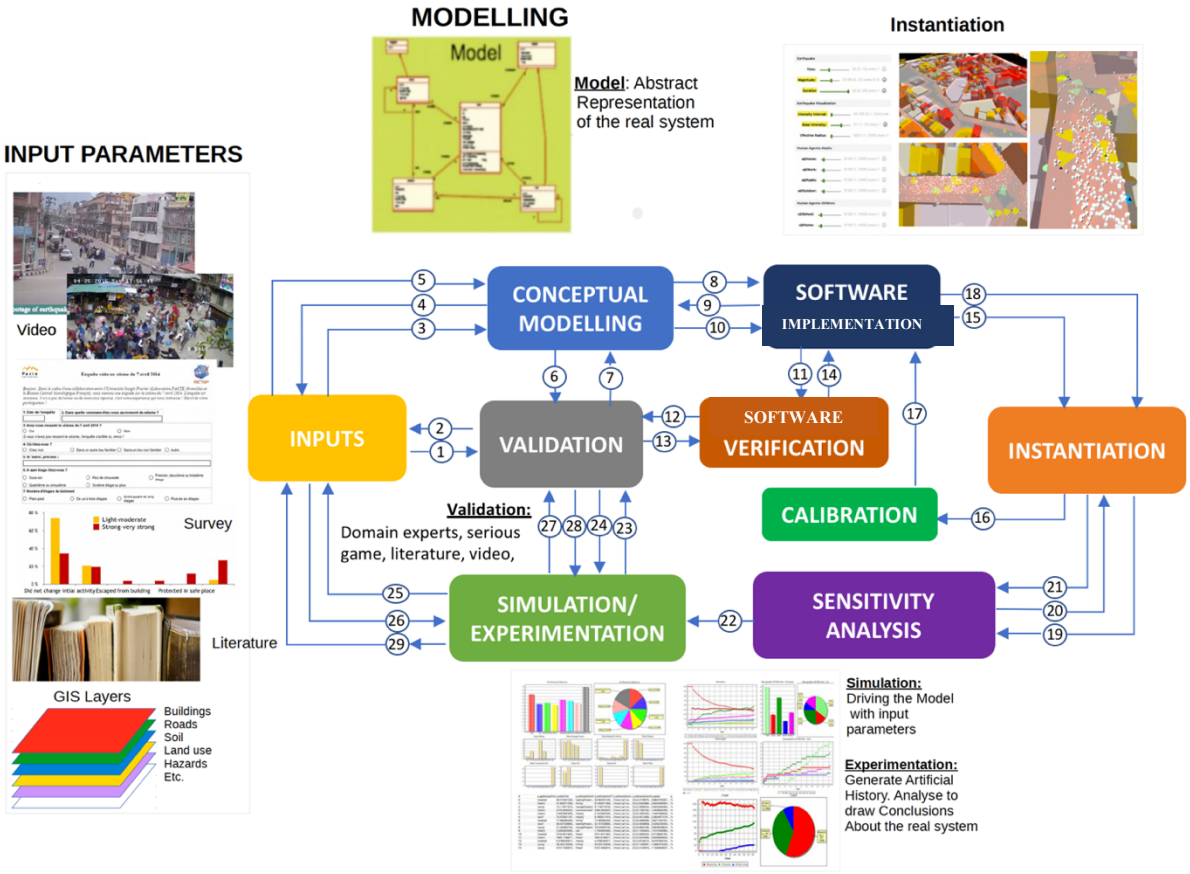

Figure 8 Detailed methodology carried out to develop a simulation of earthquake crisis

The initial node describes the *inputs* which refer to data collected from various sources. Examples of data include (1) spatial layers such as buildings and roads; (2) macroseismic building vulnerability and damage probabilities; (3) demographic data; (4) behavioural data reported from (a) previous studies, (b) observed from collected video data. More details on inputs are discussed in Section 4.4 of this chapter.

Conceptual modelling node refers to development of the model and sub-models from the gathered data. Models developed in the study are classified into three categories: models of the (1) physical crisis environment, (2) the individual, and (3) social dynamics. The models include the: (1) model of the individual and social interaction based on social attachment, or the attachment model; (2) conceptual agent-based model described in the diagrams, (3) motion and navigation of individuals in free space, (4) model of the spatial environment, (5) model of the seismic crisis environment, (6) the multi-agent model design. The models are discussed in more details in Chapter 5.

Software implementation refers to the process of transforming the conceptual model into software code. This involves translating the objects, agents and interactions into the syntax of the software environment used. The GAMA platform, that was used in this study, is further discussed in Section 4.5.1.

Software verification[12] refers to the node where the software code of the model is checked to ensure compliance with the design of the conceptual model. The software code is also checked for errors, first with respect to syntax and then for runtime errors. The runs are checked visually and also parametrically. In the adopted methodology, every node's contribution is checked, what each ensures goodness of fit and realism.

Instantiation refers to the initialisation of the model by setting the spatial layers and parameters for crisis scenarios. For example, initial layers include buildings, street network, safe area locations, and danger zones, etc. Initial parameters are from the collected data mentioned in the input node. Some examples of initial parameters are (1) heterogeneous agent population with respect to demographic characteristics, (2) maximum movement speeds of agents, (3) strength of social bonds, (4) time of day, (5) intensity of the earthquake felt in the area, (6) duration of the shaking, (7) probabilities for behaviours, etc. These layers and parameters are further discussed in Chapter 5.

Calibration[13] of the multi-domain model in the study physical and social developed in this study requires different methods. Calibration with existing data and making sure they are used in the instantiation of the model is what is only possible with the model. Examples of data used for calibration of the model include population distributions, damage and vulnerability probabilities. So far, no earthquake event of damaging nature has occurred in the city of Grenoble and has been experienced by the current population. Evacuation data in the IRIS or city scale for a damaging event is also not available. Is making sure that when realistic parameters are used, this is also calibration? Comparison with casualty statistics from previous earthquake events. Calibration base on the probabilities for actions detailed in previous studies. Social interactions produce delays.

Sensitivity Analysis[14] was used to test the dominance of parameters in the study with respect to effects on number of arrivals on safe areas. Owing to many sub-models used and many parameters in the study (geotechnical, 2D/3D space), sensitivity analysis will be done only on the social attachment parameters. An example is the effect of: (1) presence or absence of social attachment, and (2) perception distance during night time or daytime scenarios. These parameters refer to Chapter 5, models and Chapter 7, experiments.

The *simulations/experiments* run the code using the parameters. This generates new simulation data such as artificial histories for agents. This data is used to create visualisations, develop analyses, draw conclusions, and make comparisons with the real system. Examples of experimental scenarios to test effects on evacuations are (1) daytime and night time population distributions, (2) presence or absence

[12] "Computerised model verification ensures that the computer programming and implementation of the conceptual model are correct" (Sargent, 2000).
[13] Calibration as used here is "determining model parameters using real world data" (Darvishi & Ahmadi, 2014).
[14] Sensitivity analysis consists of changing the values of the input and internal parameters of the model to determine the effect on model behaviour and output (Sargent, 2000).

of social interactions in evacuations, (3) geographic scale used (a) 2 IRIS, (b) 6 IRIS and (c) 69 IRIS or city scale. The experiments are discussed in Chapter 7, and results in Chapter 8.

Validation[15] is central to the modelling process and it involves comparing the model, the simulation runs, and results of parameters, to reality. Consultation with experts (both scientific and practitioners) are done to validate the code the simulation runs. Particular attention is given to the realism the code imparts to the simulation. This also requires explaining to the experts how the code is written to explain agents in the simulation environment. The modes of validation adopted include consulting with domain experts, revisiting literature, cross checking with and collected survey and video data. Validation is done in the following (1) checking the code, (2) visual inspection of (a) agent locomotion, (b) debris generation, (c) social interaction of agents, (d) casualties and injuries; (3) statistical results. The benefit of having a GIScience environment is both its visual and parametric nature. Validation can proceed via visual inspection of agent behaviours in the microscopic pedestrian simulation as well as the ability to inspect parameters using statistical analysis and data visualisations such as graphs. An example of non-realistic behaviour which can be checked visually and parametrically are agents moving through barriers like buildings, debris, or natural features such as water bodies like rivers. Movement of agents in strict geometric patterns like straight lines and following corners is also not realistic. Video recordings of simulation runs are taken. These are used to evaluate the realism in agent movement in the synthetic crisis environment.

Figure 8 illustrates the 29 steps involved in this methodology. (1) Inspecting input data for fitness and possible inclusion to the model. Examples of input data are spatial data layers (e.g. buildings, roads), population, human factors (age, disability, and speed), behaviours observed in past earthquakes, vulnerability of buildings and probabilities for damage, etc. There are further discussed in Section 4.4. This also includes collected video data of actual earthquake disaster events. Video data allow for the very detailed study of microscopic behaviours as disaster events unfold. These behaviours are not usually described in detail in written reports. Having the video data allows for calibration of agent movements, social interactions, and interactions of individuals with the crisis environment.

(2) Input data is validated as acceptable for use in building the model. Data is modified when needed. For example, the original shapefile of buildings data does not contain building typology and vulnerability. The typology and vulnerability is however included in the IRIS boundary shapefile layer. The data is in the macro scale at the level of the IRIS. For assigning the data to buildings, The such as adapting the data from a source originally at the macro scale, and scaling it down to the micro scale, i.e. to the building level. An example is the macro seismic assessment of vulnerability which is evaluated over large areas. Values can be in percentages, but buildings need to be assigned a category for typology, vulnerability and damage. This can involve finding new data when inputs are missing. Another example is the location of egress points or doorways from buildings, which are often not available. Therefore, doors are added to the spatial database by digitisation and editing vector attributes. For population data, the number assigned to different land uses, are likewise not provided in its raw form. The distribution has to be derived from the population dataset.

(3) Inputs are used in developing the conceptual design of models and sub-models. Interactions of agents and model components are presented in diagrams described in Chapter 5. Each model component is also designed. For example, spatial data like buildings and roads, are used to develop the crisis environment.

[15] In general, validation as defined by Darvishi and Ahmadi, is the process that helps to understand whether a model can produce valid or correct outcomes (Darvishi & Ahmadi, 2014). As used by Sargent and defined in Schelinger, validation is the "substantiation that a computerized model within its domain of application possesses a satisfactory range of accuracy consistent with the intended application of the model" - (Schlesinger, 1979; Sargent, 2000). Validation techniques, from those discussed by Sargent, employed in this study, include animation, event validity, face validity (consultation with experts), animation/video, parametric or statistical analysis of simulation results, parameter variability-sensitivity analysis, and graphical representation (Sargent, 2000; Darvishi & Ahmadi, 2014).

Evacuation behaviour data derived from previous studies are used to define the probabilities for individual actions and resulting group behaviour. (4) Conceptual models are checked with the available quantitative and qualitative data. (5) Design of conceptual models are finalised with the final set of inputs. (6) Conceptual model undergoes validation via consultation with experts, checking available literature, and collected video (e.g. first-person point of view from mobile devices, CCTV cameras and news report). (7) Finalisation of the validated model. (8) The conceptual model is transformed into software code. (9) The initial software model is checked to match the conceptual model. (10) The initial software model is finalised. (11) The code of the initial software model undergoes code verification. (12) Consultation with experts to validate the software code. (13) Integration of expert comments on the software code. (14) Software model is finalised.

(15) The software model is initialised or instantiated using preliminary parameters. This involves running the model in the designed user interface using the GAMA platform. The user interface shows the simulation in full 2D and 3D space. Dynamic interaction of model elements can likewise be seen at simulation run time. Examples are the generation of debris during the earthquake, the effect of debris on structures, pathways and human agents (injury, death, trapping, or delay), individual movement in free space, evacuation of individuals from buildings through doorways towards safe areas, and social interaction during evacuation. Data from the simulation can be viewed and inspected at simulation run time. Individual agents can be clicked on and inspected for attributes such as age, speed, social group, evacuation delay, health status (injured, dead), beliefs, desires, intentions, plans, etc. Data can also be viewed in tabular form as raw values, or as dynamic graphs and charts. The data generated from running the model is saved and visualised using GAMA and the data exploration interface has been built using Python. The tabular and chat data is dynamically displayed during simulation run-time using a web browser. Examples of data displayed are the number of agents arriving in safe areas, the number of people injured or dead, pre-evacuation behaviours and delay times in evacuation, etc. The interface also allows the inspection of code sections for syntax and run-time errors allowing for code corrections during model initialisation tests. Examples of errors normally encountered are exceptions. These are only encountered during simulation runs and can be due to many things such as vector geometry or null pointers.

(16) The model is tested and calibrated with more realistic data. Examples for the individual are movement speeds, and the angle and distance of visual perception. Examples for social aspects include, social bonds, social attachment related behaviours, probabilities for behaviours, etc. For physical aspects, the debris generation is based on earthquake intensity scenarios. (17) The model is refined using the calibrated parameters. (18) The calibrated model is instantiated using calibration parameters. (19) Sensitivity analysis is initiated. Tests for sensitivity analysis are conducted using some parameters. Parameters of focus include social bonds, perception distances, time day, presence and absence of social attachment in evacuations. (20) Checking instantiation parameters effects on sensitivity analysis. (21) When the parameters are stable or do not create variations in calculations, they can be finalised and a full sensitivity analysis using all parameters of interest can be conducted. (22) Design experiments and simulations. (23) Verify and validate design of experiments and simulation. (24) Finalise simulation and experiments. Run the simulations. (25) Check/compare simulation/experiment results with inputs/real data. (26) Checked simulation with real data. (27) Final validation of simulation and experiments results. (28) Validated results and considered to finalise output. (29) Final assessment of the simulation output. When the results are not satisfactory, the process will start again until an acceptable model producing realistic results is achieved.

This ends the discussion on the detailed methodology adopted in this work. The next sections will present the study area and sources of data that were considered in order to develop the model.

4.3 Study area

The study area considered in the study is Grenoble, France. It is a city located at the foot of the Northern Alps in the southeast of France. Its centroid coordinates are 45° 10' 57.35"N, 5° 43' 15.13"E. The maps showing the location of Grenoble with respect to the metropolitan France is shown in Figure 9. The detailed map of Grenoble showing its shape, IRIS boundaries and surrounding communes is shown in Figure 10.

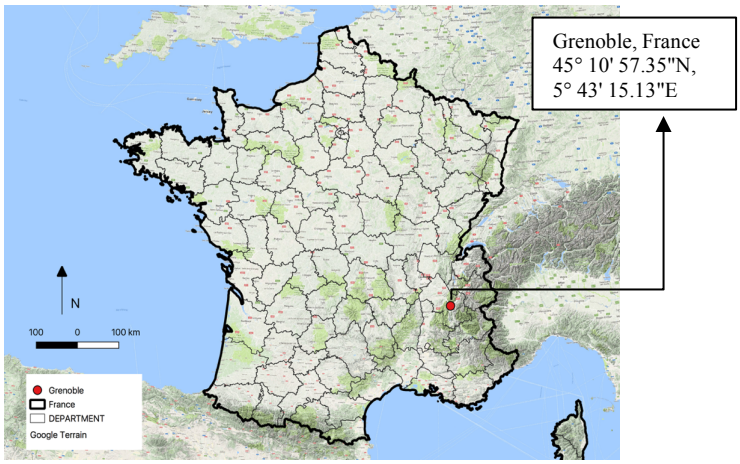

Figure 9 Location of Grenoble with respect to Metropolitan France. Map by Julius Bañgate, 2019 with data from (BRGM, 2019; Google, 2018). BRGM was the source of the Department boundaries. Google is the source of the terrain basemap.

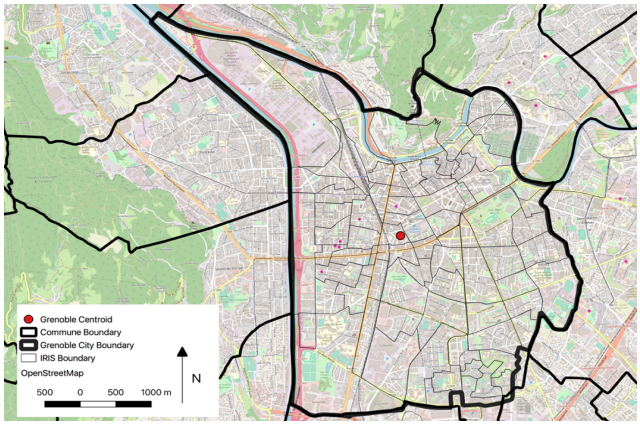

Figure 10 Grenoble city boundary map by Julius Bañgate, 2019 with data from: (Riedel_a, et al., 2015; OpenStreetMap & Contributors, 2018; BRGM, 2019). The IRIS boundary data is from Rieldel et a.l; the Commune boundary is from BRGM; the basemap is from OpenStreetMap.

Grenoble's population is 160,215 individuals according to the 2013 IRIS[16] census tracks level national census data (INSEE, 2019). The city holds great social, economic and technological importance due to the presence of many advanced research institutions and industries (AEPI, 2019; AEPI_b, 2013). Nuclear research facilities devoted to developing civilian applications are also located in the city (CEA, 2015). Grenoble's historic city centre is the venue for many social, residential, commercial and tourist activities. Due to many different activities in the city, the spatial distribution of the population within the city changes during the day, the days of the week and the seasons. The city's daily population also

[16] IRIS is a French accronym for Ilots Regroupés pour l'Information Statistique or in English 'aggregated units for statistical information' (INSEE_b, 2019). INSEE is the Intitut national de la statistique et des études économiques, it « collects, analyses and disseminates information on French economy and society" (INSEE_b, 2019).

increases due to the influx of non-residents from surrounding municipalities (André-Poyaud, Chardonnel, Charleux, & Tabaka, 2016).

The historic city centre of Grenoble hosts many old and historic buildings (Ville de Grenoble, 2013). Newer buildings can be found in the southern portion of the city as the direction of urban growth has been southward (Coppé, Enaudi, Menousse, & Munar, 2013). The presence of the Isère river and Chartreuse mountain range limits the expansion of the city towards the north. According to Dunand and Guéguen, 2012, the city centre is mainly built in masonry (Dunand & Guéguen, 2012). Also, from the same authors, suburbs surrounding the city are built with reinforced concrete. Newer suburbs located in the city's outskirts are heterogeneous and were built with either masonry or concrete. Additionally, newer suburbs located in the city's outskirts are heterogeneous and were built with either masonry or concrete.

In terms of seismicity, Grenoble lies in a zone of average seismicity (BRGM, 2019). Figure 11 shows the new seismic zones of France released in 2011. This new map shows the indicative location of Grenoble within the average seismic zone[17]. The reclassification of Grenoble to the average seismic zone communicates higher seismic risk. This significant change could help to increase the level of awareness of populations to the significance of seismic risk in Grenoble. New research, especially dealing with perceptions of risk will have to seek a way to use the data and results from previous research in their methodologies.

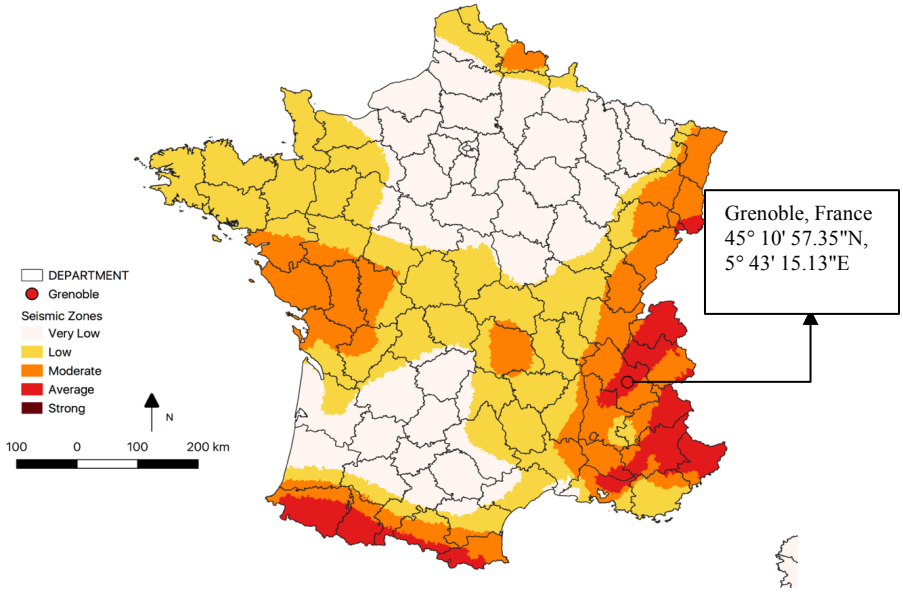

Figure 11 Seismic zones for metropolitan France May 1, 2011, article D.563-8-1 du code de l'environnement, Ministère de l'Ecologie, du Développement durable, des Transports et du Logement. Map is created by Julius Bañgate, 2019 with data from published GIS Data Source: (BRGM, 2019)

Compared to the rest of France, this region where Grenoble is located, experiences high seismic activity (Thouvenot, Fréchet, Jenatton, & Gamond, 2003). Very low magnitude/intensity earthquakes are frequently detected by seismic sensors in the city and the surrounding areas. However, the occurrence however of disastrous earthquakes are rare and have long return periods (Dunand & Guéguen, 2012).

[17] It should be noted that the older seismic zone map prior to May 1, 2011, classifies Grenoble within the lower moderate zone category (BRGM, 2019). As a consequence, prior studies used this moderate category (Beck, André-Poyaud, Chardonnel, Davoine, & Lutoff, 2010; Guéguen, et al., 2009; Dunand & Guéguen, 2012)

According to the authors, probabilistic studies project the possibility of recording intensity VII to VIII having an annual probability of 0.002 or a 475-year return period.

A local source of seismicity is the active fault in the Belledonne mountain range (ISTerre, 2019; Thouvenot, Fréchet, Jenatton, & Gamond, 2003). Another nearby fault, called the Voreppe fault, according to ISTerre team, possibly crosses the city but its activity is not known. Also, according to ISTerre team, there could still be other potentially dangerous faults that could exist in the Vercors and Chartreuse massifs that remain to be discovered. The Belledonne fault area is located southeast of the city, which can be a local source of future strong earthquakes. The return periods of earthquakes (units in magnitude, M) in the Belledonne fault zone are: M=3.5 every15 years; M=4.0 every 40 years; M5.0 every 300 years; and M6.0 every 2000 years (ISTerre, 2019). Figure 12 shows the seismicity of the Belledonne fault zone.

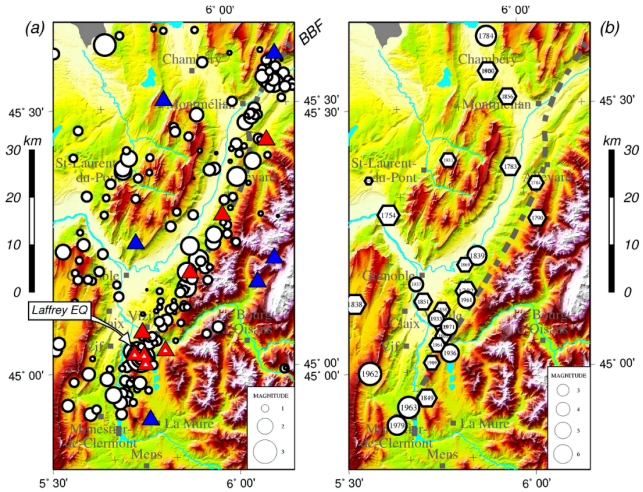

Figure 12 Seismicity of Grenoble and in the Belledonne fault area (ISTerre, 2019; Thouvenot, Fréchet, Jenatton, & Gamond, 2003). The grey broken line is the fault. The left image shows more recent earthquakes indicating magnitudes. The right image shows historic earthquakes.

Table 22 shows the historical earthquakes with reported intensities starting from intensity IV, as felt from Grenoble ($I_{Grenoble}$) (www.sisfrance.net, 2018). The intensity felt at the earthquake source of epicentre (I_{Origin}) is also indicated. It can be seen that large historical earthquakes have mostly been recorded in Grenoble at intensity V and very few at intensity VI. Intensity VII was recorded in the Corrençon earthquake of April 25, 1962. Intensities less than IV have been recorded but were not included in the table since these low intensity earthquakes are seldom perceived by the population.

Table 22 Historical earthquakes from intensity IV felt in Grenoble (www.sisfrance.net, 2018). Please note that the intensity values I_{Origin} and $I_{Grenoble}$ are expressed as real numbers and not in their roman numeral equivalents.

Date	**Time**	**Local Epicenter, Region**	**I_{Origin}**	**$I_{Grenoble}$**
12 December 1963	13 h 24 min 57 sec	Vercors (Correncon-En-Vercors), Dauphine	6	4
7 December 1963	10 h 39 min	Vercors (Correncon-En-Vercors), Dauphine	6	4
25 April 1963	13 h 36 min 11 sec	Vercors (Monteynard), Dauphine	7	5
25 April 1962	4 h 44 min 48 sec	Vercors (Correncon-En-Vercors), Dauphine	7.5	6.5
12 April 1962	13 h 38 min 5 sec	Vercors (Correncon-En-Vercors), Dauphine	5	4.5
3 March 1961	0 h 52 min 27 sec	Belledonne (Uriage), Dauphine	5	4.5
30 May 1946	4 h 41 min 38 sec	Valais (Chalais), Switzerland	7	5
18 July 1938	0 h 57 min	Queyras (Guillestre), Alpes, Dauphinoises	7	5
17 January 1937	1 h	Greivaudan (Grenoble), Dauphine	4	4
29 April 1905	1 h 59 min 15 sec	Massif du Mont-Blanc (Lac D'Emosson), Switzerland	7.5	4.5
23 February 1887	5 h 50 min	Riviera di Ponente (Imperia-Bussana), Italy	9	6
27 November 1884	22 h 57 min	Queyras (Guillestre), Alpes Dauphinoises	7	5

10 December 1882	17 h 40 min	Belledonne-Pelvoux, Alpes Savoyardes	5	5
5 August 1881	0 h 30 min	Belledonned-Pelvoux, Alpes Savoyardes	6	5.5
22 July 1881	2 h 45 min	Belledonned-Pelvoux, Alpes Savoyardes	7	5
12 November 1869	0 h 2 min	Greivaudan (Domene), Dauphine	4	4
19 May 1866	9h 12 min	Laragne (Le Motte-du-Caire), Alpes Provencales	7.5	4
25 July 1855	12 h 50 min	Valais (Visp), Switzerland	9	5
7 January 1851	23 h 30 min	Gresivaudan (Grenoble), Dauphine	5	4.5
3 April 1839	18 h 30 min	Gresivaudan (Domene), Dauphine	6	5
19 February 1822	8 h 45 min	Bugey (Belley), Bresset et Jura Bressan	7.5	5.5
2 April 1808	17 h 45 min	Piemont (Torre Pellice), Italie	8	4.5
12 September 1785	0 h 15 min	Piemont (Val de Susa, Oulx), Italie	7	4
15 October 1784	12 h 3 min	Massif de la Chartreuse (S. Chambery), Alpes Savoyardes	6.5	5
15 August 1782	16 h	Belledone (Uriage), Dauphine	6	5
15 February 1644	4 h 30 min	Alpes Nocoises (Roquebilliere), Alpes Maritimes	8	4

A map of the historical earthquakes, with intensities larger than 5 in the Grenoble vicinity is presented in Figure 13. Data is from the historical earthquake catalogue of www.sisfrance.net. The map also covers a larger area to show the relevant earthquakes occurring in Italy and Switzerland. It can be seen from Table 22 and Figure 13, that strong earthquakes occurring in far locations, such as Italy and Switzerland, are felt in Grenoble, although at lower intensities. Examples are the February 23, 1887 Riviera de Ponente, Italy earthquake occurring with intensity IX at the epicentre and felt in Grenoble as intensity VI. Another example is the May 30, 1946 Valais, Switzerland earthquake occurring with an intensity VII at the epicentre and felt in Grenoble at intensity V.

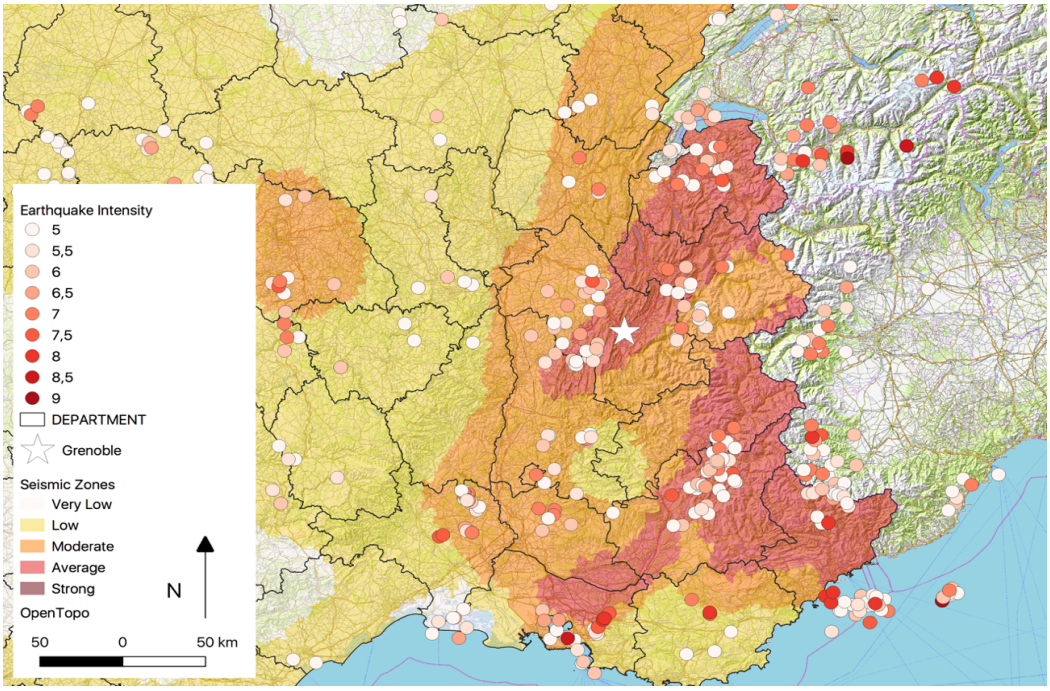

Figure 13 Location of historical earthquakes in the nearby region. Earthquakes have intensities greater than 5 around Grenoble. Earthquake data from www.sisfrance.net (www.sisfrance.net, 2018). Map by Julius Bañgate, 2019 with data on Seismic zones and boundaries from planseisme.fr (www.planseisme.fr, 2018). Topographic data from OpenTopo (OpenTopogaphy, 2018)

Grenoble is located in a small-size, deep, Y shaped sediment-filled basin that has fill materials that amplify seismic ground motion (Cornou, Bard, & Dietrich, 2003; Dunand & Guéguen, 2012). The shape of the valley and type of soil contribute to prolonging the duration of the shaking. This amplification could explain why the effect of far-occurring earthquakes are felt in Grenoble. This brings also the unfortunate consequence of the amplification for nearer earthquakes. According to Dunand and Gueguen, Grenoble can be divided into two zones of intensity amplification, based on this soil material

(Dunand & Guéguen, 2012). Zone 1 is comprised of type B soils which consist of sand and gravel. Zone 1 increments intensity values to 0.7. Zone 2, is comprised of type C soils, which consists of silt and clay. Zone 2 increments intensity by 1.5; Figure 14 illustrates these zones of amplification. It should be noted that the old historical city centre lies within Zone 2. With greater site amplification, and presence of old structures, more structural damage can be expected from Zone 2 than Zone 1. In general, according to the authors, the overall seismic risk for Grenoble is rated as moderate, when considering the probability of damage, collapse and loss.

Being in the region of average seismicity, which is one of the highest in mainland France, the risk of earthquakes to the population of Grenoble is real. However, the rare occurrence of earthquakes is seen as a possible hindrance to the development of a sound culture on seismic risk (Beck, André-Poyaud, Chardonnel, Davoine, & Lutoff, 2010). This low risk perception can result in non-definitive commitments to reduce seismic risk from authorities (Dunand & Guéguen, 2012).

A deadly earthquake on average is experienced in France every 100 years (McPartland, 2014). The last deadly earthquake was the Lambesc, Provence earthquake in 1909 (Lacassin, Tapponnier, Meyer, & Armijo, 2001). If the occurrence pattern will be the same, a disastrous tremor in France is already long overdue.

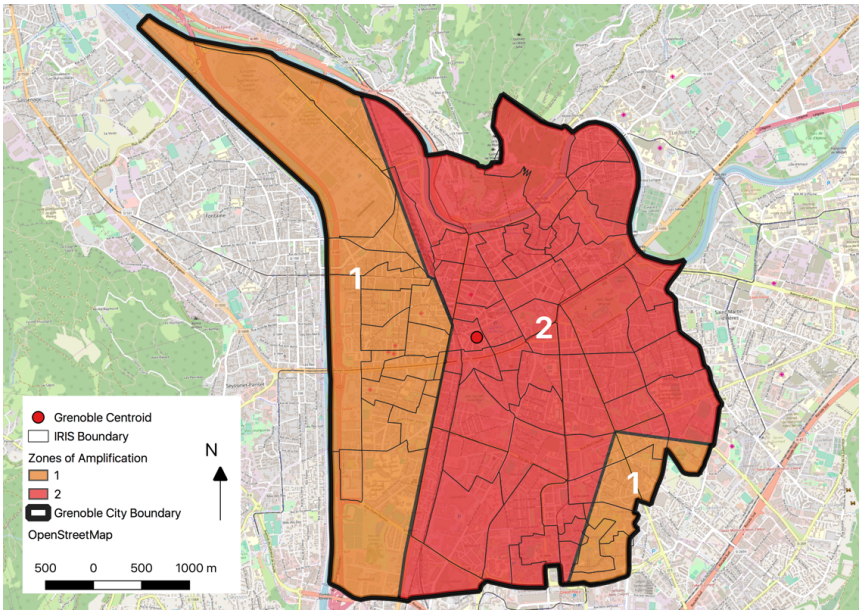

Figure 14 Grenoble zone amplification increments, zone boundaries are estimated and digitized based on a figure from Dunand & Guéguen, 2012. Map by Julius Bañgate, 2019.

The aforementioned characteristics of Grenoble make it a good site to model crisis behaviour and develop different crisis scenarios. Future earthquakes are certain but the current population has no experience with disastrous earthquakes. In the event of an earthquake, the population may fail to recognize the natural hazard and not behave in accordance with recommended behaviours during earthquake events (Beck, André-Poyaud, Chardonnel, Davoine, & Lutoff, 2010). The old structures in the city will be tested for their resilience to earthquake damage. This will also confirm if building codes are sufficient or properly complied with for newer structures. Developing the scenarios can be useful in anticipating worst-case scenarios which are necessary to enable planners to optimise efforts in evacuating populations, or respond to the needs for help or rescue.

4.4 Sources of data

The data needed to develop model and simulation scenarios come from sources from different domains. The data from different sources used in this research are detailed in Table 23. Data are categorised with respect to themes namely social (human), geospatial (spatial), and geoscience (seismic). Other descriptive fields in the table include the name of the data, its source, and purpose or how the data is used in this research.

The human population is characterised by social data. Details of the population are derived from the national statics data at the IRIS level, provided by the INSEE. The data attributes that are considered include population counts for different age groups, number of households, employment and disability. Age and disability are the major human factors when considering individual mobility. The age groups considered include child (0 to 2 years, and 3 to 14 years), adult (15 to 29 years, and 30 to 59 years), and elderly (60 + years). The age groupings include percentage values of the population that go to school, work, or who are retired. The activities of the age groups are crucial in recreating the spatial distribution of the population for different time scenarios.

The spatial distribution of the population during the day and night are derived from demographic data and mobility surveys. New data from the current research of Menin et al. on daily mobility (Menin, Nedel, Davoine, & Chardonnel, 2018) is also considered. The strength of social relationships or bonds for France are derived from the work of Suvilehto et al. (Suvilehto, Glerean, Dunba, Hari, & Nummenmaa, 2015). Social behaviours and evacuation speeds during disasters are derived from the reviewed literature presented in Chapter 2 and from gathered video data.

Geospatial vector data are used to define the crisis environment using shapefiles in the RGF-93/Lambert-93 projection. The base map on buildings footprints, road network, open spaces (parks), and natural features (rivers) are from BDTOPO (IGN, 2017). Points of interest showing locations of establishments, businesses, etc., which are not available from official sources, are derived from OpenStreetMap (OpenStreetMap & Contributors, 2018). Spatial layers not available from the aforementioned sources, such as location of building doorways, are determined using address data (Open Data Grenoble-Alpes-Metropole, 2018) or digitized from satellite images. Additional context is provided by BDTOPO, OpenStreetMap, Google StreetView, and Google Satellite imagery (IGN, 2017; OpenStreetMap & Contributors, 2018; Google, 2018). Other spatial layers such as safe areas and hazard zones are derived from GIS using spatial analysis and geoprocessing.

A comprehensive and detailed building inventory for seismic vulnerability and damage is not available for Grenoble. Damage and vulnerability probabilities for each building are derived from the work of Riedel et al. (Riedel_a, et al., 2015). Probability values are presented for each IRIS unit. The probabilities for vulnerability are used to assign buildings to different typologies. The damage probabilities are used to determine damaged buildings during different earthquake intensity scenarios.

Table 23 Description of data used for model development, initialisation of parameters and validation of results

Category	Data	Literature Source	Purpose/target
Social (Human)	Demography	National Census at IRIS level (INSEE, 2019)	Generate population based on age groups.
	Disability	National Census at IRIS level (DREES, 2017)	Add a disability attribute to individuals.
	Daily Mobility	(Menin, Nedel, Davoine, & Chardonnel, 2018)	Distribution of population in different parts of the city especially during daytime.
	Social ties/bond strength	(Suvilehto, Glerean, Dunba, Hari, & Nummenmaa, 2015)	Calibration of an individual's perception distance based on bonds to implement affiliation, perception, and recognition in the model.
	Evacuation behaviour	Literature survey detailed in Chapter 2, Questionnaire	Calibration of probabilistic assignment of crisis behaviour during evacuation.

		Survey Reports, E.g. (Beck, André-Poyaud, Chardonnel, Davoine, & Lutoff, 2010)	
	Evacuation Speed	Literature survey	Define individual speeds during evacuations.
	Video documentation of actual earthquake events	YouTube (Collection of videos from different earthquake events)	Gather pre-evacuation and evacuation behaviours during the event; Validation of realistic behaviour of agents in model and simulation.
Geospatial (Spatial)	Grenoble boundary	(Riedel_a, et al., 2015)	Define model extents, aggregated from IRIS boundaries.
	IRIS Boundary	(Riedel_a, et al., 2015)	Attributes used as probabilities for generating attributes of enclosed features (population, buildings).
	Address	(Open Data Grenoble-Alpes-Metropole, 2018)	Address/location of residences and establishments.
	Buildings	BDTOPO (IGN, 2017)	Provide location of people indoors. These also serve as barriers to movement and define the boundaries of alleyways and streets. When they are damaged during a crisis scenario they provide the source of debris.
	Road network	BDTOPO (IGN, 2017), OpenStreetMap (OpenStreetMap & Contributors, 2018)	Provide pathways, routes towards safe areas during evacuations. Centre lines of roadways are the initial safe areas. Also provides guidance to agents when evacuating to safe areas.
	Open Spaces (Parks)	BDTOPO (IGN, 2017)(IGN, 2017); OpenStreetMap (OpenStreetMap & Contributors, 2018)	Define safe areas Open space, safe areas.
	Points of Interest (POIs)	OpenStreetMap (OpenStreetMap & Contributors, 2018)	Used to define the locations of individual agents not inside home locations. Location of establishments, used to define doorways, and use/type of locations.
	Doorways	Digitised from satellite imagery	Used as starting locations for evacuation, especially during night time scenarios. Occupancy; location of "indoor" agents.
	Natural features/Rivers	BDTOPO (IGN, 2017)	Barriers to movement. These are used to restrict pedestrian movement in pathways.
	Evacuation Routes	City Planning Office, or delineated from data	Officially defined routes for evacuation.
	Danger Zones	Derived from data using geoprocessing tools	Used to define deposition areas for debris around buildings.
	Safe areas	Derived from data using geoprocessing tools, and vector editing	Areas free from debris. Used as destinations of agents during evacuations.
Geoscience (Seismic)	Vulnerability for each IRIS	(Riedel_a, et al., 2015)	Used to assign the building typology attribute (a, b, c, d, e, f) using probabilistic method.
	Damage Probability for each IRIS	(Riedel_a, et al., 2015)	Probabilistic assignment of damage to a building with respect to intensity (0,1,2,3,4,5).
	Zones of intensity amplification (based on soil type)	(Dunand & Guéguen, 2012)	Used in defining scenarios with intensity amplification.
	Video documentation of damage during actual earthquake events	YouTube (Collection of video recordings from different earthquake events)	Used for modelling damage and deposition of debris nearby structures. Videos are also used as a basis for human interaction with debris especially in encountering injuries and casualties.

4.5 Summary of the chapter

The chapter discussed the multi-disciplinary approach and detailed methodology adopted in developing the models. A description of Grenoble as the study area was presented. The discussion

revolved around the characteristics of the city and the seismicity of the area. The chapter also presented the dataset considered in the study.

It can be concluded from this chapter that adopting Grenoble as the study area for developing the model and simulation is appropriate for the following reasons: (1) it is a city vulnerable to seismic risk; (2) steps are needed to increase awareness and inspire action from local authorities and the local population to more thoroughly address seismic risk, (3) initial body of work has been done to investigate physical and social vulnerability in Grenoble (E.g. (Beck, André-Poyaud, Chardonnel, Davoine, & Lutoff, 2010; Dunand & Guéguen, 2012)); (4) data is available to build the spatial model of a synthetic seismic crisis environment, and (5) the availability of local experts from different domains to help validate the model.

The next chapters will present the other components of the detailed methodology. Chapter 5 will discuss the models, developed using the input datasets, and guided by the detailed reviews from Chapter 2 and 3. Chapter 6 discusses how the model was implemented.

CHAPTER 5. AGENT BASED MODEL OF SOCIAL ATTACHMENT

This chapter presents the *SOciaL Attachment and Crisis Evacuations (SOLACE)* model. SOLACE is developed using social attachment theory as the framework for modelling human behaviour during seismic crisis evacuations. The use of the word "solace" as the name of the model for this crisis context is appropriate. In the English language, *solace* is a noun which means comfort or consolation during times of distress or sadness. The model is the product of the multi-disciplinary methodology implemented in this work. The key components necessary to build this generic model include sub-models developed from complementary domains. *Social science* defines the models of the individual, and the interactions driven by social attachment within social groups. *Geoscience* provides the models for earthquake effects and generation of damage and debris. *GI science* defines the spatial model for the crisis environment. *Computer science* provides the multi-agent framework and tools to integrate the sub-models within a generic dynamic model and simulation environment. These domain-specific models are described in the subsequent sections.

The chapter is divided into seven sections. Each section discusses the components or sub-models that make up SOLACE. Important concepts used in developing the model are discussed in the sections[18]. Section 5.1 presents the model of the human individual agent, built using social attachment as the governing framework. Section 5.2 discusses the model for agent's individual motion and navigation in free space. Section 5.3 presents the model of the spatial environment defined by layers of geographic data. Section 5.4 presents the model of the seismic crisis environment, or the scenarios starting from earthquake shaking to evacuations. Section 5.5 describes in more details SOLACE with a UML diagram. Section 5.6 describes the software ecosystem developed to facilitate data visualisation and analysis from SOLACE. Section 5.7 presents as short conclusion.

5.1 Model of the individual and social attachment

The model of the individual integrates human factors, cognitive functions and social abilities. The mobility (i.e. means and speed of movement) of an individual in the crisis environment is primarily determined by human factors. Significant to this study are the limitations imposed by age and disability. According to social attachment theory, crises or threat situations activate attachment or affiliation (Mawson, 2005). This triggers proximity seeking behaviour towards attachment figures. Proximity seeking behaviours influence the motivations, goals, speeds and directions of individual actions.

The conceptual model for social attachment developed in this research is presented in Figure 15. In the model, the attachment figures are human individuals and groups, places, objects/property, task/routine/activity and information. Attachment between human individuals and groups are governed by the strength of social bonds. Non-human elements (like pets, places or objects) are included when they hold significance or social meaning to individuals or groups. This happens when non-human elements are involved in social interactions or can evoke memories of persons and past experiences. The significance can also be primarily economic, in the sense of monetary value or the amount of time invested (e.g. computer containing research work, etc.). Pets for example are often considered as family members (Heath S. E., Kass, Beck, & Glickman, 2001). An example of attachment to a place is a person's attachment to one's home or neighbourhood (Scannel & Gifford, 2013). For objects, it can be personal property like a wallet, mobile phone, computer, luggage, etc. The mobile phone in particular is used to connect with family members and seek information on their conditions. Working, driving and sleeping are examples of tasks or routines. Information in general refers to the safety of human and non-human attachment figures during the crisis. When attachment figures are near, information is acquired

[18] The level of detail of the concepts for developing the model are too granular to be included in Chapter 2 and Chapter 3. Also, the fine details do not fit thematically in the previous chapters, which were already very lengthy.

by seeking and direct checking on their situation. When the attachment figures are far, information can be derived from making phone calls, social media and radio and tv broadcasts.

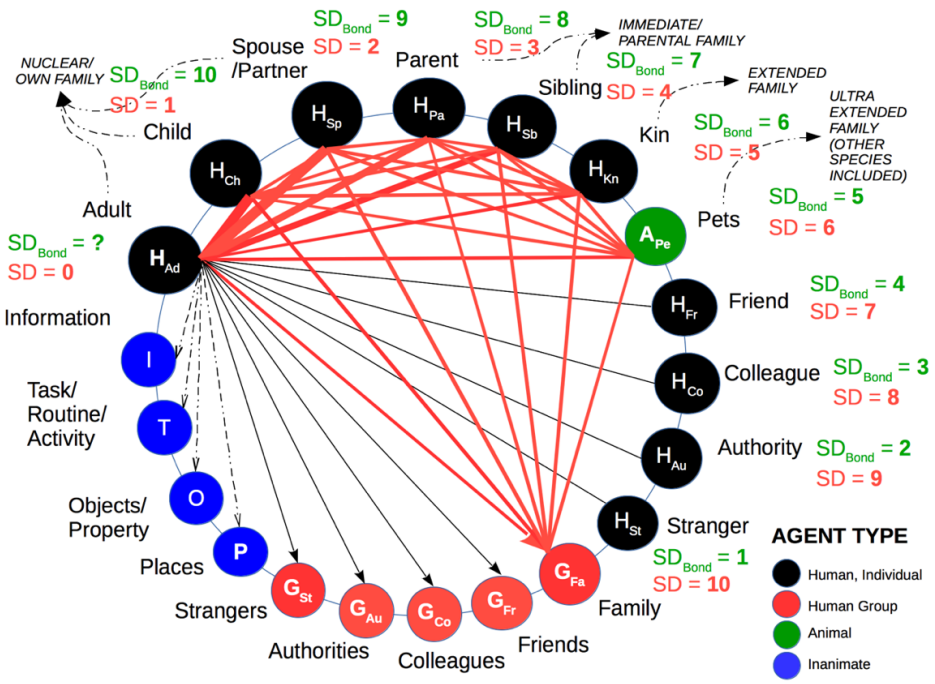

Figure 15 SOLACE Attachment Model

The succeeding sections present further details about the model.

5.1.1 Social distance and strength of bonds

In the SOLACE model, social attachment is expressed as ***social distance (SD)***, ***social distance bond strength (SD_{Bond})***, and ***affective perception distance (PD)***. The ranking used in the model are based on the notion of the strength of interpersonal ties from Granovetter (Granovetter, 1973). According to Granovetter, the strength is determined by the combination of the amount of time, the emotional intensity, intimacy and the reciprocal services that characterize the tie. In the SOLACE model, the values for parent and child (core family member) are the highest. Especially in the formative years, children spend significant amounts of time with parents. Strong bonds are likewise formed between siblings. Relatives and other kin members (grandparents, aunt, cousin, etc.), likewise can form strong ties with core family members. Individuals can also from strong ties with friends. The bonds become weaker (in decreasing order) with colleagues, acquaintances and strangers. Bonds with strangers can be formed especially during crises (see Section 2.3.4.3) (Drury, Cocking, & Reicher, 2009).

In the conceptual model shown in Figure 15, a *social distance*, ranging from 1 to 10 is used to set the priority for perceiving and reacting towards attachment figures. Social distance describes personal closeness, strong personal ties or social bond, and familiarity. The highest priority is given to individuals with the highest social bond strength with respect to the reference individual. For example, for a reference adult (H_{Ad}) who is a parent, first priority ($SD = 1$) is accorded to child (H_{Cd}) due to very high social bond $SD_{Bond} = 10$; second priority ($SD = 2$) to partner (H_{Sp}) with social bond $SD_{Bond} = 9$; third priority ($SD = 3$) to parents (H_{Sp}) with social bond $SD_{Bond} = 8$; fourth priority to siblings (H_{Sb}, $SD = 4$, $SD_{Bond} = 7$); fifth to next of kin (H_{Kn}, $SD = 5$, $SD_{Bond} = 6$); sixth to pets (A_{Pe}, $SD = 6$, $SD_{Bond} = 5$), seventh to friends (H_{Fr}, $SD = 7$, $SD_{Bond} = 4$), eighth to colleagues (H_{Co}, $SD = 8$, $SD_{Bond} = 3$), ninth to authorities (H_{Kn}, $SD = 9$, $SD_{Bond} = 2$) and last priority to strangers (H_{St}, $SD = 10$, $SD_{Bond} = 1$). Table 24 details the

mapping between social distance and social bond with respect to the relationships described in the conceptual model.

Table 24 Social distance (SD) and strength of bond (SB) from a reference adult parent

Attachment Figure	**Altruistic**		**Egoistic**		**Membership in Social Groups**				
	SD	***SD*$_{Bond}$**	**SD**	***SD*$_{Bond}$**					
Adult (H_{Ad})	0	0	10	10	Nuclear Family	Nuclear Family + Grand Parents	Close Family	Extended	Ultra extended Family (With Pets)
Child (H_{Cd})	1	10	0	0					
Spouse/ Partner (H_{Sp})	2	9	0	0					
Parent (H_{Pa})	3	8	0	0					
Sibling (H_{Sb})	4	7	0	0					
Kin (H_{Kn})	5	6	0	0					
Pets (A_{Pe})	6	5	0	0					
Friend (H_{Fr})	7	4	0	0	Friends (G_{Fr})				
Colleague (H_{Co})	8	3	0	0	Colleagues (G_{Co})				
Authority (H_{Au})	9	2	0	0	Authorities (G_{Au})				
Stranger (H_{St})	10	1	0	0	Strangers (G_{St})				

Aggregation of individuals into social groups is also included in the attachment model. The strong bonds between family members (G_{Fa}) for example are represented by the thick red lines in Figure 15. Sub-categories in the family group include (a) nuclear family which includes the couple and their child; (b) nuclear family with grandparents; (c) close family, which includes the siblings; (d) extended family with includes the next of kin or relatives; and (e) ultra-extended family which includes the pets as family members. Other social groups include friends (G_{Fr}), colleagues (G_{Co}), authorities (G_{Au}) and strangers (*GSt*). Group membership of individuals are not mutually exclusive and can overlap. A sibling or friend for example can also be a colleague. The bonds and structure of the sub-groups are context-related and adopted to French society.

The values for *SD* and SD_{Bond} presented in Table 24 represent altruistic and egoistic scenarios that will lead the experiments. In the altruistic scenario, the values for social distance *SD* are in increasing order of priority from 1 to 10. In the altruistic case, the individual does not put priority on oneself but only to others. This is represented by the zero social distance value for the human adult H_{Ad}. Also, the strength of bond SD_{Bond}, to the self is also zero in the altruistic case.

The reverse is true for an egoistic case. In this situation the reference individual only thinks of itself. Here relationships exist, but are not given priority and strength (with *SD = 10* to oneself and *SD = 0* to the rest). This would result in high social bond strength only to oneself, and zero to the rest (SD_{Bond} = 10 to oneself and SD_{Bond} = 0 to the rest). In this case no social interaction is possible. This also means that egoistic individuals would only focus on themselves, give themselves priority, and would only try to protect and save themselves. Other individuals can be perceived but only treated like other objects in the environment and treated as obstacles and barriers. The only possible interaction is maintaining distance or avoidance. This effectively reduces to individuals approximating the behaviour of particles. The individual focuses on saving only himself or.herself to reach an objective which is a safe area.

The role of familiarity in perception has been discussed in Section 2.3.4.2.

5.1.2 Visual familiarity and limits to perception imposed by distance

Complex and chaotic environments during disasters provide multiple distractions that can make the finding of other individuals difficult. Individual differences due age for example also affect the ability to focus (avoid distractions). The results of the work of Cohen & Gordon-Salant, suggested that “older adults are more susceptible to irrelevant auditory and visual competition in real-world environments”, than younger individuals (Cohen & Gordon-Salant, 2017). Also, the same authors dynamic visual scenes

provide distractions affecting listening performance. During disasters, the ability to focus to find others may be explained by (1) preferential processing during recognition tasks of personally familiar faces and voices, and (2) activation of proximity seeking behaviours due to social attachment (Keyes & Zalicks, 2016; Fontaine, Love, & Latinus, 2017; Mawson, 2005).

Familiar individuals can be perceived more easily and can then be approached or attended to faster. This familiarity influences the focus and attention of agents during navigation. Ultimately it determines their goals (destinations) and direction of movement (towards chosen goals) in the environment. Many environmental factors such as visibility and audibility limit detection and recognition. Spatial distance (proximity) is a limiting parameter in detection and recognition. As distance increases, the power to detect and recognise decreases. This section expounds on the influence of distance on the visual factors that influence recognition. The formalised equation for affective perception distance is presented as Equation 3 in section 5.1.4

Distance is the crucial parameter used in the model for agent navigation towards attachment figures. This navigation is influenced by what the agent can perceive and focus its attention within its visual field. In effect, distance acts as the spatial filter that limits the perception of non-relevant and far objects in the agent's immediate environment. Ultimately this section operationalises the link between social distance and spatial distance. In particular preferential attachment and selective perception moderated by distance. Social attachment is used as the social filter. Spatial distance acts as the spatial filter. To expound further, it is how people with different social distances (i.e. variations in strengths in social bonds) perceive each other with respect to their relative spatial distances (i.e. proximity) in the crisis environment. Important concepts are discussed here as these are important in developing the model and were not included in Chapter 2 and Chapter 3. In particular, the concepts are familiarity (social), spatial distance (spatial), lighting conditions (environment), and human vision (human factors). The objective of the section is to justify the choice of 50 meters as the effective reference perception distance used in the model. The following discussions are necessary as the search in the literature did not result in a useful reference for use in the value for perception distance.

Familiarity facilitates fast perception (detection and recognition) of attachment figures even from a distance, and in chaotic scenes (Liccione_a, et al., 2014; Kok, Taubert, Burg, Rhodes, & Alais, 2017; O'Toole, et al., 2011; Barton & Corrow, 2016; Suvilehto, et al., 2015). High familiarity naturally follows from strong attachment bonds among individuals (Suvilehto, et al., 2015). Individuals for example, are more exposed to family members through the unique pattern of historical interaction (Liccione_b, et al., 2014). Liccione et al. adds that the frequency of encounters refines the stored representation of family members in an individual's mind. As a direct consequence, this makes recognition of family members faster when compared to others. This high level of familiarity according to Liccione et al., facilitates the recognition of faces, and also discerning facial expressions. Keyes and Zalicks found that "socially important personally familiar faces are processed preferentially to socially unimportant familiar and unfamiliar faces" (Keyes & Zalicks, 2016; Gobbini, et al., 2013). The familiarity with face (1) increases identification accuracy, (2) facilitates generalization of the recognition process even at suboptimal conditions, (3) activates brain regions associated with sematic, episodic and emotional information representations of a person, (4) facilitate faster mental processing and recognition (Natu & O'Toole, 2011; Balas, Cox, & Conwell, 2007).

Spatial distance defines a limit to the recognition of other individuals and objects in the surroundings. Recognition performance degrades with increasing distance (Loftus & Harley, 2005). Faces become featureless beyond 35 meters (Maertens, 1884; Moughtin, 2003). Fortunately, even when the face is not visible, recognition of individuals is still possible. O'Toole et al. found that "human judgements of identity are likely based on the collaborative computations of multiple representations of face and body" (O'Toole, et al., 2011). Recognition of others can be through bodily shape, gait, and gestures/mannerisms during while walking or running, or a person's choice of embellishments like colourful clothing (Adilla, 1993). With these other cues, individuals can be identified even at much longer distances. For example, Adilla reported that people can identify other people even further than

500 meters. Table 25 below shows examples of distances related to visual recognition considered by other authors.

Table 25 Distances related to perception, fixation and recognition of people

Distance (meters)	What can be recognised	Source
4 to 18	Tendency to fixate on other pedestrians.	(Fotios, Yang, & Uttley, 2015)
8	Recognition performance remains at a plateau of maximum performance, approximately 90%.	(Loftus & Harley, 2005; Fotios, Yang, & Uttley, 2015)
10	Ideal facial recognition distance; Reduction of recognition performance to 75 %.	(Loftus & Harley, 2005; Fotios, Yang, & Uttley, 2015)
10 to over 50	Range of fixation distance during daytime, outdoors and in a residential area.	(Fotios, Yang, & Uttley, 2015)
>11	Pedestrians after dark may not be sufficiently visible.	(Fotios, Yang, & Uttley, 2015)
12	People can be distinguished.	(Maertens, 1884; Moughtin, 2003)
12 to 15	Reasonable distance to have a look at another person.	(Fotios, Yang, & Uttley, 2015)
12 to 24.9	Mean recognition distance.	(Fotios, Yang, & Uttley, 2015)
15	Interpersonal judgment possible.	(Fotios, Yang, & Uttley, 2015)
22	Normal identification of people in daylight is possible.	(Fotios, Yang, & Uttley, 2015; Maertens, 1884)
22.5	Person can be recognised.	(Maertens, 1884; Moughtin, 2003)
23	Reduction of recognition performance to 25%.	(Loftus & Harley, 2005; Fotios, Yang, & Uttley, 2015)
25	Facial recognition distance for public safety.	(Fotios, Yang, & Uttley, 2015)*
35	Face becomes featureless.	(Maertens, 1884; Moughtin, 2003)
50	During daytime and with normal vision, people and objects can be recognised.	(Fotios, Yang, & Uttley, 2015)
52	Fixation to unfamiliar sections during daytime.	(Fotios, Yang, & Uttley, 2015)
135	Body gestures can be discerned.	(Maertens, 1884; Moughtin, 2003)
1200	People can be seen.	(Maertens, 1884; Moughtin, 2003)

Lighting conditions affect the distances for detecting and recognising people and objects. Poor lighting conditions result in poor visibility. This situation requires people and objects to be nearer to be detected and recognised. Daytime provides the ideal lighting conditions for visibility. This visibility however can be reduced by the presence of particles like dust (due to debris collapse), smoke, fog, smog, mist and rain. Trapped individuals indoors without emergency lighting within collapsed structures lose all visibility. Night time is particularly challenging as illumination from street lights do not fully approximate visibility during daytime conditions. Earthquake disasters happening during night time can force individuals to evacuate outdoors and struggle with poor lighting conditions to seek attachment figures and safe areas. Power can also be cut from homes and streets making visibility evacuations more difficult. Moonlight can aid in visibility however is decreased during full moon towards no-moon conditions (Nichols & Powers, 1964).

Individual human factors also play a significant role in the ability to perceive other individuals and the environment. Age is a major factor as visual ability is normally poorer with increased age (Wright & Rea, 1984; Del Viva & Agostini, 2007). Young and older persons perform differently to different lighting conditions (Rahm & Johansson, 2018; Fotios & Boyce, 2015). From Rahm and Johansson's experiment, younger individuals outperformed older individuals in visual tasks when lighting is brighter. However older people are more used to and can outperform younger individuals in poorer lighting conditions. Younger individuals can detect smaller objects better than older people (Fotios & Boyce, 2015). This can enable younger people to detect small debris and avoid tripping or falling during evacuations. A composite vision score was developed by Salthouse et al. in their study of the relationship of age and vision (Salthouse, Hancock, Meinz, & Hambrick, 1996). Figure 16 shows the result of the work of Salthouse et al. In the figure, the regression analysis of visual acuity of three study groups shows the decrease of visual acuity with age using the authors' composite vision score. Each dot in the graphs represents an individual.

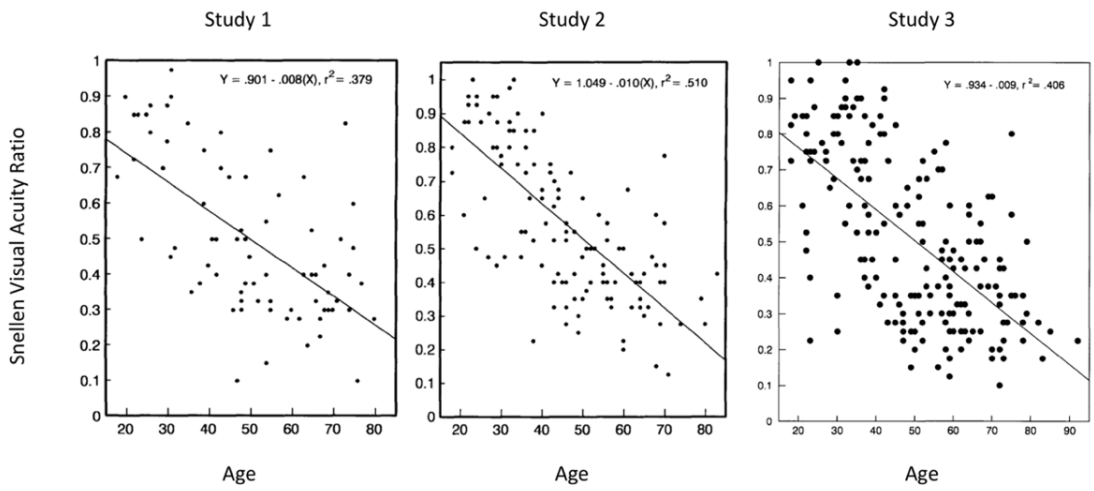

Figure 16 Regression analysis results comparing visual acuity and age in three study groups (Salthouse, Hancock, Meinz, & Hambrick, 1996)

Clarity of detail in perceiving objects can be measured by visual acuity. The Figure 17 shows the relationship of visual acuity with respect to distance. If an individual with normal vision, visual acuity 20/20, can see an object 50 meters away, it would require other individuals with poorer vision to go closer to achieve the same level of detail. A comparison of the detail for 20/20 vision with 20/200 vision shown in Figure 18.

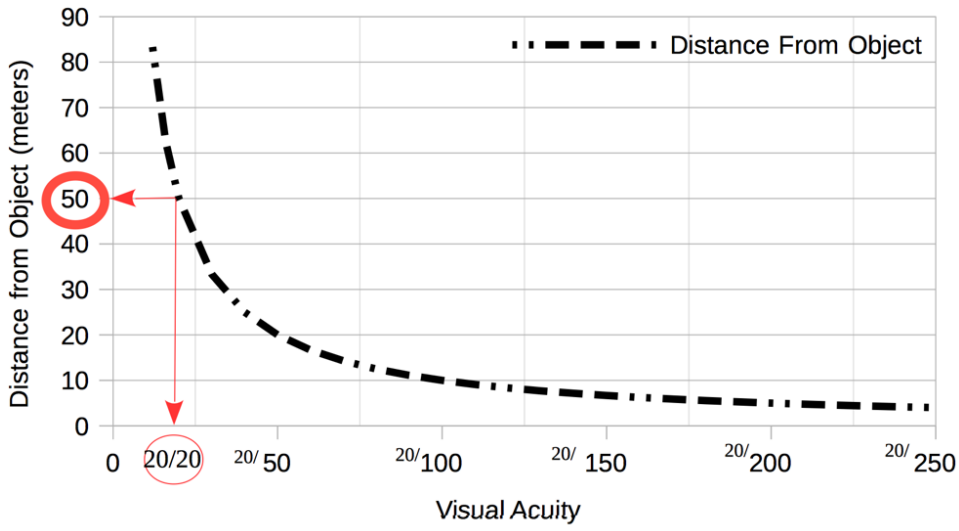

Figure 17 Visual acuity with respect to distance from object

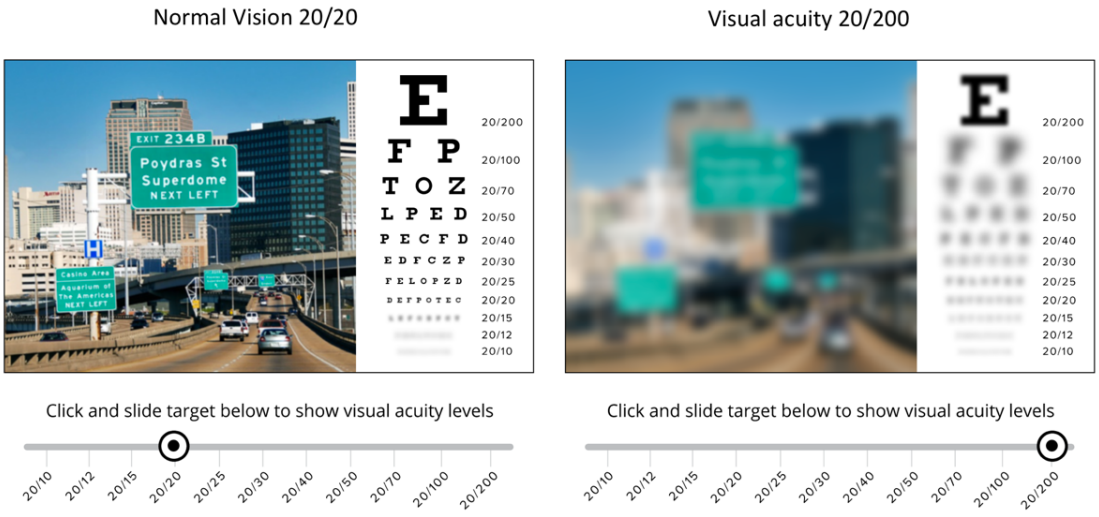

Figure 18 Visual acuity and normal vision 20/20 vs 20/200 (www.allaboutvision.com, 2018)

5.1.3 Voice familiarity and the limits to perception imposed by distance

Recognising other individuals is also possible through the familiarity of the human voice. A person is more likely to respond to a familiar voice than a non-familiar one. The response can be immediate as one's name is called by a familiar voice for example. Calling out for help, or calling the other person by name during search is often the situation when the other individual is not visible, or the perceiving person is not visible to the other. Like vision, the human voice is limited by distance. The preceding subsection discusses the role of human voice and distance in perception. Like in vision, the search in the literature did not result in the definitive spatial distance value for voice perception. This section therefore also justifies the choice of 50 meters as the reference spatial perception distance for the model.

Hearing plays an important and complementary role with vision in perceiving and recognizing other individuals (Yovel & Belin, 2013). Voices, like vision, can provide information on the speech content, age, gender, emotional state, affective state, personality, state of health and identity of a person (Kriegstein & Giraud, 2006; Sidtis & Kreiman, 2011; Barton & Corrow, 2016; Smith H. M., 2016; Lavan, Scott, & McGettigan, 2016; Yovel & Belin, 2013). During social situations, in many cases, facial and auditory information are processed by the brain simultaneously and in a similar manner (Yovel & Belin, 2013). Individuals have unique vocal signatures that facilitate recognition and identification (Fontaine, Love, & Latinus, 2017). In the context of identification however, visual recognition of faces is considered to be more superior than voice recognition (Stevenage, et al., 2012; Barsics, 2014). Humans are very good in identifying familiar voices (Fontaine, Love, & Latinus, 2017). Like in visual perception, the familiar voices of attachment figures would get the attention of focus of an individual more than others. Even in very noisy environments, listeners can better understand personally familiar voices such as from that of a spouse or a close friend than strangers (Souza, Gehani, Wright, & McCloy, 2013).

Hearing is especially useful when visual means of communication or deriving information are not possible. Examples are conversations between individuals separated by barriers such as debris, walls or structures. During zero or low visibility conditions like night time individuals can seek for help or seek others by shouting (Adilla, 1993). Trapped individuals or survivors usually tap walls to indicate their presence to rescuers. Familiar people can be identified by voice or by responding to calls with their names (Barton & Corrow, 2016; Tacikowski & Ehrsson, 2016).

Human are hardwired to respond to the cries of babies, even when they are not the parents. In the study of Young et al., hearing the cries of infants activates brain regions that make individuals more aware, attentive, active and ready to provide care (Young, et al., 2016). This activation of the flight and fight

response, and elevated level of alertness can be useful during disasters in saving the life of the child and the individuals themselves.

Table 26 Voice levels with respect to distance from source

Distance		Voice levels (dB)									
feet	meters	Normal	Raised	Very Loud	Shout_1	Shout_2	Shout_3	Shout_4	Shout_5	Baby-Cry	Scream
1.0	0.3	70	76	82	88	90	100	105	110	115	126
2.0	0.6	64	70	76	82	84	94	99	104	109	120
3.0	0.9	**60**	66	72	78	80	90	95	100	105	116
6.0	1.8	54	**60**	66	72	74	84	89	94	99	110
12.0	3.7	48	54	**60**	66	68	78	83	88	93	104
24.0	7.3	42	48	54	**60**	62	72	77	82	87	98
32.8	10	40	46	52	58	**60**	70	75	80	85	96
65.6	20	34	40	46	52	54	**64**	69	74	79	90
164.0	**50**	**26**	**32**	**38**	**44**	46	**56**	**61**	**66**	**71**	**82**
328.1	100	20	26	32	38	40	50	55	**60**	65	76
656.2	200	14	20	26	32	34	44	49	54	**59**	70
1640.4	500	6	12	18	24	26	36	41	46	51	**62**
2296.6	700	3	9	15	21	23	33	38	43	48	59
3280.8	1000	0	6	12	18	20	30	35	40	45	56

Hearing decreases with increasing distance from the source. Sound pressure level[19] decreases by 6 decibels for every doubling of distance from the source (www.EngineeringToolBox.com, 2018).

In social settings, the distance for talking with normal voice levels at 60 dB is usually at 1 to 4 meters. For outdoor activities like playing games, people talk with raised or very loud voices at distances of 5 to 10 meters. Table 26 provides the different voice levels with respect to distance from the source. It is calculated using the inverse square law and with the tool provided by the Engineering Tool Box website (www.EngineeringToolBox.com, 2018). The sound pressure level at the source location is indicated and measured from a reference of 1 ft from the source. The voice levels farther away from the source both in feet and meters is indicated. The highlighted row is for the voice levels at 50 meters from the source. The black diagonals indicate voice levels for near person conversation at 60 dB. The intersection between 50 meters and Shout_4 (105 dB) is highlighted in red. Figure 19 provides the graph of these values. Figure 20 shows the buffer distances from various locations within the UGA campus.

The calculated decibel values in Table 26 are for ideal conditions where (1) there is absence of noise, and (2) sound can travel unimpeded from the source to the receiver. Unfortunately modelling the propagation of sounds in urban environments is complicated. Sounds can be absorbed, dampened, scattered or reflected by different objects present in the environment. This is made more complicated by urban configurations which consists of large streets, small alleys and the tall buildings. The presence of ambient noise sources can make hearing difficult and requires talking with more effort (Pearsons, Bennett, & Fidell, 1977). For simplicity the study adopts 50 meters, as a convenient value to serve as the maximum perceptible range for a loud shout to be heard. It is implied that individuals in real crisis situations, make the effort to be heard by others farther away by shouting at greater than 105 dB. Coincidentally, 50 meters is also the visual perceptible distance for recognizing people and objects.

[19] From Engineering Toolbox, the typical subjective description of sound pressure level: 0-40 dB, quiet to very quiet; 60 – 80 dB, noisy; 100 dB, very noisy and > 120 dB, intolerable. The threshold for hearing is 0 dB. A normal conversation where individuals are 1 meter apart is at 60 dB. The sound of rustling leaves or a mosquito is 20 dB. A whisper is 30 dB. A quiet street and office, and whispered speech is at 50 dB. Laughter is 65 dB. The threshold for discomfort is 110 dB. A siren 30 meters away is heard at 120 dB. (www.EngineeringToolBox.com, 2018).. An infant's cry can go up to 115 dB. Screams approximate infant cries (Begault, 2008).

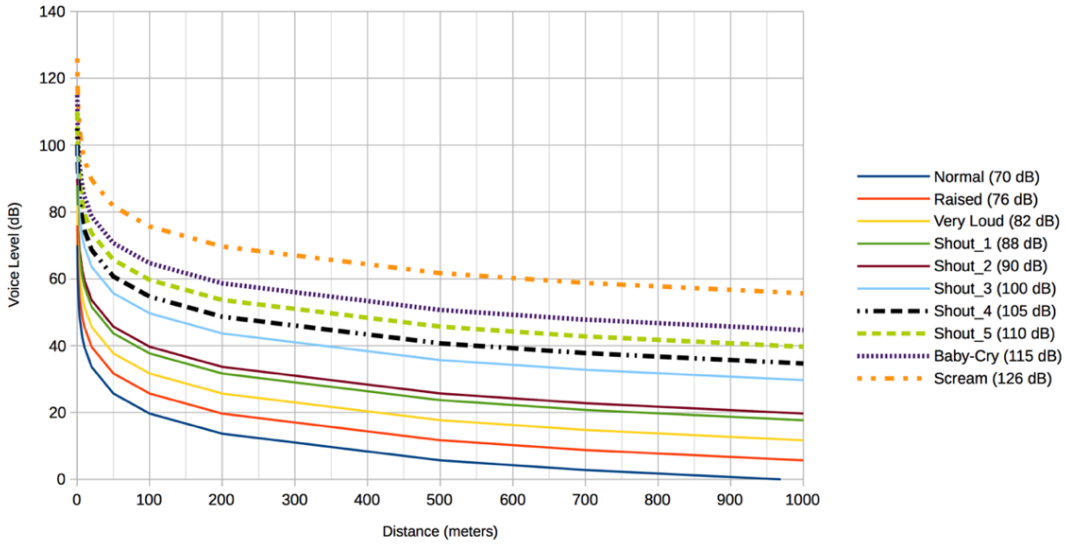

Figure 19 Voice levels at a distance from source calculated using the Inverse Square Law. As reference 0 dB, threshold for hearing; 20 dB, sound of rustling leaves or a mosquito; 40 dB, quiet room, home, bird call; 60 dB normal conversation where individuals are 1 meter apart; 80 dB is a road with busy traffic; 100 dB, motor horns 7 meters away; 120 dB, siren 30 meters away; 140 dB, is the threshold for pain. (Engineering Toolbox, 2018).

Older people tend to produce sounds at lower decibels (Begault, 2008). It will therefore take more effort for older individuals to shout or cry for help, and be heard over long distances. Hearing others likewise is a challenge for older people as decreased hearing performance and hearing loss is also common as individuals grow older (Humes, 2007; Kolarik, Moore, Zahorik, Cirstea, & Pardhan, 2016).

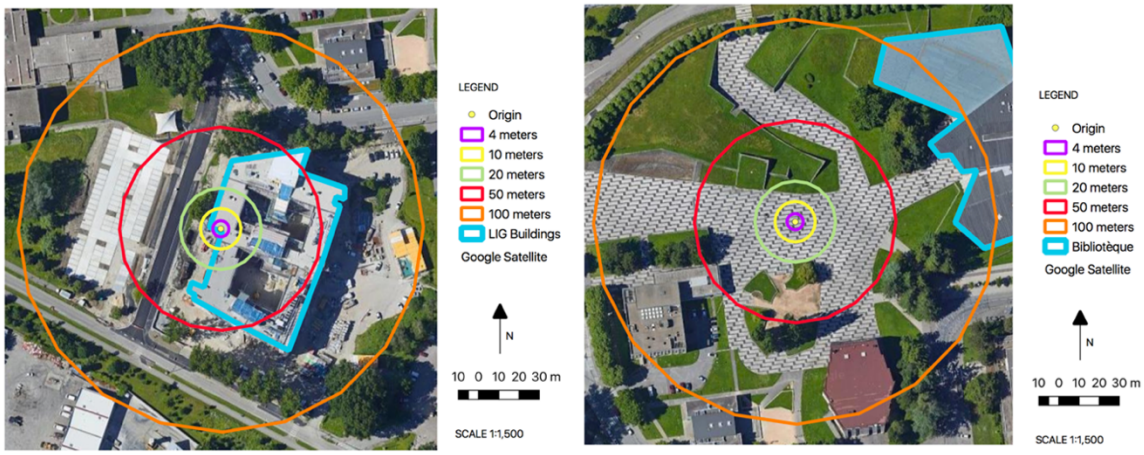

Figure 20 Example visualisation of distances from a noise point source outside the LIG Building on the UGA Campus. The left image is the LIG building. The image on the right is the open space in front of the University Science Library. The normal conversation distance is 1 to 4 meters. Beyond 4 meters individuals need to talk louder or at much higher decibels to be heard by other individuals. To be heard at the level of a normal conversation at 50 meters, in ideal situations, from the origin, the voice level has to be at 105 dB (Shout_5 in Table 26).

5.1.4 Affective Perception Distance

According to Mawson, proximity seeking behaviours are activated during threat situations. Proximity seeking behaviours during disasters to succeed (i.e. finding the person being sought; or arrival in the location of the person being sought) requires attachment figures to be perceived. The distance or range within which attachment figures are perceived is defined in this work as affective perception distance, PD_{Bond}. Equation 3 presents a formalisation to calculate PD_{Bond}.

Equation 3

$$PD_{Bond} = PD_{Normal}^{k} \times (1 + \frac{1}{10} \times SD_{Bond})$$

In Equation 3, PD_{Normal} refers to the *normal perception distance* within which people and objects are recognised. The value used for PD_{Normal} is 50 meters. The main justification for the use of 50 meters, is that at this range with normal lighting conditions and normal vision, it is possible to detect and recognise of people and objects (Fotios, Yang, & Uttley, 2015). This was discussed in section 5.1.2. The second justification has been extensively discussed in Section 5.1.3. It was shown in that section that, at 50 meters it is possible to hear another individual at the level of a normal conversation (60 dB). This can be provided that effort to shout at 115 dB is made from the source of the noise.

The constant k is the bias imposed by the environment (i.e. visibility). For full visibility during daytime, the value of $k = 1$. With low visibility during night time, the value for $k = 0.2$. For reduced visibility due to fog/snow, $k = 0.8$. Appropriate assumptions and values for k need to be made to successfully apply the affective perception distance equation in simulations.

Values for PD_{Normal} can likewise be affected by human factors h_f. In this work, this is expressed in Equation 4. PD_{Normal} is relative to a person. It can also be diminished or shortened by poor vision or poor hearing, which can be due to age. Equation 5 likewise shows the proposed formalisations for the human factors vision $h_{f_{vision}}$ and voice $h_{f_{voice}}$. Equation 5 specifies the dominant situation applicable to calculate h_f. When there is visibility or $k>0$, $h_{f_{vision}}$ is used. When there is no visibility $k=0$, $h_{f_{voice}}$ is used. The supremacy of vision, specifically with face recognition over voice has been established in Sections 5.1.2 and 5.1.3. This work therefore considers more parameters related to vision and visibility, than voice.

Equation 4

$$PD_{Normal} = h_f \times PD$$

Equation 5

$$h_f = \begin{cases} h_{f_{vision}}, & k > 0 \\ h_{f_{voice}}, & k = 0 \end{cases}$$

For the current model, a simplification is applied by considering the value $h_{f_{vision}} = 1$. This means that agents regardless of age are considered to have (1) normal (or optimal) vision and hearing, and (2) strong vocal ability for shouting. This simplification is due to the difficulty of finding data quantifying visual and auditory acuity, and strength of voice, with respect to distance, for the study area population. However, when these data are available, it is possible to generate models and equations to quantify $h_{f_{vision}}$ and $h_{f_{voice}}$.

In the case of vision, deriving from the work of Salthouse et al., $h_{f_{vision}}$ uses the values of the Snellen Visual Acuity Ratio (SVAR) (Salthouse, Hancock, Meinz, & Hambrick, 1996). This ratio ranges from 0 to 1 and relates visual acuity with age. The graphs from the work of Salthouse et al., are presented in Section 3.1.2. An approximate value for $h_{fvision}$ for example can be calculated from the regression equation from Study 3 of Salthouse et al.'s work. This is show in Equation 6.

Equation 6

$$h_{fvision} = SVAR = 0.934 - (0.009 \times Age)$$

Figure 21 shows the PD_{Normal} values when *SVAR* is equated to $h_{fvision}$. The decrease in visual acuity with age is shown. The reference visual perception distance of 50 meters likewise decreased with age.

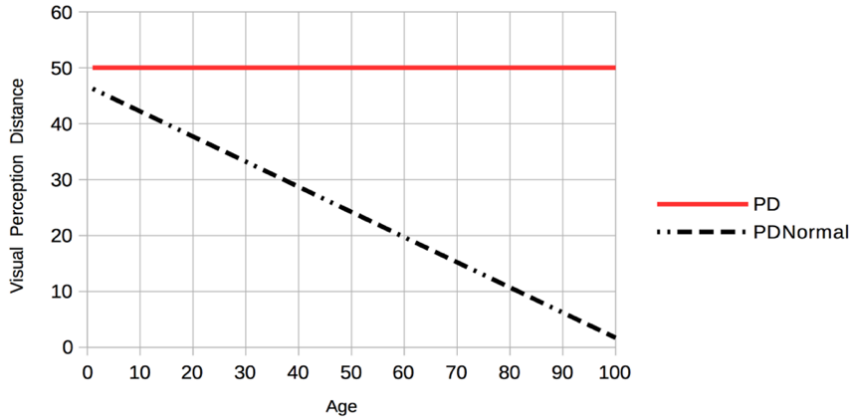

Figure 21 PD_{Normal} values with respect to values with respect to Age based on Salthouse et al.'s Snellen Visual Acuity Ratio and 50 meters visual perception distance (Salthouse, Hancock, Meinz, & Hambrick, 1996)

To illustrate the use of affective perception distance as a spatial filter, consider for example a parent perceiving a child (where $SD_{Bond} = 10$), with respect to a crowd of strangers ($SD_{Bond} = 1$), during daytime. This will result in PD_{Bond} =100 for the child and PD_{Bond} =55 for the strangers. This means that a parent may be able to recognise the child, even at 100 meters. This is twice the normal perception/recognition distance. Strangers will need to be very close to be perceived. If the child and strangers are at the same distance, the child will be perceived first.

The values for strength of emotional bonds for France for different relationships have been quantified (Suvilehto, et al., 2015). These values shown in Table 27, can be used as values for strength on bonds, SD_{Bond} in Equation 3. Unfortunately, the value for child is not included in the study of Suvilehto, et. al. In the model, the maximum value of 10.0 is assumed as the strength of bond between parent and child and is used in Equation 3.

Table 27 Mean strength of emotional bonds for France (Suvilehto, et al., 2015)

Relation	Partner	Parent	Sibling	Kin	Friend	Acquaintance	Stranger
Strength of Bond	8.82	7.77	7.51	5.29	7.57	3.84	2.17

The results of applying Equation 3 using data from Table 27 is shown in the graph in Figure 22. The graphs illustrate the "boosting effect" of social attachment in the perception of other individuals.

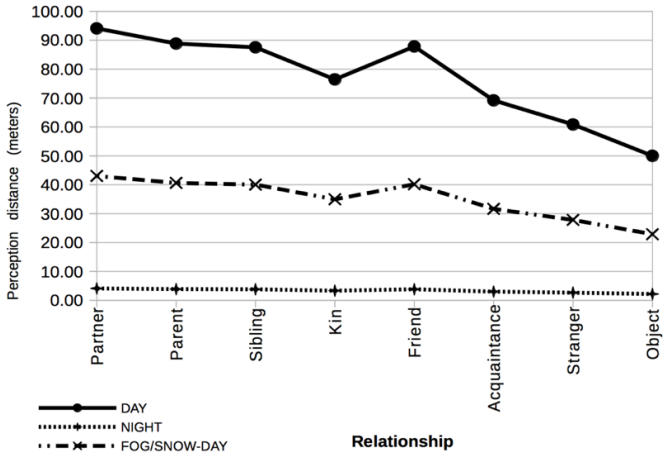

Figure 22 Perception distance influenced by social bond strength

For the perception distance of normal environment objects, for which an individual has no bond, PD_{NoBond}, the value of $SD_{Bond} = 0$. This will reduce Equation 3 to Equation 7.

Equation 7

$$PD_{NoBond} = PD^{k}_{Normal}$$

Perception of locations and destination can be based on knowledge of the location of the attachment figures. Consider, Equation 8, in the situation where knowledge of the location is known, $K_n = 1$, $PD_{knowledge} = \infty$. This means that, when an individual perceives using knowledge, or knows the location of an attachment figure, distance is not a factor. It also means that visual perception of the final destination/goal is not necessary. In the model, familiarity with the area is assumed. Knowledge of the route towards the destination is implied. Means to acquire this knowledge using maps or getting instructions is assumed to be available to individuals. To navigate, the individual needs only to maintain heading or direction towards the known location of the goal. This is for example shown in Section 7.1.2. The limiting factors in maintaining the goal are priority of the current goal with respect to other goals, or the amount of time allotted to reach a goal. If knowledge is not available $K_n = 0$, $PD_{Knowledge} = 0$. When the knowledge is uncertain or between 0 and 1, $PD_{Knowledge} = PD_{Bond}$. When the knowledge of other attachment figures is uncertain, agent's focus on what is occurring in their immediate environment.

Equation 8

$$PD_{Knowledge} = \begin{cases} \infty, & K_n = 1 \\ PD_{Bond}, & 0 > K_n < 1 \\ 0, & K_n = 0 \end{cases}$$

An example for the case when $K_n = 1$, is a situation where the location of children, who are in school or in the home, is known to the parents. Parents would move toward these locations during disaster to recover their children regardless of the distance within the study area. A first priority for a parent for example is to fetch a child from school first, before heading to an evacuation site. Other examples of perception using knowledge are heading to the nearest safe areas, official evacuation sites or the location of one's home.

An example where knowledge can be zero $K_n = 0$ is in the case of tourists experiencing a disaster in an unfamiliar place. In this case evacuation destination choice can be based solely on inputs from immediate and direct visual perception. Knowledge can be gained by consulting an evacuation map,

engaging in social interaction, or seeking information from social media or other sources. Another example is the lack of awareness of what is happening, such as when a person is sleeping. In this case, perception of the shaking is not possible therefore not resulting to any continuing with current activity.

Social attachment is also related to delay time. Actions such as seeking loved ones in the immediate crisis environment and via phone before evacuating, is an example of social attachment at work. Another example is the hesitation to leave without securing property. Delay time is further discussed in Section 5.5. Pre-evacuation behaviours are detailed in Table 28.

5.2 Individual motion and navigation in free space

Realistic motion and navigation of individuals are modelled in SOLACE using affective perception distance, object perception distance, perception angle (or angle of vision for eyesight), and immediate perception area. Individuals move in free space, towards the direction of attachments figures or target locations such as roads and safe areas.

Figure 23 illustrates this model for motion and navigation. The figure shows (1) the individual as a blue triangle labelled H; (2) the rotation of the individual from its centroid to change direction or orientation or heading indicated by blue thick arrows; (3) immediate perception area inside the yellow-orange triangle. This triangle is formed inside the perception angle indicated by the thin blue arrows; (4) the perception area with the perception angle that oscillates or swings in front of the agent to indicate gaze direction and attention; (5) a random step or "footstep" inside the perception area that can be taken by the agent to move forward; changes to the heading and perception area/angle occurs during every "footstep"; (6) location of attachment figure; (7) perception line that indicates that the attachment figure is detected by the agent as indicated by the red arrow; the detection of the attachment figure is only possible when it is inside the perception angle and within the perception distance range; (8) the affective perception distance range PD_{Bond}; it is possible to lose track of the attachment figures if they are beyond the PD_{Bond}; (9) a step along the forward direction of perception line that indicates movement towards the attachment figure; (10) barriers such as buildings, debris and bodies of water that may exist between the agent and the attachment figure.

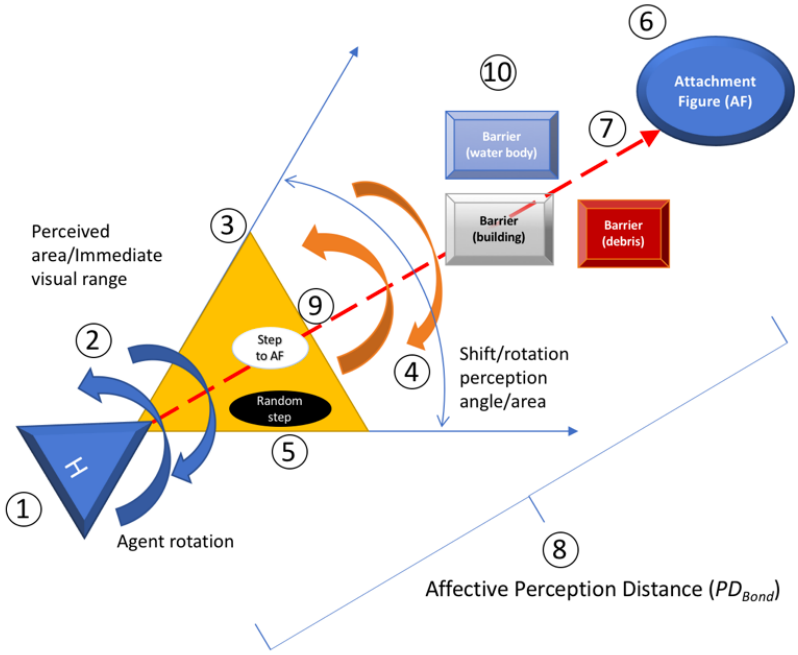

Figure 23 Movement and navigation of the individual in the SOLACE model

When moving, the individual scans the environment for attachment figures. The individual can scan within a defined perception angle for vision. This perception angle and the short forward distance from the individual defines the immediate perception area where near objects are visible. Scanning of the environment is made by changing the orientation of the perception angle and area. The orientation is changed by swinging the perception area in the front of the individual. If no attachment figure is found, an intermediate target is determined inside its perception area, and the individual moves forward. This is similar to making a forward footstep. If an attachment figure is detected, the footstep is made in the direction of the attachment figure, within the perception area.

After every footstep, the scan of the environment for attachment figures is repeated. This re-scan is necessary as locations of people can dynamically change. Also, it is possible to encounter other attachment figures to whom one may have a stronger bond. This can result in a change in target individuals. Also, bidirectional social interaction is possible only when individuals face or see each other. Otherwise it will reduce to a leader-follower scenario. When a barrier is encountered, individuals can change direction and try to move around the barrier. Examples of barriers are debris, building walls or water bodies. Presence of dead individuals can also force the change in direction of movement. The speed of movement is defined by human factors. For example, younger individuals can walk or run faster than older adults. Those with disability or other form of limited mobility will be slower compared to average active adults.

An example scenario of an adult parent agent navigating towards a child agent traversing the crisis environment is shown in Figure 24. (1) An adult agent is located at home and indoors. (2) Another agent is perceived outdoors and the agent follows it outdoors. (3) The road is perceived and the agent heads towards and travels on it. (4) The obstacles such as debris are perceived and avoided by the agent. (5) A group of adults and children is encountered and the agent decides to follow the group. (6) Agent arrives near the school with a crowd of adults in children in front of the school. The adult agent manages to perceive and locate the child from a distance. (7) The adult agent heads towards the child. (8) The child follows adult-parent. (9) The adult agent perceives a group of adult and child agents congregating in the safe area. (10) The adult and child arrive in the safe area.

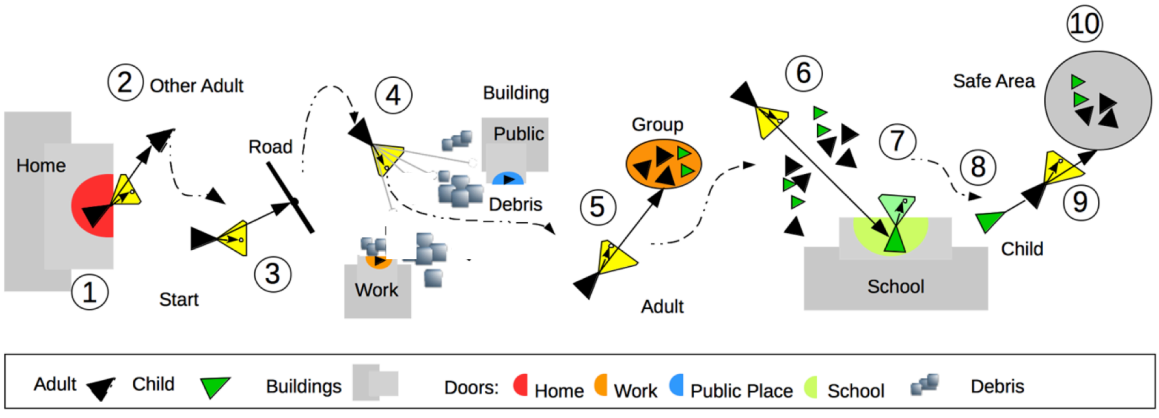

Figure 24 Example of agent movement in SOLACE model

5.3 Model of spatial environment

A vector-based approach is used in the research. A realistic representation of Grenoble's urban form and in 3D is facilitated by using a GIS. The geographic layers used are illustrated in Figure 25. The layers used are: (1) IRIS boundaries defining the extent of study area; (2) natural features such as rivers and other bodies of water; (3) road network defining pathways; (4) buildings; (5) doorways; (6) open spaces; (7) danger zones; (8) safe areas; (9) evacuation routes; (10) earthquake hazard occurring at time

T; (11) damage and debris created during the earthquake; and (12) spatial distribution of human population at time T.

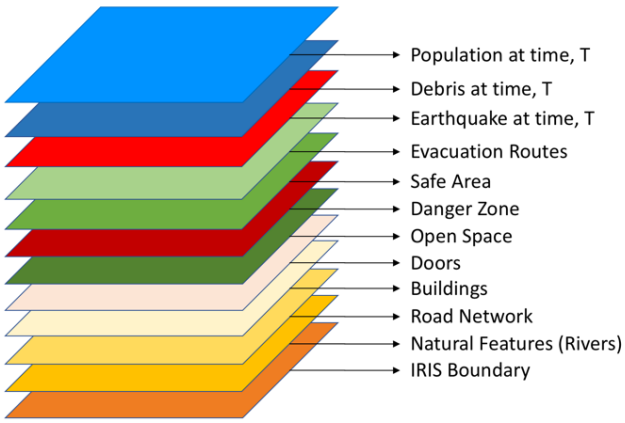

Figure 25 SOLACE Spatial data model

Additional GIS data modelling was used to generate some of the spatial layers. This includes (1) free space; (2) danger zones; (3) safe areas; and (4) spatial distribution of population at different time scenarios. Figure 26 shows the types of spaces in the study area which can act as barriers (buildings, other built features, natural features); or allow movement (free space). For the free space areas, these are further categorised as safe areas to move about, or dangerous as it exposes the agent to the risk of falling debris.

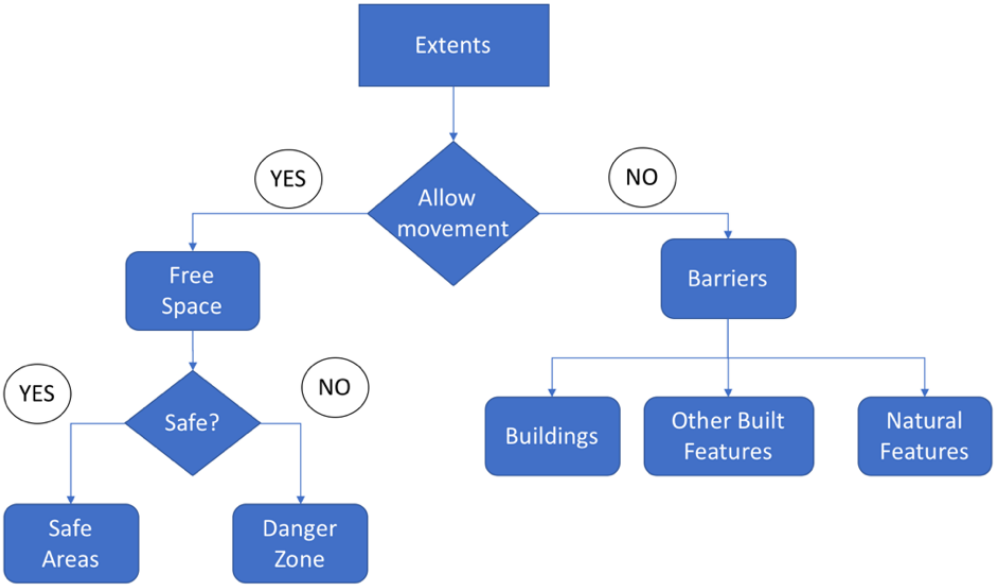

Figure 26 Study area features that act allow agent movement or as barriers

Free space defines areas where individuals are able to move around. It is generated from subtracting layers that define barriers from the extents of the study area. The layers defining barriers include (1) buildings, (2) doorways, (3) other built features (e. g. train tracks), and (4) natural features (e. g. rivers). This is illustrated in Figure 27.

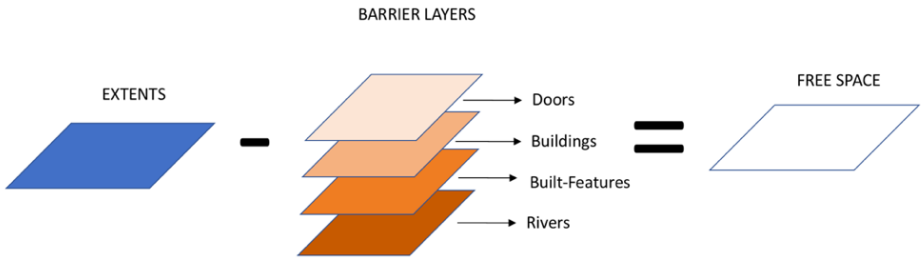

Figure 27 Extracting free space by subtracting barrier layers from extents

Danger zones define areas around buildings where debris may be deposited. This is illustrated by Figure 28. A buffer zone defining the danger zone is generated using a GIS. The distance around the edge of a building equivalent to half the height (H) of the structure is used to generate this danger zone. The value (H/2) is adopted due to the absence of a model for the field of debris deposition around structures in Grenoble. This distance parameter can be changed later when a better model for debris deposition is developed.

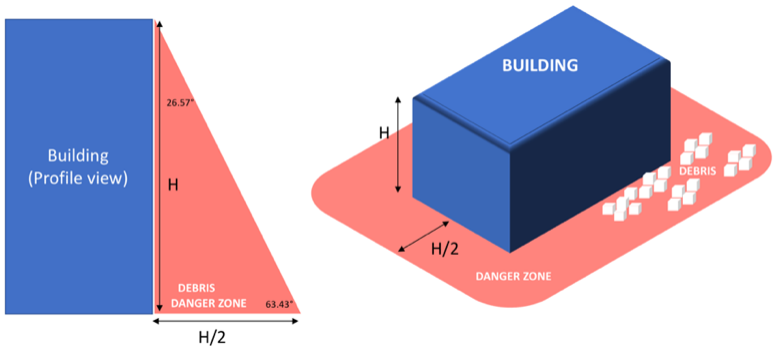

Figure 28 SOLACE danger zones

This value of H/2 is however a conservative estimate, as video footage of collapsing structures can produce debris even beyond the length of the height, H of a structure. For safety during threat of building collapse during fires, firemen usually establish a collapse zone around buildings with a distance of 1.5 times the height of a structure (1.5 x H) (Naum, 2018; Dansbach, 2009). This assumes that the structure will topple forward from its base, with its full height. The additional 50% of the height is the added measure for safety. This distance greatly contrasts with the 6-meter perimeter debris deposition distance from an intensity VII earthquake from the study of Rojo et al. (Rojo, Beck, & Lutoff, 2017). The observations were from the earthquake debris damage resulting from the 2011 Lorca Spain earthquake (MW 5.5, Intensity VII). Their study analysed 9 cases, representing damage from 3 and 4 storey buildings. However, some areas may have taller buildings and debris may fall beyond 6 meters.

Safe areas are free spaces that do not fall within buildings and danger zones. This is shown as the green zone in Figure 29. In simulation experiments, an agent is considered to have reached safety when the agent is already in the green zone. Specific locations within safe areas can be designated as meeting spots during disasters. This is analogous to evacuation assembly points set in place by authorities[20]. In the figure, this is indicated by the dark green circle in the safe zone. The distribution of safe spots can be modified easily in GIS environments. This provides the capability to test the effectiveness of different patterns or configurations of safe spots distribution within urban areas to optimise evacuations. Within

[20] Officially designated areas are marked with evacuation assembly point signs image source: International Standards Organisation (IS0, 2019)

cities, officially designated safe areas for evacuations normally include parks, parking lots and large open venues for sporting events.

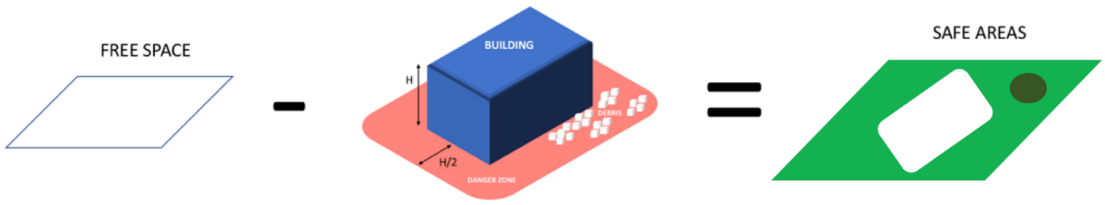

Figure 29 SOLACE Safe Areas extracted by the subtracting building footprint and danger zone from free space

The spatial and temporal distribution of people in indoor and outdoor locations, for each IRIS, is based on data from the national census data. Values from this data are used as upper limits to generate the synthetic human population for daytime, night time, weekday, and weekend scenarios. The IRIS level population values distributed to the level of buildings (to define occupancy for building with specific uses such as home, school, work, public place) and open spaces (such as parks and pedestrian walkways). The distribution is random but based on building use, open space type, and activity during different times of the day. For example, during the night or during weekends, most of the population will be distributed in homes. During a regular workday, the working population will be located in work places. Non-working individuals, such as the retired population, can be distributed in residential homes or parks.

5.4 Model of seismic crisis environment

A simplified conceptual model for the earthquake scenario in SOLACE is shown in Figure 30. From the figure, an ***earthquake (Eqk)***, occurring at an epicentre, of given magnitude and duration triggers the crisis scenario. The effect of the earthquake on people, structures, and the soil is expressed as *intensity*. As shown in the figure, buildings are represented by piles of squares. Each square is a floor in the building. The colours of each floor represent the intensity at each floor. Lighter tones mean less intensity, while darker red tones refer to more intense shaking in the floor. Different soil types represented as hexagonal tiles. Different types of soil will have different amplification effects on building shaking. For Grenoble, two zones of intensity amplification (see Figure 14), based on soil types, have been identified (Dunand & Guéguen, 2012) .

From the figure, in the first case, *Case 1*, buildings and soil near the epicentre of the earthquake are exposed to more shaking and therefore higher intensities. For reference, the observed differences in the behaviours of people at different intensities has been detailed in Table 1. Upper floors are also subject to much higher intensities than lower floors. Human occupants in the upper floors may therefore experience these much higher intensities and this may trigger self-protective actions and evacuation behaviours. Occupants in the lower floors may feel less shaking or may not even be aware of the earthquake. High intensities can result in damage indoors and outdoors. In the figure, debris damage is generated in the danger zone outside the structure as a grey block. The amount of damage and debris generated depends on the (a) building height, (b) typology, (c) vulnerability class, (d) damage probability, (e) earthquake intensity and the duration of the shaking. In case 1, the building, is a well-built structure with four floors. It is able to withstand high intensities from a nearby quake with very few debris damage.

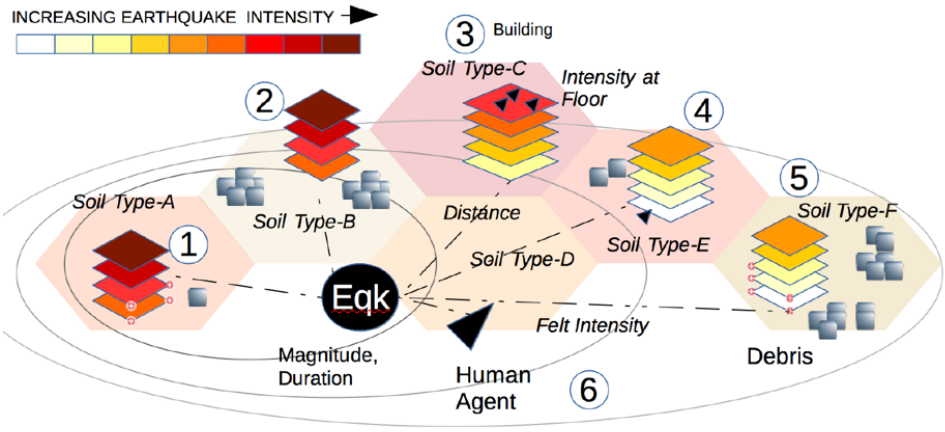

Figure 30 SOLACE earthquake modelling

Case 2, shows a building which is poorly built and with weaker material. It has the same number of floors as in Case 1, a similar distance to the epicentre, and soil type in the same amplification zone. More damage and debris are generated for this case. *Case 3* shows a well-built structure, compliant with building codes, and consisting of more floors. The distance from the epicentre is similar to the first two cases. This structure is not damaged or create debris. This case also shows people located in the uppermost floor. The individuals experience the intensity of the shaking relative to their building floor. *Case 4* shows a moderately-built structure but located farther away from the epicentre; it suffers minor damage and produce few debris. *Case 5* shows a poorly built structure, located farther away from the epicentre, but on a soil-type belonging to the higher intensity amplification zone. This situation produces more damage and debris. *Case 6* shows human individuals located outdoors. At the ground level, people experience the earthquake based on the response of the soil and distance from the epicentre.

For this this conceptual model, simple equation to quantify felt intensity of the individual at the building floor level, $b_{feltIntensity}$ is shown in Equation 9. Parameters included are: earthquake intensity, $eq_{Intensity}$; distance from the earthquake epicentre, $eq_{Distance}$; and building floor, b_{floor}. The $eq_{Intensity}$ is calculated from Equation 10, the reference intensity $ref_{Intensity}$, value considered and is corrected for amplification due to soil type.

Equation 9

$$b_{feltIntensity} = eq_{Intensity} \times \left(1 + \frac{(0.95 \times b_{floor})}{eq_{Distance}}\right)$$

Equation 10

$$eq_{Intensity} = \begin{cases} ref_{Intensity} + 0.7, & Zone = 1 \\ ref_{Intensity} + 1.5, & Zone = 2 \end{cases}$$

Damage to structures and creation of debris are determined by assigning vulnerability and damage probabilities from Rieldel et al. (Rieldel, et al., 2014) to the building data. Debris blocks are created for each intensity scenario considered. Lower intensities create fewer debris with a smaller footprint. The dimension of debris blocks is increased with increasing intensity. This is analogous to a larger debris footprint, from greater damage, due to larger intensities. The types of debris created for intensity V, VI, VII and VIII are based on the size of footprint, and created as small squares, with dimensions in meters (n x n meters). The typologies are small (1m x 1m), medium (2m x 2m), large (3m x 3m) and huge debris (4m x 4m) respectively. For larger intensities, an additional meter for every unit increase in intensity is added to the dimension of the square debris block. This is shown in Equation 11.

Equation 11

$$n = \begin{cases} 0, & Intensity < V \\ 1, & Intensity = V \\ n + (Intensity - V), & Intensity > V \end{cases}$$

Equation 12 is used to calculate the number of debris, n_{debris} , blocks to be created. One parameter is damage category, c_{Damage}. The damage categories are 0, 1, 2, 3, 4 and 5 in the order of increasing damage effects. The number of debris produced for each vulnerability class is k_{Debris}. This is derived using Equation 13. Other parameters used for generating the number of debris are earthquake intensity, $eq_{Intensity}$, from Equation 10; height of the building in meters b_{Height}; and constant, l_{Debris} to limit the drawn debris blocks in the model/simulation for faster computation. The l_{Debris} value for intensity V, VI, VII and VIII are 100, 500, 1000, 1500 and 2000 respectively.

Equation 12

$$n_{Debris} = c_{Damage} \times k_{Debris} \times eq_{Intensity} \times b_{Height} \times \frac{1}{l_{Debris}}$$

The parameter k_{Debris} is the rate of debris production probability for each building vulnerability class. Vulnerability classes are a, b, c, d, and e in the order of decreasing damage production. Masonry structures for example are assigned to vulnerability class a, and can produce more debris than reinforced concrete, which belongs to class e. The number of debris produced is probabilistic and can fall within a range. For example, masonry structures can produce a minimum of 1 to a maximum of 10 debris blocks. The rules for deriving k_{Debris} is shown in Equation 13. The vulnerability classes are *a*, *b*, *c*, *d* and *e*. The maximum debris counts for each class are a', b', c', d' and e' respectively where $a' > b' > c' > d' > e'$. Example values for each class are 10, 7, 5, 3 and 1 respectively.

Equation 13

$$k_{debris} = \begin{cases} kd \in [1, a'], & VC = a \\ kd \in [1, b'], & VC = b \\ kd \in [1, c'], & VC = c \\ kd \in [0, d'], & VC = d \\ kd \in [0, e'], & VC = e \end{cases}$$

5.5 SOLACE multi-agent model and UML diagram

The SOLACE multi-agent model is described by the simplified UML diagram in Figure 31. All elements of the model are agents interacting in geographic space. (1) The *earthquake agent* is the phenomenon that is generated in the environment, triggers the crisis scenario, and affects all agents. Its attributes include magnitude, duration and intensity. (2) *Soil* agents amplify the intensity of the earthquake. Their attributes include type and zone. (3) Building agents are located within a soil agent. Their attributes include typology (construction material), use, and height. (4) Debris agents are produced when building agents are damaged due the intensity of the earthquake. (5) Danger zone agents are located at the perimeter of building agents. These zones are areas of deposition for debris agents. These also define areas where exposed individuals can be injured, killed or trapped by debris. (6) *Safe area* agents are evacuation zones that are located outside danger zone agents. They can be a designated shelter, an open space, or road sections. (7) The individual human agents are heterogeneous with different characteristics defined by age, gender, roles, social group, etc. Human agents occupy indoor and outdoor locations in the environment. They can only move in free space. Interactions with the environment and

socially with other human agents are possible. Examples of behaviours during evacuations include move to safe area, seek family members, follow a leader, etc.

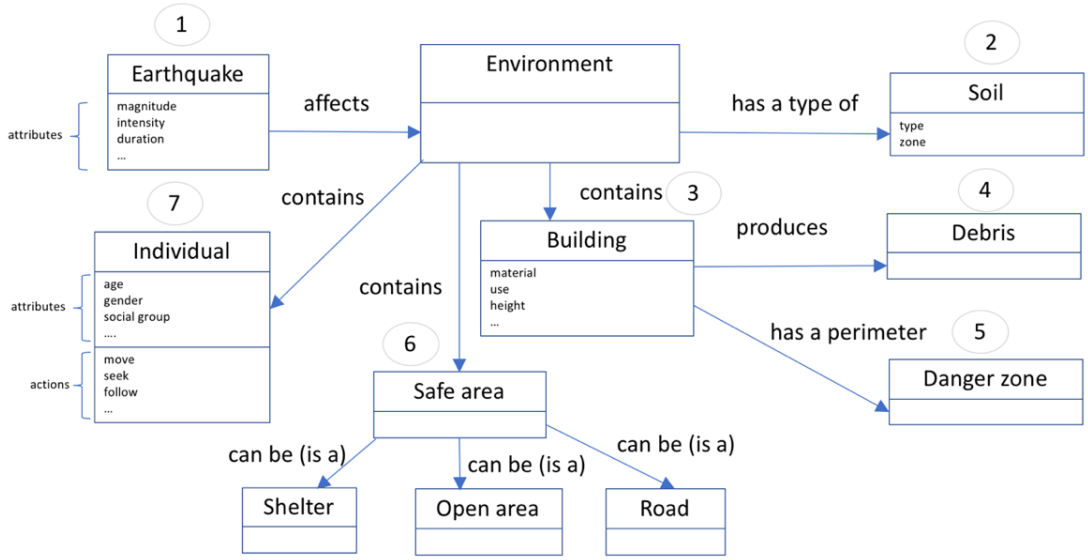

Figure 31 SOLACE simplified UMLClass diagram

A probabilistic approach is applied in how agents choose pre-evacuation behaviours. This is used in calculating the delay time in evacuating buildings. The steps for this approach include the following. (1) A list of pre-evacuation actions or behaviours is prepared. Each of the behaviours is based on SOLACE social attachment model. The attributes for each behaviour includes (a) a range of time to complete the action, d and (b) the probability to be selected for a probability scenario, $Prob_{Sc} = i$, and (c) a *GOTO* parameter, which bootstraps egress from a building. Examples of this actions include proceed to safe area and rescue child from school. Table 28 presents the complete list of pre-evacuation behaviours. Probability scenarios can be (a) uniform probability, all can be selected, probabilities for each action $p = 1$. (b) uniform probability of $p = 0.5$ for all actions. (c) randomly assigned probability value, $p = random(0,1.0)$, (d) probability assigned by an expert, or (e) probabilities derived from a survey. This is shown in Equation 14. (2) The number of behaviours for each agent is determined by selecting a random value, N from the count of possible actions. This is shown in Equation 15. (3) N actions are selected from the PeB_{List} to derive the actions for each agent. This new set of actions comprise the $PeB_{selected}$ list, shown in Equation 16. It is possible that the number of actions in the $PeB_{selected}$ is not equal to *N*. The probability values assigned to some actions may additionally act as a filter, the values may be too small to be included in the final list of pre-evacuation actions.

Equation 14

$$PeB_{List} = [b_0(d_0, p_0, GOTO_0), b_1(d_1, p_1, GOTO_1), \dots, b_n(d_0, p_0, GOTO_n)], \qquad Prob_{Sc} = i$$

Equation 15

$$N = random\,[length(PeB_{List})]$$

Equation 16

$$PeB_{selected} \subseteq PeB_{List}$$

Table 28 Pre-evacuation behaviours in the SOLACE model

Context	Micro-Actions	Examples
Information	Observe immediate environment	Look outside windows
	Confirm with others when in a group	Talk to colleagues to confirm is an earthquake or if situation is life threatening.
	Seek information from media	Turn on radio, check the Internet, watch news on TV
	Document event	Take photos, video, selfie
	Inform others	Notify others on social media, post photos, live video; Call others
Self	Protect self	Seek cover under the table
	Stabilise self	Maintain balance during shaking
	Move away from object	Move away from walls and furniture
	Walk or run during shake	Immediate egress from building
	Walk or run after shake	Wait for shaking to stop and egress from the building
	Evacuate to safe area	Go any open area such as roads, parks
	Evacuate to assigned area	Go to officially designated safe are
	Freeze	Stay immobile because of fear.
	Weigh options and decide	Choose route and possible exits before egress
	Continue current task	Proceed with task as normal. Remained and continued working; Woke up but slept again; Continued driving
	Stopped current task	Stopped working and observed the environment
	Stay still	Remain immobile and continue to observe shaking
	React, scream	Screaming out of fear
	React, enjoyed the experience	Not fearful but enjoyed having experienced a quake
	React, hope for shaking to stop	Fearful and hope for the shaking to stop
	Do nothing	Stay immobile and do nothing. It can be because the shaking is not felt, or not considered as a threat to the self.
	Waited for shaking to stop	Wait for shaking to stop before egress
	Pray	Pausing and praying for personal safety.
	Move Out	Immediate egress from buildings
	Stay indoors	Stay inside for fear of falling debris from higher floors.
Family	Phone/call family member	Calling family members who are outdoors to confirm their safety
	Seek nearest family member	Find other family members inside homes before evacuating.
	Get kids immediately	Getting babies and other children before egress
Others	Help	Calming others; Assist injured, elderly and disabled
	Follow towards exit.	Copy others actions like heading towards egress
	Check on dependent	Check on the elderly or children before evacuation
	Protect someone	Shield others from debris or falling furniture
Property	Turn-off gas	Close gas mains and stoves.
	Close doors and windows	Close doors or windows to avoid being robbed
	Hold/prop objects	Prop furniture, large TV sets
	Grab objects	Get personal property like wallets, documents, computer
	Grab emergency kit	Get emergency, survival, or first aid kits

Egress of agents from buildings proceed immediately when a behaviour with the GOTO parameter is selected. When no GOTO parameter is selected, the durations of all selected actions are totalled before egress. An immediate change in behaviour to egress can be triggered when a human agent perceives debris or other human agents who are injured or deceased. The model for egress with pre-evacuation behaviours is shown in Figure 32.

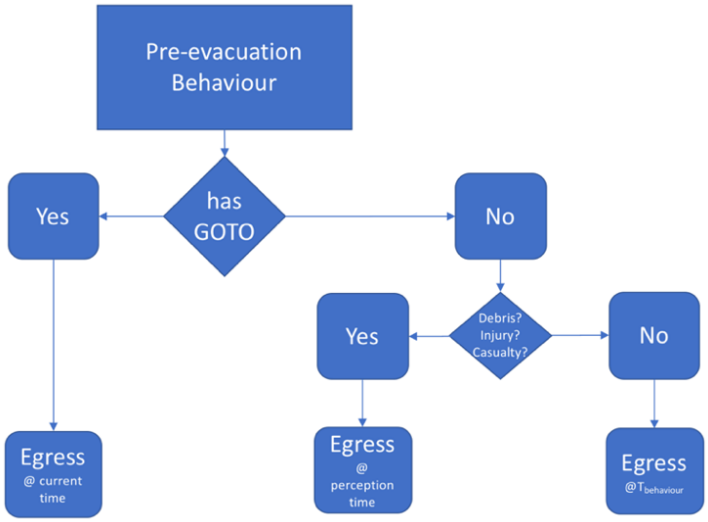

Figure 32 Model for building egress

Delay time to leave a building, T_{Delay} is calculated, for an agent at a building floor, B_{floor} by summing the durations for all the selected pre-evacuation actions, $T_{Behaviour}$, and adding the time required to travel through building floors to the ground level, T_{floor}. Calculations for $T_{Behaviour}$ and T_{Delay} is shown in Equation 17 and Equation 18 respectively. When an agent has a behaviour with a *GOTO* parameter, the value for $T_{Behaviour}$ = 0.

Equation 17

$$T_{Behaviour} = \sum_{i=0}^{n} d_i \quad , \; where\ d_i \text{ time for } b_i \in PeB_{selected}$$

Equation 18

$$T_{Delay} = T_{Behaviour} + (B_{floor} \times T_{floor})$$

During pedestrian evacuation, agent decision making, behaviour and social interaction are implemented using the BDI approach. Table 29 illustrates several examples of an individual agent's beliefs, desires and possible actions in different contexts. Desires can be contradictory to each other. As an example, seeking family member involves putting oneself in danger.

Table 29 Examples of BDI implemented with social attachment in SOLACE

Context	**Beliefs**	**Desires**	**Actions**
Normal situation	None	None	None
During extreme earthquake	I'm not safe	Be safe	Seek attachment figures/objects, protect self, egress, evacuate
During moderate earthquake	I'm safe, my building is safe	None	None
At safe area with family	I'm safe	Stay safe	Stay
At safe area but missing family member	I'm safe, my family member is unsafe	Stay safe, family member is safe	Seek family member, call, return to danger area

This decision-making process is shown in Figure 33. The human agent (1) is sensitive to the environment and dynamically evaluates the current context, (2) formulates a belief about the situation, (3) each belief is associated with a desire, and the highest priority desire is selected, (4) the highest priority desire becomes the agent's intention, (5) a plan of action is chosen to achieve that selected intention, and (6)

the context is re-evaluated. The described process repeats until the desired context, for example, being safe, is reached.

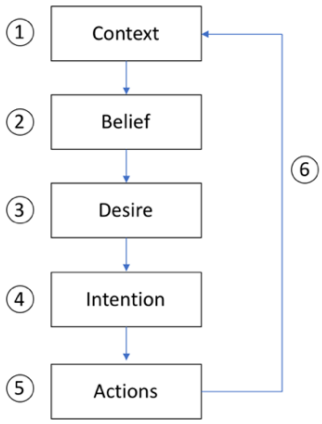

Figure 33 Human agent decision making

Behaviours considered for the model and implemented using BDI are listed in Table 30. The table details how agents interact with targets in the crisis environment and among themselves. BDI acts as a dynamic switch and facilitates agent cognitive decision making especially during agent social interactions. BDI is able to manage the (1) different relationships for each specific agent as shown in the social attachment model in Figure 15, (2) dynamic social interactions resulting from relationships using PD_{Bond} as a measure of priority, and (3) conflicting scenarios during evacuations. Examples of conflicting scenarios are (1) attachment related pre-evacuation behaviours such as retrieving property before evacuating to safety, (2) when an adult agent needs to move away from the location where a dead agent is present, but that agent is a close family member. BDI also is used to enable movement of agent movement towards goals such as head toward safe areas.

Table 30 Evacuation behaviours modelled/implemented taking into account BDI

Agent	**Target**	**Micro-Actions**	**Reason/motivation**
Human agents (adult and child)	Earthquake	Perceive earthquake	Physical threat
	Debris	Perceive and move away from	Physical threat
		Change pre-evacuation behaviour	Physical threat; seek refuge/safety
	Road centreline	Move to centre of road	Seek refuge/safety
	Safe area	Move to safe area	Seek refuge/safety
		Slow down when inside safe area	Seek refuge/safety
	Doors	Move from	Egress to seek refuge or attachment figures
		Move towards	Affiliation/proximity seeking (attachment to place, property, location of attachment figures)
	Buildings, bodies of water, fenced areas (train tracks)	Avoid, move away from	Physical barrier
	Injured or dead adult and child	Change pre-evacuation behaviour	Indication of immediate threat
	Injured adult or child	Perceive and move towards	Help others in need
Adult	Adult family member	Perceive and move towards	Affiliation/proximity seeking
	Child family member	Perceive and move towards	Affiliation/proximity seeking
	Child family member when role of adult is parent	Perceive and move towards	Affiliation/proximity seeking
	Adult kin	Perceive and move towards	Affiliation/proximity seeking
	Child kin	Perceive and move towards	Affiliation/proximity seeking
	Adult friend	Perceive and move towards	Affiliation/proximity seeking
	Child friend	Perceive and move towards	Affiliation/proximity seeking
	Adult colleague	Perceive and move towards	Affiliation/proximity seeking

	Child of colleague	Perceive and move towards	Affiliation/proximity seeking
	Adult stranger	Perceive and move towards	Affiliation/proximity seeking
	Child stranger	Perceive and move towards	Affiliation/proximity seeking
	Child when role of adult is teacher	Perceive and move towards	Affiliation/proximity seeking
	Adult who is elderly or disabled	Perceive and move towards	Help others in need
Child only	Adult family member	Perceive and move towards	Affiliation/proximity seeking
	Adult family member when role of adult is parent	Perceive and move towards	Affiliation/proximity seeking
	Child family member (sibling)	Perceive and move towards	Affiliation/proximity seeking
	Adult kin (uncles/aunts)	Perceive and move towards	Affiliation/proximity seeking
	Child kin (cousins)	Perceive and move towards	Affiliation/proximity seeking
	Adult friend	Perceive and move towards	Affiliation/proximity seeking
	Child friend	Perceive and move towards	Affiliation/proximity seeking
	Adult "colleague" who is a teacher	Perceive and move towards	Affiliation/proximity seeking
	Adult "colleague" who is not a teacher but in school	Perceive and move towards	Affiliation/proximity seeking
	Child colleague (classmate)	Perceive and move towards	Affiliation/proximity seeking
	Adult stranger	Perceive and move towards	Affiliation/proximity seeking
	Child stranger	Perceive and move towards	Affiliation/proximity seeking

5.6 Software application model and system architecture

A multi-platform approach used to implement SOLACE. This strategy is used to take advantage of available software tools for data processing, simulation, dynamic data reporting, and 2D/3D visualisation.

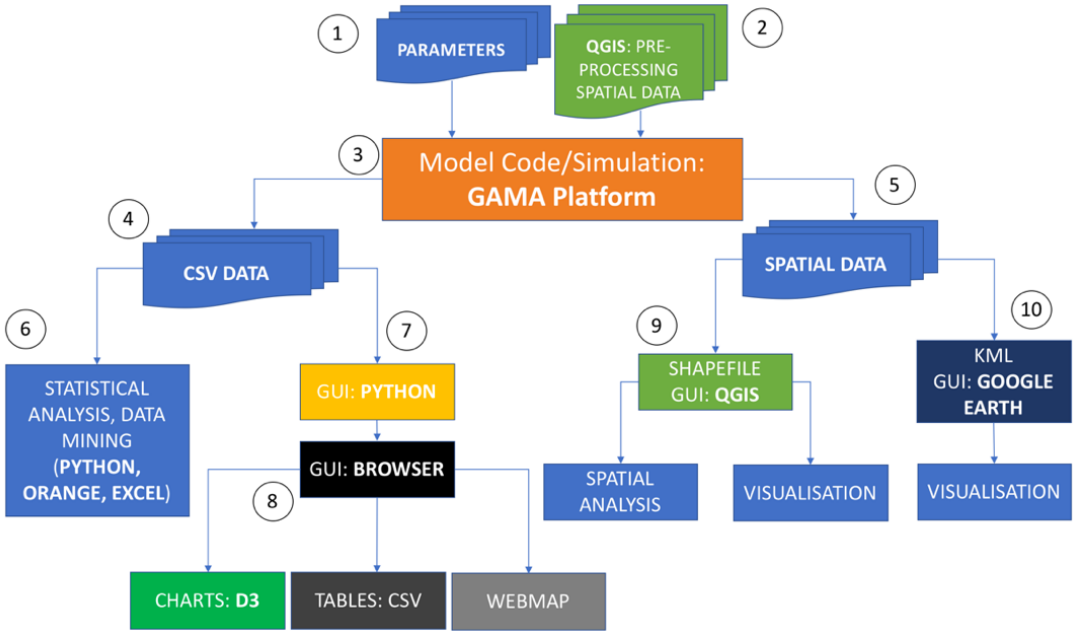

Figure 34 SOLACE System Architecture

The architecture and complimentary roles of the technologies are shown in Figure 34. (1) Model parameters are derived from data. (2) Spatial data are pre-processed using Quantum GIS (QGIS) (QGIS Development Team, 2018). (3) The model code is written using the BDI architecture with the GAMA Platform (Grignard, et al., 2013). (4) Output of the simulation runs are saved at every time step as text files in CSV form. (5) Spatial data outputs include shapefiles and KML files. (6) Statistical analysis and data mining tools are used to process the CSV data. (7) A custom user interface developed using Python

facilitates dynamic data visualisation using a web browser. (8) The web browser uses JavaScript to display D3 charts and tables, and Leaflet/Folium web maps. (9) QGIS is used to process shapefiles for spatial analysis and dynamic 2D and 3D map visualisations and animations. (10) Google earth is used to visualise and create animations using KML files within photorealistic 3D scenes and street views.

5.7 Summary of the chapter

The chapter discussed the different components that make up SOLACE. The model uses social attachment are the framework for behaviours during seismic crisis situations. The behaviours included in the model are consistent with Mawson's social attachment theory (Mawson, 2005). Affiliation activated by the treat from earthquake, prompts proximity seeking behaviours towards attachment figures. Familiarity facilitates the recognition of attachment figures from a distance. The role of distance in recognition of personally familiar individuals has been highlighted in the chapter. Distance is relevant to the model in the following concepts (1) social distance SD_{Bond}, (2) affiliation distance (PD_{Bond}), and (3) spatial distance for recognition tasks, modulated by human factors and environment conditions. Distance functions as a filter to prioritise perception and actions such as movement towards attachment figures. Affiliation distance is the direct expression of social attachment in SOLACE. It functions as a dynamic spatial filter in the prioritisation of attachment figures for proximity seeking behaviours. The location of an attachment figure defines the direction of agents during motion.

This function of distance as a filter highlights the importance of the accurate representation of geographic space to achieve a realism in the evacuation model. The spatial model of the crisis environment is built using real geographic data. With this dataset, the 2D and 3D distribution of earthquake effects on environment objects (buildings) and human agents are simulated. The effects of earthquakes shaking is more severe when closer to the source and at much higher floors. Human agents are located in building floors and outside. Taller buildings with poor construction produce more debris at farther distance from the structures. Vulnerability and damage probabilities of buildings are derived from a macroseismic study (Riedel et al., 2014). Danger zones are areas of deposition for debris. Safe areas are zones where no debris is deposited. Safe areas generated from geoprocessing task on geographic data.

Dynamic interactions of agent elements are facilitated in the multi-agent model. These interactions include (1) damage or debris creation of buildings due to extreme shaking and long earthquake durations, (2) individual human agent interactions with earthquake damage, and (3) social interactions. The BDI architecture is used to simulate the cognitive decision making of agents implement individual and social behaviours.

The system architecture or software model for SOLACE is composed of several modules. The software code for the agent-based simulation is develop using GAML with the GAMA platform. Geographic data is managed and pre-processed using QGIS. Utilities to store data and visualise dynamic graphs of the data are developed in Python. Basic data analysis is done using spreadsheets.

To conclude, SOLACE has been developed using different components, with social attachment as the core motivation and foundation for the model. In the chapter, this was shown from the development the core social attachment model, evacuation behaviours, and agent-based software model and architecture.

CHAPTER 6. IMPLEMENTATION, CALIBRATION & VALIDATION OF THE SOCIAL ATTACHMENT MODEL

This chapter details the relevant workflows and key software code implemented to develop SOLACE. Geospatial data that defines the crisis environment are pre-processed using the GIS tools available in QGIS (QGIS Development Team, 2018). The prepared data is used in agent-based modelling using the GAMA platform (Grignard, Taillandier, Gaudou, Vo, & Drogoul, 2013). A highly visual approach was used in the many steps using QGIS and GAMA. Dynamic data visualisations tools to explore simulation results were likewise developed using Python, JavaScript, D3 and viewed in the browser using HTML.

The chapter is divided into the following sections. Section 6.1 discusses the use of GIS in preparing the spatial model of the crisis environment. Section 6.2 discusses the use of ABM in developing the code for the model. Section 6.3 discusses the hardware configuration used to run SOLACE. Section 6.4 details the activities involved to calibrate the model. Section 6.5 provides the short summary and conclusion to the chapter.

6.1 Spatial data processing workflows

Spatial data used in the agent-based model were prepared using geoprocessing[21] with GIS. The key geoprocessing tasks involved (1) deriving safe areas and danger zones, (2) integrating damage and vulnerability attributes to building data, and (3) editing and creating new data such as adding doorways to buildings. Doors have been created by selecting nodes from building polygon outlines. Other tasks to integrate attribute information are attribute joins, spatial joins, and editing data tables.

Vector data were also integrated with attribute data using GIS. Attribute data include vulnerability and damage probabilities from Quantum GIS or QGIS, which was used to process the spatial thematic data layers. Thematic layers include buildings, safe areas, free areas. Processing included vector data editing and attribute encoding. These finalised thematic layers were used as inputs to the agent-based model and simulation in GAMA. This workflow is shown in Figure 35. This represents the generic process for each data which will be detailed in the following subsections.

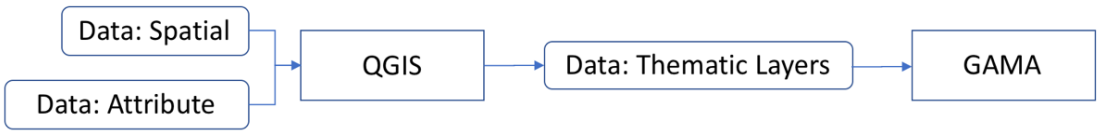

Figure 35 Spatial data processing workflows

Spatial data and non-spatial attribute data were prepared for integration into the agent-based model using GIS. Quantum GIS or QGIS was used to process the spatial thematic data layers. Thematic layers include buildings, safe areas, free areas. Processing included vector data editing and attribute encoding. These finalised thematic layers were used as inputs to the agent-based model and simulation in GAMA.

[21] Geoprocessing includes procedures for data manipulation and processing of geospatial data (Sherman, 2008). Example operations on data using QGIS are buffer, clip, difference, dissolve, intersect, and union (Roth, 2018). Vector editing was also done to simplify data.

6.1.1 Deriving safe areas and danger zones

The workflow for deriving safe areas and danger zones is shown in Figure 36. The layers used include shapefiles from BDTOPO, OpenStreetMap and the IRIS boundaries from Riedel et al., 2014 (Riedel, Guéguen, & Dunand, 2014). Preparing the data for integration into the model includes (1) geoprocessing and (2) building the attribute tables. Figure 37 shows the GIS layers used. Figure 38 shows the zoomed in version. Table 31 provides the details and characteristics of the data.

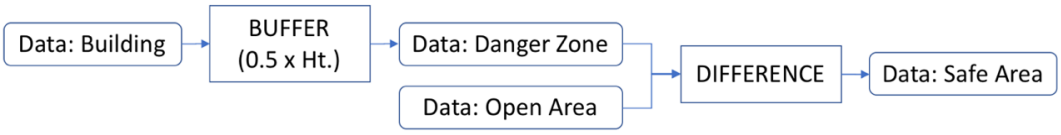

Figure 36 Geoprocessing workflow for the creation of danger zones and safe areas

Figure 37 Spatial layers used in the model at the scale of the city of Grenoble

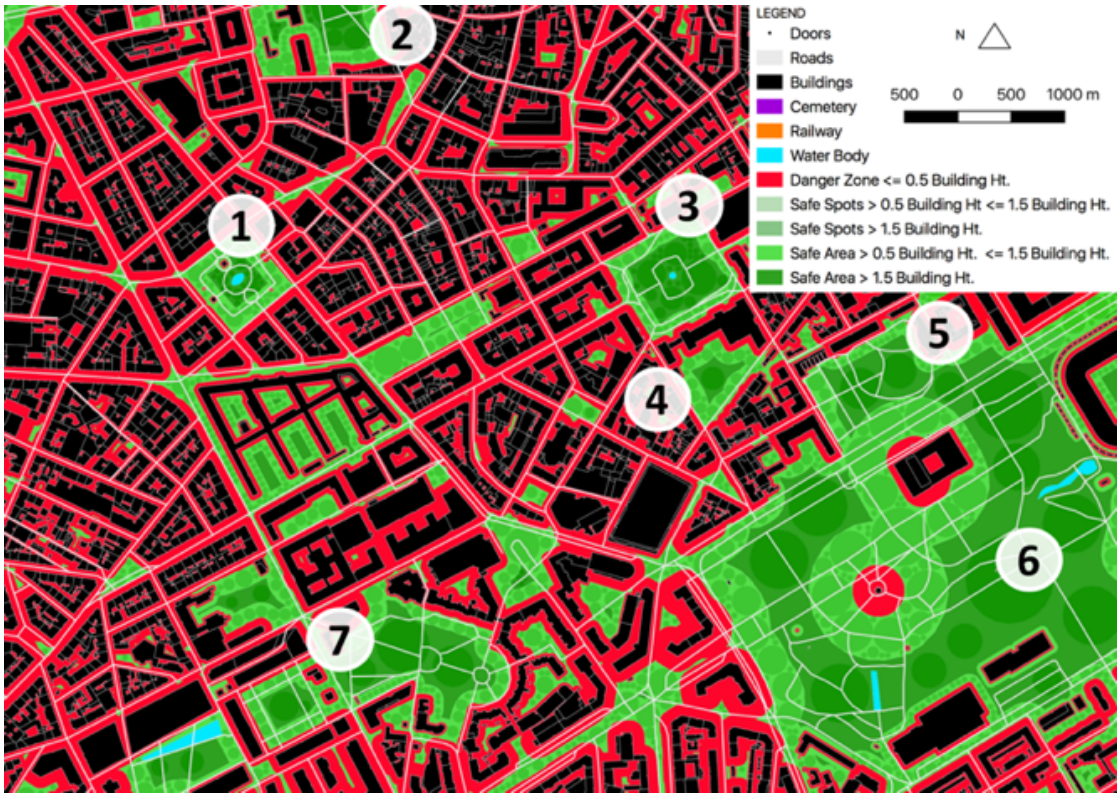

Figure 38 Safe areas and danger zones in the city center of Grenoble. Danger zones are the red areas around buildings. The width of the zone or the distance from the building is half the height of the structure. The safe areas are the green coloured spaces. Large open spaces suitable for evacaution in the figure are (1) Place Victor Hugo, (2) Parc Jardin de Ville, (3) Verdun, (4) Parc du Département de l'Isere, (5) Parc Jadin des Plantes, (6) Parc Paul Mistral, and (7) Parc Jardin Hoche.

Table 31 Data layers in Figure 37 and Figure 38

Category	Data	Colour	Source	Purpose/target
Geospatial (Spatial)	Grenoble boundary	Pink	(Riedel_a, et al., 2015)	Define model extents, aggregated from IRIS boundaries.
	IRIS Boundary		(Riedel_a, et al., 2015)	Attributes used as probabilities for generating attributes of enclosed features (population, buildings).
	Buildings		BDTOPO (IGN, 2017)	Provide location of people indoors. These also serve as barriers to movement and define the boundaries of alleyways and streets. When they are damaged during a crisis scenario they provide the source of debris.
	Road network		BDTOPO (IGN, 2017), OpenStreetMap (OpenStreetMap & Contributors, 2018)	Provide pathways, routes towards safe areas during evacuations. Centre lines of roadways are the initial safe areas. Also provides guidance to agents when evacuating to safe areas.
Geospatial (Spatial) Geoscience (Seismic)	Doorways		Digitised from satellite imagery	Used as starting locations for evacuation, especially during night time scenarios. Occupancy; location of "indoor" agents
	Natural features/Rivers		BDTOPO (IGN, 2017)	Barriers to movement. These are used to restrict pedestrian movement in pathways.
	Danger Zones		Derived from data using geoprocessing tools	Used to define deposition areas for debris around buildings
	Safe areas		Derived from data using geoprocessing tools, and vector editing	Areas free from debris. Used as destinations of agents during evacuations.

6.1.2 Scaling macroseismic damage and vulnerability data to the building level

Building vulnerability and damage was derived from IRIS level macroseismic vulnerability and damage attributes. The workflow of assigning IRIS level macroseismic data to buildings within an IRIS is shown in Figure 39. The steps involved are (1) deriving the centroids of buildings resulting to a point shapefile; (2) spatial attribute join by assigning the building centroid points to the bounding IRIS polygon; (3) attribute join operation linking the data from the building centroid points to the building polygon data. The result is a building polygon shapefile with the attributes of the IRIS layer.

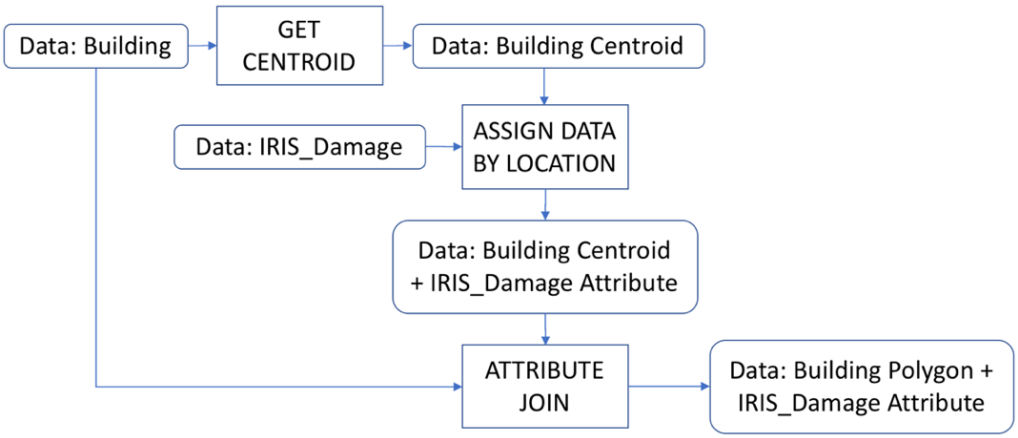

Figure 39 Assigning building with IRIS damage and vulnerability data

The fields in the resulting attribute table of the building shapefile with the combined vulnerability and damage probability data from the IRIS shapefile are detailed in Table 32. The probability values are used later in the assignment vulnerability and damage for each building. This is discussed in Section 6.2.2.1.

Table 32 Building data with IRIS attributes

IRIS data Fields	**Type**	**Description**
ID	String	Building ID
HAUTEUR	Integer	Building height
IRIS (code, Integer), IRIS_NAME (String)		IRIS Code and Name
ZONE	Integer	Soil Zone
D_pa, D_pb, D_pc, D_pd, D_ pe	Float	Probability Typology (for typologies a, b, c, d, and e)
D_d0V_p, D_d1V_p, D_d2V_p, D_d3V_p, D_d4V_p, D_d5V_p	Float	Probability Damage Degree Intensity V (for degree 0, 1, 2, 3, 4, and 5)
D_d0VI_p, D_d1VI_p, D_d2VI_p, D_d3VI_p, D_d4VI_p, D_d5VI_p	Float	Probability Damage Degree Intensity VI (for degree 0, 1, 2, 3, 4, and 5)
D_d0VII_p, D_d1VII_p, D_d2VII_p, D_d3VII_p, D_d4VII_p, D_d5VII_p	Float	Probability Damage Degree Intensity VII (for degree 0, 1, 2, 3, 4, and 5)
D_d0VIII_p, D_d1VIII_p, D_d2VIII_p, D_d3VIII_p, D_d4VIII_p, D_d5VIII_p	Float	Probability Damage Degree Intensity VIII (for degree 0, 1, 2, 3, 4, and 5)
D_d0IX_p, D_d1IX_p, D_d2IX_p, D_d3IX_p, D_d4IX_p, D_d5IX_p	Float	Probability Damage Degree Intensity IX (for degree 0, 1, 2, 3, 4, and 5)
D_d0X_p, D_d1X_p, D_d2XI_p, D_d3X_p, D_d4X_p, D_d5X_p	Float	Probability Damage Degree Intensity X (for degree 0, 1, 2, 3, 4, and 5)
D_d0XI_p, D_d1XI_p, D_d2XI_p, D_d3XI_p, D_d4XI_p, D_d5XI_p	Float	Probability Damage Degree Intensity XI (for degree 0, 1, 2, 3, 4, and 5)
D_d0XII_p, D_d1XII_p, D_d2XII_p, D_d3XII_p, D_d4XII_p, D_d5XII_p	Float	Probability Damage Degree Intensity XII (for degree 0, 1, 2, 3, 4, and 5)

Figure 40 shows map of the buildings, IRIS and resulting buildings with IRIS attributes. Different colours represent IRIS boundaries. The buildings are the black polygons on the leftmost image. The

centre image shows IRIS boundaries as large polygons with different colours. The buildings assigned with attributes with respect the enclosing IRIS are shown in on the rightmost image. Here the buildings reflect the colours of the enclosing IRIS.

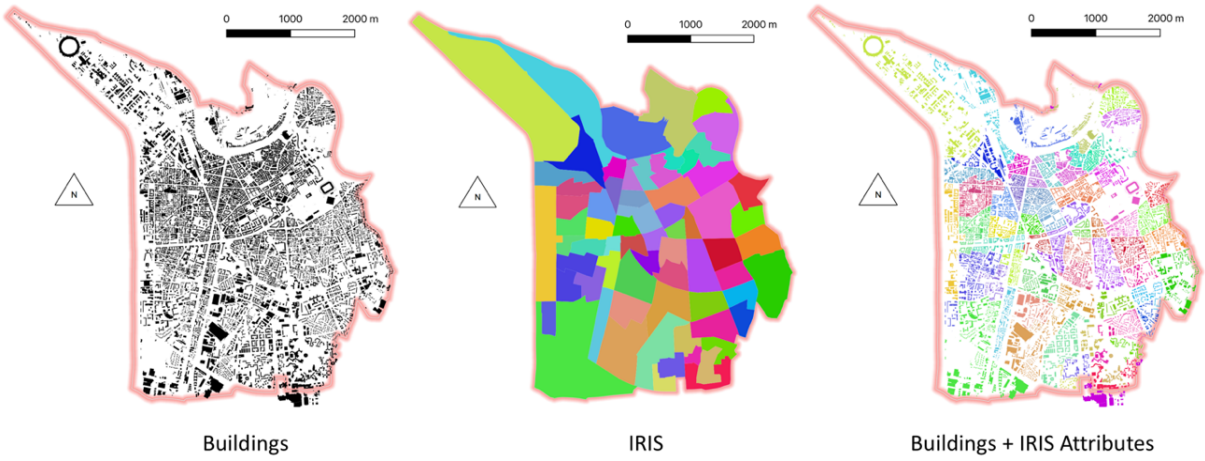

Figure 40 Building data with IRIS layer attributes

6.1.3 Spatial data subsets

The Grenoble study area covers 69 IRIS boundaries and contains a large number of spatial elements with complex geometries. This includes buildings, danger zones, safe areas, etc. Each layer, which is composed of many individual components, introduces complexity. During simulation runs, very high model complexities result in very slow processing times. The strategies adopted on vector data to manage complexity and speed up data processing are: (1) minimise the number of individual vector elements; (2) use simple geometries; (3) simplify attribute tables and minimize number of fields; and (4) create smaller subsets of the data.

To facilitate testing, calibration and some experiments on the model, smaller spatial subsets of the data were used. The subsets are small, medium and large areas. The large set covers the entire city of Grenoble. Figure 41 shows the two subsets of the data. The figure includes (1) small area covering two IRIS zones in the old historic centre, namely Victor Hugo and Grenette, and (2) medium area showing a map covering nine IRIS zones. The nine IRIS zones are Victor Hugo, Grenette, Aigle, Championnet, Génissieu, Hoche, Jean Jaurès, Préfecture, and Saint-André.

The spatial layers used in the model for each spatial subset are detailed in Table 33. The categories for the vectors are boundary, building, building damage, danger zone, doors, roads, safe areas, land cover and land use, and other layers. The number of vector elements or records for each layer is indicated. In Table 33, it can be noticed that for building damage and danger zones, layers for each intensity scenario are presented. For example, Building_Damage_Int5 and Danger_Zone_Int5 for an intensity V earthquake scenario. For the building damage layer, only buildings with damage are considered (i.e. damage class >= 1). Similarly, for the danger zone only danger zone polygons containing the buildings with damage are considered. Higher intensities result in more damaged buildings and damaged zones. This strategy of deriving subsets of the building data with respect to intensity scenarios gives a fewer number of vector polygons. This speeds up the simulation experiments.

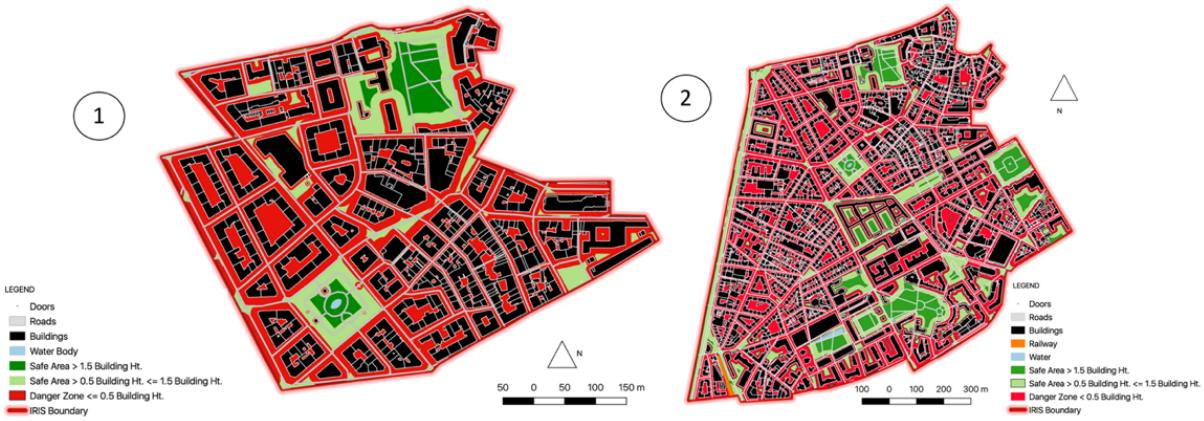

Figure 41 2-IRIS Subset (Left), 9-IRIS Subset

In the case of safe areas (or evacuations areas), *Safe Area* polygons are fewer in number than Safe Spots. Safe Area polygons however define very large zones and have more complex geometries. Safe Areas, in general, refer to safe areas away from buildings. Safe Spots are small circles within the Safe Area polygon footprint and offer more precise destinations for agent displacements. Safe spots are analogous to meeting spots or rally points. This is also useful in distributing evacuating agents in a more realistic pattern similar to those observed in real evacuations. The use of these two types of safe areas was tested in the experiments.

Table 33 Number of vector elements for the model for each layer

Category	**Fields**	**Type**	**Number of vector elements**		
			Small Area	**Medium Area**	**Large area**
Boundary	IRIS	COUNT	2	9	69
	Boundary	Polygon	1		1
Building	Building_Outline	Polygon	73		6244
Building damage for each Intensity scenario	Building_Damage_Int5	Polygon	12	56	426
	Building_Damage_Int6	Polygon	116	439	3491
	Building_Damage_Int7	Polygon	304	1037	7984
	Building_Damage_Int8	Polygon	386	1485	11588
	Building_Damage_Int9	Polygon	459	1768	14493
	Building_Damage_Int10	Polygon	471	1872	15994
	Building_Damage_Int11	Polygon	472	1899	16611
	Building_Damage_Int12	Polygon	473	1902	16717
Danger Zone for each damaged building	Danger_Zone_Int 5	Polygon	20	83	553
	Danger_Zone_Int 6	Polygon	144	571	4530
	Danger_Zone_Int 7	Polygon	394	1402	10561
	Danger_Zone_Int 8	Polygon	503	1985	15315
	Danger_Zone_Int 9	Polygon	598	2384	19090
Doors	Door_Centroid	Point	380	1492	10865
Roads	Roads	Polygon	203	727	6169
Safe Areas	SafeArea >0.5	Polygon	34	184	
	SafeArea >0.5 <=1.5	Polygon	32	177	1477
	SafeArea > 1.5	Polygon	3	25	726
	Safe Spots >0.5 <=1.5	Polygon			16634
	Safe Spot > 1.5	Polygon			120
Land cover and Land use	Water Body (e.g. river, pond)	Polygon	1	3	20
	Rail	Polygon	0	1	8
	Cemetery	Polygon	0	0	1
Other layers	Mask	Polygon	1	1	1
	Extent	Polygon	1	1	1
	Free Space	Polygon	3	13	171

6.1.4 Vector data modification (adding doors, carving out doorways and simplify layers)

Modifications in the vector data layer were necessary to implement the crisis scenario and ensure mobility of agents. Of particular concern was providing precision for source locations for agents and a single means for egress of structures. Egress points are necessary for more accurate results for evacuation times.

Doors in buildings play a key role in the model. These are where indoor agents are generated, free to move about "indoors", and egress during evacuations. Doors in the shape of semi-circles are carved-out of building polygons. Doors are placed in the side of buildings close to roads. Attributes for doors indicate the use of the building such as home, school, work and public area. In the model, at least one door is created for each building polygon. Buildings are considered as barriers in the model. Doors are the parts of buildings where movement of agents is possible. Figure 42 illustrates the different types of doors in buildings. Table 34 shows the attributes of doors.

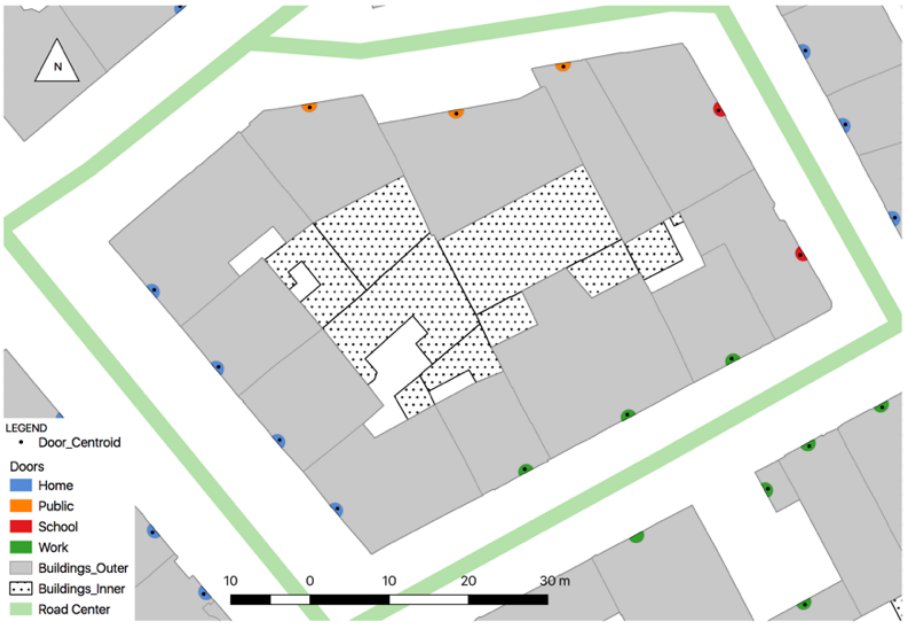

Figure 42 Doors and buildings in SOLACE. Human agents are generated inside door polygons at the start of the simulations.

Table 34 Attributes for doors

Fields	**Values**
Use	Home, School, Work, Public
Building_ID	ID of enclosing building
IRIS	Name of enclosing IRIS boundary

The use of doors as starting points for agent motion is a simplification and compromise. The main reason is that the simulation deals with pedestrians emerging from buildings and evacuating towards safe areas. In this way there is no need to model agents moving from different floors in the building to the door; rather the agents' exits are timed (i.e. staged delays) to reflect which floor they may be on and their pre-evacuation activities. The other reasons are (1) a common point is needed for egress, (2) buildings have at least one door and locations can be validated from street photographs, (3) there is more control in managing egress times of agents through pre-evacuation delay times, (4) unnecessary navigation delays by building wall barriers are generated when agents are generated indoors, and (5) no data is available for building indoor layouts or floor plans.

Other modifications on the data are simplifications of building layers. Only buildings close to streets, or "outer buildings" are retained and used in the model. "Inner buildings" are edited out and not included. This is to lessen the number of building polygons, minimize model complexity and improve processing times. Inner and outer buildings are shown in Figure 42.

6.2 Agent based modelling workflow

The software code for SOLACE is written in GAML within the GAMA development environment. GAMA was chosen for the model due to its (1) easy to read high level programming syntax, (2) open source framework, which makes examples available, (3) capability to seamlessly integrate geospatial data, (4) capacity to build in BDI architecture, (5) tools to inspect agent characteristics, (6) crisp and excellent opengl 3D map display, and (7) export csv and shapefile data.

A modular strategy was adopted to manage the code. This is shown in Figure 43. The set of modules includes (1) scenario and shapefile generator for building vulnerability and damage, BuildingDamageScenario.gaml; (2) shapefile data manager Data_Shapefile.gaml; (3) population data definition file Data_Population.gaml; (4) social perception distance definition file Data_SocialAttachment.gaml. (5) human species definition file, Species_Human.gaml; (6) adult species definition file Species_Adult.gaml; and (7) child species definition file Species_Child.gaml; These are imported into the main module SOLACE.gaml.

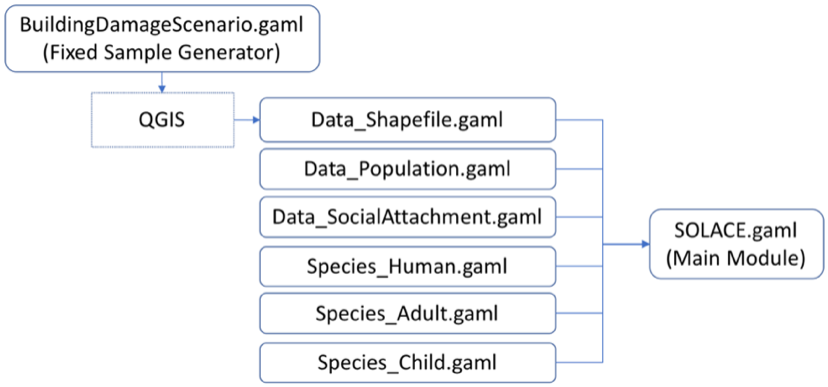

Figure 43 SOLACE Code Modules

The SOLACE.gaml main module imports and integrates the aforementioned modules. It also contains code components for the (1) parameter interface, (2) initialisation, (3) output data management, (4) other species, (5) experiments, and (6) display.

6.2.1 GAMA simulation user interface

The simulation user interface for SOLACE is shown in Figure 44 and Figure 45. The Map View window provides a visually rich map environment to dynamically view the simulation in 2D or 3D. As shown in Figure 44, the Mode parameters view provides the interface for changing values for the (1) population of agents, (2) intensity and duration of earthquakes can be changed, (3) day or night context, etc. These dynamic settings facilitate the testing of "what if" scenarios without changing the code. This however requires restarting the simulation. Also shown in Figure 45, the Model parameters view with dynamic controls such as sliders used to change parameter settings. Examples are changing layer opacities or the vertical exaggeration of buildings. These dynamic controls when modified do not require the reloading of the simulation. The changes are immediately applied in the next simulation time step.

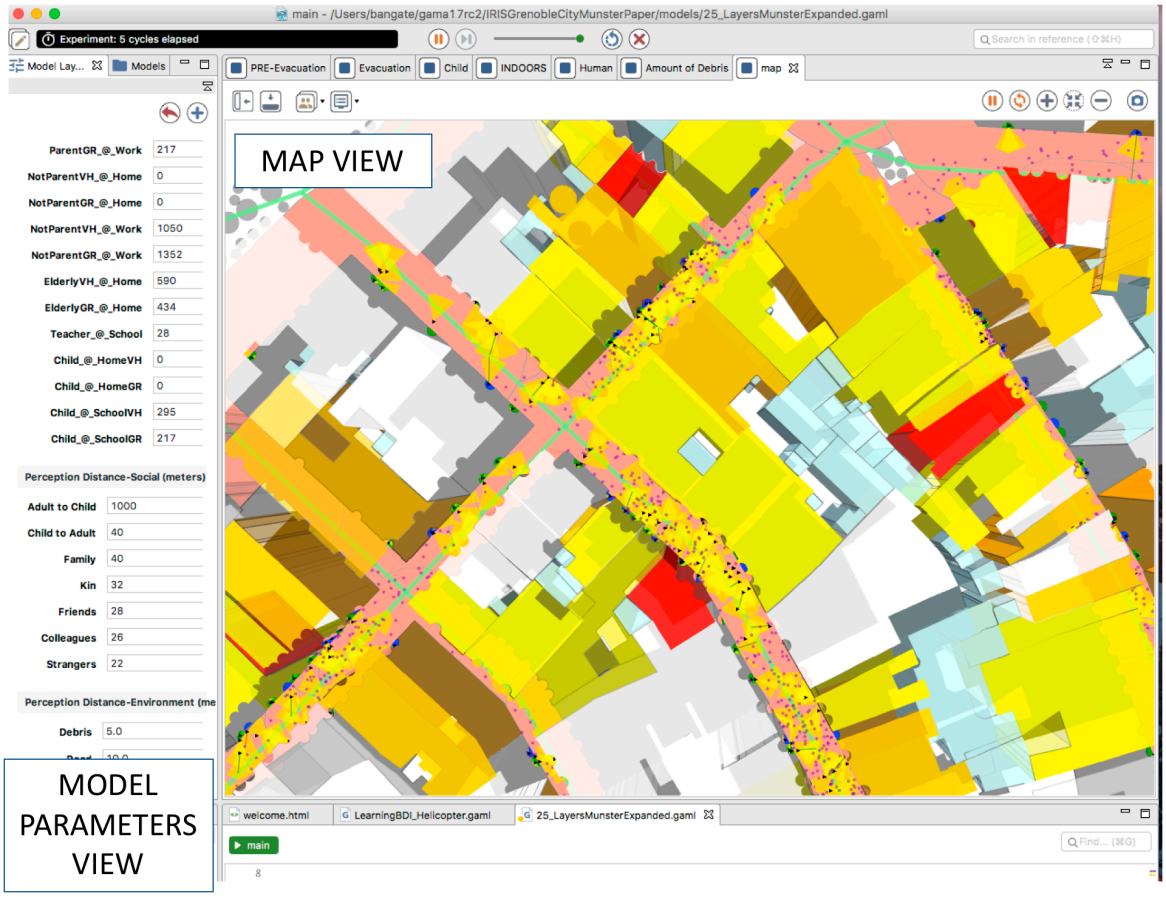

Figure 44 SOLACE user interface using GAMA (2D)

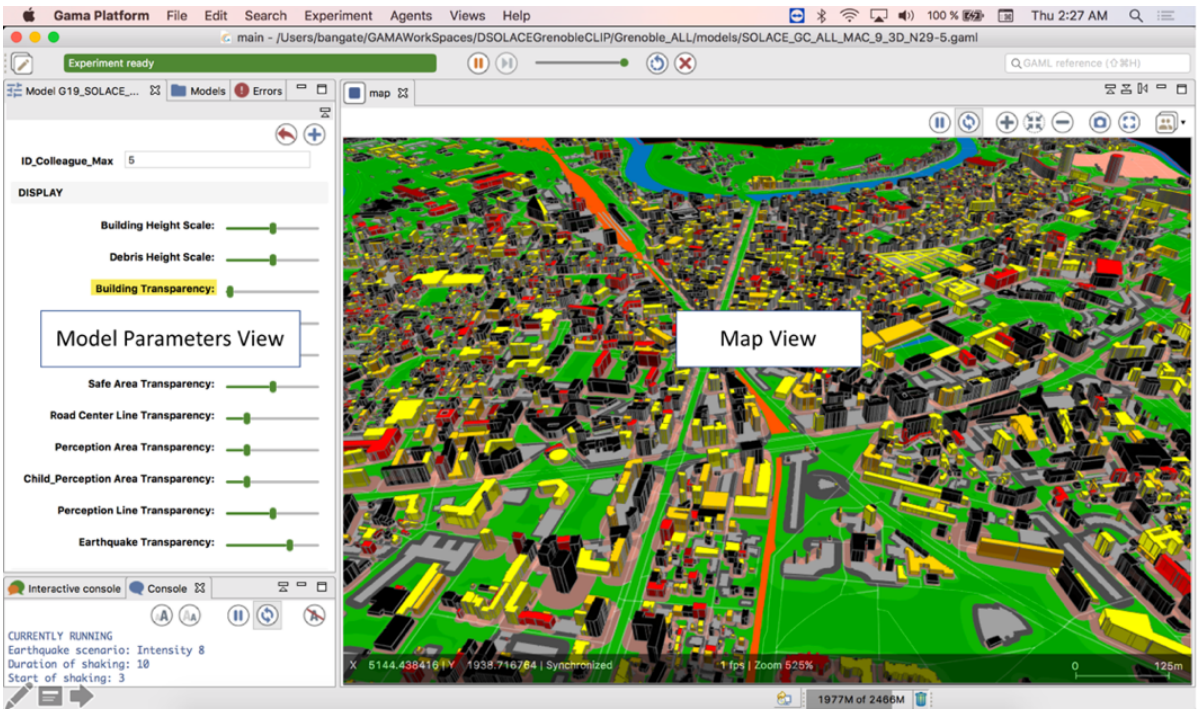

Figure 45 SOLACE user interface using GAMA (3D)

6.2.2 Use of probabilities in generating agent populations

Attribute data gathered from different sources are in macroscopic form. That is, data describe characteristics of large areas such as the IRIS level. Examples of this data are macroseismic assessments and demographic characteristics. The values are usually in percentages and are linked to IRIS boundaries or polygons. Disaggregating these data for generating heterogeneous populations of microscopic agents requires the use of probabilities.

In the study, the percentages are used as probabilities to generate the heterogeneous population of agents. The *flip()* operator, available in GAMA is used to evaluate the probabilities (GAMA Development Team, 2018). When evaluating a float value representing a probability, a boolean is returned. When the result is *true*, a parameter is assigned a value. For example, for a building located in an IRIS with 50 percent *masonry* structures, if *flip(0.5)=true*, the building is assigned the typology *masonry*.

6.2.2.1 Use of probabilities in generating agent populations and assigning vulnerability and damage to every building (GAML Code)

The probabilistic method is used to assign attributes on vulnerability or typology of damage for each building. The building shapefile with IRIS level macroseismic data evaluated with QGIS in Section 6.1.2, is further processed using GAML code. The shapefile is first accessed as shown in the pseudocode shown *Code 1*. The GAML code for this is shown in the Code 30 (Appendix).

Code 1

```
buildingIntensityVShapefile <- path to the building shapefile;
```

Attributes from shapefiles are made readily accessible in GAMA provided that the field names are indicated together with the declaration of the parameter type. Examples of field names indicated in *Code 2* are *D_pa*, *D_pb*, *D_pc*, *D_pd*, *D_pe*, *D_d0V_P*, *D_d1V_P*, *D_d2V_P*, etc (see Table 32). The field values are of type float. These are used as probabilities in SOLACE. The GAML code is shown in Code 31 (Appendix).

Code 2

```
Value for D_pa; Value for D_pb; Value for D_pc; Value for D_pd; Value for D_pe;

Value for D_d0V_P; Value for D_d1V_P; Value for D_d2V_P; Value for D_d3V_P;
Value for D_d4V_P; Value for D_d5V_P;

Value for D_d0VI_P; Value for D_d1VI_P; Value for D_d2VI_P; Value for D_d3VI_P;
Value for D_d4VI_P; Value for  D_d5VI_P;

. . . . .
```

For example, in the *Code 3*, to get the typology *typeVC*, the *D_pa* value is evaluated first, if its *flip(D_pa)* results in the value of 1, the *typeVC* is assigned the value *a*. When this happens, the succeeding probabilities, *D_pb*, *D_pc*, and *D_pd* are not evaluated. However, if the first in the list, *D_pa* results in a 0 value, the next parameter *D_pb* is evaluated similar to *D_pb*. The *flip()* function with the probability valued is evaluated until the value of 1 is reached, and the appropriate typology is assigned. This evaluation is shown in Table 35. The GAML code is shown in Code 32.

Code 3

```
Assign typology for building
     - evaluate probability flip function using probability value for typology a
          - if True the value "a" is assigned, and calculation finishes
          - if False the next typology is evaluated
               - evaluate probability flip function using probability value for typology b
                    - if True the value "b" is assigned, and calculation finishes
                    - if False, the next typology is evaluated
                         . . .
                        - if True assign the value for the typology, and calculation finishes
                        *when value is False evaluation continues until typology e is reached
```

Table 35 Evaluating probabilities for building typology typeVC with the flip() function. The assigned value to typeVC is contained within the braces (i.e. "a", "b", "c", "d", or "e").

Parameter	***flip₁()***	***flip₂()***	***flip₃()***	***flip₄()***	***flip₅()***
D_pa	True, ["a"]	False	False	False	False
D_pb	-	True, ["b"]	False	False	False
D_pc	-	-	True, ["c"]	False	False
D_pd	-	-	-	True, ["d"]	False
D_pe	-	-	-	-	True, ["e"]

The calculation for the values of the damage scenarios (0 to 5) for the different intensity scenarios from V to XII are similarly derived using the *flip()* function. The scenarios are *typeDCV*, *typeDCVI*, *typeDCVII*, *typeDCVIII*, *typeDCIX*, *typeDCX*, *typeDCXI*, and *typeDXII*. The evaluation is implemented using *Code 4*. The GAML code is shown in Code 33. The evaluation for the scenario *typeDCV* is shown in Table 36.

Code 4

```
Assign damage for intensity V
    - evaluate probability flip function using probability value for Intensity V, level 0
      damage
        - if True assign the value 0 and calculation finishes
        - if False, evaluate next level
              - evaluate probability flip function using probability value for Intensity V,
              level 1 damage
                 - if True assign the value 1, and calculation finishes
                 - if False, evaluate next level
                      . . .
                      - if True assign the value for the level, and calculation finishes
                      *when value is False evaluation continues until level 5 is reached

Assign damage for intensity VI, VII, VIII, IX, X, XI and XII
     -  evaluated in the a similar manner to intensity V but using the respective probabilities
     for intensity and level of damage
```

Table 36 Evaluating probabilities for building damage typeDCV during an intensity V earthquake scenario with the flip() function. The assigned value is contained within the braces (i.e. 0, 1, 2, 3, 4, or 5).

Parameter	***flip₁()***	***flip₂()***	***flip₃()***	***flip₄()***	***flip₅()***	***flip₆()***
D_d0V_P	True, [0]	False	False	False	False	False
D_d1V_P	-	True, [1]	False	False	False	False
D_d2V_P	-	-	True, [2]	False	False	False
D_d3V_P	-	-	-	True, [3]	False	False
D_d4V_P	-	-	-	-	True, [4]	False
D_d5V_P	-	-	-	-	-	True, [5]

The result of the code is a buildings' shapefile containing the attributes for vulnerability and damage for each seismic scenario. This is used as the probabilistic vulnerability and damage scenario for the multi agent simulation. New scenarios can likewise be generated by running the GAMA code. The line of code for saving the shapefile with the appropriate field names is shown in Code 5 . The GAMA code is shown in Code 34

Code 5

```
save building data as shapefile to a directory with the following attributes id, height,
typology assignment (a to e), and damage probability from intensity V to XII
```

The maps for vulnerability and damage probability for intensity VIII earthquake generated from the resulting building shapefile are shown in Figure 46.

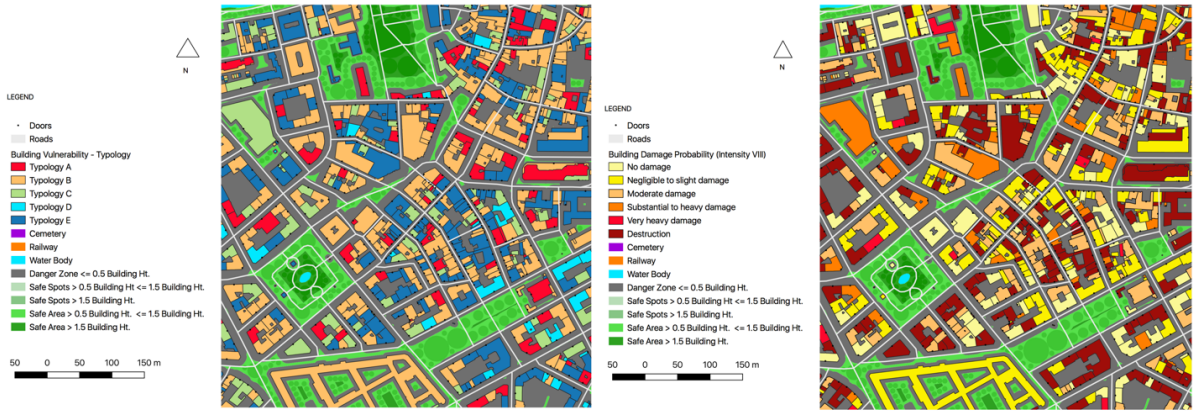

Figure 46 Left: Building Vulnerability – Typology (A to E); Damage: Building Damage (0 to 5) for Intensity VIII Scenario.

The building shapefile data is used to create the building agents in SOLACE. For example, creating the building agents for an intensity VI earthquake scenario requires the lines of code shown in Code 6. The GAMA code is shown in Code 35.

Code 6

```
Load into the model the building shapefile for the intensity VI scenario from a
specific directory.
```

In the init section of the code, the building agent is created as shown in Code 7. The GAMA code is shown in Code 36.

Code 7

```
Create the building agent from the from the building shapefile for intensity  VI
scenario.
```

In the definition of the building species agent, the parameters are derived directly from the building shapefile attribute fields. As shown in Code 8, the field names are ScBH1_VC, ScBH1DV and HAUTEUR for vulnerability, damage and height respectively. The appearance of building agents are defined in the aspect section. The colours are assigned to the respective vulnerability class (a, b, c, d and e) and damage category (0, 1, 2, 3, 4 and 5). The depth parameter calls the HAUTEUR field values to render the building heights in 3D. The GAMA code is shown in Code 37.

Code 8

```
Building species for intensity VI scenario
     - characteristics
         - building height (HAUTEUR * height multiplier)
         - building vulnerability class (a, b, c, d or e)
         - building damage for intensity VI (0, 1, 2, 3, 4, and 5)
     - drawing the building
         - based on vulnerability
              - type a (Red)
              - type b (Green)
              - type c (Blue)
              - type d (Yellow)
              - type e (Violet)
         - based on damage at intensity VI
              - damage 0 (White)
              - damage 1 (Yellow)
              - damage 2 (Orange)
              - damage 3 (Red)
              - damage 4 (Maroon)
              - damage 5 (Black)
```

The result of Code 6, Code 7, and Code 8 are shown in Table 37 and Table 38. Table 37 shows the building agents drawn in the simulation with respect to vulnerability class. The vulnerability classes are from A to E in the order of decreasing vulnerability. Table 38 shows building damage category from 1 to 5 in the order of increasing damage.

Table 37 Building Vulnerability Class in the order of decreasing vulnerability

Typology	**A**	**B**	**C**	**D**	**E**
Colour	red	green	blue	yellow	violet
3D		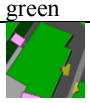		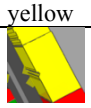	
Examples (Grünthal, European Macroseismic Scale 1998, 1998)	Masonry (rubble stone, adobe-earth brick)	Masonry (simple stone, unreinforced with manufactured stone units)	Masonry (massive stone, unreinforced with RC[22] floors); RC (frame w/o ERD[23], walls withour ERD)	Masonry (reinforced or confined); RC frame with moderate ERD); Timber structures	RC walls and RC frame with high level of ERD; Steel structures.

[22] RC – Reinforced concrete
[23] ERD – Earthquake Resistant Design

Table 38 Building Damage Grade in the order of increasing damage

Damage Class	**0**	**1**	**2**	**3**	**4**	**5**
Colour	White	yellow	orange	red	maroon	Black
3D	Not displayed					
Damage (Grünthal, European Macroseismic Scale 1998, 1998)	No damage	Negligible to slight damage (no structural damage, slight non-structural damage)	Moderate damage (slight structural damage, moderate non-structural damage)	Substantial to heavy damage (moderate structural damage, heavy non-structural damage)	Very heavy damage (heavy structural damage, very heavy non-structural damage	Destruction (very heavy structural damage)

A 3D snapshot of Grenoble showing an intensity VIII earthquake scenario for building vulnerability and damage are shown in Figure 47 and Figure 48 respectively. In both figures, the displayed buildings are those with damage grades greater or equal to 1 (>=1). To further clarify, black grey spaces between buildings indicate locations for buildings that are not damaged.

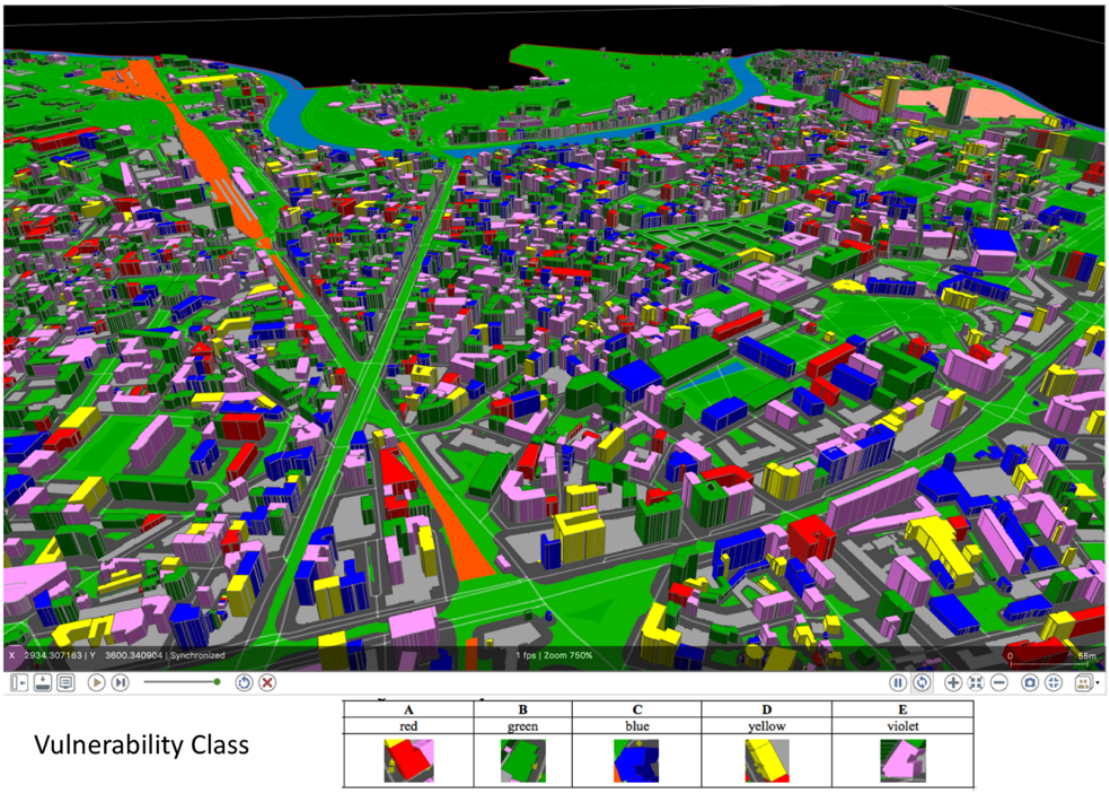

Figure 47 Building vulnerability classes from left to right are from A to E in the order of decreasing vulnerability.

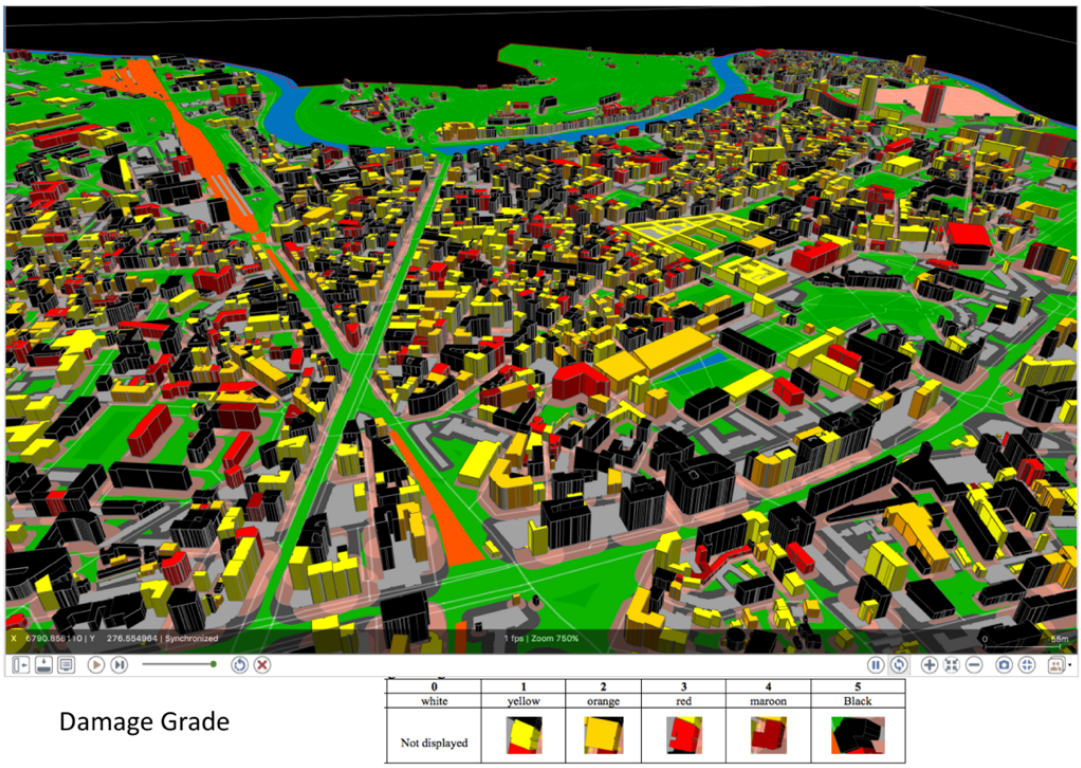

Figure 48 Building damage at Intensity VIII scenario. Values are from from left to right are from 1 to 5 in the order of increasing damage.

6.2.2.2 Debris creation

Building agents create debris agents. The debris agents are deposited in the danger zone surrounding the building. The amount of debris created depends on the building attributes such as vulnerability.

A reflex defined in the buildings species is used to create debris during the start of the earthquake and within its duration. This statement is expressed in Code 9. The GAMA code is shown in Code 38. The approach used to create debris is probabilistic.

Code 9

```
Create debris for every time step from the start of the earthquake until the shaking stops
```

Probability to produce debris for each typology is defined in Code 10. The equivalent GAMA code is shown in Code 39. A probable random integer *k_debri*s, is picked from a range of values between 1 to 10. Typologies that are highly vulnerable to damage create more debris. Typologies are from *a*, *b*, *c*, *d*, and *e*, in the order of decreasing vulnerability. For example, in Code 10, for a Type a structure such as masonry, a *k_debris* random value from 1 to 10 debris is picked. For a structure with minimal vulnerability type e, such as engineered reinforced concrete, a *k_debris* value between 0 and 1 is picked.

Code 10

```
Number of debris created (k_debris)based on building typology
     - if the building typology is "a" then
          - generate a random number of debris between 1 and 10
     - if the building typology is "b" then
          - generate a random number of debris between 1 and 7
     - if the building typology is "c" then
          - generate a random number of debris between 1 and 5
     - if the building typology is "d" then
          - generate a random number of debris between 0 and 3
     - if the building typology is "e" then
          - generate a random number of debris between 0 and 1
```

The number of debris *n_debris* created for each time step is calculated as shown in Code 11. The equivalent GAMA code is shown in Code 40. The debris agent is created in the danger zone adjacent to (or nearest) the damaged building. The footprint of the debris block is simplified to the shape of a square. The dimensions of the debris block increase with increasing intensity. This is analogous to having more debris covering the ground with increased damage from increasing intensity. The purpose of this simplification is to facilitate faster simulation times by lessening the number of debris agents created.

Code 11

Number of debris created (n_debris) based on intensity, damage and height

- if the intensity is V
  - n_debris is calculated for each building using the following:

$$n_{_debris} = \frac{damage \times \#\ of\ debris\ for\ building\ typology \times intensity \times building\ height}{denominator}$$

  - calculating n_debris

$$n_{_debris} = \frac{\text{ScBH1DV} \times k_debris \times 5 \times HAUTEUR}{650}$$

  - create the **small debris** agents in random location within the danger zone around the building. The number of small debris agent around the building should be equal to *n_debris*.
- if the intensity is VI
  - calculate n_debris for each building for intensity 6

$$n_{_debris} = \frac{\text{ScBH1DVI} \times k_debris \times 6 \times HAUTEUR}{500}$$

  - create the **medium debris** agents in random location within the danger zone around thebuilding. The number of medium debris agent around the building should be equal to *n_debris*.
- if the intensity is VII . . .
- ...
- if the intensity is XII . . .

As indicated in Code 11 and Code 40, (1) intensity V earthquake produces smallDebris with a dimension of 1x1 meter; (2) intensity VI produces mediumDebris (2x2 meter) (3) intensity VII produces bigDebris (3x3 meters); intensity greater than VIII produces huge debris (4x4 meters). In the calculation for *n_debris*, the relevant parameters are the typology expressed in *k_debris*; damage level (*ScBH1DV* for intensity V, *ScBH1DVI* for intensity VI, *ScBH1DVII* for intensity VII, *ScBH1DVIII* for intensity VIII, *ScBH1DIX* for intensity IX, *ScBH1DX* for intensity X, *ScBH1DXI* for intensity XI, and *ScBH1DXII* for intensity XII); the intensity of the earthquake and height of the building; and a value for each intensity are used as a denominator. The purpose of the denominator together is to lessen the number of debris agents produced. A large number of agents greatly slows down the simulation. This lesser number of debris agents for higher intensities however is compensated by the larger footprints occupied by debris. The intensity related parameters are detailed in Table 39.

Table 39 Intensity related parameters in the calculation of debris values are 0, 1, 2, 3, 4 and 5.

Scenario	Field for Vulnerability Class	Field for Damage Grade (0, 1, 2, 3, 4 or 5)	Debris type	Dimensions	Denominator
Intensity V	ScBH1_VC	ScBH1DV	smallDebris	1x1 meter	650
Intensity VI	ScBH1_VC	ScBH1DVI	mediumDebris	2x2 meter	500
Intensity VII	ScBH1_VC	ScBH1DVII	bigDebris	3x3 meter	1000
Intensity VIII	ScBH1_VC	ScBH1DVIII	hugeDebris	4x4 meter	1500
Intensity IX	ScBH1_VC	ScBH1DIX	hugeDebris	4x4 meter	1500
Intensity X	ScBH1_VC	ScBH1DX	hugeDebris	4x4 meter	1500
Intensity XI	ScBH1_VC	ScBH1DXI	hugeDebris	4x4 meter	1500
Intensity XII	ScBH1_VC	ScBH1DXII	hugeDebris	4x4 meter	1500

To implement building collapse at Damage level 5 (which usually occurs starting from Intensity VI), debris are directly created in buildings' doorway and footprint, during the duration of the earthquake at each simulation time step. That is the doorway that has the same ID as the building. The implementation is shown in Code 12. The equivalent GAMA code is shown in Code 41. Figure 49 shows the debris blocks in the simulation.

Code 12

```
If the intensity is VI and the damage level for the building is 5
     - create huge debris in the door or inside the building
```

Figure 49 Violet squares are debris created by damaged buildings during the duration of the earthquake in the simulation. Debris are generated within danger zones. Snapshot of a simulation for intensity..

6.2.2.3 Spatially distributed heterogeneous human agent populations

In the model, human agents are divided into two categories: adult and children. Child agents are less than 15 years old. Adult agents are greater than or equal to 15 years old. This grouping is based on the available demographic data for each IRIS unit. Age groups for children are from 0 to 2 and 3 to 14. For adults, the ages are grouped 15 to 29, 30 to 59, and greater or equal to 60.

Human agents are created for each IRIS region based on the population. Human agents can be created in indoor or outdoor locations within each IRIS boundary. The number of agents created in each location is based on daily activity and is dependent on the time of day. During night time, agents are created inside homes. During daytime, agents are distributed in the home, work, school, public and outdoor locations. For indoor locations, human agents are created in the centroid of doorways. For outdoor, human agents are created in free space.

The generation of the heterogeneous human agent population and its spatial distribution in the model is implemented in the following code sections. Code 13 shows the parameters needed such as list of locations (use), age group (age group), speeds (evacSpeedMax) and probabilities for disability with respect to age groups are indicated. A parameter disabilityON functions as a switch to include, or not, the disability parameter. This is useful in some experiments to determine the impact of disability in the population. The equivalent GAMA code is shown in Code 42.

Code 13

```
//General parameters in generating human agents
List of building locations based on use or activity
     - Home, Work, School, Public, "Outdoor"
List of age groups
     - "adult", "elderly", "child";
List of ranges maximum values for evacuation speeds for age group
     - adult (0 to 3.8 m/sec]
     - child 0 to 2 yrs old (0.0 m/sec)
     - child 3 to 14 (0.0 to 2.23 m/sec)
     - elderly (0 to 1.11 m/sec)
     - disabled (0 to , 1.77)
List of probability for disability based on statistical data on age
     - 0.012, 0.024, 0.013, 0.028, 0.039, 0.035, 0.090, 0.067, 0.123,
       0.102, 0.125, 0.124, 0.217,0.229, 0.423, 0.361
Setting if disability to is considered
     - if disability is not considered
          - disabilityON <- false;
     - if disability is considered
          - disabilityON <- True
```

Code 14 shows the list of IRIS locations considered. The equivalent GAMA code is shown in Code 43. This list can change depending on the IRIS units considered.

Code 14

```
List of IRIS locations considered
     -  "Crequi_VHugo", "Grenette", "AIGLE","CHAMPIONNET","GENISSIEU","HOCHE","JEAN
        JAURES","PREFECTURE,…,"WALDEC ROUSSEAU"
```

Code 15 shows the format of the data for each IRIS in the list in Code 14. The equivalent GAMA code is shown in Code 44. The population for each age group in different locations is indicated as a list. The age groups are 0 to 2, 3 to 14, 15 to 29, 30 to 59, and greater than 60. The locations are home, work, school, public and outdoors. The data shown in Code 15 is for night time conditions where people are assigned to homes. A percentage parameter, pctPop is also used to limit the population considered. Limiting the number of human agents considered in the simulation is useful in experiments. A full population (or 100% or pctPop = 1.000) for the whole of Grenoble is possible however this is computationally expensive and takes a very long time to complete.

Code 15

```
//Generating population for night time scenario (E.g. All agents are at home)
- Multiplier (pctPop) is used to generate a Percentage of the population.
     - if pctPop = 0.002, this means that 2% of the indicated population is generated
- distribute the population for age groups based on activity/location
     - population distribution (example Adult 30 – 59 y.o. for 1 IRIS unit)
          - Adult (30 to 59 y.o.) at Home: pctPop x Estimated value (= 660)
          - Adult (30 to 59 y.o.) at Work: pctPop x Estimated value (= 0)
          - Adult (30 to 59 y.o.) at School: pctPop x Estimated value (= 0)
          - Adult (30 to 59 y.o.) at Public: pctPop x Estimated value (= 0)
          - Adult (30 to 59 y.o.) at Outdoor: pctPop x Estimated value (= 0)
```

Code 16 shows the data for daytime scenario. The equivalent GAMA code is show in Code 45. Notice the values for different locations. The full population is used as indicated by the pctPop value of 1.000 or 100%.

Code 16

```
//Generating population for day time scenario (E.g. Agents are at different locations)
- Multiplier (pctPop) is used to generate a Percentage of the population.
     - if pctPop = 1.000, this means that 100% of the indicated population is generated
- distribute the population for age groups based on activity/location
     - population distribution (example Adult 30 – 59 y.o. for 1 IRIS unit)
          - Adult (30 to 59 y.o.) at Home: pctPop x Estimated value (= 0)
          - Adult (30 to 59 y.o.) at Work: pctPop x Estimated value (= 594)
          - Adult (30 to 59 y.o.) at School: pctPop x Estimated value (= 0)
          - Adult (30 to 59 y.o.) at Public: pctPop x Estimated value (= 0)
          - Adult (30 to 59 y.o.) at Outdoor: pctPop x Estimated value (= 66)
```

Code 17 shows the list grouping age group data from different IRIS units. The equivalent GAMA code is shown in Code 46 . Shown is the list for the 30 to 59 age groups. This is used in Code 18 to generate populations in batches using age groups.

Code 17

```
List of population of adults (30 – 59 y.o.) for each IRIS location
 - "Crequi_VHugo", "Grenette", "AIGLE","CHAMPIONNET","GENISSIEU","HOCHE","JEAN
    JAURES","PREFECTURE,…,"WALDEC ROUSSEAU"data for list<list> I30_59
];
```

Code 18 shows how agents are generated in the model. The GAMA code is shown in Code 47.This code uses Code 13 to Code 17. Code 18 loops over the lists and creates the agents for ease age group, use and IRIS location. Disability is also assigned to agent when the parameter disabilityON = true. Assignment of disability is probabilistic and uses the flip() function. The speed of the individual is assigned based on the range of values for the age group.

The human agents created in the simulation are detailed in Table 40. Agents are point locations rendered as simple 2D or 3D graphics in the map. A triangular perception area representing gaze, and attention is also shown for each active agent. Agents within the angle formed by the perception area, and when in range, can be perceived by the agent. When the other agent is perceived a perception line is drawn. This perception area also indicates the direction of movement. Screenshots of the agents from 2D and 3D versions of the simulation are also provided. The three health conditions of agents are also presented.

This include healthy, injured and deceased or dead agents. Deceased agents are inactive and therefore do not have perception areas.

Code 18

```
- Generate the population of agents with respect to the age groups for each IRIS location.
      - assign age
      - assign location (home, work, school, public, or open area)
      - assign role
      - assign speed
      - if disability is considered
            - assign disability (based on probabilities for age groups)
            - change previously assigned speed and assign new speed based on disability
```

Table 40 Human agents in SOLACE

Agent	Type	Function	Description		Screenshot	
					3D	**2D**
Adult	Point	Social, Cognitive	Age > 15 years old. Exhibits cognitive and social behaviours during earthquakes and evacuations.	**Healthy**. 3D: Black head. Grey body. Yellow perception area. 2D: Small blue triangle. Yellow perception area.		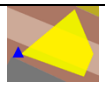
				Injured. 3D: Red head. Yellow perception area. 2D: Red small triangle. Yellow perception area		
				Deceased. 3D: White head inside debris. No perception. No movement. 2D: White triangle inside debris. No perception area.		
Child	Point	Social, Cognitive	Age <= 15 years old. Exhibit cognitive and social behaviours during earthquakes and evacuations.	**Healthy**. 3D: Green head and body. 2D: Orange square. Green perception area.		
				Injured. 3D: Red head, green body, green perception area. 2D: Red square. Green perception area.		
				Deceased. 3D: White head, green body, inside debris, no perception area. 2D: White square, inside debris		

6.2.2.4 Creating non-human agents

Non-human agents included in the simulation are grouped into environment, hazard and safe areas. The agents are detailed in Table 41. Except for earthquake and debris, these layers are created directly from shapefiles. The workflow is similar to the creation of building agents discussed in Section 6.2.2.1. This workflow is illustrated in Figure 50. The steps involved in creating agents from shapefiles include: (1) specifying a *shapefileName* and the path to the shapefile; (2) creation of the species *speciesName* from the shapefile; (3) defining the species *speciesName* with the relevant parameters (i.e. int, float, string) and specifying how the species is drawn in the aspect section; and (4) display the agent by calling the species *speciesName* in the experiment.

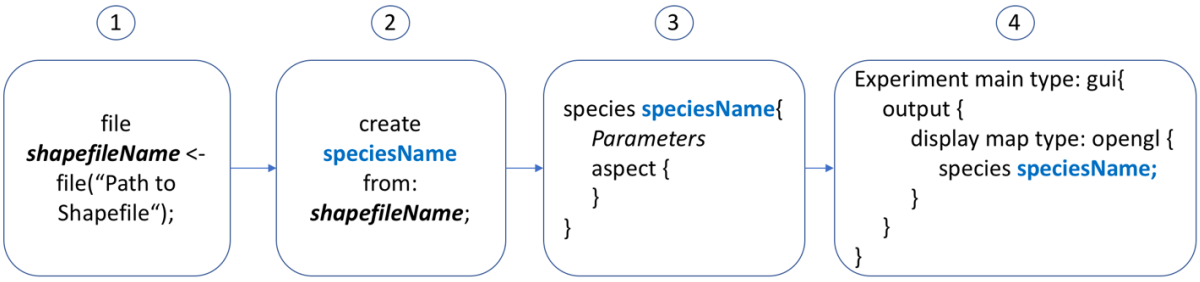

Figure 50 Creating non-human agents from shapefiles

Table 41 Non-human agents in SOLACE

Category	Agent	Type	Function	Description	Screenshot 2D
Environment	Free Space	Polygon	Allow free movement	Allows movement of human agents. Includes doors, roads and danger zones.	Not displayed
	Road centre	Polygon	Pathway	White intersecting linear polygons indicating road centre line. Allows movement of human agents; Provides guidance; Initial destination to in early evacuation	
	Door	Point	Source of agents	Semi circles located on the sides of buildings. Starting location of indoor agents	
	Building	Polygon	Barrier, Debris Source	Structures that are vulnerable to earthquake shaking	
	Water Body	Polygon	Barrier	Includes rivers and ponds	
	Railway	Polygon	Barrier	Fenced area, Railway zone	
	Cemetery	Polygon	Barrier	Fenced area, Cemetery zone	
Hazard	Earthquake	Point	Barrier	The phenomena and hazard being modelled. Increasing intensities	
	Debris	Polygon	Phenomena	Created during earthquake shaking by buildings and deposited around Danger Zones	
	Danger Zone	Polygon		Orange area around buildings. The width of the zone is half the height of the building. Site for debris deposition	
Safe areas	Safe area > 0.5 Bldg Ht.	Polygon	Evacuation Destination	Contiguous areas away from buildings (> 0.5 x height of building)	

6.2.3 Complex multi-agent dynamics

In the SOLACE model, human agents respond to presence of other human agents and environment objects (or non-human agents). Objects in the environment either function as barriers, hazards or safe areas. Barriers such as buildings and bodies of water, restrict movement and require that human agents to move around them. Hazards such as earthquake and debris force human agents to move away. Safe areas are sought by human agents when evacuating. Social interaction governed by social attachment facilitates the movement of human agents towards attachment figures. Implementation of interactions

of human agents and other agents in the simulation are defined using a mix of simple reflexes and the BDI architecture.

6.2.2.1 Interactions with barriers

Human interaction with, and navigation around, barriers such as building agents are defined in simple reflexes. Code 19 is an example of a reflex that allows an adult agent to avoid nearby building polygons when these are close to it by a distance lesser than 5 meters. In Code 19, the agent can change its forward direction when nearby buildings are detected. This is indicated by the heading parameter. The GAMA code is shown in Code 48.

Code 19

```
Avoid buildings when they are nearby (less than 2 meters away)
     - when a building is nearby
        - change direction or heading
        - move forward in the new direction
```

6.2.2.2 Interactions with debris in the environment (avoidance, injury, death)

Human agents can be hit by debris causing injury or death. In the GAML code this is handled as a reflex. The flip () function in GAMA is used here to define the probability for the injury or death. Currently the value is 0.5 or 50 percent probability for each case. The reflex in Code 20 can be read as: an adult can be hurt by small debris when it is outdoors, the intensity of the earthquake is V, the agent is active or healthy and the time is during the duration of the earthquake. Also, when the adult agent is very near the centre of the debris, there is a probability that it can be dead or injured. A child agent has a similar reflex. The equivalent GAMA code is shown in Code 49.

Code 20

```
An agent is hurt by debris when its location (outdoors) overlaps the location of debris at
the instant the debris is created. The intensity is V and debris are created in the first 10
seconds.
     - a probability of (50%) evaluated to determine is the agent is dead
          - if true, the agent is dead.
          - if false, the agent is injured.
```

By default agents perceive and avoid debris. This is also implemented as a reflex as shown in Code 21. The equivalent GAMA code is shown in Code 50.

Code 21

```
An agent can avoid debris when it is active (i.e. not dead)
     - detect all nearby debris
     - select the nearest debris
     - change location away from debris
```

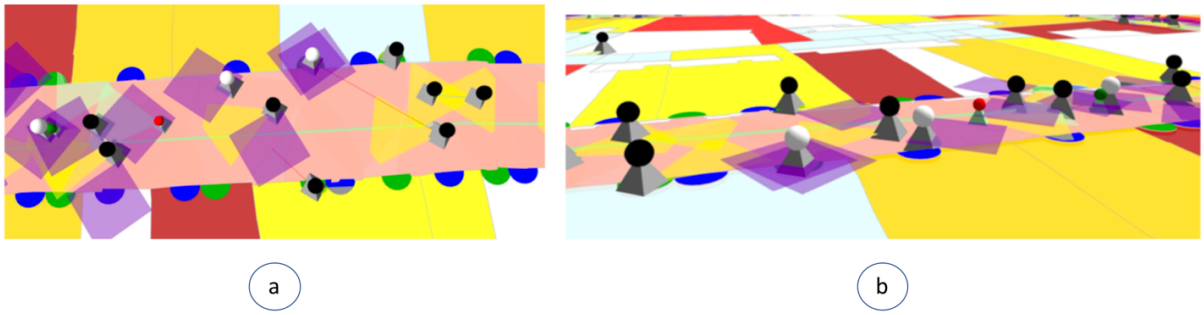

Figure 51 Effect of debris on human agents. Healthy adult and child agents have black and green heads respectively. Injured agents have red heads. Dead agents have white heads and do not have perception areas. (a) Top view. (b) Side view.

6.2.2.3 Defining social relationships

Social relationships or groupings are defined in the agent by adding an ID attribute. Each agent is assigned an ID for all possible relationships. These are family, kin, friend and colleague. When agents share the same ID, they belong to the same group. If agents do not share the same ID in any of the aforementioned relationships, they are strangers.

The ID assignment for family members and colleagues are based on the building-door ID and floor number they occupy at the start of the simulation. For example, in work environments, individuals sharing the same *building+floor ID* string are colleagues. In a similar fashion, adult teachers with students in a class will share the same *building+floor ID* string. This is shown in Code 22. The equivalent GAMA code is shown in Code 51.

Code 22

```
Assigning agents with IDs for family (idFamily) and colleage (idColleague) at the start of
the simulation
     - assign the agent to a door in a building located in floor/level.
     - extract the building ID
     - generate relationship ID by combining the building ID with the building floor number.
       Agents having the same relationship ID are in the same social group.
          - if the location of the agent is "Home", the generated relationship ID is for a
            Family relationship.
          - if the location of the agent is "Work", the generated relationship ID is for a
            Colleague-Work relationship.
          - if the location of the agent is "School", the generated relationship ID is for a
            Colleague-School relationship.
```

Kin and friend relationships are assigned a random value based on a range. This is shown in Code 23. The GAMA code is shown in Code 52. The ranges for *idKinMax* and *idFriendMax* can be changed in the simulation model parameter interface during testing. Having very small ranges to pick random values for *idKinMax* and *idFriendMax* produces many relatives and friends. Very large ranges produce many strangers.

Code 23

```
Assigning agents with IDs for kin (idKin) and friend (idFriend) at the start of the
simulation. Agents having the same relationship ID are in the same social group.
     - for idKin a random value is assigned based on the maximum value for kin (idKinMax)
     - for idFriend a random value is assigned based on the maximum value for friend
       (idFriendMax)
```

6.2.2.4 Social attachment implemented with BDI

Social attachment is implemented in the model through (1) attachment-based pre-evacuation behaviours resulting in delayed egress from buildings, and (2) perception of other human agents during evacuations. The simulation uses the basic features of GAMA's BDI architecture to implement social attachment. Basic features only include the use of predicates, beliefs, desires, intentions and plans[24].

Code 24 shows the BDI predicates used in plans and reflexes of a human adult agents. The equivalent GAMA code is shown in Code 53.

Code 24

```
List of BDI predicates used by adult agents
 - normal, adult_move_to_Door, stay_feelsafe, moveout, adult_move_to_road,
   adult_move_to_safearea, adult_helpInjuredAdult
```

Code 25 shows the BDI predicates used in plans and reflexes of a human child agent. The equivalent GAMA code is shown in Code 54.

Code 25

```
List of BDI predicates used by child agents
     - child_move_to_safearea, child_move_to_road, child_move_to_adultTeacher,
       child_move_to_adultFamily, child_move_to_adultFamilyParent, child_move_to_adultKin,
       child_move_to_adultFriend, child_move_to_adultColleague, child_move_to_adultStranger,
       child_move_to_childFamily, child_move_to_childKin, child_move_to_childFriend,
       child_move_to_childColleague, child_move_to_childStranger
```

Pre-evacuation behaviours are triggered by the detection of noticeable earthquake shaking. A portion of the reflex for detecting earthquakes and assigning pre-evacuation action is show in Code 26. The full code determines pre-evacuation actions and calculates delay time to egress. When the decision of the agent is to leave, the next choice of evacuation actions is determined by BDI parameters. This is shown in Code 26. The equivalent GAMA code is shown in Code 55.

Code 26

```
When the earthquake is detected by the agent
     - remove the existing belief and desire of the agent for a normal (or no earthquake
        situation)
     - add the following desires
          - adult_move_to_road, adult_move_to_safearea, adult_move_to_adultFamily,
            adult_move_to_childFamily, adult_move_to_childFamily_Parent, adult_move_to_adultKin,
            adult_move_to_childKin);adult_move_to_adultFriend, adult_move_to_childFriend,
            adult_move_to_adultColleague, adult_move_to_childColleague,
            adult_move_to_adultStranger, adult_move_to_childStranger,
            adult_Teacher_move_to_child, adult_helpInjuredAdult
```

Perception of other human individuals are determined by the perception distance range. The values for perception distance are contained in the *Data_SocialAttachment.gaml* file and imported into the *SOLACE.gaml* main module. The values for perception distance are shown in Code 27. The values are in the calculated using the perception distance bond equation. The values are for day, night and snow scenarios respectively. The equivalent GAMA code is shown in Code 56.

[24] Features of BDI that are not used are the social architecture, emotions, norms, persistence and personality.

Code 27

```
The perception distances (meters) used for day, night and snow scenarios for
     - //perception distance (format: DAY, NIGHT, SNOW)
     - child (PD_Child) <- [100.0, 100.0, 100.0];
     - family (PD_Family) <- [100.0, 100.0, 100.0];
     - partner (PD_Partner) <- [94.10, 4.11, 43.03];
     - parent (PD_Parent) <- [88.85, 3.89, 40.63];
     - kin (PD_Kin) <- [76.45, 3.34, 34.96];
     - friends (PD_Friends) <- [87.85, 3.84, 40.17];
     - acquaintances (PD_Acquintance) <- [69.20, 3.03, 31.65];
     - stranger (PD_Stranger) <- [60.85, 2.66, 27.83];
```

The perception of other human agents using perception distance is implemented in a BDI plan. An example of a plan is shown in Code 28. The equivalent GAMA code is shown in Code 57. The plan is for an adult moving towards an adult family member. The adult can move if it is active (i.e. not deceased), if it is not in an evacuation zone, and if its location is less than the perception distance for family member. Also, the adult should have the same ID as the nearest adult. If the previously stated conditions are true, then the other adult will be detected and the adult can move towards the other adult.

In the simulation interface, when human agents perceive another agent, perception lines are drawn. The colour of the perception line indicates the relationship between the two agents. Table 42 details the perception lines that are defined in the simulation interface. This table also includes the perception lines when agents detect elements in the environment or non-human agents.

Code 28

```
Active adult agent moves towards a family member when the family member is perceived by the
agent (is nearby)
     - perceive family member
     - move towards family member
```

Table 42 Perception lines available for the model – adult agents perceiving others/objects

Agent	Target	Relationship with the target	Type	Perception Line Colour	Illustration
Adult	Adult	Family	BDI	Blue	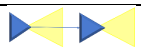
		Kin	BDI	Violet	
		Friend	BDI	Magenta	
		Colleague	BDI	Yellow-Green	
		Stranger	BDI	Yellow	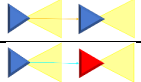
		Injured	Reflex	Turquois	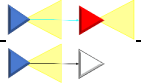
		Dead	Reflex	Black	
	Child	Family	BDI	Blue	
		Kin	BDI	Violet	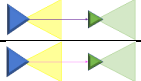
		Friend	BDI	Magenta	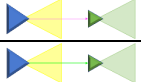
		Colleague	BDI	Yellow-Green	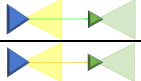
		Stranger	BDI	Yellow	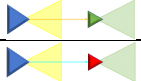
		Injured	Reflex	Turquois	
		Dead	Reflex	Black	
	Environment	Road	BDI	White	
		Safe Area	BDI	Forest green	

		Debris	Reflex	Magenta	
Adult	Child		BDI	Orange	
Adult – Parent	Child	Family	BDI	Red	
Adult - Teacher	Child	Authority	BDI	Red	
Child	Adult - Teacher	Subordinate	BDI	Red	
	Adult - Parent	Family	BDI	Red	
	Adult	Family	BDI	Blue	
		Kin	BDI	Violet	
		Friend	BDI	Magenta	
		Colleague	BDI	GreenYellow	
		Stranger	BDI	Yellow	
		Injured	BDI	Turquois	
		Dead	Reflex	Black	
	Child	Family	BDI	CornflowerBlue	
		Kin	BDI	Violet	
		Friend	BDI	Magenta	
		Colleague	BDI	GreenYellow	
		Stranger	BDI	Yellow	
		Injured	BDI	Turquois	
		Dead	Reflex	Black	
	Environment	Road	BDI	White	
		Safe Area	BDI	Light Green	
		Debris	Reflex	Magenta	

6.2.4 Versions of running the simulation

Running the simulation is done in several ways, full, limited or headless (Table 43). The first is running with the full interface as shown in Figure 44 or Figure 45. The full interface is useful for visualising the map, tables, code, charts, etc. This approach however requires more computer processing resources resulting to longer processing times. The longer duration becomes more significant when running the simulation with a large population of agents. The second way is a limited approach (or a semi-headless mode) where displays of the map and charts are disabled. The facilities for inspecting code errors and table attributes are still active. These allows for checking the simulations during runtime. This saves computing resources and allows for faster processing times compared to the full interface version. The third option is the full headless mode where the simulation is run only in the terminal. This approach is the fastest as is utilises the least resources. However, it provides no possibilities to inspect the simulation during runtime. Also, initial tests using the headless version SOLACE would fail during the simulation test runs and therefore not utilised.

The limited approach was fully utilised in running the simulations and generating the data for analysis. This provided the opportunity to check the simulation, inspect the errors and check the generated data. The saved simulation data is saved as a CSV file and visualised and analysed with tools that were developed external to the model. This tool is discussed in Section 6.2.5. The strategy of using a separate visualisation tool allowed the simulation to only generate the simulation data. The developed browser-

based chart display, allowed for the dynamic updates to chart of simulation results on-the-fly or during simulation runs.

Table 43 Ways of running SOLACE

GAMA Feature	Function	Full	Limited	Headless
Editor	Write and edit GAML code	✓	✓	-
	Save CSV and shapefile data via the code	✓	✓	-
	Add/remove height parameter for 3D display via the code	✓	✓	
Models	Manage models	✓	✓	-
Errors	Check runtime errors	✓	✓	-
Parameters	Set and modify parameters	✓	✓	-
Tables	View simulation data	✓	✓	-
	Manually save CSV data during a time step	✓	✓	-
Map Display	View and explore simulation in 2D/3D. Pan, zoom and rotation of simulation space possible	✓	-	-
	Manually export screenshots	✓	-	-
	Screen capture video via external application (Eg. Quicktime, Kazam)	✓	-	-
Charts	View charts	✓	-	-
Via Terminal	Run GAML code via terminal, parameter testing and calibration	-	-	✓

6.2.5 SOLACE data visualisation user interface

The SOLACE data visualisation user interface was developed to dynamically view data from the simulation external to the GAMA environment (Figure 52 and Figure 53). Tables and charts are available in the GAMA platform. These features however add to the processing load of the application making the simulation run more slowly. Having the chart and table feature outside of the GAMA environment gives a faster simulation. The technologies used to develop the dynamic view of tables and charts were Python, JavaScript, D3 and html (Figure 54). The purpose of the dynamic displays is mainly to allow the viewing of simulation results in real time. The display in the web browser is refreshed to reflect the updated data coming from running the SOLACE the simulation. Simulation results can likewise be viewed, graphed and analysed using standard spreadsheets. This however requires more processing steps, longer times, and is not dynamic.

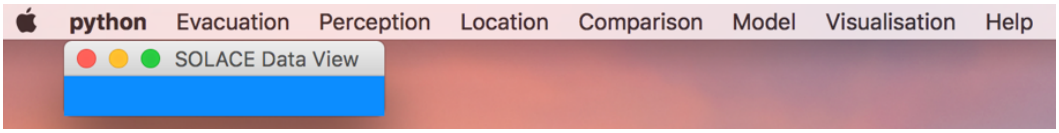

Figure 52 SOLACE data view user interface

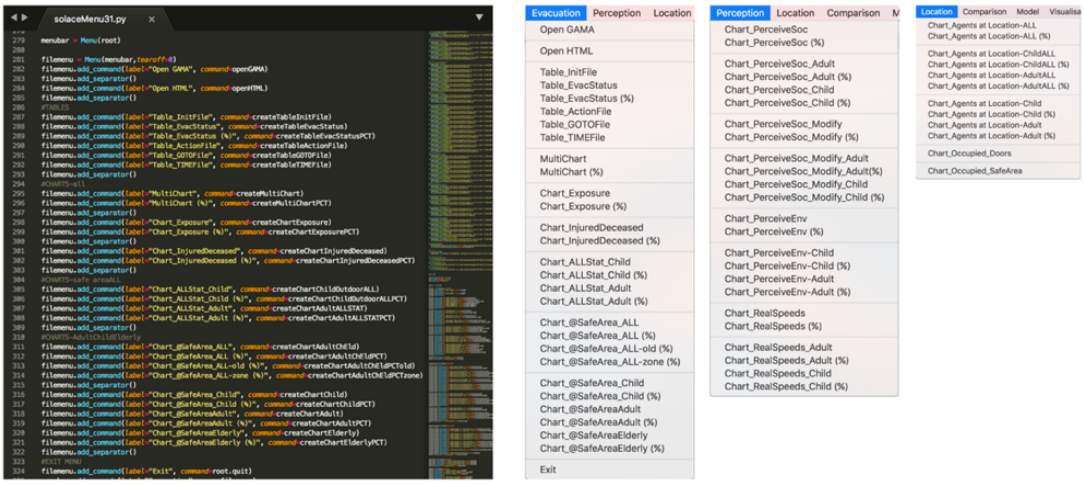

Figure 53 Python code creating the SOLACE menu items for creating charts displaying information for evacuation, perception and location

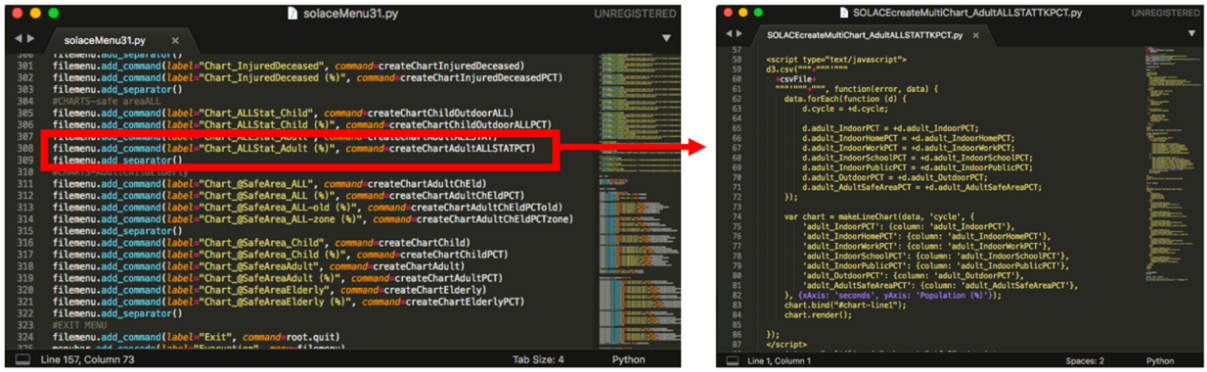

Figure 54 Python code for displaying data as a chart or a table in the browser. An html file is created using python. In the code, D3 is used to embed the data using javascript.

6.2.6 Simulation data

Evacuation simulation data is stored as CSV[25] files. The CSV files produced by the simulation are described in Table 44. A set of these six CSV files are created for each simulation run. New data at every simulation timestep is appended to the files[26]. The six CSV files record (1) initial simulation parameter values *Table_InitFile*, (2) evacuation status in raw values *Table_EvacStatus*, (3) evacuation status in percent values *Table_EvacStatus (%)*, (4) actions chosen by agents during re-evacuation *Table_ActionFile*, (5) time for each action chosen during pre-evacuation *Table_TIMEFile*, and (6) set of actions which includes a GOTO pre-evacuation action *Table_GOTOFile*. The machine time duration is also recorded when each cycle completes. This facilitates inspection of simulation performance or calculation of average time per time step.

[25] Comma Separated Variables/Values, CSV files

[26] GAMA has a built-in table showing default simulation data for all agents during every time step. This data however is not saved automatically and is discarded after each simulation run. A portion of the code in SOLACE is dedicated to saving the data in an aggregated form. The aggregated data is displayed in dynamic tables and charts to facilitate real-time monitoring of simulation results. The results are viewed through dynamic tables and charts viewed and updated in a browser.

Table 44 Tables available in the Python UI

Table	Description	Number of fields/ Parameters
Table_InitFile	Values of key parameters at the start of simulation	12
Table_EvacStatus	Values of parameters at every timestep in raw counts	132
Table_EvacStatus (%)	Values of parameters at every timestep in percent	132
Table_ActionFile	Pre-evacuation actions chosen by agent. Used to quantify delays. Applies the probabilities for each action.	47
Table_TIMEFile	Time allocations for each action based on ranges.	47
Table_GOTOFile	Pre-evacuations actions with the GOTO parameter. Set of actions with the GOTO parameter is needed to be selected for an agent to egress a structure.	15

The CSV files are accessible using the SOLACE Data View interface as shown in Figure 55. The table showing the data for evacuation status is displayed on a web browser page as shown in Figure 56. The table showing the data for pre-evacuation actions and consumed time for the actions are shown in Figure 57.

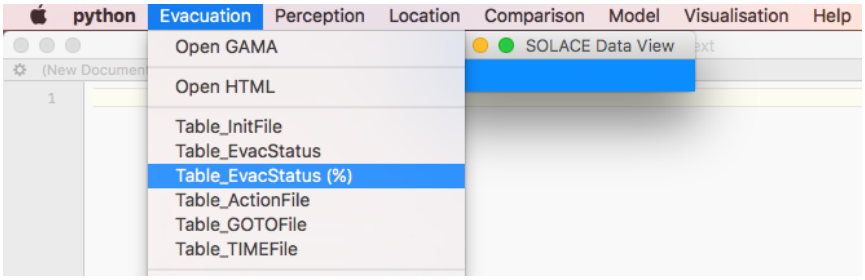

Figure 55 Evacuation progress file in percent. Dynamic D3 browser-based tables to monitor and inspect generated tables compare evacuation progress in real time.

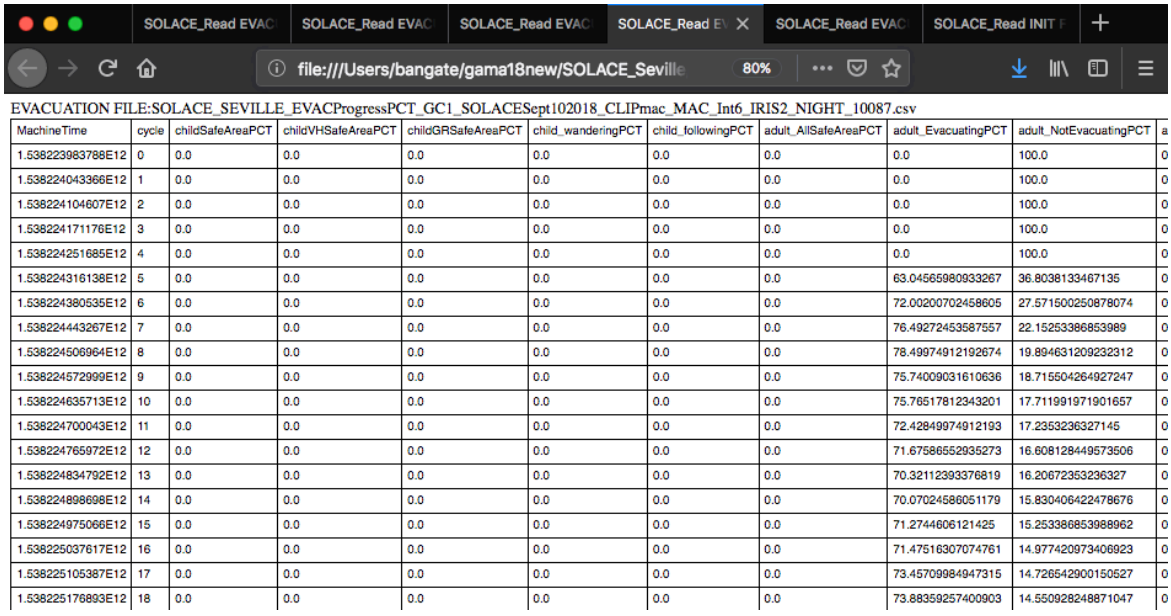

EVACUATION FILE:SOLACE_SEVILLE_EVACProgressPCT_GC1_SOLACESept102018_CLIPmac_MAC_Int6_IRIS2_NIGHT_10087.csv

MachineTime	cycle	childSafeAreaPCT	childVHSafeAreaPCT	childGRSafeAreaPCT	child_wanderingPCT	child_followingPCT	adult_AllSafeAreaPCT	adult_EvacuatingPCT	adult_NotEvacuatingPCT	a
1.538223983788E12	0	0.0	0.0	0.0	0.0	0.0	0.0	0.0	100.0	0
1.538224043366E12	1	0.0	0.0	0.0	0.0	0.0	0.0	0.0	100.0	0
1.538224104607E12	2	0.0	0.0	0.0	0.0	0.0	0.0	0.0	100.0	0
1.538224171176E12	3	0.0	0.0	0.0	0.0	0.0	0.0	0.0	100.0	0
1.538224251685E12	4	0.0	0.0	0.0	0.0	0.0	0.0	0.0	100.0	0
1.538224316138E12	5	0.0	0.0	0.0	0.0	0.0	0.0	63.04565980933267	36.8038133467135	0
1.538224380535E12	6	0.0	0.0	0.0	0.0	0.0	0.0	72.00200702458605	27.571500250878074	0
1.538224443267E12	7	0.0	0.0	0.0	0.0	0.0	0.0	76.49272453587557	22.152533868853989	0
1.538224506964E12	8	0.0	0.0	0.0	0.0	0.0	0.0	78.49974912192674	19.894631209232312	0
1.538224572999E12	9	0.0	0.0	0.0	0.0	0.0	0.0	75.74009031610636	18.715504264927247	0
1.538224635713E12	10	0.0	0.0	0.0	0.0	0.0	0.0	75.76517812343201	17.711991971901657	0
1.538224700043E12	11	0.0	0.0	0.0	0.0	0.0	0.0	72.42849974912193	17.2353236327145	0
1.538224765972E12	12	0.0	0.0	0.0	0.0	0.0	0.0	71.67586552935273	16.608128449573506	0
1.538224834792E12	13	0.0	0.0	0.0	0.0	0.0	0.0	70.32112393376819	16.20672353236327	0
1.538224898698E12	14	0.0	0.0	0.0	0.0	0.0	0.0	70.07024586051179	15.830406422478676	0
1.538224975066E12	15	0.0	0.0	0.0	0.0	0.0	0.0	71.2744606121425	15.253386853988962	0
1.538225037617E12	16	0.0	0.0	0.0	0.0	0.0	0.0	71.47516307074761	14.977420973406923	0
1.538225105387E12	17	0.0	0.0	0.0	0.0	0.0	0.0	73.45709984947315	14.726542900150527	0
1.538225176893E12	18	0.0	0.0	0.0	0.0	0.0	0.0	73.88359257400903	14.550928248871047	0

Figure 56 Evacuation progress file in percent viewed from a web browser. Dynamic D3 browser based tables to monitor and inspect generateted compare evacuation progress in real time.

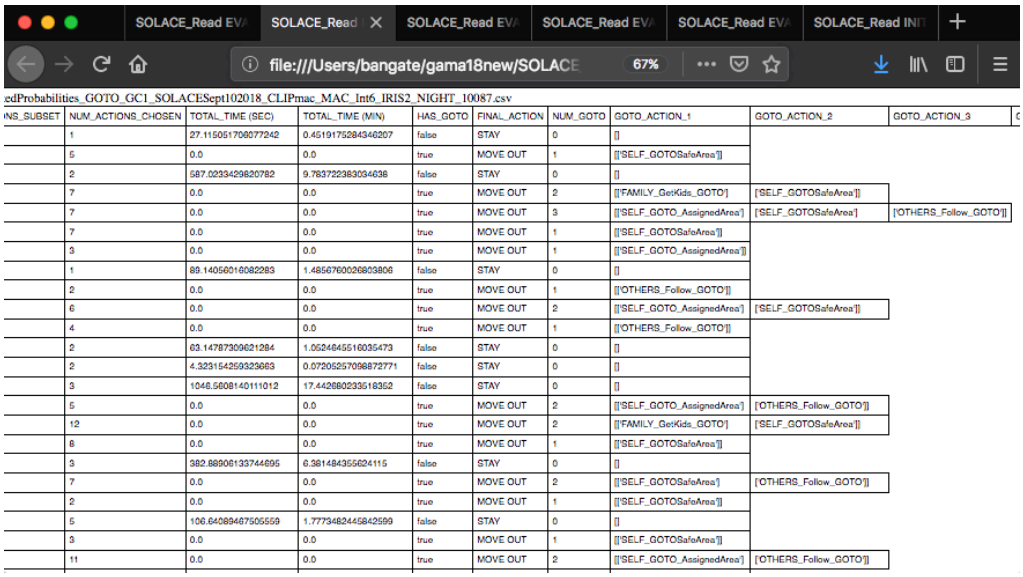

edProbabilities_GOTO_GC1_SOLACESept102018_CLIPmac_MAC_Int6_IRIS2_NIGHT_10087.csv

NS_SUBSET	NUM_ACTIONS_CHOSEN	TOTAL_TIME (SEC)	TOTAL_TIME (MIN)	HAS_GOTO	FINAL_ACTION	NUM_GOTO	GOTO_ACTION_1	GOTO_ACTION_2	GOTO_ACTION_3
	1	27.115051706077242	0.4519175284346207	false	STAY	0	[]		
	5	0.0	0.0	true	MOVE OUT	1	['SELF_GOTOSafeArea']		
	2	587.0233429820782	9.783722383034636	false	STAY	0	[]		
	7	0.0	0.0	true	MOVE OUT	2	['FAMILY_GetKids_GOTO']	['SELF_GOTOSafeArea']	
	7	0.0	0.0	true	MOVE OUT	3	['SELF_GOTO_AssignedArea']	['SELF_GOTOSafeArea']	['OTHERS_Follow_GOTO']
	7	0.0	0.0	true	MOVE OUT	1	['SELF_GOTOSafeArea']		
	3	0.0	0.0	true	MOVE OUT	1	['SELF_GOTO_AssignedArea']		
	1	89.14056016082283	1.4856760026803806	false	STAY	0	[]		
	2	0.0	0.0	true	MOVE OUT	1	['OTHERS_Follow_GOTO']		
	6	0.0	0.0	true	MOVE OUT	2	['SELF_GOTO_AssignedArea']	['SELF_GOTOSafeArea']	
	4	0.0	0.0	true	MOVE OUT	1	['OTHERS_Follow_GOTO']		
	2	63.14787309621284	1.0524645516035473	false	STAY	0	[]		
	2	4.323154259323663	0.07205257098872771	false	STAY	0	[]		
	3	1046.5608140111012	17.442680233518352	false	STAY	0	[]		
	5	0.0	0.0	true	MOVE OUT	2	['SELF_GOTO_AssignedArea']	['OTHERS_Follow_GOTO']	
	12	0.0	0.0	true	MOVE OUT	2	['FAMILY_GetKids_GOTO']	['SELF_GOTOSafeArea']	
	8	0.0	0.0	true	MOVE OUT	1	['SELF_GOTOSafeArea']		
	3	382.88906133744695	6.381484355624115	false	STAY	0	[]		
	7	0.0	0.0	true	MOVE OUT	2	['SELF_GOTOSafeArea']	['OTHERS_Follow_GOTO']	
	2	0.0	0.0	true	MOVE OUT	1	['SELF_GOTOSafeArea']		
	5	106.64089467505559	1.777348244584259	false	STAY	0	[]		
	3	0.0	0.0	true	MOVE OUT	1	['SELF_GOTOSafeArea']		
	11	0.0	0.0	true	MOVE OUT	2	['SELF_GOTO_AssignedArea']	['OTHERS_Follow_GOTO']	

Figure 57 GOTO file viewed from a web browser. Dynamic D3 browser-based tables to monitor and inspect generated compare evacuation progress in real time.

6.2.7 Dynamic time series charts

Dynamic charts facilitate the visualisation of stored CSV data from the simulation. Technologies used to develop the dynamic charts are Python, Javascript, D3 and html. The charts are made accessible by a customised interface developed using Python. A python code is called by the user interface menu options. The python code (1) calls the chosen CSV file. D3 javascript is used to render the page in the web browser. The simulation user interface together with sample web charts are shown in Figure 58. The list of charts produced from the simulation using the custom tool are detailed in Table 45. The categories of the chart include evacuation, perception and location for the different types of agents (adult, child and elderly).

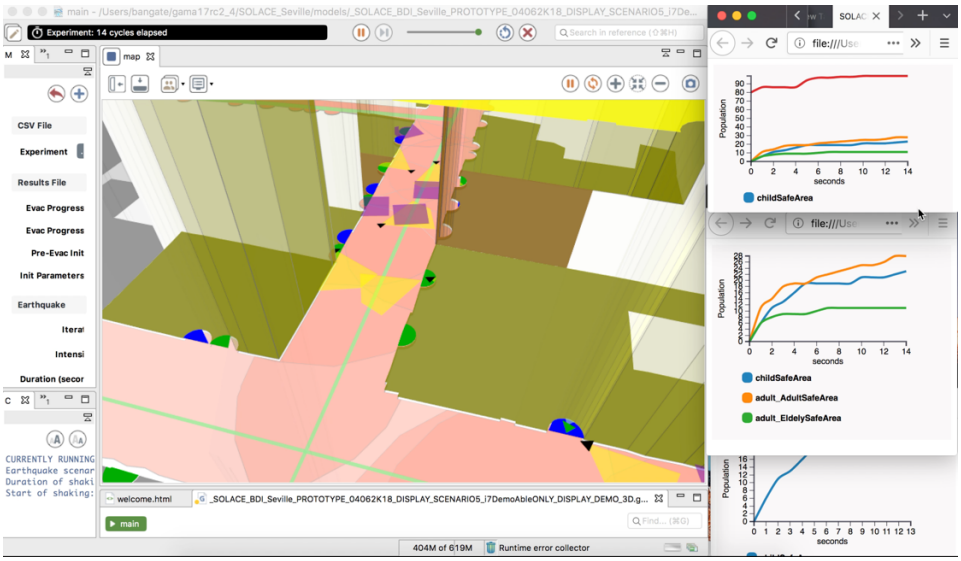

Figure 58 Dynamic D3 browser-based charts to monitor and compare evacuation progress in real time

Table 45Time series charts available in the Python UI

			Adult		Child		Elderly		All	
Chart	**Category**	**Parameters per Chart**	**Raw**	**%**	**Raw**	**%**	**Raw**	**%**	**Raw**	**%**
Multichart	Evacuation	4							✓	✓
Chart_Exposure	Evacuation	7							✓	✓
Chart_InjuredDeceased	Evacuation	4							✓	✓
Chart_ALLStat	Evacuation	7	✓	✓	✓	✓				
Chart_@SafeAreaAll	Evacuation	15	✓	✓	✓	✓	✓	✓	✓	✓
Chart_PerceiveSoc	Perception	10	✓	✓	✓	✓			✓	✓
Chart_PerceiveSoc_Modify	Perception	8	✓	✓	✓	✓			✓	✓
Chart_PerceiveEnv	Perception	12	✓	✓	✓	✓			✓	✓
Chart_RealSpeeds	Perception	10	✓	✓	✓	✓			✓	✓
Chart_Agents at Location	Location	12	✓	✓	✓	✓			✓	✓
Chart Occupied Doors	Location	10							✓	✓

6.3 Hardware considerations

SOLACE can run in GAMA installed in desktop and server environments. However, running on a remote server with a more powerful hardware configuration is preferred. Table 46 details the hardware configurations used to develop SOLACE and eventually run simulation experiments. Machines should have many hardware cores (>= 40) and a large memory footprint (>=141GB). GAMA is able to optimise simulation performance using parallel processing. Having many cores speeds up parallel processing greatly. This enables large simulation experiments to complete simulation time steps at much faster speeds. Large simulation experiments cover large geographic areas such as (1) several city blocks, (2) many IRIS units, and (3) the entire city. Large geographic areas involve many geographic entities, all of which are agents, resulting in many complex interactions. Large area simulations with cognitive agents especially utilizing BDI is computationally expensive and result in very slow simulation runs. Simulation experiments covering small area can be run on a laptop or desktop with 8 effective cores.

Table 46 Hardware Platforms used for developing and running SOLACE simulations

Machine	**Processor**	**Arch**	**Physical Cores**	**Effective Cores**	**Memory (GB)**	**Swap (GB)**	**Minutes per Cycle (Ave)**		
							2IRIS	**6IRIS**	**69IRIS**
LIG Server (Debian Linux)	Intel(R) Xeon(R) CPU E5-2640 v4 @ 2.40GHz	X86_64	40	40	141G	18.6	0.66 mins per cycle	2.64 mins per cycle	-
LIG Docker	Intel(R) Xeon(R) CPU E5-2620 v4 @ 2.10GHz	X86_64	8	8	23 G		-	-	18.83 mins per cycle
Fab Lab (Ubuntu Linux)	Intel(R) Xeon(R) CPU E5-1650 v3 @ 3.50GHz	x86_64	12	12	31.3G	2.0	0.82 mins per cycle	-	-

Laptop (MacOSX)	Intel Core i7 1600 MHz DDR3 @2,5 GHz	x86_64	4	8	16G		1.18 mins per cycle	-	-

Table 46 shows the configuration of running SOLACE on a Linux server and a client machine accessing the data. The server can be left alone running the simulation experiments. The simulations can be run in full, limited and headless modes. The limited mode, as discussed in Section 6.3.3, is preferred in running SOLACE as it can write the simulation data in the designed CSV file format. CSV files can be accessed by the client machine to produce analysis and direct visualisations of the data. Retrieving the simulation data from the server can be done using the ssh and rsync protocol in Linux or the Mac.

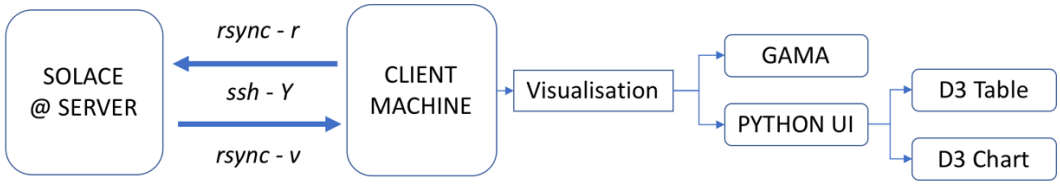

Figure 59 SOLACE Server Configuration

6.4 Calibration, simulation and validation

Calibration of the model required using the data from diffing sources. These sources include behavioural data reported from the reviewed literature. Video data from several earthquake events from all around the world were likewise reviewed, and behaviours noted to verify or enrich the gathered behaviours from literature, as there has been no observed behaviours from actual disastrous earthquakes in the Grenoble study area. Finally, scientific and operational experts were consulted in order to validate the model.

6.4.1 Calibrating population data

Concerning pedestrian mobility and speeds, Testing model runs if agents behave as expected. Mobility in free space. Respecting barriers. Navigation via shortest paths. Dynamic social interaction between agents. Origin and destination actions. Casualty generation. Debris generation. Delay via pre-evacuation actions. Multi-scale testing of agent behaviour (indoor, outdoor, city block, IRIS, city level).

Behaviour data noted from survey results reflected in the reviewed of the model required using the data from multiple sources. The behaviours are implemented in the model area listed in Table 28 from Chapter 3. These behaviours are from sources also mentioned in Chapter 3 such as Table 10.

6.4.2 Checking disaster video footage

Pedestrian behaviour from video recordings of simulation runs were compared with video from earthquake events from different countries. The videos include indoor and outdoor footage taken from mobile devices and CCTV cameras.

6.4.2.1 Indoor video – pre-evacuation behaviours

Agents egress from doors of buildings at different time intervals. Indoor behaviour in the model is defined to mimic real word scenarios. Examples of indoor video data are (a) May 12, 2015, Nepal earthquake (Bajracharya, 2018) and (b) March 11, 2011 Sendai, Japan earthquake (No Comment TV, 2018). In Figure 60-a, pre-evacuation behaviours include seeking protection under the table, exchanging

information with colleagues, waiting for others to make the move, mimicking others and managing personal property.

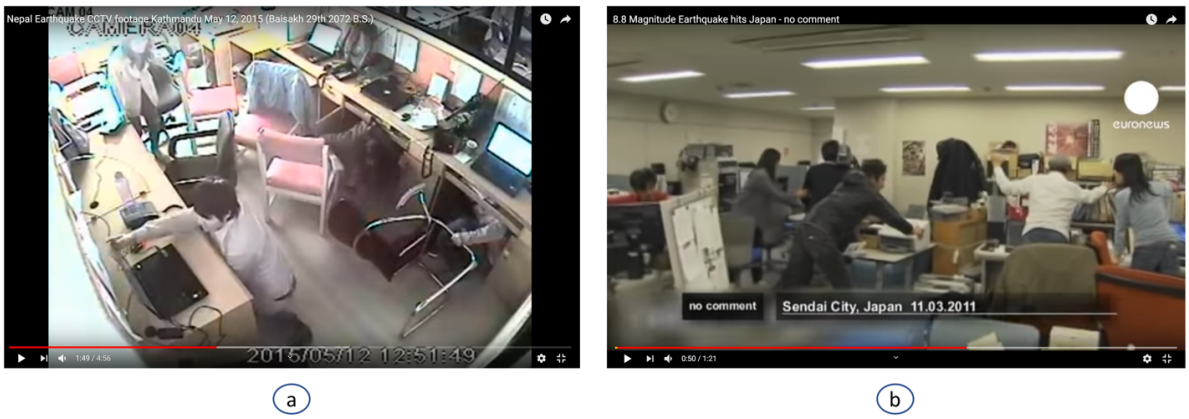

Figure 60 Validating social dynamics in the simulation by comparing with video from indoor scenes. (a) Nepal, May 12, 2015 earthquake. (b) March 11, 2011 Sendai, Japan earthquake.

Similarly, in the simulation runs, agents are probabilistically assigned pre-evacuation behaviours. This results to variations in the triggering of different possible behaviours. Like in video and journal reports, some agents do no immediately move out of the structures. The timing of egress from structures vary due to the actions assigned to the agents during pre-evacuation.

6.4.2.2 Outdoor video – pedestrian evacuation behaviours outdoors

The realism of the dynamics of agent behaviour during the runs of the simulation is checked with video taken during earthquakes from outdoor locations. Figure 61-a shows the CCTV footage from a market in Asan, Nepal during the April 25, 2015 earthquake (Pokhrel, 2018). In the video, individuals converge at the centre of this market square to seek safety. The annotated lines, indicate gaze and direction of movement. Most of the lines point towards empty spaces farther away from structures. A single line can be seen moving towards the opposite direction. The circles show close grouping of individuals. Hugging and holding hands can indicate close relationships. Figure 61-b is the result from simulation. The yellow and green perception areas located in front of agents similar to the Asan video, indicate gaze, intent to move to a direction, and direction of movement. The perception drawn between agents indicate relationship. Clustering and close proximity can likewise be observed among agents as they move towards safe areas. The clustering can be forced, due to the narrowing of passageways resulting from the presence of debris. This can also be due to social interaction among individuals with close relationships.

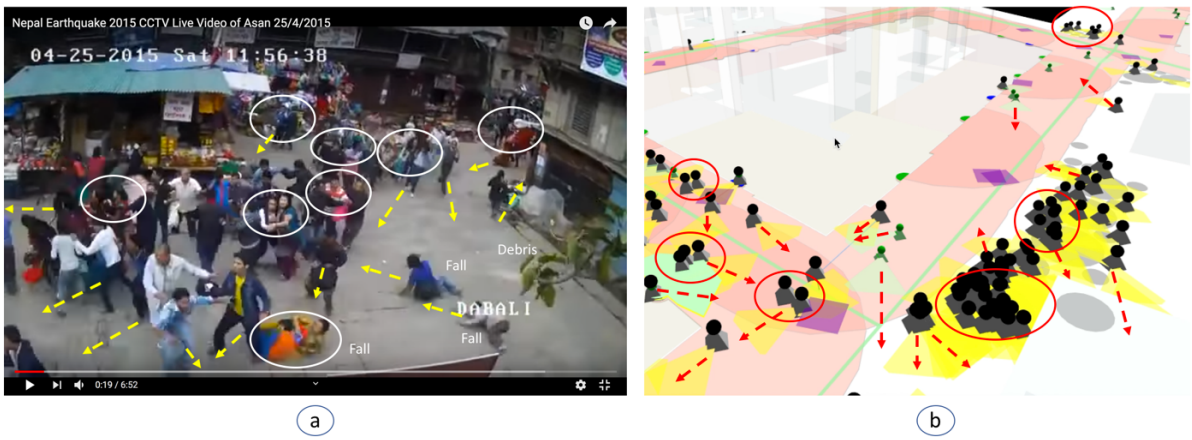

Figure 61 Emergent spatial patterns of social dynamics in the simulation by comparing with video from outdoor scenes. (a) Asan, Nepal, April 25, 2015 earthquake (b) simulation showing agent dynamics.

The pattern created by pedestrian clusters in a large open space in shown in Figure 62. Figure 62-a shows the pattern created in Zocalo Square, Mexico City during the Sept. 19, 2017 earthquake (Hollogram Studio Viral, 2018). Figure 62-b shows the spatial pattern of agent distribution in the park, Place Victor Hugo in Grenoble. The patterns in Figure 62-a and Figure 62-b are somewhat similar in the sense that more agents cluster in the outer sections of the park fronting the main pedestrian passageways.

Figure 62 Emergent spatial patterns of social dynamics in the simulation by comparing with video from outdoor scenes. (a) Zocalo Square, Mexico City during the Sept. 19, 2017 earthquake (b) clusters of agents in Place Victor Hugo, Grenoble.

Social interaction with respect to the presence of debris, injuries and deaths as replicated in the model are likewise checked with real video data. Figure 63-a shows the effect of debris damage during the Mexico earthquake on Sept. 19, 2017 (Yoti, 2018). The group of individuals in the figure are helping an old lady injured by falling debris. Figure 63-c shows this scenario implemented in the model. Debris can injure or kill agents. The default action of agents when perceiving debris is to move away. However, when an injured or dead agent is perceived, depending on the strength of attachment bond, agents can move toward the stay with the injured or dead agent. In the model, it is possible for agents to move through debris.

Figure 63 Emergent spatial patterns of social dynamics in relation to presence of debris, injuries and deaths. (a) pedestrian scene from Mexico earthquake on Sept. 19, 2017 (b) simulation showing agent interaction width debris and other agents. In the figure, injured agents have red head and dead agents have white heads. Healthy agents have black (adult) and green heads (child). (c) pedestrian scene, Christchurch, New Zealand

6.4.3 Consultation with experts to validate the model

Validation of the model and simulation required the opinion of experts from the different domains covered by the study. The experts consulted are social scientists, computer scientist, geoscientists and practitioners (Figure 64). The overall assessment is a general acceptance of the model as a first attempt to simulate evacuation behaviour integrating social, spatial and geophysical aspects.

Figure 64 Consultation with experts

The model and simulation have likewise been presented in three multi-disciplinary conferences focusing on risk. During the ISCRAM 2017 Conference in Albi France, the review of literature for the basis of social attachment has been presented. At the ICTDM 2017 conference in Munster Germany, initial results of the model were discussed. At the Risk 2018 Conference in Spain more results from the model

was presented. The general opinion gathered from the conferences that the model can be useful, similar to the results of the consultation with experts.

6.5 Summary of the chapter

This chapter presented the implementation of SOLACE. Different aspects of the model from (1) geospatial data pre-processing, (2) agent-based model code and simulation implementation, and (3) data visualisation. The discussions focused on how social attachment was implemented in the model.

CHAPTER 7. DESIGN OF EXPERIMENTS

This chapter details the design of experiments. It presents the scenarios used to evaluate the effect of social attachment on pedestrian evacuations during earthquakes. The sensitivity of social attachment to different parameters is determined. This short chapter is divided into the following sections. Section 7.1 describes the experiment scenarios. Section 7.2 provides a general description of the experiments. Section 7.3 provides a short conclusion.

7.1 Experiment scenarios

Different simulation experiments are designed to evaluate the influence of different parameters on evacuation using the model. Each parameter tested seeks to answer the research questions described in Section 1.4 of Chapter 1. In particular, Question 1 is focused on the role of social attachment on evacuations. Question 2 explores the effect of knowledge; Question 3 looks at the role of the number of close bonds; Question 4 compares the effect of time of day: Question 5, effect of the presence of disability; Question 6, effect of the presence of casualties; Question 7, effect of intensity; and Question 8, the effect of the radius of danger zones around buildings.

The research questions explored in this research fall into three general categories. The categories include (1) *social aspects* as the framework for evacuations; (2) *human factors*, that impose limits to human mobility during evacuations; and (3) the *physical context* of the earthquake crisis environment. The experiment scenarios are grouped into the following themes shown in Table 47.

Table 47 Themes for the research questions

Theme	Research Question	Topic	Keywords	Number of Experiments
Underlying social aspects	1	Role of Social Attachment	Attachment	120
	2	Effect of Knowledge	Knowledge	30 (Set 1) 2 (Set 2) 30 (Set 3)
	3	Role of Number of Close bonds	Social Bonds	30
Human Factors	4	Time of day (Day vs Night)	Visibility, Population Distribution	60
	5	Disability (With disabled, No disabled)	Disability, speed, mobility	40
Crisis Environment	6	Casualties	Dead, Injured, Intensity	40
	7	Intensity	Debris, Intensity	40
	8	Radius of Danger Zones	Danger Zones	23

7.1.1 Question 1. Role of social attachment

This question tries to determine the effect of social attachment on evacuation arrivals in safe areas. The two scenarios considered are **With Attachment** and **No Attachment**. Experiments are conducted for different intensities and the time of day for the 2 IRIS areas. The radius used for the danger zone is half the height of buildings. The perception distance for the safe area is 20 meters. The reference perception distance (PD_N) used is 50 meters. The maximum value used for IDs for family and kin groups is 50. Individuals with disability are included in the simulation. The parameters are presented in Table 48. The results are presented in section 8.3.1.

Table 48 Parameters and values for question 1 experiments

Coverage	Intensity	Time	$Radius_{DZ}$	PD_{SA}	PD_N	ID_{Fam_Kin}	Disability	Attachment
2 IRIS	4,5, 6 or 8	Day or Night	H/2	20 m	50 m	50	Yes	W-A/N-A

7.1.2 Question 2. Role of knowledge

This question looks at the influence of the knowledge of safe areas in evacuations. The hypothesis is that when locations of safe areas are known, it would lead to more individuals arriving in safe areas. Knowledge of the location of safe areas allows individuals to perceive safe areas and makes possible goal directed spatial navigation (towards safe areas). This will eventually result in more evacuation arrivals. Also linked to this hypothesis is that, with directed spatial navigation guided by knowledge, the time required to navigate towards safe areas is lessened resulting to reduced evacuation times and therefore early arrivals in safe areas.

Conversely, if individuals do not have knowledge of the location of safe areas, goal directed spatial navigation is not possible; they are not able to navigate towards safe areas. Individuals are able to reach safe areas only by chance. This may result in very low arrivals in safe areas. It may also require longer times for individuals to chance upon arriving in safe areas.

Two sets of experiments were done to test these hypotheses. In the first set, the safe areas are in very close proximity to the initial locations of the agents. This set uses the standard safe areas around buildings. In the second set of experiments, a single safe area is defined in a location far from the initial location of agents. This single safe area can be reached by a 15-minute walk in ideal conditions. Ideal conditions mean that (1) movement towards safe areas is done immediately and fast; (2) shortest path is taken to navigate towards safe areas; (3) evacuation is not disturbed by other actions; and (4) the shortest path is not blocked.

7.1.2.1 SET 1. Nearby safe area

Perception distance is used as the indicator of knowledge of the safe area. The variable parameter in the experiment is the perception distance of safe areas (PD_{SA}). The values used for limited knowledge are 20 meters and 50 meters. These values are within the visual perception distance. Aside from being equated to limited knowledge, these limited ranges also allow individuals to recognize and discover safe areas when they fall within their perception distance. For high or absolute knowledge, 10 kilometres is used. The experiments are conducted over 2 IRIS areas. The effect of debris is eliminated by using Intensity IV. Night time is used to ensure that all individuals start from indoor locations. A No Attachment scenario is used to also eliminate the effect of social influence through social bonds. The other parameter constants used in the experiments are presented in Table 49.

Table 49 Parameters and values for question 2 experiments

Coverage	Intensity	Time	$Radius_{DZ}$	PD_{SA}	PD_N	ID_{Fam_Kin}	Disability	Attachment
2 IRIS	4	Night	H/2	20 m/50 m/10 km	50 m	50	Yes	N-A

PD_{SA} (Perception Distance Safe Area), $PD_{SÀ}$ (Perception Distance Normal), W-A (With Attachment), N-A (No Attachment), H (Building Height), DZ (Disaster Zone)

7.1.2.2 SET 2. Single safe area far from population initial location – free space navigation

Considering the surprising results of set 1 (see Section 8.3.2.1), the effect of long (10 km) and short (20-meter) perception distance in finding a single safe area is tested by a simple experiment using a subset of the model data shown in Figure 65. In this experiment, 5 % of the population for the 2 IRIS area (244 adults, 17 children) is generated within the IRIS 2 boundary. Evacuation of agents towards a single safe

area 500 to 600 meters from the IRIS 2 boundary is recorded for the duration of 5400 cycles. In Figure 65, the safe area is a single circle located south east of the IRIS 2 area in Parc Mistral[27]. The evacuation catchment radius around the safe area is shown in Figure 66. It is possible to reach this middle green safe area within 15 minutes by walking when the average walking speed is 1.4 meters per second. By running with an average speed of 3.0 meters per second, it is possible to reach the safe area within 7 minutes. Intensity IV earthquake during night time is considered for the scenarios. The simulation is recorded for 5400 cycles (i.e. 1 hour 30 minutes).

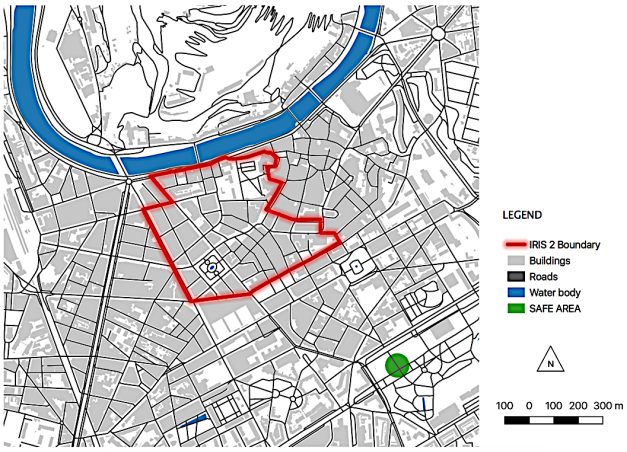

Figure 65 Simple experiment on individual navigation through urban pathways.

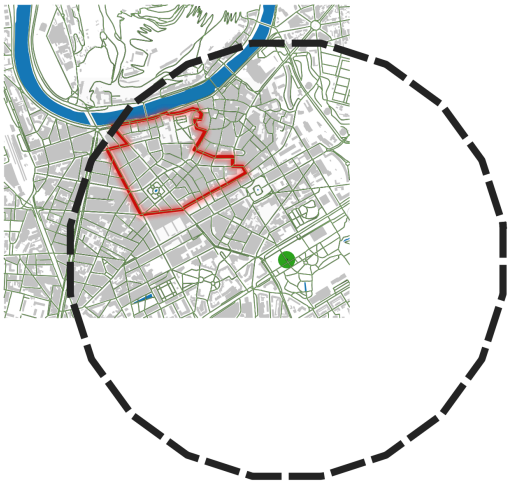

Figure 66 Catchment radius of the safe area defined by the black circle drawn with thick broken lines.

7.1.2.3 SET 3. Single safe area located in a distant location from the population initial location, with shortest path navigation, percentage of the population with knowledge of safe area

In this set of experiments, improvements on the use of knowledge in the navigation strategy of agents to reach safe areas is implemented. The improvement is the ability of agents to evacuate using the

[27] As a reference, the distance from Parc Victor Hugo to the safe area in Parc Mistral, using the nearest major roads (Boulevard Agutte Sembat and Boulevard Maréchal Lyautey) is approximately 900 meters. Using this path, at the comfortable walking speed of 1.4 meters per second (Bohannon, 1997; Fritz & Lusardi, 2009), it will take approximately 11 minutes to reach the safe area.

shortest paths to move towards the nearest safe area. In these set of experiments, when an agent has knowledge of the safe area, individual agents are also able to select and head towards the nearest shortest possible route to use for navigation. When taking the shortest route, agents focus in reaching the safe area and stay within road centrelines. For roads enclosed by buildings on both sides, road centre lines the farthest locations from the buildings, and can be considered safer when evacuating. Agents are able to strictly follow the shortest path road centreline (implemented as snapping to the vector centreline) when they are very close to the centre line by at least 1 meter. Prior to this close proximity to the centreline, agents are able to move freely in free space and are able to interact with other agents. This navigation using shortest path road centrelines is in shown in Figure 67.

Figure 67 Agent navigation towards safe area using the shortest path. Agents (small yellow triangles on roads) move from initial building locations (dark grey and light grey polygons) towards the safe area (green circle) by way of shortest paths defined from road centrelines (white-orange vector lines). The intensity simulated is Intensity IV, which explains the absence of debris damage and therefore blocked pathways.

Three sets of experiments were conducted using this navigation strategy. The summary of the parameters used in this set of experiments is show in Table 50. Testing the effect of knowledge was done by varying the percentage of the population with knowledge of the safe area. In the first set, 100% of the population have knowledge. In the second set 66% of the population have knowledge. In the last set, 0% of the population have knowledge. The experiments were run until it reached 6000 cycles. This is equivalent to 1 hour and 40 minutes evacuation time. This long duration was allowed due to the initial observation that it was not possible to have the agents reach the safe area within 900 cycles (equivalent to 15 minutes). The earthquake intensity simulated is intensity VI. The scenario used is for night time. This ensures that agents are in home environments.

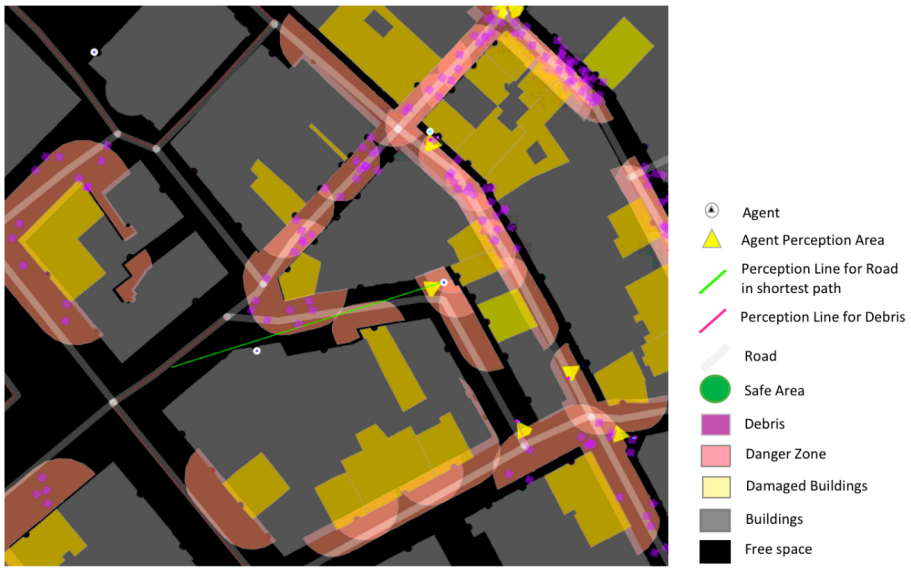

Figure 68 Agent navigation around blocked pathways. The agent with the long and green perception line has perceived a road segment which is part of the shortest route (white with thin red centreline). In its current location, the agent is able to travel freely in space as it navigates towards the portion of the shortest path towards safe zones. Buildings without damage are shown as grey polygons. Damaged buildings are yellow-orange polygons. Debris blocking roadways are shown as violet squares. Red polygons surrounding damaged buildings are danger zone.

Table 50 Parameters and values for question 2 experiments – set 3

Coverage	Intensity	Time	$Radius_{DZ}$	Knowledge Safe Area	PD_N	ID_{Fam_Kin}	Disability	Attachment
2 IRIS	6	Night	H/2	100%/60%/0%	50 m	50	Yes	N-A

7.1.3 Question 3. Role of the number of close bonds

This question looks at the influence of the number of close bonds on evacuation. The hypothesis is that there would be few evacuation arrivals when there are many close bonds. This is due to the high likelihood that closely bonded individuals will hesitate to leave each other especially in danger zones. Staying in the initial locations during the earthquake to be with others can result in non-evacuations, or delayed arrivals in safe areas.

To answer this question two types of with attachment scenarios are compared. The first scenario has many individuals sharing many close bonds (i.e. family, kin and friends). The second scenario has many individuals with weak bonds or having many strangers. It should be noted that social attachment during disasters can form with strangers. The bond however is much weaker than with closely bonded individuals.

The social bonds in the experiments is defined by group membership and implemented as perception distances. Closely bonded individuals are more familiar to each other. This familiarity facilitates recognition and perception event at much longer distances. This familiarity also imposes bias or acts as spatial and preferential attachment filter. For example, when two other individuals fall within the perception angle, the one with the stronger bonds to the perceiver is perceived over the other with lesser bond. The variable used in the experiment to implement the two scenarios is the range of the ID for kin and friends. The ID for family members is assigned from building ID and floor number. The range of 50 is used for the scenario with many close bonds. The range of 1000 is used for the scenario with many strangers. The parameters used in the experiments are detailed in Table 51. The results of these experiments are shown in section 8.3.3.

Table 51 Parameters and values for question 3 experiments

Coverage	Intensity	Time	Radius$_{DZ}$	PD$_{SA}$	PD$_{N}$	ID$_{Kin_Friends}$	Disability	Attachment
2 IRIS	4	Night	H/2	20m	50 m	50 or 1000	Yes	W-A

PD$_{SA}$ (Perception Distance Safe Area), PD$_{SÂ}$ (Perception Distance Normal), W-A (With Attachment), N-A (No Attachment), H (Building Height)

7.1.4 Question 4. Effect of time of day

This question looks at the influence of the time of day on evacuations. The main variable tested in the experiments is time of day. Experiment results of day and night scenarios are superimposed and compared in the context of different earthquake intensities. The two main differences between night and day scenarios are (1) initial locations of individuals at the start of the simulation, and (2) length of perception distances.

The hypothesis for this question is that there will be more arrivals in safe areas during the day than night time. This is based on the several ideas. First, the daytime scenario already has an advantage since some individuals are already outdoors and can already be in safe areas; and are spatially more spread out at different indoor locations (i.e. homes, schools, work areas and public places). During night time all individuals are indoors in homes. Second, individuals can see farther during the daytime than night time. The third reason is that attachment bonds between family members are very strong which can delay evacuation. During daytime, individuals exposed strengths of bonds since they can be co-located with non-family members. The parameters used in the experiments are detailed in Table 52.

Table 52 Parameters and values for question 4 experiments

Coverage	Intensity	Time	Radius$_{DZ}$	PD$_{SA}$	PD$_{N}$	ID$_{Kin_Friends}$	Disability	Attachment
2 IRIS	4, 6 or 8	Day or Night	H/2	20m	50 m	50	Yes	W-A

PD$_{SA}$ (Perception Distance Safe Area), PD$_{SÂ}$ (Perception Distance Normal), W-A (With Attachment), N-A (No Attachment), H (Building Height)

7.1.5 Question 5. Effect of the presence of disability

This question looks at the scenario when disability is considered in the population of evacuees. The two scenarios considered are With Disabled and No Disabled in the context of with attachment and no attachment for Intensity VI. The hypothesis is that for the population with disabled, there will be lesser overall arrivals in safe areas. This is based on the premise that disabled individuals are slower to evacuate. The evacuation of non-disabled individuals may be influenced by the disabled due to social attachment. The parameters used in the experiments are detailed in Table 53.

Table 53 Parameters and values for question 5 experiments

Coverage	Intensity	Time	Radius$_{DZ}$	PD$_{SA}$	PD$_{N}$	ID$_{Kin_Friends}$	Disability	Attachment
2 IRIS	6	Day	H/2	20m	50 m	50	Yes or No	W-A/N-A

PD$_{SA}$ (Perception Distance Safe Area), PD$_{SÂ}$ (Perception Distance Normal), W-A (With Attachment), N-A (No Attachment), H (Building Height)

7.1.6 Question 6. Effect of the presence of casualties

This question looks into the effects of the presence of casualties (i.e. injured and deceased) on the route during evacuations. Interactions with casualties along the route may influence the evacuation of individuals. Strong social attachment bonds may result in individuals staying with casualties who are attachment figures. On the other hand, the presence of casualties may act as cues that can trigger immediate evacuation to safe areas. This may happen especially when individuals share very low

attachment bonds and may move away from casualties. The hypothesis for this question is that more interactions in the route will result in lesser arrivals in safe areas.

The scenarios considered with attachment, day conditions at intensities 4, 5, 6 and 8. The parameters for the experiments are shown in Table 54. The results include (1) casualties, (2) interactions with casualties, and (3) arrivals in safe areas.

Table 54 Parameters and values for question 6 experiments

Coverage	Intensity	Time	Radius$_{DZ}$	PD$_{SA}$	PD$_{N}$	ID$_{Kin_Friends}$	Disability	Attachment
2 IRIS	4, 5, 6 and 8	Day	H/2	20m	50 m	50	Yes	W-A

PD$_{SA}$ (Perception Distance Safe Area), PD$_{SÂ}$ (Perception Distance Normal), W-A (With Attachment), N-A (No Attachment), H (Building Height)

7.1.7 Question 7. Effect of intensity

This section looks at the role of intensity with respect to the number of arrivals in safe areas. Results from previous questions were actually presented in the context of different intensities. The discussions however focused on the social and behavioural aspects. This section will provide the physical context particularly related to the debris damaged produced at different intensities and its impact on evacuations. The scenarios considered with attachment, day conditions at intensities 4, 5, 6 and 8. These are the same set of experiments used in Question 6 (see Section 8.3.6). For reference, the parameters for the experiments are shown in Table 54.

7.1.8 Question 8. Effect of the radius of danger zones and availability of safe areas

This section looks at the effect of the radius of danger zones on the number of arrivals in safe areas. Taller buildings will have larger danger zones around them. Large danger zones around buildings define the area with the largest probability where an individual can be trapped or hit by falling debris (and therefore can be killed or injured). Areas with many adjacent buildings will have overlapping danger zones. This define overlapping probabilities or risk. Larger danger zones effectively push safe areas farther away from buildings. This means that an increased distance needs to be traversed by individuals during evacuations. This in effect increases the required time to reach safe areas.

In this section, the hypothesis is that large radius for danger zones would result in lesser arrivals in safe areas. The parameters considered for the experiments are detailed in Table 55.

Table 55 Parameters and values for question 8 experiments

Coverage	Intensity	Time	Radius$_{DZ}$	PD$_{SA}$	PD$_{N}$	ID$_{Kin_Friends}$	Disability	Attachment
IRIS2, IRIS9, IRIS69	VI	Night	H/2 or 6 m	20m	50 m	50	Yes	W-A/N-A

PD$_{SA}$ (Perception Distance Safe Area), PD$_{SÂ}$ (Perception Distance Normal), W-A (With Attachment), N-A (No Attachment), H (Building Height)

Figure 69 shows the map of available safe areas for the radius of danger zone from (a) half the building height, and for (b) uniform 6 meters around buildings. By visual comparison it can be seen that there are more safe areas available to individuals if the radius used is 6 meters. The safe areas for the radius of half the height of building occur as patches and farther away from buildings.

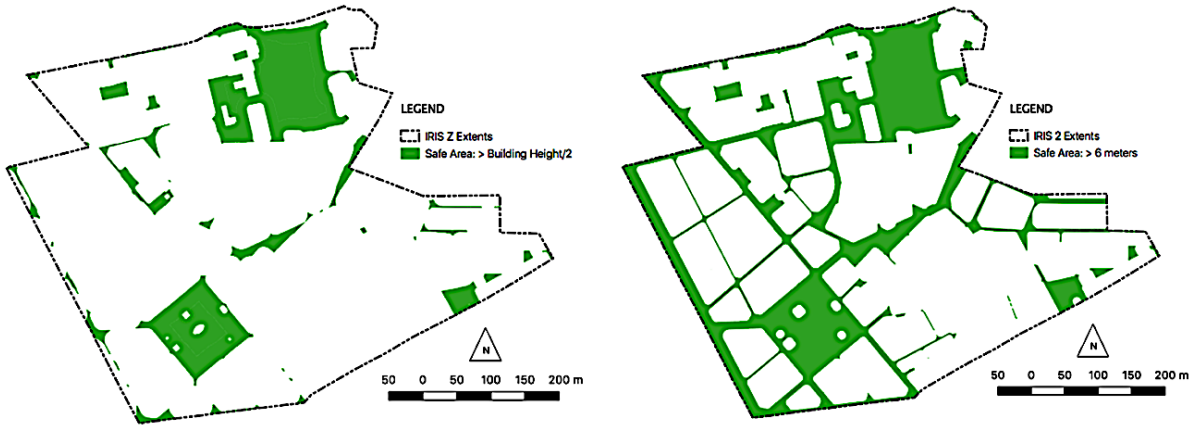

(a) (b)

Figure 69 Map of available safe areas (a) > Half the height of buildings (b) uniform 6 meters around buildings

Table 56 shows the comparison of the values for available safe areas for the IRIS 2 coverage used in the experiments. It can be seen that the percentage of available safe areas is much greater for the 6-meter radius and is at 25.24% of the total area. For the radius using half the height of the building, the available safe area is just 14.37 % of the total coverage. Figure 70 shows the pie chart for the distribution of danger zone, barriers and safe areas.

Table 56 Size of danger zones, safe areas and barriers (in square meters and percent)

Radius of danger zone from building (meters)	Danger Zone (DZ), (sq. meters)	Barriers (B) sq. meters	Safe Area (SA) sq. meters	DZ %	B%	SA%	TOTAL %
Half of building Height (H/2)	103436.90	139396.54	40759.93	36,47	49,15	14,37	100
6 meters	72631.37	139396.54	71565.46	25,61	49,15	25,24	100

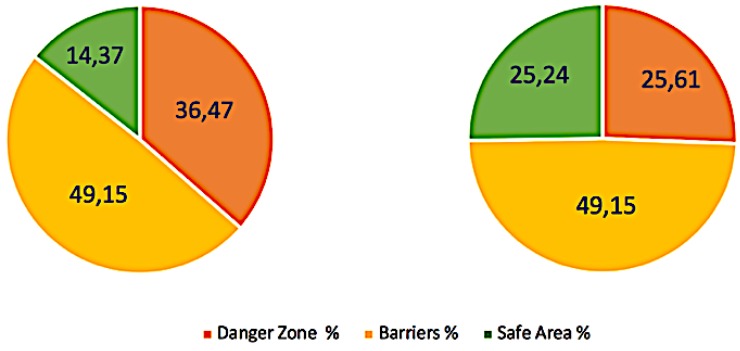

(a) (b)

Figure 70 Available safe areas (a) > Half the height of buildings (b) uniform 6 meters around buildings

7.2 General description of experiments and simulation with the model

The workflow for the experiments is shown in Figure 71. (1) The scenario is defined in the GAML code. This requires setting the appropriate data such as the shapefiles, population and perception distance. The parameters for the scenario are set. The prefix for the filenames of the resulting CSV files is set. (2) The experiment is run in limited display mode. (3) A CSV file is extracted from the results folder. (4) Data is visualised using the SOLACE data view tool. Analyses of the data and comparison with results from other scenarios are done using spreadsheets.

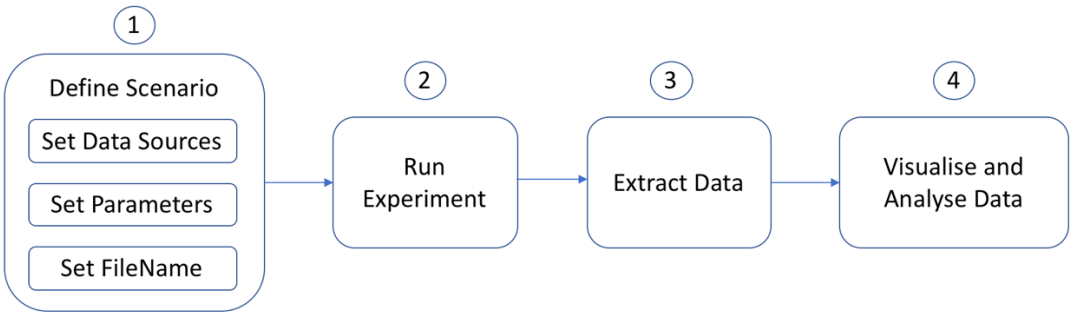

Figure 71 Workflow for the experiments

7.2.1 Time

Earthquakes are sudden onset events. Ideally, evacuations need to be immediate and fast. That is, pedestrians need to be in outdoors, and in safe areas after a very short time after an earthquake event. The model and simulation experiments are used to investigate the very first few seconds after an earthquake. The duration of agent evacuation data recorded for each simulation experiment is 15 minutes. One simulation time step is equivalent to 1 second. This 15-minute period translates to 900 timesteps for each experiment. This duration is set in the simulation as shown in Code 29. The equivalent GAMA code is shown in Code 58. For longer duration observations, the value can be changed in the code or in the model parameter interface.

Code 29

```
End the simulation 900 cycles after the start of the earthquake.
```

During the initial tests, it was observed that large numbers of agents greatly reduce the speed of the simulation run. A single run of an experiment using the small area subset with 2 IRIS units, and target duration of 1800 timesteps (30 minutes), finishes after approximately one day on a machine with 40 cores and 141GB memory. In the new experiments, the number of agents was reduced or minimised to ensure that simulation run completes in the required timestep (900 timesteps or 15 minutes). The strategy adopted to limit the number of agents is the use of a smaller spatial coverage for the experiments. In GAMA, all elements of the model are agents. This includes the buildings, roads, roads, debris, etc. The complex geometries of spatial layers add to processing times. The population of cognitive human BDI agents likewise requires longer processing durations. The city population of Grenoble is 64,000 individuals from the census data. This large number of BDI agents results in very slow simulation runs.

7.2.2 Spatial extents

A majority of the experiments for sensitivity analysis was implemented using the smallest data subset covered by 2 IRIS units. This 2 IRIS subset includes a small population of human and environment agents. The objective is to generate many results from multiple simulation runs. Adopting this small area makes reaching this objective possible. A smaller number of experiments was conducted on the moderate sized subset covering 9 IRIS units. The city scale simulation covering 69 units was implemented last with a very limited number. The reason for using subsets is to optimise the time available for the experiments. This is also due to limitations of the computer hardware that greatly impact the speed of simulation runs.

7.2.3 Parameters

The simulation experiments use different types of values for parameters. The values are relative to the scenario considered. The parameters used in the model are shown in Table 57. The last column indicates the parameter modified for each change in scenario. At the top of the list are the parameters usually modified before the start of each experiment scenario. These include intensity, time of day, building damage and danger zone. The remaining parameters are modified for situations that require fine tuning of values.

Table 57 Initial simulation parameters

Description	**Parameter**	**Type**	**Modified to set scenario**	**Values**
Intensity	*eqIntensity*	Int	Yes	IV, V, VI or VIII
Context or Time of day	*Context*	Int	Yes	Day or Night
Building Damage	Shapefile for damage scenario at intensity	Shapefile	Yes	
Danger Zone	Shapefile for damage scenario at intensity	Shapefile	Yes	
Duration of Earthquake	*eqDuration*	Int	No	10 cycles
Time for start of earthquake	*eqTime*	Int	No	3rd cycle
Base Shapefiles	Shapefiles defining environment	Shapefile	No	Roads,
Agent Population	IRIS population	Int	No	IRIS population
Perception Distance (meters)	PD_Child, PD_Partner, PD_Parent, PD_Kin, PD_Friends, PD_Acquaintance, PD_Stranger, PD_Family, PD_debris, PD_road, PD_safeArea, PD_walls	Float	Yes	Day, Night, Snow [100.0, 100.0, 100.0] [94.10, 4.11, 43.03] [88.85, 3.89, 40.63] [76.45, 3.34, 34.96] [87.85, 3.84, 40.17] [69.20, 3.03, 31.65] [60.85, 2.66, 27.83] [100.0, 100.0, 100.0] 10 meters, 20 meters, 4 meters, 5 meters
Separation Distance (meters)	separation_Others, separation_Deceased, separationDebris	Float	No	1 meter 5 meters 5 meters
Avoidance Distance (meters)	avoidance_Others, avoidance_Deceased, avoidance_Debris	Float	No	1 meter 5 meters 5 meters
Probabilities	evacSpeedMax, probDisability, actionProbabilities, preEvacActions_Master, preEvacActions_TimeRANGE_MASTER	Float	No	List of speeds in m/sec List of probability values List of action probabilities List of actions List of time ranges for actions
Social Group ID_string	idFamily, idColleague	String	No	BuildingID+Floor#
Social Group ID_float	idKinMax, idFriendMax,	Float	No	50, 50
Species definition	Adult, Child, Human	Species	No	
Behaviours	Behaviours	String	No	List of behaviours
Behaviour Probabilities	Probability for each behaviour	Float	Yes	Probabilities for behavours

7.3 Summary of the chapter

This chapter presented the design of simulation experiments for different scenarios. The objective of the experiments is to determine the impact of parameters on evacuation using the model. The focus of each experiment highlighted merits of model components to provide realism in simulating earthquake evacuations. The defined scenarios show that the model SOLACE is flexible and can be configured to represent and design different earthquake scenarios. Parameters can be adjusted to the level of complexity needed in experiments. Fine tuning probabilities used in the simulation is possible by changing the values as needed in the GAML code. The limit to the number of experiments that can be performed is defined by the capacity of hardware. Multiple scenarios can be explored especially when an HPC infrastructure is used.

CHAPTER 8. RESULTS

This chapter presents the results of experiments covering different earthquake evacuation scenarios. The chapter is divided into the following: Section 8.1 provides a brief introduction; Section 8.2 describes the charts used in presenting the results; Section 8.3 discusses the experiment results with respect to the research questions; and Section 8.4 summarises and concludes the chapter.

8.1 Introduction

The relevance to evacuation of different parameters is tested in each scenario. The effect of the parameters on evacuation is evaluated based on the number of arrivals in safe areas. As the objective of evacuations is saving lives, a large percentage of arrivals in safe areas is used as the measure of evacuation success. The scenarios are compared solely on this criterion.

The data on the number of agents reaching safe areas are recorded over 900 simulation cycles. In the experiments, one simulation cycle is equivalent to 1 second. For each experiment run of 900 cycles, this is equivalent to simulating the first 15 minutes of evacuation immediately after the earthquake event. The experiment scenario evaluating the effect of knowledge is a special case where data for 6000 simulation cycles is used for analysis. Section 7.1 indicates the respective details on simulation parameters and experiment scenarios. The different scenarios are presented in Table 47 and the default parameters used in the simulation are shown in Table 57.

8.2 Description of charts used

Several charts are used to present simulation results in this chapter. The types of charts used are histograms, time series, x-y scatter plots and pie charts. The data is from the CSV file generated from each simulation run. The charts are processed using MS Excel.

The comparisons of scenario results are presented using histogram charts accompanied by time series plots. The histogram plots show the values of arrivals of agents at the 900th or 6000th cycle. Time series charts are used to plot the values from the 1st to the 900th cycle or 6000th. X-Y scatterplots are used to compare results involving the different earthquake intensities: 4, 5, 6 and 8. Time series plots may likewise accompany X-Y scatterplots. Pie charts are also used for easy comparison of results.

8.3 Answers to research questions

The results of experiments covering the eight research questions (discussed in Section 1.4 of Chapter 1, and experiment design elaborated in Section 7.1 and Chapter 7), are presented in this section.

8.3.1 Question 1: Does social attachment affect the number of arrivals in safe areas?

Figure 72 and Figure 73 show the results for day and night evacuations respectively for Intensity IV. Figure 74 and Figure 75 show the results for day evacuations at intensities V and VI respectively. Figure 76 and Figure 77 show the day and night evacuations respectively for Intensity VIII. The summary of the percentage arrivals and calculated differences are presented in Table 58.

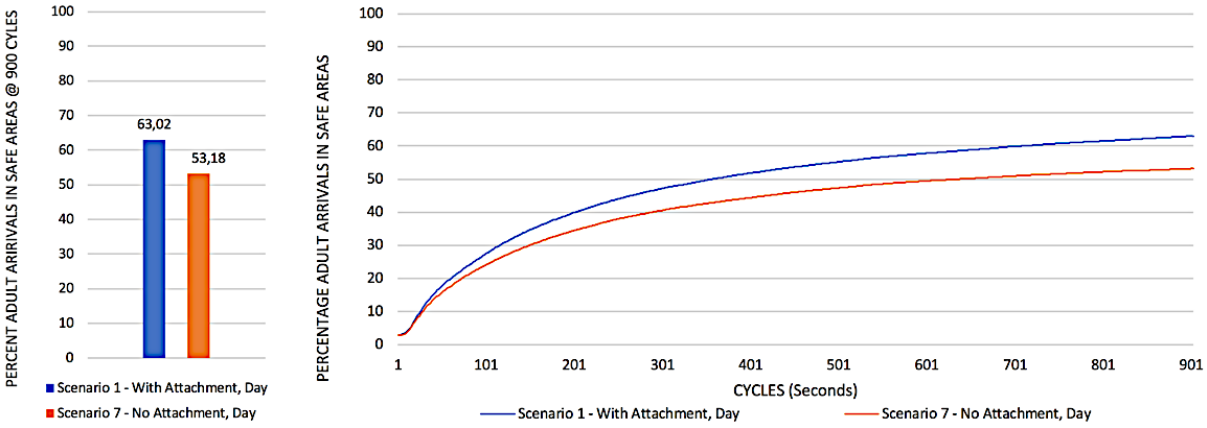

(a) (b)

Figure 72 Adult arrivals in safe areas, Intensity IV – Day (a) histogram, (b) timeseries

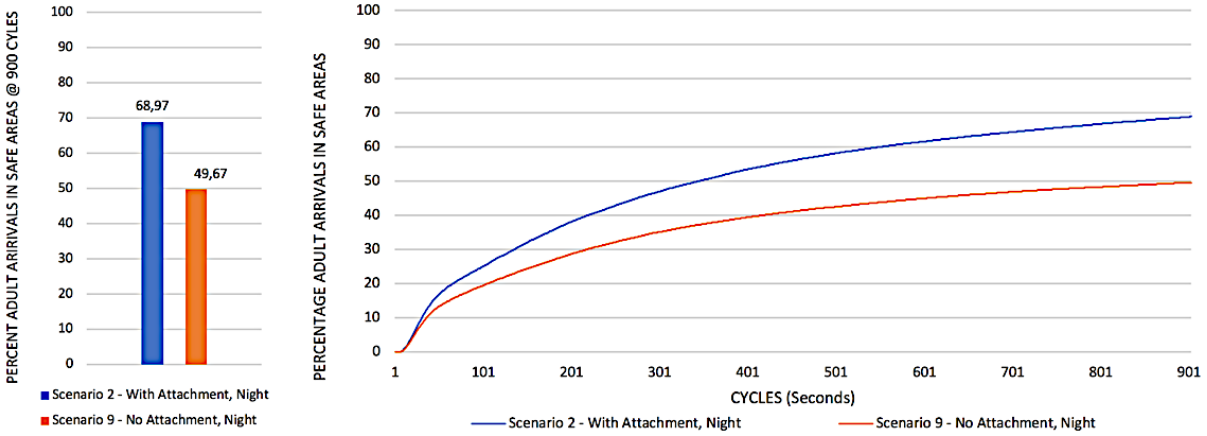

(a) (b)

Figure 73 Adult arrivals in safe areas, Intensity IV - Night (a) histogram, (b) timeseries

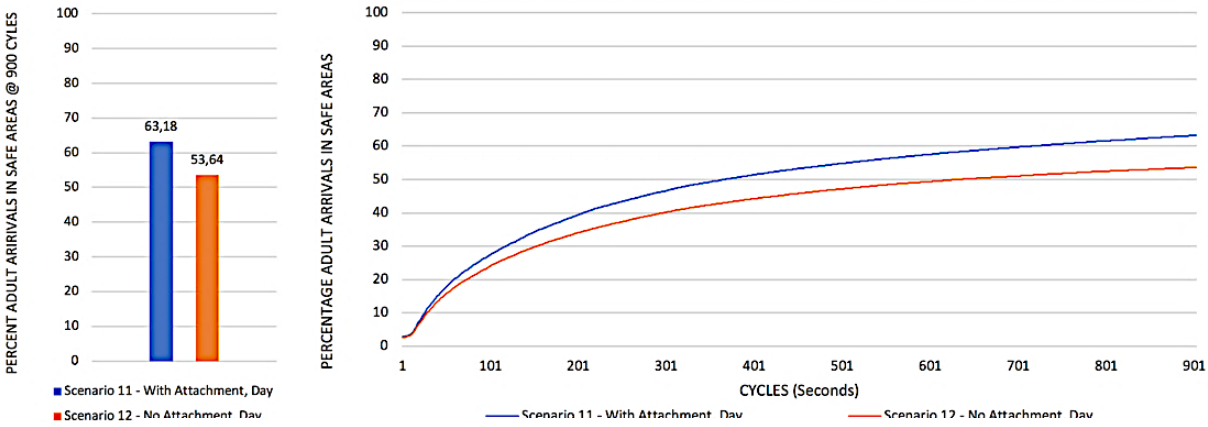

(a) (b)

Figure 74 Adult arrivals, Intensity V – Daytime (a) histogram, (b) timeseries;

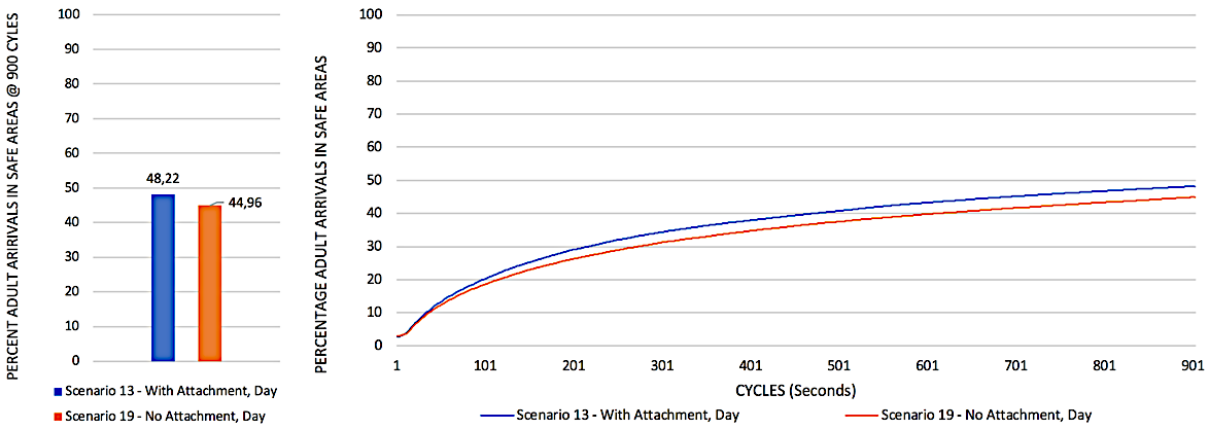

(a) (b)

Figure 75 Adult arrivals, Intensity VI – Daytime (a) histogram, (b) timeseries

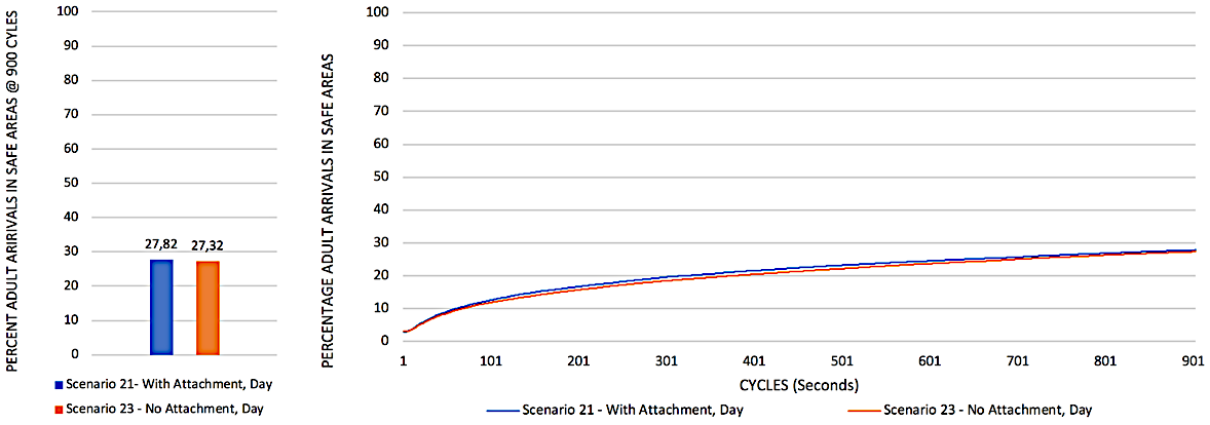

(a) (b)

Figure 76 Adult arrivals, Intensity VIII – Day (a) histogram, (b) timeseries

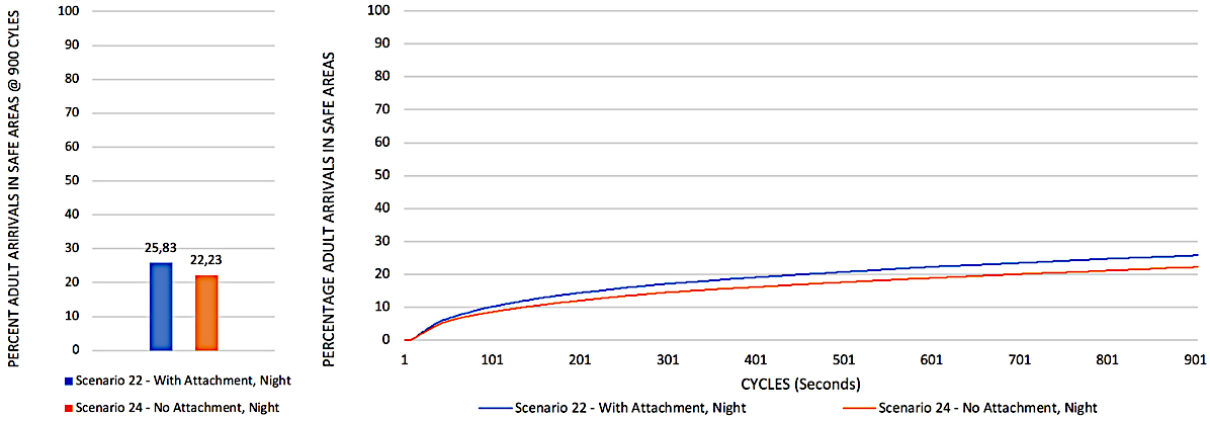

(a) (b)

Figure 77 Adult arrivals, Intensity VIII – Night (a) histogram, (b) timeseries

In the six charts shown in Figure 72 to Figure 77, it can be seen that evacuations **With Attachment** result in more arrivals in safe areas than evacuation with **No Attachment**. This trend is consistent for

both day and night conditions. The difference between **With Attachment** and **No Attachment** is more pronounced or larger for night conditions as shown in Figure 73 and Figure 77. Here **With Attachment** dominates **No Attachment** with differences of 19.30% for Intensity IV and 3.6% for Intensity VIII, respectively.

Comparing day and night conditions with respect to intensities reveal that the difference for **With Attachment** and **No Attachment** is much greater for night than day conditions. For Intensity IV this can be seen by comparing Figure 72 with Figure 73. In this case, the 19.30 % difference for the night condition is greater than the 9.84 % difference for the day condition. For Intensity VIII, this is seen by comparing Figure 76 with Figure 77. In this case, the 3.6 % difference for the night condition is greater than the 0.5 % difference for the day condition.

Comparing **With Attachment** and **No Attachment** with respect to intensity, it can be seen that the difference becomes smaller as the intensity increases. This trend can be seen from Figure 72 and Figure 77 and from values in Table 58. The difference is largest for Intensity IV and becomes very small at Intensity VIII. This is consistent for both day and night conditions. Table 58 shows the summary values and calculated differences from the experiments. The difference is derived by subtracting with-attachment and no-attachment results.

Table 58 Difference in percentage arrivals in the With Attachment and No Attachment scenarios

	Day		**Night**		**Difference (With Attachment – No Attachment)**		
Intensity	**W-A**	**N-A**	**W-A**	**N-A**	**Day (%)**	**Night (%)**	**(Night – Day) %**
Intensity IV	63.02	53.18	68.97	49.67	9.84	19.30	9.46
Intensity V	63.18	53.64	-	-	9.54	-	-
Intensity VI	48.22	44.96	-	-	3.26	-	-
Intensity VIII	27.82	27.32	25.83	22.23	0.5	3.6	3.1

W-A (With Attachment), N-A (No Attachment)

Figure 78 shows the X-Y plots of the values from Table 58. Figure 78-a shows the values for **With Attachment** and **No Attachment** for the day condition with respect to intensities. For both scenarios, a decreasing trend can be seen in the number of arrivals at intensity becomes higher. The difference between the two scenarios also decreases. Figure 78-b plots the arrivals for both the day and night time condition for both the **With Attachment** and **No Attachment** scenarios at intensities 4 and 8 respectively. The larger differences in arrivals at Intensity IV implies that attachment has significant influence on evacuation at the lowest intensity. The clustering of the data points at the higher Intensity VIII shows that the influence of attachment becomes negligible at higher intensities.

From the results of these experiments, it can be concluded that the number of arrivals in safe areas is expected to be larger when social attachment plays an active role in the evacuation. That is, agents are able to socially interact, with the interaction facilitated by social attachment. This however can only happen when agents are mobile, can interact, and able to move towards safe areas. At higher earthquake intensities, barriers can hinder social interaction and the may block access to safe areas. In this situation, the beneficial effects of social attachment to evacuation is muted by the presence of barriers.

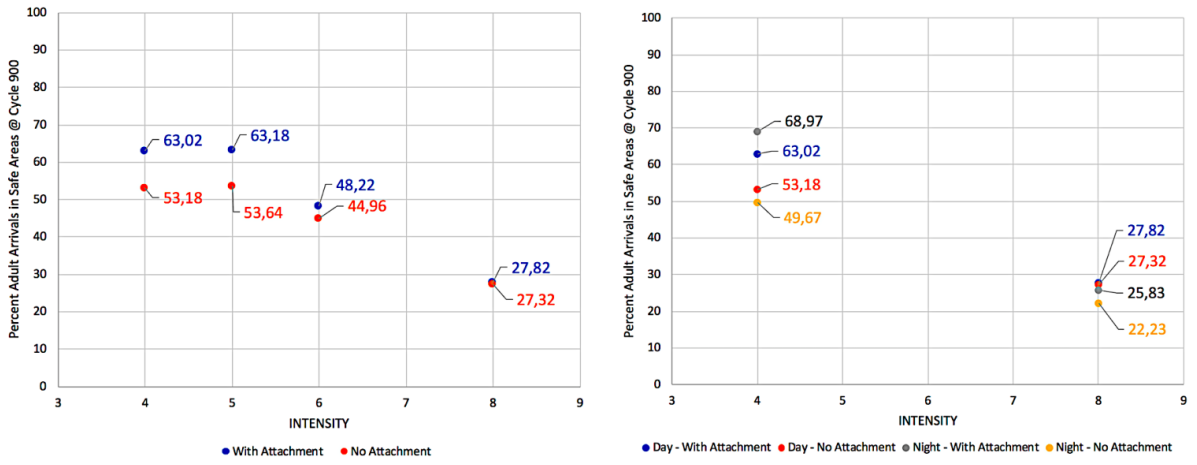

(a) (b)

Figure 78 Comparison across different intensities – (a) Daytime only for Intensity IV, 5, 6 and 8, (b) Extreme values Intensity IV vs Intensity VIII for Day and night time scenarios

To further illustrate the beneficial effects of social attachment on evacuation, please consider how individuals perceive goals in the **No Attachment** and **With Attachment** scenarios shown in Figure 79.

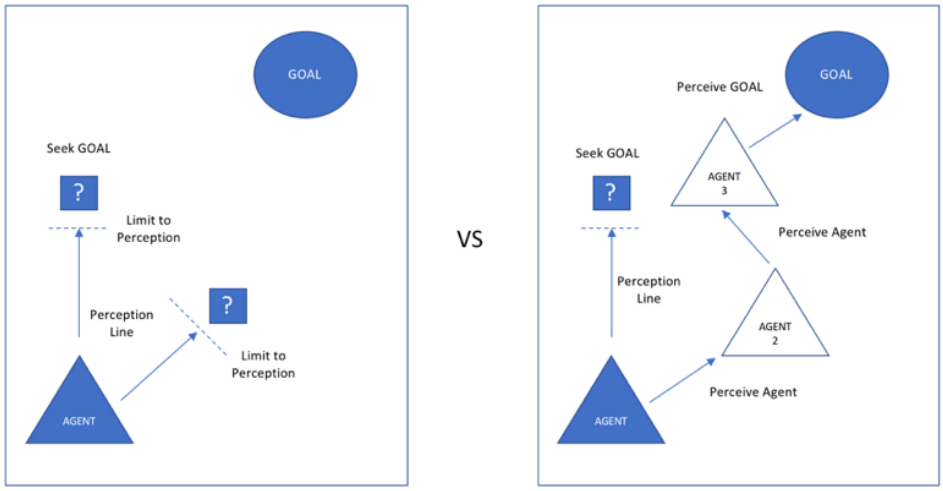

(a) (b)

Figure 79 Perceiving Goals: (a) no social attachment, (b) with social attachment

For the **No Attachment** scenario shown in Figure 79-a, perception of a goal (such as a safe area) will be limited by the range of perception (distance) of the individual. When the goal is not perceived, the individual continuously seeks for it in the environment. The small forward movements (footsteps) guided by limited vision would reduce to a random walk (Barbosa, et al., 2018; Natapov, Czamanski, & Fisher-Gewirtzlan, 2016; Rudnick & Gaspari, 2004). The individual needs to be close enough to a goal to be able to perceive a goal. When the goal is perceived, the individual is guided towards the goal by a perception line. This leads to perceptually directed behaviour (M., Klatzky, Golledge, & Philbeck, 1999); or biased random walk (Rudnick & Gaspari, 2004); or goal directed behaviour or wayfinding (Brunyé, Gardony, Holmes, & Taylor, 2018). Please refer to the model of the agent illustrated in Figure 23 of Section 5.3 Chapter 5. In this no attachment scenario, the evacuation is solely by-individual, i.e. the agent is alone and left to its own means and sets of behaviours in navigating towards safe areas.

In the With Attachment scenario shown in Figure 79-b, the limited perception of individuals is effectively extended by the perception of the attachment figure, and an ultimate goal, by perception distance propagation (Weiss, 1978) or (forward markov chain) (e.g. nodes in a view graph (Franz, Mallot, & Wiener, 2005))) (Dalton, Hölscher, & Montello, 2019). This is also called indirect perception (Vaez, Burke, & Alisadeh, 2016) or indirect search (Kunze, Doreswamy, & Hawes, 2014). This results to the individual being indirectly guided to the goal, which in this case can be a safe area. To illustrate perception distance propagation, consider for example an Agent perceives and moves towards another Agent 2, who perceives and moves towards Agent 3, who in turn perceives a Safe Area. The Agent effectively moves closer to the safe area guided by the previous position of Agent 2, who was in turn also guided by the position of Agent 3. However, it may be the case that Agent 3 is not headed towards the safe area. This may lead the Agent to move farther away from the goal. Also, the perception of other agents may likewise be discontinued due to: (1) other agents moving out of range caused by (a) differences in speeds, (b) blocked pathways, (c) complex layout of built environment; or (2) shifting of gaze or attention. When attachment figures are not in range, movement of agents reduce to a random walk.

For earthquake evacuations any movement away from initial vulnerable environments is important. With social attachment, the presence of attachment figures can pull agents away from vulnerable locations. Familiar agents, when within visual range and perception angle, are readily perceived by an agent. Distance acts as a filter for preferential attachment. This may help facilitating the clustering of individuals or the formation of evacuation groups. Having many individuals in a group and moving in the same direction, provides many possible targets or attachment figures. A large group has a high probability being noticed or perceived. Other individuals not within the cluster of individuals, but within range, may gravitate towards group members, further increasing group size. Social attachment therefore presents the agents with many intermediate goals. This results to more possibilities during social interactions. This is illustrated in Figure 80. Different pre-evacuation behaviours would ensure different egress time from buildings. Individuals that are first to egress, but remain within range, can provide the direction for evacuating social group members.

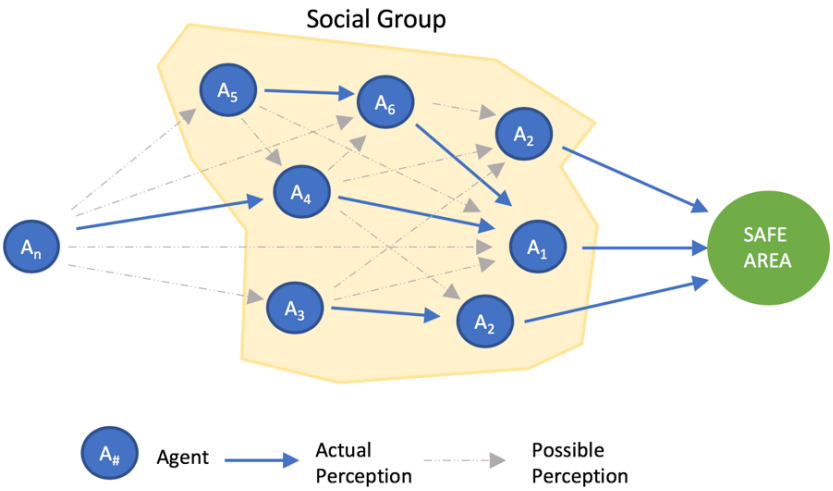

Figure 80 Creation of Social Groups facilitated by social attachment

The beneficial effect of social attachment on evacuation can therefore be summarized to (1) initiate movement from initial locations by having attachment figures as intermediate goals; (2) trigger group formation and evacuation as groups; (3) provide individuals with increased degrees of freedom for multi-modal goal seeking and action (e.g. following), modulated by attachment bonds and spatial proximity; (4) increased probability for goal-directed (seeking) behaviours facilitated by the presence of attachment figures; (5) extension of perception distance by perception distance propagation or indirect perception. These insights provide explanation to the result that With Attachment result in more arrivals in safe areas than No Attachment.

The almost similar trends in arrivals for high Intensity VIII scenario can be due to the isolating influence of debris. The presence of debris in pathways from high intensity earthquakes results in limited individual mobility and reduces the possibility for perception distance propagation. There will still be social interactions but these may be localised away from safe areas. The individuals physically may not be able to escape these island traps. Individuals who are outside this island traps, may likewise be attracted to groups in isolated pockets delaying or completely ignoring going to safe areas. When this happens, the beneficial effect of social attachment for evacuation to safe areas is muted at increased intensity. This is eventually cancelled out for Intensity VIII as show in Figure 78-b. The small advantage though of social attachment for the night time condition for the high intensity scenario is highlighted in

Figure 77-b. For Intensity VIII, the cause of the low number of arrivals, aside from low mobility, is due to the high number of casualties.

The large difference in the agent arrivals between Intensity IV and VIII highlights the importance of mobility (Table 58 and Table 59). The difference between arrivals for With Attachment and No Attachment in daytime is 35.2% and 25.86% respectively. For the night time, the values are 43.14% and 27.44% respectively. From the values, it can be seen that there are more arrivals for the low Intensity IV scenarios than for Intensity VIII. Unlike the high Intensity VIII scenario previously described, no debris are generated in Intensity IV. Evacuation is not hampered by blocked pathways and individuals are able to interact. In this context, the main factor that can influence the arrivals is the duration of pre-evacuation actions, prior to egress from buildings.

Table 59 Difference in percentage arrivals in the with attachment and no-attachment scenarios for Intensity IV and VIII

	Day		Night		Difference (With attachment – no attachment)		
Intensity	**W-A**	**N-A**	**W-A**	**N-A**	**Day (%)**	**Night (%)**	**(Night – Day) %**
Intensity IV	63.02	53.18	68.97	49.67	9.84	19.30	9.46
Intensity VIII	27.82	27.32	25.83	22.23	0.5	3.6	3.1
Difference (Intensity IV – Intensity VIII)	35.2	25.86	43.14	27.44	9,34	15,7	6,36

W-A (With Attachment), N-A (No Attachment)

To summarise and answer the research question: social attachment is beneficial to evacuation especially when mobility towards safe areas is possible. The social interactions made possible by social attachment increases the probability for individuals to reach safe areas. With social attachment, the mode of evacuation is individually or in groups. With no social attachment, evacuation is exclusively an individual effort. The probability of reaching safe areas is much greater than with no attachment case where evacuation purely rests on the individual without the influence of others.

8.3.2 Question 2: Does the knowledge of nearby safe areas affect the number of arrivals in safe areas?

8.3.2.1 Set 1. Nearby safe areas

Table 60 lists the almost similar results for the number of arrivals in safe areas for the three distances defining knowledge. Figure 81 gives the charts showing the effect of knowledge of the location of safe areas. It can be seen from Figure 81-a that the difference is very small at the 900th cycle. The trend in the time series plot shown in Figure 81-b also shows that this difference is consistently small from the 1st to the 900th cycle.

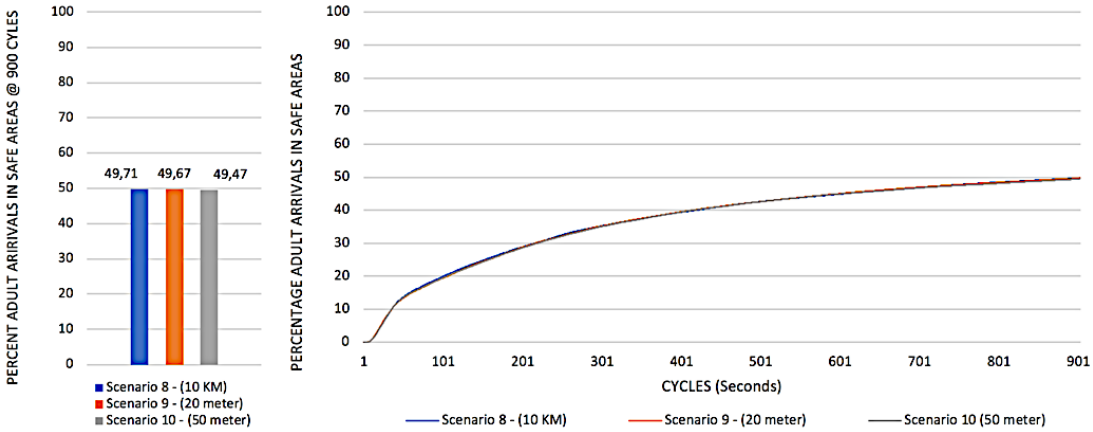

(a) (b)

Figure 81 Effect of knowledge of safe areas on adult arrivals, Intensity IV – Night (a) histogram, (b) timeseries

Table 60 Effect of knowledge of safe areas on adult arrivals

Coverage	**20 meters**	**50 meters**	**10 km**
Percentage Arrivals	49.67	49.47	49.71

The results of this set of experiments showed that the different ranges of perception distance used to represent knowledge does not produce noticeable differences in the number of agent arrivals in safe areas. This result is opposite to the hypothesis that the number of arrivals of agents with the scenario with absolute knowledge (perception distance of 10 km) to be greater than the 50-meter and the 20-meter perception distances.

The main reason for this similarity in the plots, can be the close proximity of safe areas from the initial locations of individuals. This relatively short distance cancels out the advantage of absolute knowledge. If the safe areas however are very far (such as greater 500 meters), the scenario with absolute knowledge may have more arrivals. This is possible because with the far distance, absolute knowledge can enable goal directed behaviour to reach safe areas. In the situation where the safe area is very far, when the perception distance is 20 or 50 meters, individuals will only engage in undirected random walks. In this case, the probability of reaching safe areas will be very low.

8.3.2.2 Set 2. Single safe area far from population initial location – free space navigation

The results of these experiments are shown in Table 61. Very few arrivals in the safe area were recorded within 5400 cycles. For example, the first arrival in experiment 1 occurred at the 1892nd cycle. The duration between succeeding arrivals is also very long: in the same experiment, the 2nd individual arrived at the 2758th cycle, and the 3rd in the in the 4815th cycle respectively. For scenario where individuals had short perception distance of 20 meters, no arrivals were observed. These simple experiments showed that the 10 km safe area perception distance provided the individuals the capability to detect the safe area. The results of the simple experiment indicate that long perception distance ranges, or absolute knowledge of safe area locations is useful when navigating towards a remote safe area.

Table 61 Simple experiment. Number of arrivals after 5400 cycles (1 hour 30 minutes)

	No Attachment	
Coverage	**20 meters**	**10 km**
Number of Arrivals	0	3

The small experiment with a single safe area in a far location resulted in very few agents reaching safe zones. This proves the following: (1) safe zones that are far can be found when individuals know where they are (can be perceived) even at far away distances; (2) far located safe zones require more time for evacuation. This longer length of time is due to (a) longer distances to travel; (b) almost finite average walking/running speeds; and (c) Even when the destination is known, the possibility to get disoriented and lost is high, especially in cities dissected by many pathways. Taking a wrong turn in city streets has the potential to increase getting lost. To be able to find far safe areas faster, (a) routes towards safe areas also need to be specified or marked for direction guidance; (b) high familiarity with city streets; (3) nearby safe zones need to be provided/accessible for individuals for immediate evacuations. Nearby zones would ensure that even without knowledge of specific safe areas individuals will be able to discover safe areas with random visual search; (4) many individuals are able to reach safe areas when nearby. Faster evacuation time is needed for earthquake events. Reaching safe areas with the least amount of time can make accounting for missing individuals faster; (5) the model needs improvement in terms of navigation and search strategies or ensuing guidance (markers) to direct individuals in safe areas that are far away. This is similar in real situations.

Another possible reason could be the continuous forward movement of individuals when they start to emerge from buildings. Egress is done even without the benefit of having the final goal of arriving at a definitive safe area location. When no goal is detected, random walk enables agents to move farther away from source locations. Moving forward increases the probability of finding safe areas especially when they fall within the range of perception.

Another possible contributing factor to this result could be the structure of the urban area. Roadways act as intermediate goals providing agents guidance in navigating urban space. Buildings act as barriers that constrain the movement within roadways and open spaces. Even with absolute knowledge of safe areas, individuals are forced to navigate around buildings to reach safe areas. Dense urban centres with many buildings, dissected by many roadways can pose navigation challenges in reaching safe areas.

8.3.2.3 Set 3. Single safe area located in a distant location from the population initial location, with shortest path navigation, percentage of the population with knowledge of safe area

The results of this set of experiments are shown in Table 62 and Figure 82. It can be seen from Figure 82 that for the scenarios with populations of agents with 100% and 66 % knowledge, agents start arriving in safe areas after approximately 1100 cycles. The scenario with 0% of the population having no knowledge of the safe area do not have arrivals. The experiments with the most arrivals in the safe area are the experiments with 100% of the population having the knowledge of safe area locations. The arrivals peaked at an average of 83% at the 6000th cycle. The second set of experiments with 66% of the population having knowledge of safe areas, reached the peak of average arrivals at approximately 53%. The experiments with the population with 0% knowledge continue to have no arrivals at the 6000th cycle.

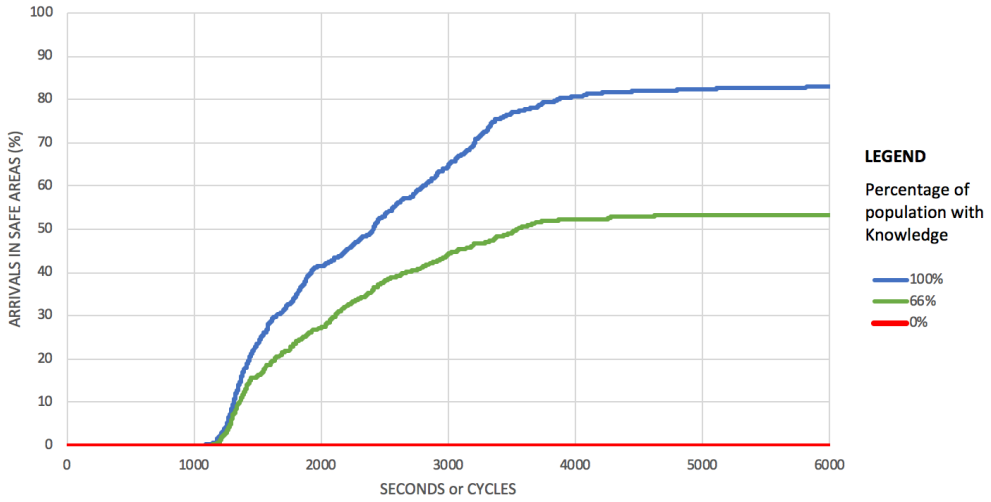

Figure 82 Results of evacuation with knowledge

Table 62 Number of arrivals after 6000 cycles

	Percent of the Population with knowledge of safe areas		
	0 %	**66 %**	**100 %**
Percentage Arrivals	0 %	53.33 %	82.91 %

The result from the set of experiments confirm the importance of knowledge in the search for safe areas during evacuations. This is especially true if the location of the safe area is far and difficult to reach. Complex configurations of city environments can make navigation complicated for agents, especially when pathways are blocked and agents need to find alternative pathways. It is also impossible for trapped agents to move out of damaged zones.

For both the 66% and 100% knowledge scenarios, it can be seen from Figure 82 that not all of the agents with knowledge arrived in safe areas. This can be due to different possible reasons. One possible reason are the pre-evacuation behaviours assigned to agents. An agent with knowledge agent may have been assigned behaviours which consume a considerable amount of time. Some agents with knowledge may also have chosen to stay and not evacuate. Some agents may likewise be trapped, injured or have died from debris.

With the result that knowledge is important, several improvements in the scenarios therefore can be done to improve the chances of agents arriving in safe areas within the least amount of time (less than 15 minutes). That is, placement of safe areas must be as close as possible to agents so that the safe areas can be reached easily and faster by agents. This underscores the importance of the strategic placement of safe areas in urban environments. This can be ensured in the creation of city evacuation plans.

Using the experiment data as an example, and shifting the centre of the15-minute walking radius to the centre of the boundary (IRIS 2), the different scenarios for placement of safe areas shown in Figure 83 could be tested. In Figure 83-a, several safe areas can be placed in open areas outside the red IRIS 2 boundary. Each agent with knowledge can choose the nearest safe area. This can minimise travel time and effectively allow agents with knowledge to reach safe areas much faster. A large number of safe areas likewise present agents with more options, as pathways to some areas may be blocked by debris. Locating safe areas closer and closer to the boundary such as in Figure 83-b and Figure 83-c and even inside the boundary as in Figure 83-d, can improve evacuation times and the number of safe area arrivals.

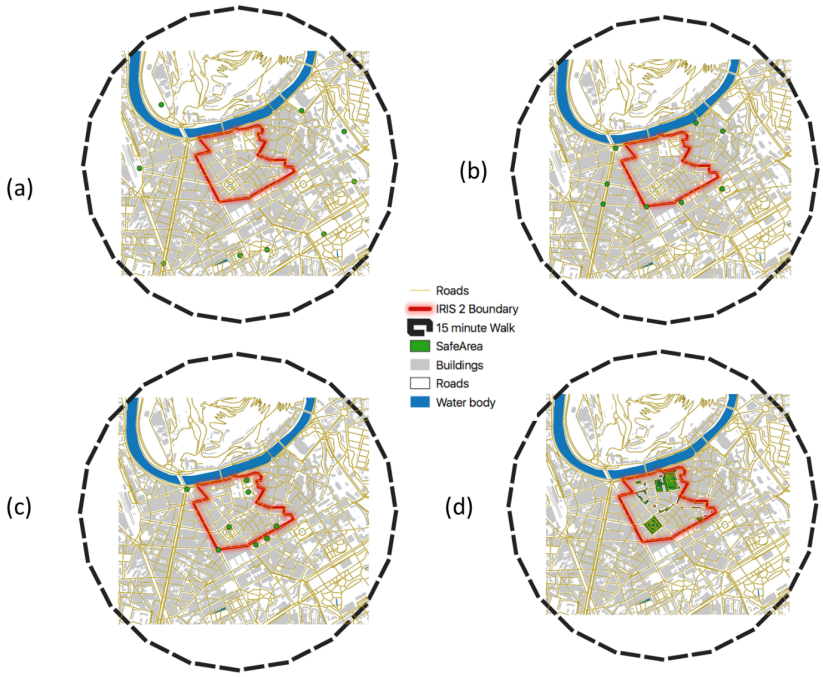

Figure 83 Possible configurations of safe areas to improve evacuation. (a) Open areas far from the boundary. (b) Open areas closer to the boundary. (c) A mix of boundaries outside and inside the boundary. (d) Safe areas away from buildings inside the boundary.

8.3.2.4 Short conclusion from 3 sets of experiments

The summary of the results of the scenarios is shown in Table 63.

Table 63 Summary of results for experiment on evacuation with knowledge

Experiment Set	**Scenario**	**Arrivals in safe areas**
Set 1 – Safe areas are located nearby (Greater than Half of the building height), 900 Cycles	Limited Knowledge – 20 meters PD_{SA}	49.67 %
	Limited Knowledge – 50 meters PD_{SA}	49.47 %
	Broad Knowledge – 10 kilometres PD_{SA}	49.71 %
Set 2 – Single safe area far from population, 5400 Cycles	Limited Knowledge – 20 meters PD_{SA}	0%
	Broad Knowledge – 10 kilometres PD_{SA}	3 Agents
Set 3 – Single safe area far from population, Percentage of population with broad knowledge and with shortest path navigation, 6000 Cycles	0 % Knowledge	0 %
	66 % Knowledge	53.30 %
	100 % Knowledge	82.91%

From Table 63, it can be seen that the knowledge of nearby safe areas is important and this makes a huge difference in the number of arrivals in nearby safe areas. This is especially true when the location of an identified safe areas is far from the initial locations of evacuating populations. For safe areas that are located far away from individuals, successful evacuation requires that the shortest path directly leading to the safe area is also known, and used by evacuating individuals. Random walks directed in the opposite direction of safe areas, or agents doing actions that consume time away from actually evacuating to safe areas, result in either delayed- or non- arrival in safe areas.

The ideal scenario for successful evacuations is that 100% of individuals are knowledgeable of where safe areas are, and of what routes to. However, in reality only a percentage of individuals in a locality may have knowledge of safe areas and the associated shortest paths. Locals would have the advantage of having more knowledge of routes, and are therefore expected to move towards the direction of safe areas with ease. Having no knowledge is difficult at shown by the experiments. From the experiments it was shown that increasing the knowledge of populations of where safe areas are, can help ensure the greater number of arrivals in safe areas.

The detrimental effect of limited knowledge of the location of safe areas can be minimised or cancelled out by ensuring that safe areas are in close proximity and are easy to find. This close proximity allows for the possibility that safe areas can be directly sought or discovered by agents even through random walks. This point is clearly demonstrated in Figure 81. The results from Figure 81 showed that there are arrivals in safe areas which are located very near the evacuating agents. Also, in this case, there seemed to be no discernible difference for agents navigating with knowledge or no knowledge of the location of safe areas.

8.3.3 Question 3: How does the number of close bonds affect evacuation?

Figure 84 presents the charts showing the effects of the number of social bonds on evacuation. It can be seen from Figure 84-a that at the 900th cycle, there are more arrivals in safe areas for the scenario where there are many close bonds than for the scenario with many strangers. The difference in the number of arrivals is 13,14 %. The time series plot in Figure 84-b shows the scenario with many close bonds consistently having more arrivals in safe areas than the scenario with many strangers from the 1st to the 900th cycle. The difference between the arrivals from the two scenarios also seem to grow larger from the 1st to the 900th cycle.

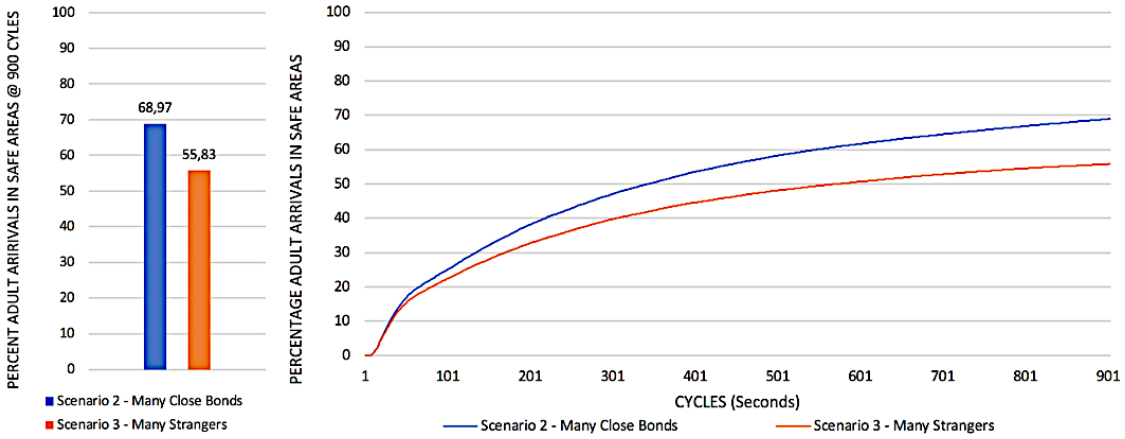

Figure 84 Effect of the number of social bonds on adult arrivals in safe areas,

The result is contrary to the hypothesis that there will be few arrivals if there are more social bonds. However, the result of having more arrivals for the scenario with many close bonds is consistent with the results from Question 1 (in Section 8.3.1). This helps confirming that when attachment is present in evacuations, it results in more arrivals in safe areas.

The contribution of Question 3 is in highlighting the role of strong and weak social bonds in evacuations. Having many close bonds in the population makes available to individuals a large pool of attachment figures that can provide guidance during evacuations. This large pool can facilitate the creation of supergroups that can help pulling group members towards safe areas resulting in more arrivals.

Weak social bonds with strangers likewise facilitate evacuation. Although arrivals are fewer that of the scenario with many close bonds, arrivals with strangers are much greater than for the scenario with no attachment. This is shown in Figure 85 and Table 64. The scenario with strangers results in arrivals which are 6.16% greater than for no attachment. The trend in the time series plot in Figure 85-b shows that the arrivals in the weak attachment scenario with more strangers is consistently greater than that for no attachment. The difference also increases from the 1st to the 900th cycle.

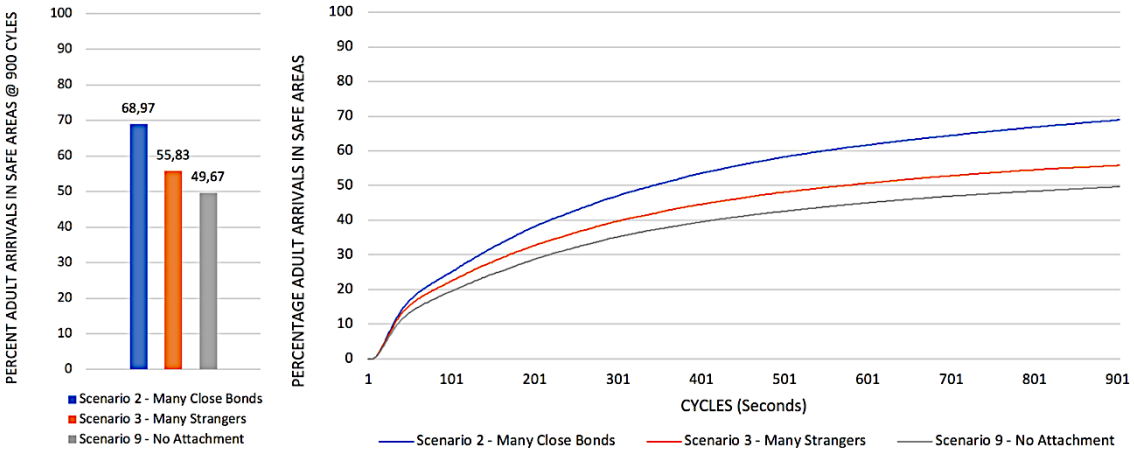

Figure 85 Effect of the number of social bonds compared with No-Attachment Intensity IV – Night (a) histogram, (b) timeseries

Table 64 Effect of social bonds on the number of arrivals in safe areas

	No Attachment Bonds	**Many Strangers**	**Many Close Bonds**
Number of Arrivals	49.67	55.83	68.97

The hypothesis was that there would be few evacuation arrivals when there are many close bonds, since individuals will be constrained from leaving original locations, due to the strong attraction towards attachment figures. The results showed that this is not the case. What had not been fully considered is the possibility that individuals may move together or follow others when they egress and head to safe areas. Also, individuals will have different styles in responding to threat situations resulting in variations in pre-evacuation behaviours. Social bonds in real populations are inherently variable and intermixed. Some will be first to make a move or exit, and others just follow. This facilitates perception distance propagation and actually benefits evacuations. Strong attachment bonds would prompt others to follow. This is shown in Figure 84 and Figure 85. These same strong bonds can also motivate individuals to search or fetch others, even moving towards danger zones, before moving to safe areas.

As a conclusion to answer the question, a large number of close bonds result in greater arrivals in safe areas than when there are many strangers. The weak social bond with strangers also benefits evacuations and results in more arrivals in safe areas than the case when there is no social attachment at all. The results of these experiments highlight the importance of having more close bonds in communities to facilitate evacuations.

8.3.4 Question 4: How does the time of day affect evacuation?

Figure 86, Figure 87 and Figure 88 compare the effect of night and day on the number of arrivals in safe areas for Intensity IV, VI and VIII respectively. From the figures, the advantage of the day condition can be seen in the first cycle. There are agents already located in safe areas. However, from Figure 86 and Figure 87, it can be seen that this advantage is erased as the arrivals for the night condition, both for the Intensity IV and VIII, overtake the arrivals for the day scenario. The difference between the night and day condition for Intensity IV is the largest at 5.69 %. For Intensity VI, the difference is smaller at 1.07 %. The time series plots in Figure 86-b and Figure 87-b show the gradual increase in arrivals for the night condition finally overtaking the values for the day condition. This happens at cycle 305 for Intensity IV, and much later at cycle 650 for Intensity VI.

The situation for Intensity VIII however is different as shown in Figure 88. The daytime condition seems to maintain its advantage (in this case 2.88 %) on number of arrivals over the night condition. This can be seen from the timeseries plot in Figure 88-b. At the 900th cycle the arrivals in day condition is greater than the night condition by 1.99%.

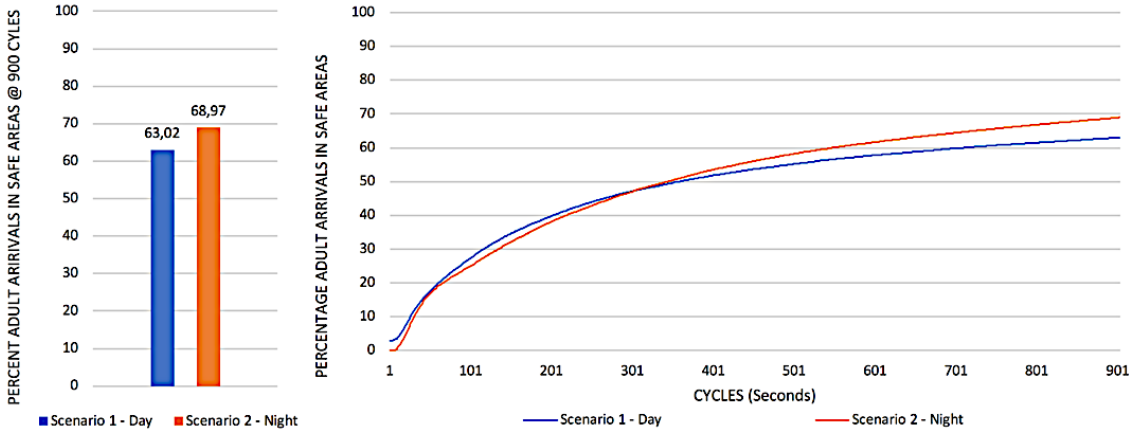

(a) (b)

Figure 86 Effect of the time of day on evacuation, Intensity IV: (a) histogram, (b) timeseries

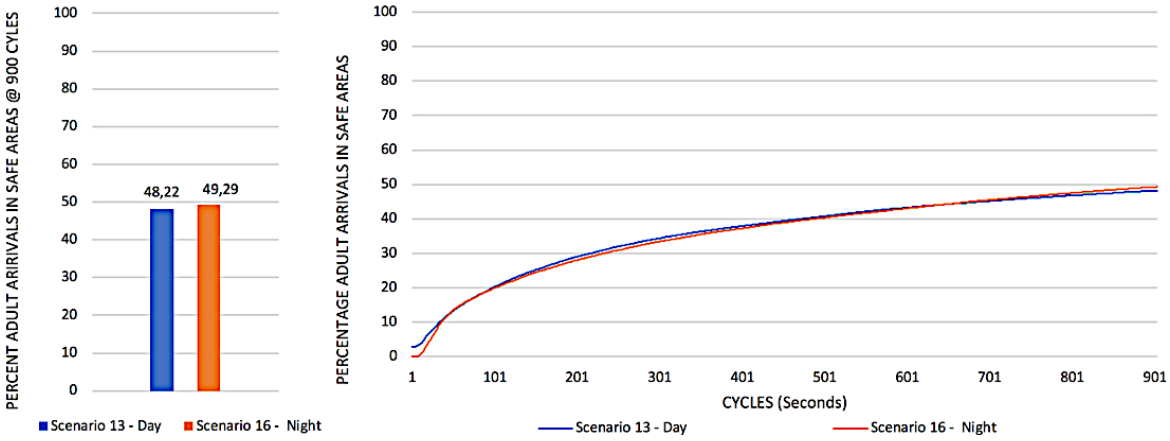

(a) (b)

Figure 87 Effect of the time of day on evacuation, Intensity VI: (a) histogram, (b) timeseries

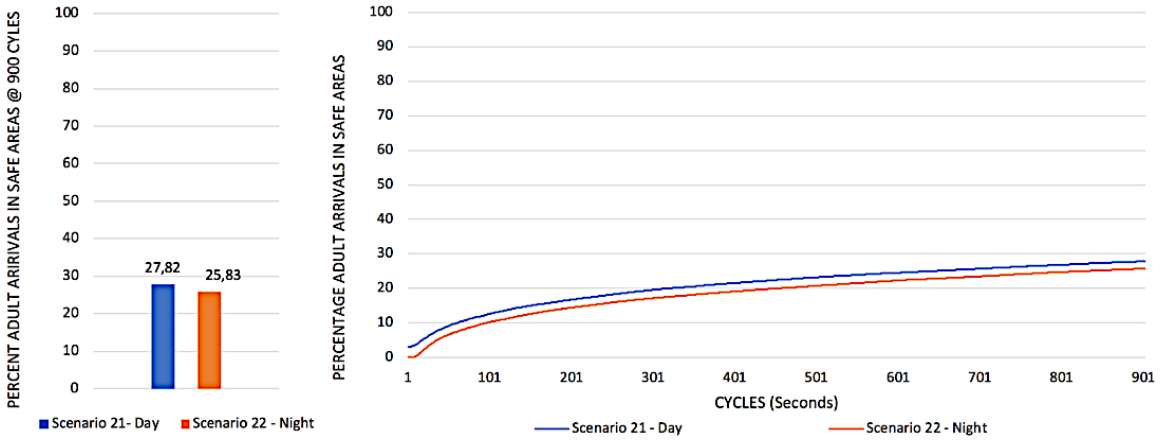

(a) (b)

Figure 88 Effect of the time of day on evacuation,Intensity VIII: (a) histogram, (b) timeseries;

Table 65 shows the summary of the results of the difference in percentage arrivals with respect to the time of day. Figure 89 shows the x-y plot of this summary.

Table 65 Difference in percentage arrivals with respect to time of day at the 900th cycle

Intensity	Day	Night	Difference (Night – Day)
Intensity IV	63.02	68.71	5.69
Intensity VI	48.22	49.29	1.07
Intensity VIII	27.82	25.83	- 1.99

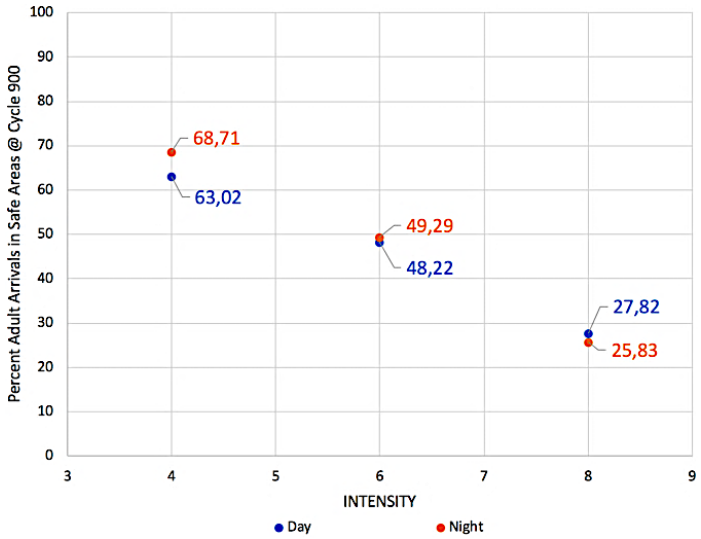

Figure 89 Comparison of day vs night time evacuation arrivals with respect to intensity at the 900th cycle

This has been presented to be true for day and night conditions and for all intensities considered. The observed large difference in the Night condition than the Day condition however comes as a pleasant surprise and is seemingly counter intuitive. It is counter intuitive in the sense that perception distances for attachment figures are much shorter during night than day conditions. One would expect the day condition to have more arrivals in safe areas. However, as previously mentioned, this is surprisingly not the case with social attachment. This result actually highlights the role of social attachment in evacuations.

The significance of social attachment particularly for the night condition may be explained in particular by perception distance propagation or indirect perception. Even with shorter perception distances, individuals are effectively able to perceive goals such as safe areas through others. Perception distance propagation however is not enough to explain the dominance of social attachment. For social attachment to be applied, attachment figures need to be within perception range. In this context, location plays a very significant role. For night conditions individuals are co-located at home with family members who they share very strong social bonds. In this situation the influence of social attachment is effectively optimal. Evacuation is done as a family group. Leading evacuating family members provide a very strong pull, guiding other member in the direction of safe areas. In addition, homes may likewise be located in places close to safe areas.

Night time conditions with attachment facilitates the formation of groups with members that are initially co-located or close together. The short perception distance for attachment figures during night time ensures this situation. Only attachment figures that are close are perceived by individuals. Other attachment figures outside this short perception distance range are effectively filtered out. The short perception distances during night time and strong bonds between members would ensure the creation of more compact cohesive groups. These factors present during night time conditions could explain the large number of arrivals in safe areas.

For the day condition with attachment, individuals may be co-located with non-family members for whom the strength of social bonds vary. Individuals are present in different types of locations, e.g. home, school, work, public places and outdoors, based on their daytime activity. This can result in to the formation of different groups based on social bonds that are weaker than family bonds. Individuals may eventually shift to groups with whom individuals they share stronger bonds. This is especially true when groups are headed in different directions. This shifting of perception may impact the number arrivals in safe zones.

From the results in these set of experiments, it can be concluded that the time of day affects the evacuation arrivals in safe areas. Consistent with the results from Question 1, the combination of night time, with-attachment and low intensity conditions produce the more arrivals in safe areas, than the daytime condition. This result also further validates and strengthens the finding that social attachment facilitates more arrivals in safe areas.

The contribution of the results from Question 4 are the findings that (1) the arrivals for night time, while much lesser than daytime at the start of the simulation, become much greater than daytime arrivals at later cycles; (2) The difference between night time and daytime arrivals become much lesser with increasing intensities. (3) For increasing intensities, the cycle where night time arrivals become much greater than daytime is shifter to a much later time; and (4) for the highest intensity considered, the daytime scenario is able to maintain its initial lead and is able to maintain slightly more arrivals than night conditions. This can be seen from the time series chart in Figure 88-b, where the day and night plots are almost parallel.

The discussion on the benefits of social attachment for night-time evacuations have been elaborately discussed in Question 1. Question 4 adds the insight that (1) time of day with social attachment is significant for low intensities. (2) At slightly higher intensities, the effect of time of day is diminished such that the difference is very small. (3) At very high intensities the effect of time of day with attachment is cancelled out. This can be seen from similar trend in the day and night plots in Figure 88-b. This can be interpreted as almost similar rates of arrivals in safe areas. The daytime arrivals are only greater because of the individuals already located in safe areas at the start of the simulation.

8.3.5 Question 5: How does disability affect the number of arrivals in safe areas?

Figure 90 shows the results of the scenario were disabled individuals are included in the evacuation scenario with attachment. The without attachment scenario is shown in Figure 91. From the histograms both of Figure 90-a and Figure 91-a, it can be seen that the number of arrivals for the case with no disabled is slightly greater than that with disabled at the 900th cycle. The small differences for the percentage arrivals are detailed in Table 66. For the with attachment scenario the difference is 0.68%. For the no attachment scenario, the difference is 0.45%. Comparing between with attachment and no attachment, the difference is for no disabled at 3.49%, which is slightly larger than for with disabled at 3.26%. The time series charts in Figure 90-b and Figure 91-b show almost similar plots with the with the population without disabled generally having slightly more arrivals.

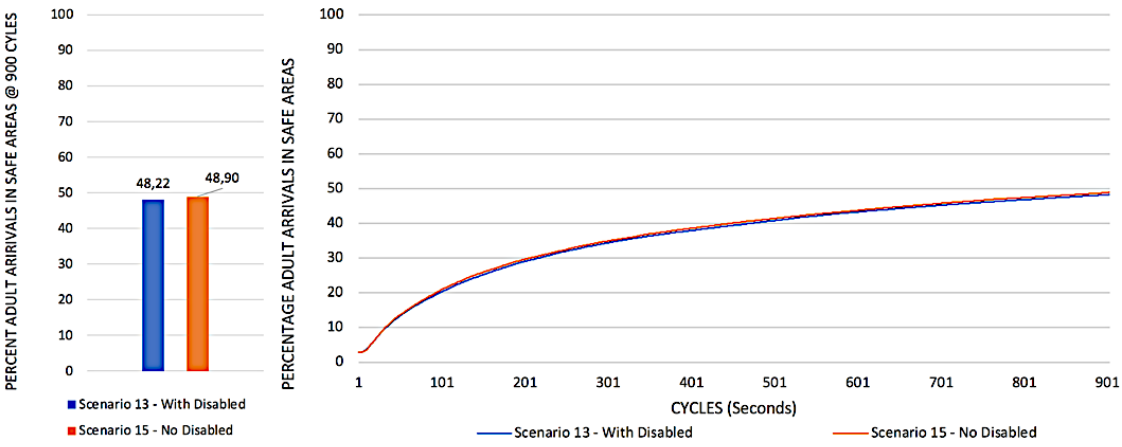

(a) (b)

Figure 90 Effect of the presence of disabled, Intensity VI – With Attachment: (a) histogram, (b) timeseries;

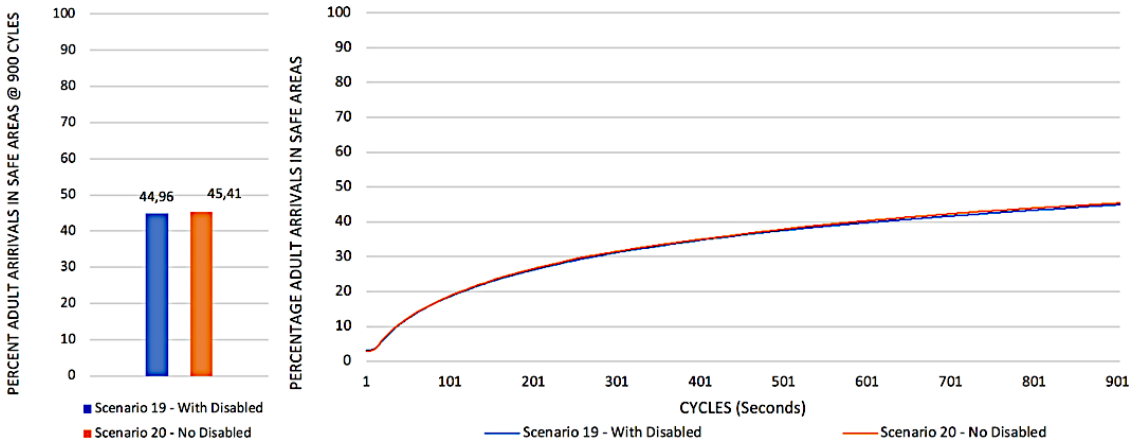

(a) (b)

Figure 91 Effect of the presence of disabled, Intensity VI – No Attachment: (a) histogram, (b) timeseries

Table 66 Difference in percentage arrivals with respect to presence of disabled at the 900th cycle

Scenario	With Disabled %	No Disabled %	Difference (No Disabled – With Disabled) %
With attachment	48.22	48.90	0.68
No Attachment	44.96	45.41	0.45
Difference (With Attachment – No Attachment)	3.26	3.49	0.23

From the results it can be concluded that the presence of disabled in the evacuating population has a slight effect on evacuation arrivals in safe areas. This confirms the hypothesis that arrivals are lesser when disability is present in the population. The small difference in the results for the scenarios can be mainly due to the small number of disabled individuals in the population. Another reason can be that the daytime condition at Intensity VI, considered for the experiments, already yield relatively low arrivals in safe areas. The differences may be larger if (1) there are more disabled in the population; (2) night conditions; and (3) low Intensity IV.

To briefly conclude and answer Question 4, the presence of disabled in the population affects the total number in safe areas. The situation where there are no disabled results to more arrivals than populations with disabled.

8.3.6 Question 6: Does the presence of casualties on the route affect the number and time of arrivals in safe areas?

Figure 92-a shows the number of active individuals[28] with respect to the number of deaths and injuries shown in Figure 92-b and Figure 92-c respectively. It can be seen that the low intensity earthquakes produced very few casualties, ranging from 0 to 5 percent. However, the higher Intensity VIII earthquakes resulted to a large percentage of deaths reaching 39.38%, and many injuries at 21.68 %.

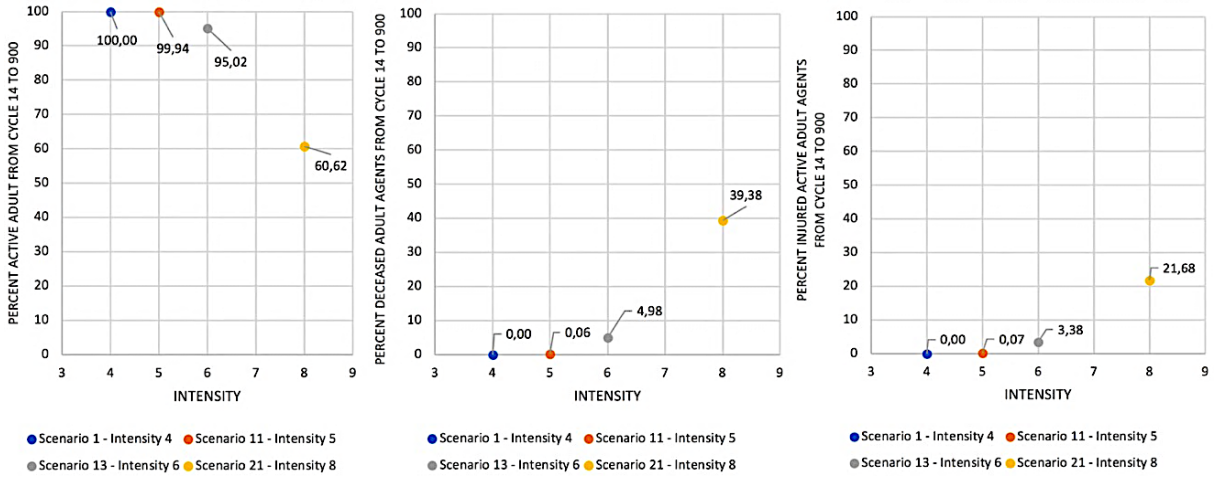

(a) (b) (c)

Figure 92 Casualties on the route, (a) active agents, (b) deceased, and (c) active injured adult agents

Figure 93 focuses on active agents and casualties for the large Intensity VIII day and night conditions. Figure 93-a shows the number of active agents at 60.62% for the day and 58.12% for the night condition. From Figure 93-b and Figure 93-c, it can be seen that the numbers of casualties are high. For the deceased, there are 39.38% and 41.88 percent for day and night respectively. For the injured, there are 21.68% and 23.13% for day and night respectively. Also, it is noticeable that there are more casualties for the night time than the daytime scenario. The difference however is very small. The difference in the deceased and injured for night and day are 2.5 % and 1.45 % respectively.

[28] Active individuals can move around and interact. Injured agents are active agents. Deceased individuals are immobile and cannot interact.

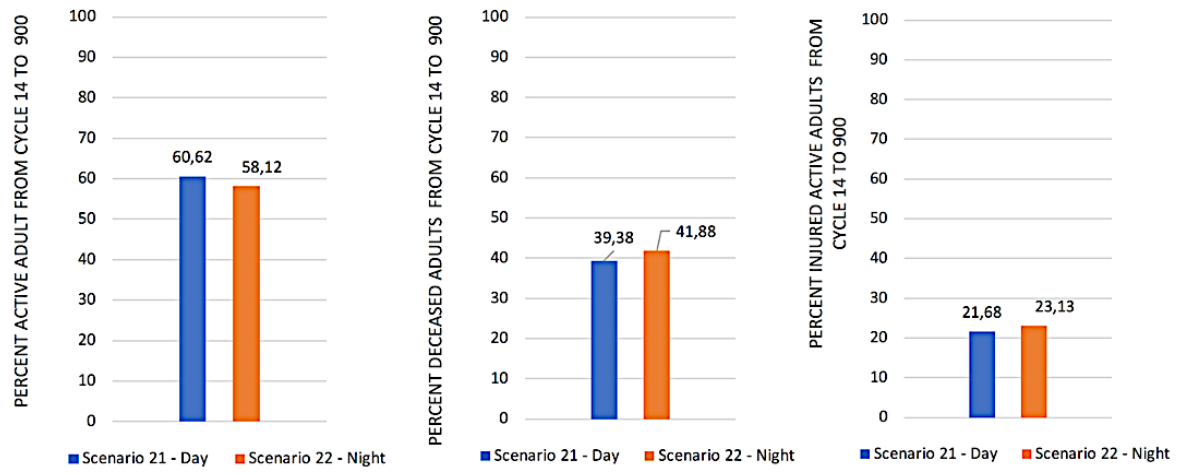

(a) (b) (c)

Figure 93 Casualties on the route, Intensity VIII, (a) number of active, (b) deceased, and (c) injured

The interactions with casualties are shown in Figure 94 and Figure 95. Figure 94 shows the number of adult agents interacting with deceased adults. Figure 95 shows adult agent interactions with injured adults. It can be seen that more interactions are generated for the high Intensity VIII than for the other intensities. Intensity VIII the generated interactions at the 900th cycle with deceased at 54.80% (Figure 94-a) and with injured at 54.05% (Figure 95-a). Intensity VI generated lesser interaction with deceased at 27.12 % (Figure 94-a) and with injured at 31.94% (Figure 95-a). Intensity V generated far lesser interaction with the deceased at 0.65% (Figure 94-a) and 2.13% with the injured (Figure 95-a). Intensity IV generated no interactions as there are no casualties.

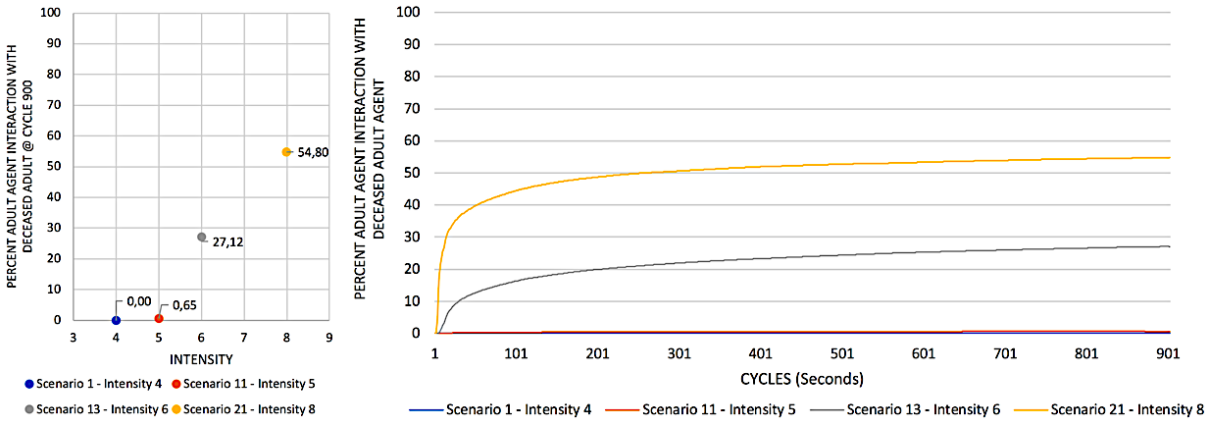

(a) (b)

Figure 94 Adult agents interacting with deceased adult agents along the route (a) histogram, (b) time series

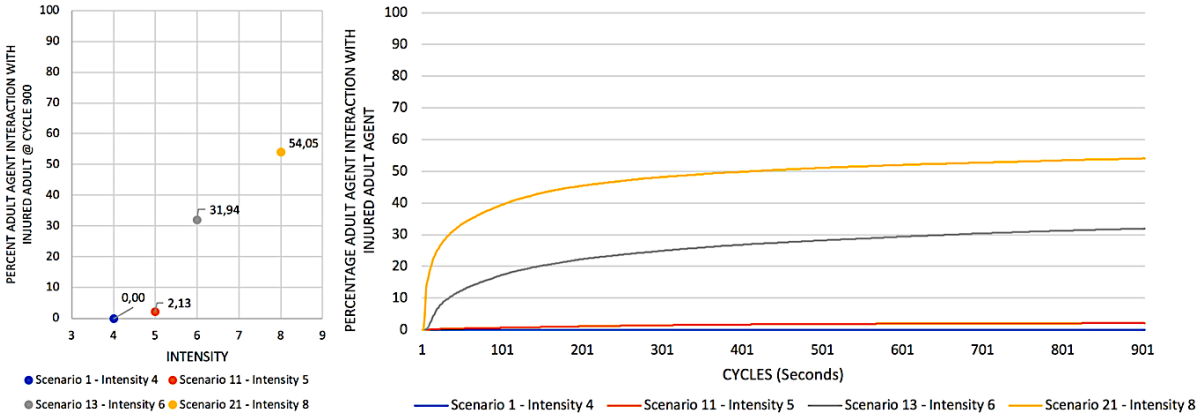

(a) (b)

Figure 95 Adult agents interacting with injured adult agents along the route (a) histogram, (b) time series

The time series plot of the social interactions with the deceased and injured are shown in Figure 94-b and Figure 95-b respectively. It can be seen that the interactions with casualties for the Intensity VIII scenario is consistently the largest compared with all the lower intensities from the 1st to the 900th cycle. Intensity VIII started the sharp increase in interactions during the very first cycles. This coincides with the period just after the earthquake where debris is produces causing casualties. The plot for Intensity V is less steep in the initial cycles and exhibits a gradual increase. Although it is consistently much less than for Intensity VIII, the trend of the plot seems parallel to Intensity VIII, especially from approximately the 150th cycle. Similar to that of Intensity VIII, from the 150th cycle the increase is gradual producing a not so steep slope in the graph. From Figure 94-b, the plots for Intensity V show almost a very flat graph due to the very-low values (less than 1%) for interactions with deceased agents. However, from Figure 95-b the interaction with injured individuals, although very small (less than 2.13%), shows a more defined gradually increasing graph. The plot for Intensity IV is flat at zero arrivals (as shown by the blue line) since there are no casualties.

The large number of interactions with casualties can be seen as direct indicators of the large damage in individuals' immediate surroundings. Gradual increase in the values, as seen in the timeseries plots, can indicate casualties being discovered on the route to safe areas. Injured individuals are able to move about and have higher probabilities of being encountered by other individuals. Multiple encounters with casualties are also possible especially when agents are trapped with the casualties in the same location.

Figure 96 shows the arrivals in safe areas with respect to intensities 4, 5, 6 and 8 respectively. At the 900th cycle, as shown from Figure 96-a, the arrivals are 63.02%, 63.18%, 48.22%, and 27.82% respectively. It can be seen that there are more arrivals for low intensities than higher intensities. In the timeseries plot shown in Figure 96-b, it can be seen that the plots for Intensity IV and 5 seem almost similar and have consistently the largest, gradually increasing values from the 1st to the 900th cycle. The lesser in arrivals is from Intensity VI, followed by the lowest arrivals from Intensity VIII. The order of the graphs for arrivals in safe areas are reversed compared to that of the graphs for interactions with casualties (Figure 94 and Figure 95).

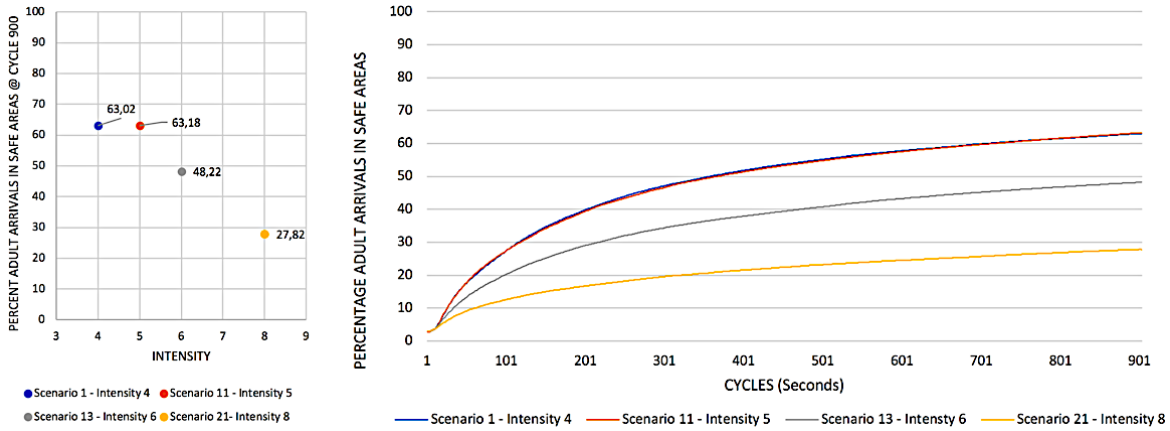

(a) (b)

Figure 96 Percent arrivals in safe areas – With Attachment, Day (a) histogram, (b) timeseries

Table 67 provides the summary comparing evacuation arrivals with respect to presence of casualties. It shows the intensity, number of active individuals, casualties, interaction with casualties, arrivals and non-arrivals in safe areas, and difference between the no-arrivals and number of deceased (NA-D).

Table 67 Percentage arrivals and interaction with casualties at the 900th cycle, Day, With Attachment

		Casualties		Interaction with Casualties		at theSafe Area		Differenc e
Intensity	**Active**	**Deceased**	**Injured**	**Deceased**	**Injured**	**Arrivals**	**Non-Arrivals (NA)**	**NA-D**
IV	100.00	0.00	0.00	0.00	0.00	63.02	36.98	36.98
V	99.94	0.06	0.07	0.65	2.13	63.18	36.82	36.76
VI	95.02	4.98	3.38	27.12	31.94	48.22	51.78	46.80
VIII	60.62	39.38	21.68	54.80	54.05	27.82	72.18	32.80

From the results presented in the section, it can be seen that the presence of casualties in the routes directly result in low arrivals in safe areas. A large number of deceased automatically lowers the number of survivors who can evacuate. For example, from Table 67, the number of active agents is significantly reduced with increasing intensity. That is, all agents are active (100%) for Intensity IV; 99.94% for Intensity V; 95.02% for Intensity VI; and lowest for Intensity VIII at 60.62%. However not many active agents are able to arrive in safe area at the 900th cycle. The arrivals are 63.02%, 63.18%, 48.22% and 27.82 percent for intensities IV, V, VI and VIII respectively. The non-arrivals are 0%, 0,06%, 4.49% and 39.38 percent intensities IV, V, VI and VIII respectively. The pie-charts showing these results are shown in Figure 97.

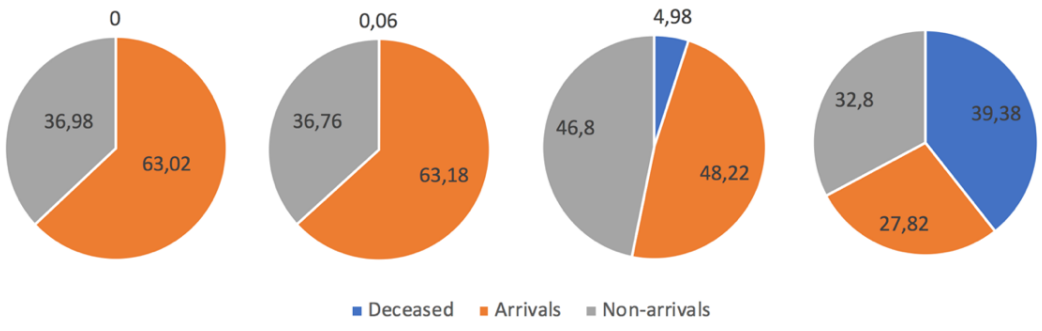

(a) Int IV (b) Int V (c) Int VI (d) Int VIII

Figure 97 Percent arrivals and non-arrivals in safe areas – With Attachment, Day (a) Intensity IV, (b) Intensity V, (c) Intensity VI, (d) Intensity VII

Structural collapse can produce many deaths and injuries especially when people are directly exposed to damage. The number of deaths shown in Figure 97 is high at 39%, especially for the Intensity VIII Scenario. This was calculated with the maximum 50 % probability of dying or getting injured when hit by debris. The 50% is similar to the death and injury percentages (shown in Table 68) used in the calculation of Coburn et al's lethality ratio[29] (Coburn_1, Spence, & Pomonis, 1992; Coburn & Spence, 2002). Estimating casualties with models for earthquakes is a difficult task and has been the subject of many studies which are use either empirical, hybrid and analytical methods (Jaiswal_2, Wald, & Hearne, 2009). The USGS uses the PAGER platform in issuing fatality estimates. Alexander investigates the 1:3 ratio of deaths to injuries during earthquakes in (Alexander_2, 1985). Current casualty models used in post-earthquake event estimations involve high degrees of uncertainty and has yet to produce a very accurate results in predicting casualties (mortality and morbidity) and is an active domain needing more research (Alexander & Magni, 2013; Spence & So, 2011).

Table 68 Estimated injury distributions at building collapse, % of trapped occupants (Coburn_1, Spence, & Pomonis, 1992; Coburn & Spence, 2002)

Triage injury category	Masonry	Reinforced concrete (RC)
Dead or unsaveable	20	40
Life threatening cases needing immediate medical attention	30	10
Injury requiring hospital treatment	30	40
Light injury not necessitating hospitalization	20	10

The effect of social attachment can be subtle and difficult to quantify. The results for the Intensity IV, daytime scenario can be considered as a baseline condition. That is, it is not influenced by additional debris which can act as barriers and no casualties. The normal trend is that Intensity IV provides the largest number of arrivals and arrivals decrease with increasing intensity. The arrivals however from Intensity V (63.18%) is slightly larger than from Intensity IV (63.02%). Also, the trend in the time series plot in Figure 8.20-b show arrivals in Intensity V becoming larger than Intensity IV. It is a curious case which may imply that social attachment, triggered while encountering casualties, may have some beneficial effects, however small, in promoting the evacuation of other individuals.

To briefly summarise and answer the question, the high number of casualties in the route contributes to the low number of arrivals in safe areas especially for high intensities. High damage in the environment is equivalent to high exposure causing the casualties. Presence of the damage likewise limits mobility of individuals and can concentrate interactions in confined locations. Increased probability of interactions among attachment figures or casualties are possible in these situations. However, limitations in mobility does not allow individuals to reach safe areas. In the situation of high intensities resulting to extreme damage and casualties, the benefit of social attachment and interactions is cancelled out and does not result in more arrivals in safe areas during immediate evacuation.

More precision in the model in terms of casualties (population exposure) can be achieved if the following are used in the model: (1) more accurate probabilities for succumbing to injury and death when exposed to debris and damage during building collapse; (2) accurate building occupancy data during different times of the day; (3) precise locations of individuals at different times of the day; (4) updated building data (a) door locations; (b) floor layouts, (c) vulnerability. The benefit of using the model is the ability to explore different scenarios, the results of which can be used for efforts related to preparedness. In the simulation runs, exposure to debris hazard is the prime determinant of injury or death. This exposure is determined by the location of agents. This location is also defined by daily mobility.

[29] *Lethality ratio* is the ratio of the number of people killed to the number of occupants present in collapsed buildings of a particular building class (e.g. masonry or reinforced concrete (RC)) (Coburn_1, Spence, & Pomonis, 1992; Coburn & Spence, 2002). Fatality rate is a similar term used in PAGER (So & Pomonis, 2012).

8.3.7 Question 7: Does intensity affect the number of arrivals in safe areas?

In the previous section discussing Question 6, Figure 97 and Table 67 showed the effect of intensity on evacuation for the 2-IRIS coverage area. From Figure 97, it can be seen that the number of arrivals in safe areas decrease with increasing intensity. The low Intensity IV and V conditions have larger number of arrivals compared to intensities VI and VI. This is mainly due to the very few casualties resulting from debris damage. Large numbers of debris likewise are barriers that can completely block passageways hindering movement towards safe areas.

Figure 98 shows the average count of debris created at different intensities. Debris are generated around vulnerable buildings at every cycle for the duration of the shaking. From Figure 98 it can be seen that Intensity VIII resulted in the largest value in the number of generated debris with 3976 debris blocks. Intensity VI comes second with 995 debris blocks, then Intensity V with 14 debris blocks, and lastly Intensity IV with no debris.

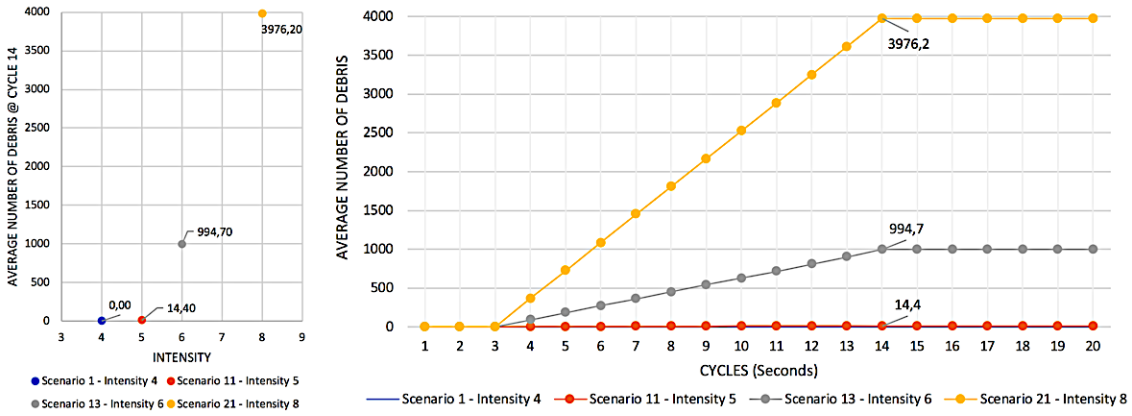

(a) (b)

Figure 98 Number of Debris and Intensity –(a) histogram at 14th Cycle, (b) timeseries 0 to 20th Cycle

The dimensions of the debris created during the experiments are different for each intensity. The difference in dimension result in different footprints when created around vulnerable buildings in danger zones. Larger debris footprints are more dangerous since these increase the probability of hitting an individual. Debris when created during the duration of the earthquake can pile up or overlap in danger zones. Debris with larger footprints can fill pathways more easily effectively blocking evacuation routes. The types of debris and those produced in the experiments are shown in Table 69. The dimension of debris for different intensities are 1 x 1 meter for Intensity V; 2 x 2 meters for Intensity VI; and 4 x 4 meters for Intensity VIII. From the experiments, the total effective amount of debris, in square meters, are 14.4 for Intensity V; 3978.8 for Intensity VI; and 63619.2 for Intensity VIII.

Table 69 Debris production with respect to intensities

Intensity	Debris Type	Size (meter)	Footprint (sq.m.)	Number Debris	Total debris (sq.m.)	Deaths (%)	Injuries (%)	Arrivals (%)
Intensity IV	-	-	-	0	0	0	0	63.02
Intensity V	Small	1 x 1	1	14	14	0.06	0.07	63.18
Intensity VI	Medium	2 x 2	4	994	3978	4.98	3.38	48.22
Intensity VII	Large	3 x 3	9	-	-	-	-	-
Intensity VIII	Huge	4 x 4	16	3976	63619	39.38	21.68	27.82

The large difference in arrivals in safe areas between high intensity and lower intensity events can be explained by the impact of the debris. Debris generates casualties and defines physical limits to the mobility of individuals moving towards safe areas. This is demonstrated by the number or deceased from Intensity VIII is the largest at 39.38% deceased and 21.68% injured. The total casualties (i.e.

deceased + injured) therefore would be 61,06% of the population. Arrivals in safe areas are likewise very low at 27.82%. The active uninjured population accounts for just 33.24%.

Debris hinder swift evacuation when it blocks shortest paths towards safe areas. Consider for example the damage during the August 24, 2016 Amatrice, Italy earthquake shown in Figure 99 and Figure 100. The earthquake occurred with a magnitude of 6.0 and an estimated maximum EMS[30] intensity of X (Quest, et al., 2016). In the areas that suffered the most damage, debris from collapsed building walls deposited into adjacent pathways. Trapped individuals needed to be rescued from collapsed structures.

Figure 99 Debris damage during the August 24, 2016 Amatrice, Italy earthquake (Mag. 6, Int X) (Legi il Firenzepost, 2016; Quest, et al., 2016)

Figure 100 Damage during the August 24, 2016 Amatrice, Italy earthquake (Mag. 6, Int X) (Mesa, 2016; Quest, et al., 2016)

Table 70 and Table 71 show the level of building damage for the intensity scenarios with respect to the different coverage areas (2-IRIS, 9-IRIS, and 69-IRIS). The values in Table 70 are raw counts while that in Table 71 are in percentages. The levels of damage are in increasing order from 1 to 5. For the more detailed discussion on building damage grades, please refer to Table 7. From the values in Table 70 and Table 71, it can be seen that the number/percentage of buildings with different levels of damage increases with intensity. Large numbers of damaged buildings are expected to produce more debris, especially for the buildings with level 5 damage. The experiment conducted was for the IRIS-2 coverage

[30] EMS Intensity – European Microseismic Scale Intensity

and it produced a significant number of debris as shown in Table 69. Running the experiments for the IRIS-9 and IRIS-69 can simulate this damage scenario.

Table 70 Number of buildings with different levels of damage for each intensity scenario (Probabilistic)

	2-IRIS					9-IRIS					69-IRIS				
Int	**1**	**2**	**3**	**4**	**5**	**1**	**2**	**3**	**4**	**5**	**1**	**2**	**3**	**4**	**5**
IV	0	0	0	0	0	0	0	0	0	0	0	0	0	0	0
V	11	0	0	0	0	41	0	0	0	0	323	0	0	0	0
VI	24	73	0	0	0	73	282	0	0	0	471	2074	0	0	0
VII	67	32	10	140	0	230	118	25	453	0	1406	839	173	3253	0
VIII	97	94	36	9	150	373	316	172	32	592	2483	2213	1271	291	5330

Table 71 Percentage of buildings with different levels of damage for each intensity scenario (Probabilistic)

	2-IRIS					9-IRIS					69-IRIS				
Int	**1**	**2**	**3**	**4**	**5**	**1**	**2**	**3**	**4**	**5**	**1**	**2**	**3**	**4**	**5**
IV	0	0	0	0	0	0	0	0	0	0	0	0	0	0	0
V	2.8	0	0	0	0	2.8	0	0	0	0	2.8	0	0	0	0
VI	6.2	18.9	0	0	0	4.9	19.0	0	0	0	4.1	17.9	0	0	0
VII	17.4	8.3	2.6	36.3	0	15.5	7.9	1.7	30.5	0.0	12.1	7.2	1.5	28.1	0
VIII	25.1	24.4	9.3	2.3	38.9	25.1	21.3	11.6	2.2	39.9	21.4	19.1	11.0	2.5	46.0

The probabilistic distribution of building damage for the aforementioned coverage areas for the intensity VIII scenario are shown in Figure 101, Figure 102 and Figure 103 respectively. From the figures, it can be seen that the distribution of damage is spread out in the coverage areas. The areas with the high concentration of level 5 damage are expected to produce the most casualties. These areas will likewise have many blocked routes hindering the evacuations of individuals to safe areas.

Figure 101 Buildings with damage for Intensity VIII within the 2-IRIS coverage area

Figure 102 Buildings with damage for Intensity VIII within the 9-IRIS coverage area

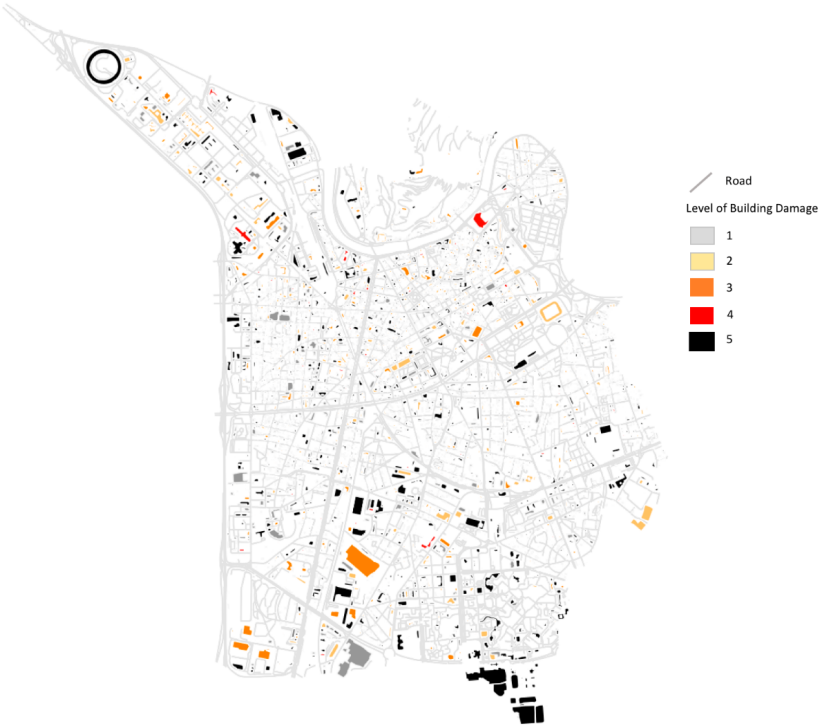

Figure 103 Buildings with damage for Intensity VIII within the 69-IRIS coverage area

To briefly conclude and provide the answer to the question, intensity affects the arrivals in safe areas. Larger intensities would result more damage and eventually to lesser arrivals in safe areas. This is mainly due to increased casualties. Debris likewise hinder physical mobility, trapping individuals who wish to move towards safe areas.

The study of the effects of earthquakes at different intensities are equally important. Extreme or large intensity earthquakes are rare. However, smaller earthquakes intensity quakes are much more common. Cumulative effects of small earthquake events are greater (Gaillard, 2019). This more common occurrence directly implies more people are exposed to its effects. The cumulative effects of earthquakes are also therefore greater across populations at different time scales or generations or histories.

8.3.8 Question 8: How does the radius of the danger zone around buildings affect the number of arrivals in safe areas?

Figure 104 shows the effect on evacuation of a large radius used to delineate the danger zones around buildings. It can be seen that the radius of half the height of the building has fewer and much slower arrivals in safe areas. For the case where a uniform 6-meter radius is adopted to delineate the danger zone, more arrivals are observed.

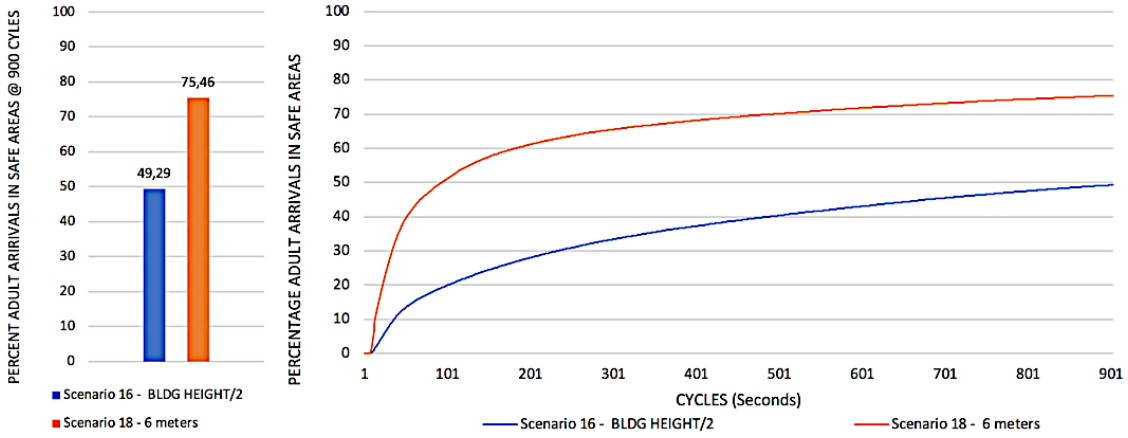

(a) (b)

Figure 104 Effect of radius of the danger zone on evacuation – With Attachment (a) histogram, (b) timeseries

Large danger zones around buildings provide greater area and probability for debris damage to be deposited in large street sections. This also increases the probability for individuals to be trapped, injured or killed by debris. Larger radius for danger zones likewise decreases the effective area allotted for safe zones. Larger danger zone radius likewise increases the evacuation travel distance from buildings to safe zones. Blocked pathways force individuals to find other routes. This can make travel distances much longer. The nearest safe zone from a cluster of vulnerable structures can be very far. Longer distances result in much longer travel times or in this case evacuation time to reach safe zones. Individual evacuations times may exceed the cut-off time of 15 minutes. Arrivals beyond the 15- minute cut-off time is not counted. Larger danger zones therefore have the effect of decreasing the number of arrivals in safe areas.

The amount or area of safe zones and their spatial distribution, defines accessibility and also affect evacuations. Figure 105 shows the spatial distribution available safe areas in the extents for IRIS 2, IRIS 9, and IRIS 69. The radius of the danger zone considered is half the height of buildings.

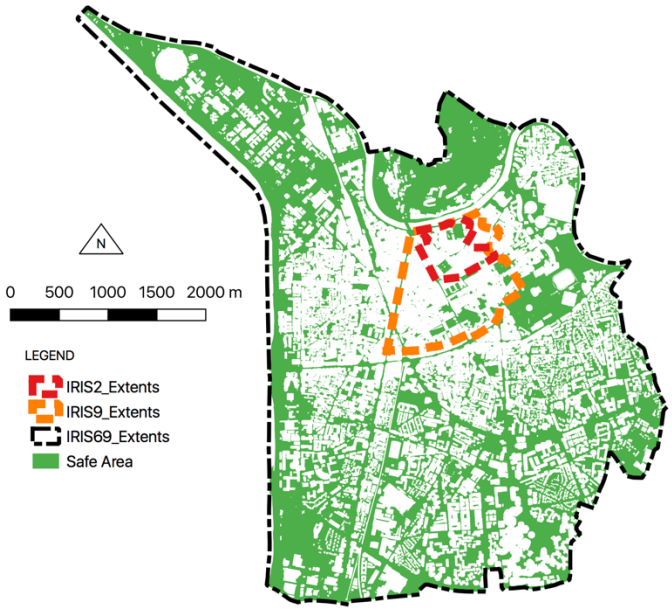

Figure 105 Safe areas with respect to extents (IRIS 2, IRIS 9 and IRIS 69)

Table 72 shows the total areas of safe areas available to agents. The radius of the danger zone considered is half the height of the building. The pie charts in Figure 106 shows the danger zones, safe areas and barriers in the thee IRIS extents. It can be seen that for the amount of safe areas in decreasing order is from IRIS 69, IRIS 9 and IRIS 2 respectively. Also, the ratio of available safe area to danger zones is much greater in IRIS 69, than IRIS 9 and IRIS 2 with values of 2.10, 0.50 and 0.39 respectively. This trend is similar when comparing the ratio of safe areas to barriers. For IRIS 69, there are more safe areas than barriers. This means that there is more probability for agents to find safe areas than encountering barriers. The subsets IRIS 9 and IRIS 2 cover Grenoble's urban core with more buildings or barriers. This is illustrated by the ratio of safe areas to barriers of 0.37 and 0.29 respectively.

Table 72 Available areas for IRIS extents with danger zone at half the height of adjacent buildings

Coverage	Area	Danger Zone (DZ)	Barriers (B)	Safe Area (SA)	DZ %	B%	SA%	TOTAL %	SA/DZ
IRIS 2	283593.37	103436.90	139396.54	40759.93	36.47	49.15	14.37	100.00	0.39
IRIS 9	1271099.83	448314.43	599988.85	222796.55	35.27	47.20	17.53	100.00	0.50
IRIS 69	18190865.09	4019368.72	5711486.26	8460010.11	22.10	31.40	46.51	100.00	2.10

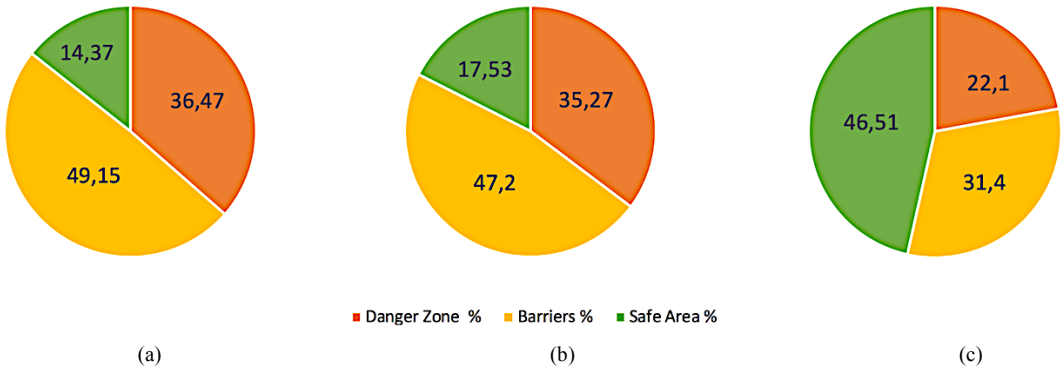

Figure 106 Danger zones, safe areas, and barriers (a) IRIS 2, (b) IRIS 9, (c) IRIS 69

Figure 107 shows the effect of increased coverage from IRIS 2, IRIS 9 and IRIS 69 on evacuation. With the increase in coverage, comes the increase in available safe areas to agents. From Figure 107-a, it can be seen the 69-IRIS coverage area has the most arrivals in safe areas compared to the IRIS-2 and IRIS-9. This can be explained by the fact that there are more safe areas accessible to agents. From Figure 106

it can be seen that the 69-IRIS coverage has 46.51 % of its extents devoted to safe areas. Also, from Figure 106, it can be seen that the area covered by barriers (or buildings) is the smallest at 31.4%. Conversely, this means that agents have more free space for navigation. Agents can likewise move more easily towards safe areas. The danger zone for the 69-IRIS coverage is also the smallest at 22%. This means that this coverage has Accordingly, the arrivals for the 9-IRIS coverage ranks second in the percentage of arrivals as seen from Figure 107. Also, it has 17.53 % of its extents classified as safe areas. The last with respect to the number of arrivals is the 2-IRIS coverage, with the smallest percentage of safe areas in its extent coupled with the largest percentage for barriers at 49.15%. Aside from having fewer safe areas as options for evacuation, many barriers restrict navigation.

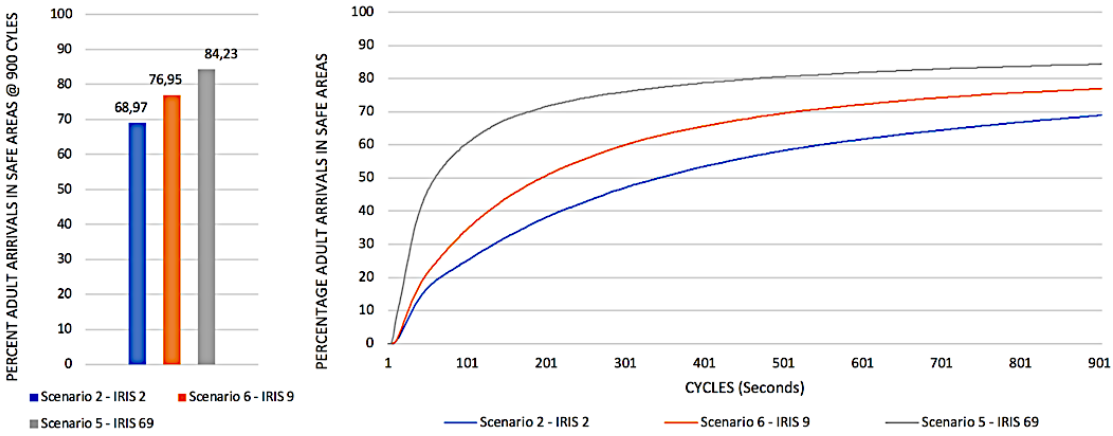

(a) (b)

Figure 107 Effect of increased coverage and availability of safe area (a) histogram, (b) timeseries

To briefly conclude and provide an answer to the research question, the radius used in the delineation of danger zones affects the arrivals in safe areas. A small radius such as 6 meters will lead to more arrivals in safe areas. This is due to the following (1) makes the distance of safe areas shorter to traverse and therefore it is faster to reach, (2) minimises the deposition area of debris, therefore reducing the probability for casualties. When safe areas are readily accessible due to the reduced area of danger zones, the probability of reaching safety is higher. For more clustered urban centres, safe areas are fewer and farther away from buildings or individual source locations. Urban areas with more open spaces will have many safe areas that can be easily reached by individuals during evacuations.

8.4 Summary of the chapter

A summary of the results is shown in Table 73, Figure 108 and Figure 109. In Table 73, the arrivals in safe areas are presented for each scenario. The last two columns present the hypothesis and the conclusion on the verification of the hypothesis respectively.

Table 73 Summary of results

Research Question	Parameter	Scenario	Arrivals in Safe Areas
Q1: Attachment	With Attachment	Int IV-Day	63.02 %
		Int V-Day	63.18 %
		Int VI - Day	48.22 %
		Int VIII – Day	27.82 %
		Int IV-Night	68.97 %
		Int V-Night	-
		Int VI – Night	-
		Int VIII – Night	25.83 %
	No Attachment	Int IV-Day	53.18 %
		Int V-Day	53.64 %
		Int VI - Day	44.96 %
		Int VIII – Day	27.32 %
		Int IV-Night	49.67 %

		Int V-Night	-
		Int VI – Night	-
		Int VIII – Night	22.23 %
Q2: Knowledge	Limited Knowledge - Nearby Safe Area	PD_{SA} = 20 meters	49.67 %
	Limited Knowledge - Nearby Safe Area	PD_{SA} = 50 m	49.47 %
	Broad Knowledge – Nearby Safe Area	PD_{SA} = 10 KM	49.71 %
	Limited Knowledge (Far Safe Area)	PD_{SA} = 20 meters	0%
	Limited Knowledge (Far Safe Area) – 5400 Cycles	PD_{SA} = 10 KM	3 arrivals
	100% of Population with Knowledge (Far Safe Area) – 6000 Cycles	PD_{SA} = 10 KM	82.91 %
	66 % of Population with Broad (Far Safe Area) – 6000 Cycles	PD_{SA} = 10 KM	53.30 %
	0% of Population with Broad knowledge (Far Safe Area) – 6000 Cycles	PD_{SA} = 10 KM	0 %
Q3: Number of Close Bonds	No Bonds		49.67 %
	Few Close Bonds (Many Strangers)		55.83 %
	Many Close Bonds (Few Strangers)		68.97 %
Q4: Time of Day	Day	Int IV-Day	63.02 %
		Int VI – Day	48.22 %
		Int VIII - Day	27.82 %
	Night	Int IV- Night	68.71 %
		Int VI – Night	49.29 %
		Int VIII - Night	25.83 %
Q5: Disability	With Disabled	With Attachment	48.22 %
		No Attachment	44.96 %
	No Disabled	With Attachment	48.90 %
		No Attachment	45.41 %
Q6: Casualties	Few Casualties	Int IV	63.02 %
		Int V	63.18 %
	Many Casualties	Int VI	48.22 %
		Int VIII	27.82 %
Q7: Intensity	Low Intensity (IV, V)	Int IV	63.02 %
		Int V	63.18 %
	Moderate Intensity (VI)	Int VI	48.22 %
	High Intensity (8)	Int VIII	27.82 %
Q8: Radius of Danger Zone	Small Radius	6 meters	75.46 %
	Large/Variable Radius	H/2	49.29 %

From Table 73, it can be seen that with respect to attachment (Question 1), the scenario **with attachment** resulted to more arrivals in safe areas than **no attachment**. With respect to knowledge (Question 2), having knowledge (of safe areas and the shortest paths towards safe areas) results to more arrivals in safe areas, than no-knowledge or limited knowledge. With respect to close bonds (Question 3), having more close bonds during evacuation results to more arrivals in safe areas than having no bonds, or limited bonds.

With respect to time of day (Question 4), night time evacuations resulted to more arrivals in safe areas than during daytime scenarios. This result is actually consistent and directly follows from the results from Question 1 and Question 4. During night time scenarios, individuals are in home locations with family members with whom they share strong attachment bonds.

With respect to the presence of disability in the population (Question 5), the results are not very conclusive as the results are very similar. The arrivals however for with no disabled is just a bit higher. This is maybe due to the considered small population of disabled in the population. Significantly increasing the population of disabled in the simulation may provide clearer results. Also increasing simulation cycles may also show more discernible differences.

With respect to the number of casualties (Question 6), more casualties from high intensity earthquakes, result in fewer arrivals in safe areas than less casualties. With respect to earthquake intensities (Question 7), low intensity earthquakes result in more arrivals than higher intensities result in fewer arrivals in safe areas. With respect to the radius of danger zones from buildings (Question 7), a large radius for danger zones result in lesser arrivals in safe areas than danger zones from smaller radius.

Figure 108 shows a histogram of the percentage arrivals of agents in safe areas the 900th cycle after the start of the earthquake in the simulation. The horizonal axis of the graph shows the respective scenarios (1 to 24); intensity (IV, V, VI and VIII), with attachment (Yes or No); the time (Day or Night); and the standard or default case (Yes or No). Bounding boxes clustering the results into intensities are provided to facilitate easy reading. Lines also divide the sections in the bounding boxes with respect to attachment and time of day. It can be seen from Figure 8.1 that scenarios with attachment have more arrivals than scenarios with no attachment. This is also more noticeable for night time scenarios in low intensity experiments.

The time series graphs for the experiment scenarios are shown in Figure 109. The graphs show the progress of arrivals of adult agents in percentages values at every cycle or second during the evacuation. The total duration recorded is 900 cycles reckoned from the start of the earthquake. The curves are drawn as 4-line types. They correspond to the same grouping of intensities as in

Figure 72. Light solid lines show Intensity IV; dotted lines show Intensity V; darker solid lines show Intensity VI; dashes with dots show Intensity VIII. It can be seen from Figure 8.2 that, increasing intensities lead to lesser and much slower arrivals.

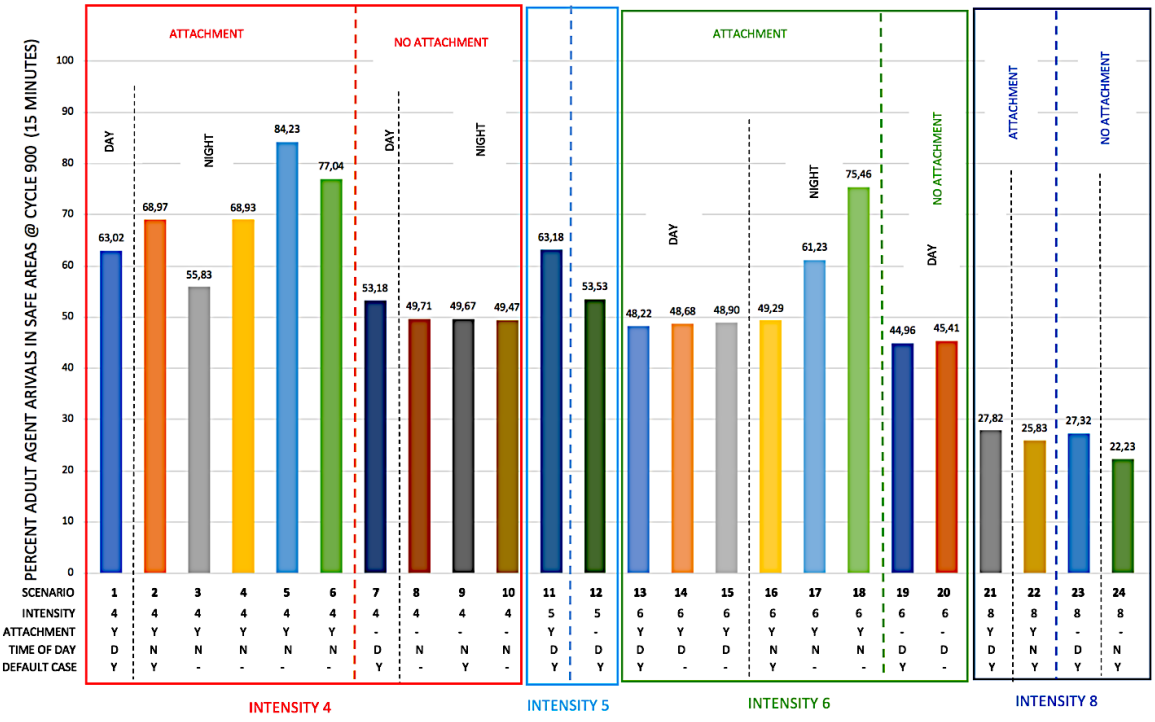

LEGEND: Y = Yes; - = No, D = Day; N = Night

Figure 108 Evacuation arrivals of adults in safe areas at cycle 900 (15 minutes) for all scenarios.

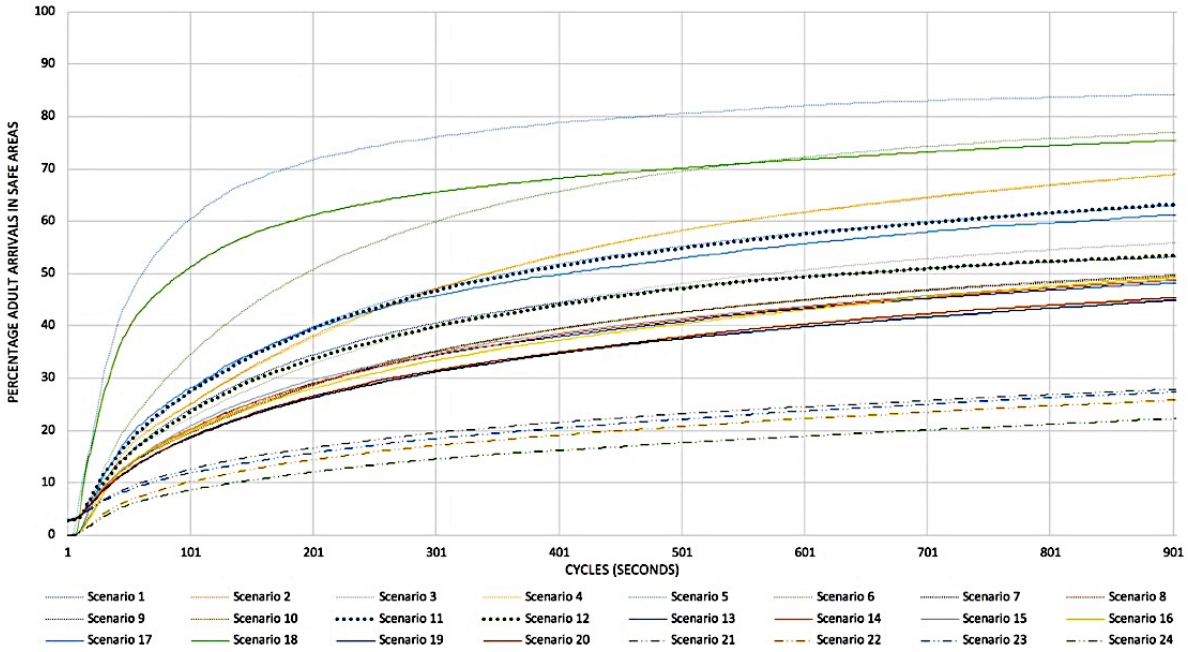

Figure 109 Evacuation arrivals of adults in safe areas at cycle 900 (15 minutes) for all scenarios.

CHAPTER 9. CONCLUSION

9.1 Synthesis and conclusions

This study sought to answer different research questions related to the social aspects of earthquake evacuations. For this purpose, a multi-agent model was conceived and implemented with GAMA. Table 74 details these answers with respect to the hypothesis posited at the start of this work.

Table 74 Summary of answers to research questions

Research Questions	Hypothesis	Hypothesis Confirmed?
Q1: Does social attachment affect the number of arrivals in safe areas?	**YES**. Social attachment can affect the number of arrivals in safe. Lesser arrivals are expected with social attachment.	**YES**, social attachment affects the number of arrivals. **However**, contrary to the hypothesis, there are actually more arrivals in safe areas when social attachment is considered.
Q2: Does having the knowledge of nearby safe areas affect the number arrivals in safe areas?	**YES**, knowledge of the location of nearby safe areas increases the number of arrivals in safe areas.	**YES**. Hypothesis confirmed.
Q3: How does he number of close bonds affect evacuation?	The number of close bonds in the population affect evacuations and can result in lesser number of arrivals in safe areas.	**NO.** There were actually more arrivals in safe areas when there are many closely bonded individuals in the evacuating population.
Q4: How does the time of day affect evacuation?	Daytime evacuation result in more arrivals in safe areas. Night time evacuation, result in fewer arrivals.	**NO**. Actually, there were fewer arrivals in safe areas during daytime. More arrivals in were observed during night time.
Q5: How does disability affect the number of arrivals in safe areas?	Presence of disabled individuals in the population will result in lower number of arrivals in safe areas.	**YES**. Hypothesis confirmed.
Q6: Does the presence of casualties on the route affect the number and time of arrivals in safe areas?	The presence of casualties in the route can trigger evacuations and therefore result in more arrivals in safe areas.	**NO**. Although the presence of casualties can trigger the evacuation of other individuals, this is also an indicator of the extreme vulnerability of the structures in the same location. More casualties are expected and therefore less arrivals in safe areas.
Q7: Does intensity affect the number of arrivals in safe areas?	High intensities will result in lesser number of arrivals in safe areas.	**YES.** Higher intensities result in greater building damage. This can result in injuries, deaths and the trapping of survivors through blocked pathways. This effectively lessens arrivals in safe areas.
Q8: How does the radius of danger zones around buildings (and consequently the size of safe areas) affect the number of arrivals?	Large radius of danger zones around buildings (and consequently fewer safe areas) decreases the number of arrivals in safe areas.	**YES.** Large danger zones result in lesser number of arrivals in safe areas especially for higher intensities.

Evacuation is a complex dynamic process and many elements need to be modelled for it to be realistic, believable and useful for scientific research and policy[31] development. At the very core of this research are people. With human beings as the primary concern, it is necessary to know the reasons and motivations behind people's behaviours during evacuations. A good understanding of these underlying motivations gives the strong foundation for modelling and implementing the behaviours observed from disasters videos, and those gathered from literature.

Social dynamics influence evacuations. This is supported by the findings of this research (in Section 8.3.1) that shows how social attachment plays a beneficial role in evacuations. Specifically, more people can arrive in safe areas when social attachment is present and it facilitates social interaction during evacuation. Social attachment defines core motivations for individual micro-actions or behaviours (Mawson_a, 2005). Social attachment bonds provide the basic ingredient necessary for group formation. The emergence of social groups is the result of proximity seeking behaviours activated during threat.

The results of this research also showed that knowledge of the location of safe areas is important for successful evacuations. Knowledge enables reaching safe areas using shortest pathways (by avoiding blocked roads). What has not been implemented is the direct sharing of knowledge during social

[31] Policies related to disaster risk reduction, response, preparedness, mitigation, and management

interactions. This could be approached by building on the results of the social attachment and knowledge experiments. When social interaction includes the transfer of knowledge, by way of communication, the location of safe areas can spread in the population therefore effectively increasing the arrivals in safe areas. When individuals decide to keep the information to themselves (or not share with others), or avoid social interactions, the percentage of knowledge of safe areas will not change. When this happens as in the results from Section 8.3.2.3, one can expect a fewer number of arrivals in safe areas.

Information on safe areas and shortest pathways can still be acquired by individuals through evacuation maps, signals/arrows or directional sensors installed in strategic locations in cities. Acquiring knowledge in this manner has not been implemented, but as in the case above, it could be considered. As in the spread of knowledge by social interaction above, humans with knowledge who share information are akin to information kiosks, however they are mobile. In improving the simulation, in-place or static sources of information can be added, in such a way that when agents approach this information source, knowledge about the shortest path to the nearest safe area is acquired, and the agent proceeds to evacuate accordingly using this knowledge. Evacuation information and knowledge systems for smart cities of the future for example may integrate this strategy. Such systems can provide accurate real time information especially on the status of damage on evacuation pathways thus aiding evacuation. This point further stresses the important role of information in evacuations. Moving further, agents acquiring this information, can share these with others. In this manner, the knowledge is spread, and eventually this increases the chance that other evacuees can reach safe areas.

Having more social bonds facilitates evacuations. That is, the more social bonds the individual have, the possibility in reaching safety is increased. Knowledge of where to go of course is needed for successful evacuations. This was shown in Section 8.3.3. This result is consistent with the results from Section 8.3.1, and therefore further strengthens the role of social attachment in evacuations. This means that when social bonds are present, even at strengths that are weaker than core family bonds, it is enough to influence how individuals evacuate, and eventually ensure arrivals in safe areas.

The influence of human factors that limit mobility, or the distance with which others can be perceived, were also tested in two sets of experiments. Day and night time evacuation scenarios were used to test the effect of visual perception distance (in Section 8.3.4). The night scenario was found to result in more arrivals in safe areas than daytime. This is contrary to the expected result that daytime arrivals were supposed to have more arrivals due to the longer perception distances available to agents. The advantage offered by night scenarios is that during night time agents are mostly at home with close proximity of their family. This cancels out the advantage of longer perception distances. That is, they can see their family members. The close proximity and preferential attachment to be close to agents with stronger bonds (in this case), facilitates group formation[32], and evacuation as groups. This leads to more individuals reaching safe areas. During daytime scenarios, agents are more distributed (or scattered) in different locations. In these locations, the strength of social bonds can vary and can also be weak. Therefore the formation of groups can be more difficult. The results of these experiments, although originally focused on visual perception distance, further strengthen the role of social interactions in facilitating evacuations. It could be interesting to explore the scenario where agents are at home locations with family members during daytime (such as on a weekend, or a holiday), in order to see if a greater number of agents arrival in safe areas when compared to the night time scenario results. This can be further explored in future experiments with the model.

The impact of the presence of disability (i.e. with mobility impairments) on evacuation population was explored in Section 8.3.5. The result did not show a significant difference in the number of arrivals for between the population of disabled or non-disabled agents. This can be due to the short 15 minute

[32] Note that the groups formed in the simulation are composed of loosely coupled individuals. That is, agents are not locked to a group or to an individual. Agents can move in and out of groups, depending on who and what they perceive. Agents implement multi-modal behaviour and can move in different directions.

duration considered for the evacuation. The results however showed that a slightly higher number of arrivals in the population without disabled agents (Figure 90 and Figure 91). In reality, disability is disadvantageous to mobility. Increasing the simulation time could establish if this is the case. Real populations include individuals with disability and this should be included in simulations to make results more realistic. In order to make evacuations plans to be more inclusive, they should be based on studies that include disability.

Large intensity earthquakes cause considerable damage to structures that result in many injuries and deaths. The influence of different intensities resulting to casualties (injuries and deaths) was presented in Section 8.3.6. Increasing intensities result in an increasing number of deaths and casualties and fewer arrivals in safe areas. The other cause is the presence of debris that blocks pathways that trap survivors. The production of debris at different intensities is presented in Section 8.3.7. More debris are generated with increasing intensities.

The results of the impact of large danger zones around buildings are presented in Section 8.3.8. From the results, it can be seen that large danger zones result in fewer arrivals in safe areas. Danger zones around buildings define the regions where debris damage have the highest probability of impact (by falling and deposition). Areas outside of danger zones are safe from debris, and are safe areas[33]. Falling debris puts evacuating populations at risk of injury or death especially when these zones are traversed. When people egress from buildings or pass along roadways bounded by structures, they expose themselves to the risk of falling debris. The size of danger zones around structures are physically defined by their dimensions (i.e. height and width). Tall structures effectively have large danger zones. When structures are not vulnerable (safe) to earthquakes, no damage or debris are expected to fall within its danger zone. However, when a structure is vulnerable, debris are expected to fall in their respective danger zones. Larger intensities, as described Section 8.3.7 produce more debris in the respective danger zones.

Built-up urban environments are heterogeneous and are a mix of different structures with different vulnerabilities. The danger zones of these non-vulnerable and vulnerable building can overlap and debris from vulnerable structures can affect non-vulnerable ones. When individuals from safe structures decide to evacuate, they become exposed to the damage from the adjacent vulnerable buildings. These observations further strengthen the importance of implementing strict policies for seismic building/structural codes. These policies, when properly implemented can help ensure that structures can survive earthquakes and result in minimal or no damage. When all structures are equally "built to code"[34] this can significantly reduce the risk to people during earthquakes.

To conclude, overall, the results of the experiments point to the importance of social interactions during evacuations. The behaviours of individuals are significantly affected by their social environment that responds to the challenges imposed by the physical environment produced by earthquake disasters. The capacity and tendency for social interaction are inherent in humans and need to be considered in evacuations. It was shown that social attachment is important because it can facilitate saving more lives during earthquake disasters.

9.2 Contributions

The first and main contribution of the research is to add to arguments stressing the importance of human behaviour and the social dynamics that emerge during crisis evacuations. Needless to say, people are

[33] It can be argued that the areas inside safe buildings are also safe areas. However, building-code compliant structures are not indestructible and on built on some level of safety. Earthquakes can still render some damage to buildings and aftershocks can further weaken structures leading to more damage and increased probability of collapse.
[34] Following building codes

the focus of evacuations and this is true for all types of disasters. The difference of between disasters is the nature of the hazards involved. Earthquake disasters are different in the sense that earthquakes are unpredictable, have no warning, occurs in short durations, and the effects are felt over a very large area. Focusing on human behaviour therefore can make the results of the study especially the social aspects, relevant to other evacuation research.

The second major contribution of the study is SOLACE, the multi agent-based model for earthquake evacuation implemented using social attachment. Human behaviour is complex and is difficult to model. Earthquake disasters also produce complex and challenging environments that are likewise difficult to model. The GAMA platform proved to be an effective tool to combine the social and environmental aspects needed to attempt in developing a realistic model of the crisis scenarios. The model was useful in testing some aspects of human behaviour and the physical environment. BDI in GAMA was useful in the development of cognitive agents. Using the model actually opened up more interesting question concerning different scenarios. Also, many other parameters can be added and tested in the model. This flexibility offered in the GAMA platform, means that the model can be changed, with respect to data, and the parameters used in calibrating simulation experiments. This flexibility likewise gives the model the potential to be applied to other areas.

The third major contribution is that the research supports the benefit of using accurate spatial data in dynamic multi agent-based models. Spatial data are heavily used by government institutions around the world in their planning processes (Antolfe, Doherty, & Marin-Ferrer, 2018; Fekete, et al., 2015). *Geosimulation* and *geocomputation* have been used mostly in the modelling of the dynamics of physical processes and urban systems. However most of these studies do not sufficiently integrate human behaviour and social dynamics. This is mainly due to the limits imposed by the complexity of these models that require large computing power and resources (Torrens, 2001). Concerning of multiagent models, most lack the use of spatial data. Currently there are very few agent-based models implementing complex human behaviours for evacuations with accurate geospatial data. Integrating spatial data increases the realism of multi agent models. This makes the model and the results of simulations relatable and easily explainable to other scientists from different domains, experts, and practitioners. Evacuation is very sensitive to the precision used in representing space and time in models. Modelling exposure to debris hazard requires the spatial data on buildings, their vulnerabilities, and temporal precision in generating and depositing debris in danger zones. Populations are likewise generated based on occupancy at different times of day. The scheduling of egress from structures is likewise influenced by pre-evacuation actions and the number of floors traversed by agents. Lastly, the configuration of streets and locations of safe areas contribute to the duration of evacuations and arrivals in safe areas.

9.3 Future work

The research has been very useful in testing initial insights on the effects of social and behavioural aspects on earthquake evacuation. Furthermore, the work has a lot of potential when applied to the four domains that constitute the model.

9.3.1 Improving the model

Many improvements are proposed to further increase the realism of the model. The following can be done.

The building dataset has used probabilistically assigned typologies and vulnerability attributes based on IRIS level percentages (see Section 6.1.2). An ideal dataset would be to use the actual building stock of the city with data for each building based on official seismic assessments. Desired data and attributes would include age of the building, typology, damage and vulnerability at different intensities, building design, floor plan, number of floors, elevation, locations of doorways and emergency exits, etc. Having

these values available for each building could enhance the model and increase the realism of the simulation results.

Using accurate building occupancy data for different times of the day is crucial in the modelling the distribution of populations. Although this dataset is ideal, it is unfortunately not used in the current model. The distribution of the population for the different scenarios has been probabilistically assigned based on the IRIS level population data (see Section 6.2.2.3). Data on households when available will also be useful in establishing the possible social relationships in source locations. The use of very detailed individual and household data in simulations however opens up ethical and privacy concerns (Torrens, 2001).

Officially designated safe areas and their associated evacuation routes can be used in the future scenarios. Acquiring this data for the model has not been possible. What has been used instead as safe areas are areas where debris can probably not be deposited (which is the distance away from buildings) (see Section 5.3, Section 5.4 and Section 6.1.1). An exact determination of the danger zones around buildings is likewise needed. Having this data can greatly improve the realism of simulations.

The model can be improved by adding missing physical features that also act as barriers or pose risks during evacuations. These include moving and parked cars, trams, trains, fences, trees and chimneys. The only barriers used in the model are buildings, water bodies, generated debris and fatalities. Adding these missing elements can likewise improve the realism of the evacuation scenarios.

There are many possible models that can refine the different aspect of SOLACE. For the geospatial model of the spatial environment, a more detailed urban model (2D and 3D) could be integrated. This can include a more complete set of buildings, establishments and land use. The information to include can be similar to the level of details in OpenStreetMap, GoogleMaps or Google Earth (OpenStreetMap & Contributors, 2018; Google, 2018).

The behaviour data were gathered from a mix of sources (see Table 10 and Table 28). The model can benefit from more accurate human behaviour data, preferably from earthquake survivors. However, finding these survivors and conducting interviews however can be difficult. Important details can be forgotten especially when interviews are conducted long after earthquake events. Video data during earthquakes when available are very useful since these can be analysed at different levels of detail and context (physical setting, social setting, culture, etc.). Survey data on earthquake behaviours (possible experience, possible actions) is also very useful, but require a large number of samples. It is also difficult to project possible "actual" behaviours into future earthquake events especially if the sample population has not experienced an earthquake event.

On the social aspect, an improved model on social bonds is desired. Quantification of social bonds is another active area of research where new methods are being explored. Culture also defines social structures, relationships and therefore also the strength of social bonds. New studies quantifying social bond strength with respect to different cultural settings and social environments can help improve the model. Also, integration of other models for dynamic social and psychological aspects relating to the individual can improve the model. This includes emotions, contagion, communication, spread of information, etc.

Still on the social aspect, an improved model for distributing populations in geographic space can help improve the model. New population distribution models from mobility studies, and household travel surveys can help improve the model.

Concerning the geoscience aspect, a model on how earthquakes are felt at different floor levels is particularly desirable. Earthquakes are usually felt more from the upper floors of taller buildings than on lower floors. Individuals located at lower floors usually do not sense low magnitude earthquakes. This difference in experiences in earthquakes is significant since it can result in varied behaviours from individuals residing in the same building. In addition, a more accurate model of debris creation, deposition in danger zones and the delineation of danger zones would be useful. The current model uses the method described in Section 6.2.2.2 with the amount of debris being shown in Section 8.3.7. This resulted in a large number of casualties for intensity VIII (Figure 97). A better model of debris creation and deposition could result in fewer numbers of debris and casualties.

Lastly, there is a need for a more accurate casualty model. Specifically, a method for establishing the probability of being hurt or dying when hit by debris during earthquakes is needed. Currently the model uses a 50% probability of being injured or killed by debris (i.e. agent location intersects with a debris polygon) (see 8.3.6). This probability is computed during each time that an agent is hit by debris during shaking. This interaction is shown in Section 6.2.2.2. The number of casualties using this probabilistic assignment of injury or death, is high (Figure 97). A more accurate casualty model could result in fewer casualties.

For the computer science domain there are many possible models that can be incorporated to improve the model. These can include (1) improved model for agent navigation and perception; and (2) BDI models of incorporating emotion, contagion, spread of knowledge, communication, etc. BDI can implementations can be further enhanced to accommodate large populations of cognitive agents. The performance of models can likewise be improved by using different computing infrastructures such as HPC and GRID environments.

9.3.2 Possible applications in different domains

SOLACE can be useful in exploring different what-if scenarios in each of the four domains that constitute the model.

9.3.2.1 Geospatial science

The model can be useful for urban planning in the context of ensuring the evacuation preparedness of people during disasters. The effect on evacuation of existing and future configurations of the urban space can be tested using the model. For example, different configurations or placements of safe areas, meeting points and evacuation routes can be tested in the model (see Figure 83). An evacuation efficiency rating could be developed using the model to indicate the efficiency of safe area and meeting point placements, and evacuation routes. Impact of changes in urban configurations (such as new constructions, closed roads, additional residential areas) can likewise be tested using the model.

It is possible to apply SOLACE for data at different levels of spatial detail or scale, for example the larger metropolitan area of Grenoble. Applying the model to different municipalities in France is also possible. The data on building vulnerability and damage at the IRIS level has been calculated for the whole of France by Riedel et al. (Riedel, Guéguen, & Dunand, 2014). Spatial data on buildings and roads are available as well from both government and open sources. Mixing data however from different sources can be challenging especially in ensuring goodness of fit between datasets.

Testing the flexibility of applying the model to different areas is very important. Once the model is proven flexible and useful, it can be applied in the modelling of the evacuation potential of areas outside of France. This is significant because there are many countries that are prone to earthquakes. Applying the model in these countries may help in efforts to prepare for future earthquakes. Difficulty in directly applying the model can be from the unavailability of detailed building stock data, with attributes on vulnerability and damage at different intensities. Spatial data, especially when not available from official

sources, can be acquired from OpenStreetMap. Depending on the country, very fine level of detail can be available (e.g. buildings, roads, points of interest (establishment, schools, facilities, etc.)). When data is not available, the help of the OpenStreetMap community can be sought to generate the needed map features (OpenStreetMap & Contributors, 2018; Albuquerque, Eckle, Henfort, & Zipf, 2016). The level of detail in OpenStreetMap data is sufficient to be used in the model. Data from official sources however is preferred.

Applying SOLACE at the scale of single building with a complex layout can also be explored. Indoor evacuation was actually tested at the start of the research before SOLACE was completed. The basic model for indoor evacuation tested with a complex layout is show in Figure 110. The zoomed in version of the egress point at the door is shown in Figure 111.

Figure 110 Indoor evacuation in a hospital floor with complex layout (Bañgate, 2016)

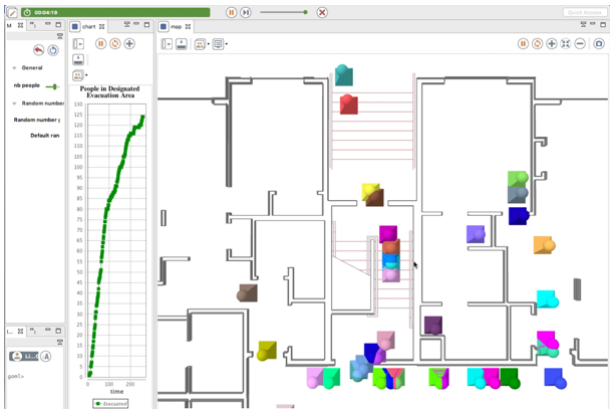

Figure 111 Egress from building (Bañgate, 2016)

SOLACE can be customised to use the spatial data for this type of indoor model. The walls for example are analogous to the building barriers. Like the buildings in the city model, the walls can have attributes for typology (e.g. wood, cement, glass), and vulnerability and damage at different levels of intensity. Weak indoor wall materials can (e.g. glass, masonry) be damaged or collapse during high intensity earthquakes. These can block pathways, cause injuries and death. The population of agents can be generated in rooms based on designed occupancy. The relationships of the agents can also be assigned.

For example, for work environments, most will be colleagues or friends. For residential apartments, most will be family members. Some indoor environments will have a complex mix of possible relationships such as in hospitals, airports, etc.

The correct geographic representations of the spatial elements is very crucial in modelling indoor evacuations. The dimensions of indoor elements need to be correct. Examples are the lengths and widths of pathways, and location and widths of egress points. Narrow widths can define bottlenecks for exiting crowds. Needless to say, this also includes correctly representing the correct size and widths of building occupants (people). Individuals with large footprints can more effectively block pathways. For example, it was found that there are higher densities and faster flow through doors in the evacuation of children than that of adults (Larusdottir & Diderichs, 2011). Figure 112 shows the layout of one of the floors of the LIG building overlaid on a Google satellite image. Having the correct geographic reference ensure that the distances to be travelled by agents are reflective of actual measurements on the ground. These distances affect estimates of travel time.

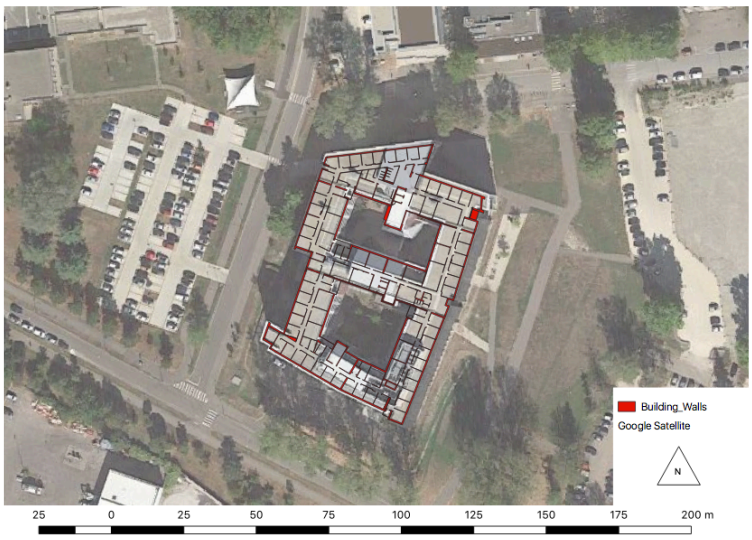

Figure 112 Floor layout of LIG Building

A wider range of spatial scales and therefore spatial complexity can be explored using SOLACE. Models can become very complex and may still give a similar result from a simpler and less complex model. Very complex models also consume large computing resources and take a long time to run. For applications such as disaster modelling that demands a level of urgency, slow simulation runs are not acceptable especially in the response stage of the crisis management cycle. In the planning stage however, highly accurate but slow simulation runs still be very useful. Finding the right mix of spatial elements with acceptable levels of model complexity may hopefully be explored in the future using the developed model.

9.3.2.2 Social sciences

In social sciences, different parameter settings for social behaviours during evacuations can be tested. A possible practical application is the testing of scenarios of compliance with recommended actions during earthquake evacuations. Ideal behaviours and durations can be set in the model (see Section 5.5). Scenarios with different levels of compliance can be tested in the simulation.

The impact of compliance to recommended behaviours can be tested with respect to present and future demographic characteristics and spatial distribution of populations. The trend in developed nations is the increase in the population of the elderly and fewer younger individuals. This makes mobility a

primary concern especially in the future. Setting population characteristics and distribution for example are shown in Section 6.2.2.3.

The influence of culture on evacuation is also a very interesting area. In the model, the influence of culture can be set using the parameter for social attachment bonds. The research established that social attachment is beneficial to evacuations. This therefore implies that communities or cultures with close attachment bonds have better chances evacuating successfully. Culture is manifested by how families and households are structured (e.g. single parents, many kids, elderly parents living with family, large family size, extended families, etc.). Culture is also manifested in the settlement patterns and organisation of urban space. Work environments have their own professional culture, and with less personal relationships. The model can be used to test the evacuation potential of different cultures in evacuation. The model therefore has the potential to be used in different spatial scales, and in other places such as other cities, other urban areas or other countries. Culture also affects behaviours and risk perception. A future work can focus on the integration of risk perception into the social model of behaviours.

9.3.2.3 Geoscience

A future work in the domain of geoscience can be the testing of the effect of the different levels of compliance to current and future building codes. Different earthquake intensity scenarios can be used to test the damage patterns using damage and vulnerability potential values of the building stock. Another area of research is exploring and improving the methodology of assigning vulnerability and damage attributes to individual buildings. This data is usually only provided for large zones (such as municipalities, IRIS/survey unit) that enclose many buildings. The data needs to be scaled down to the level of each building. A simplified method of attribute assignment needs to be explored.

Establishing the most accurate configuration of danger zones needs to be explored. That is, a more precise radius around buildings must be found. This also requires an accurate debris deposition model, as the risk of casualties is linked with exposure to debris at the base of buildings. Site effects which may amplify the seismic waves depending on the soil typology or topography, and thus lead to differences in intensity over the studied area, have also not been fully explored in the SOLACE model, and need to be addressed in future work.

Scenarios with variable intensity distribution in the study area also need to be explored in future works. In each of the experiments, a single intensity assignment for the whole study area was used. In reality however, how earthquakes are felt in landscapes vary. Also areas that are closer to the earthquake can also experience more pronounced shaking.

9.3.2.4 Computer science

A future work in the domain of computer science can be the development of a serious game based on SOLACE. The serious game can be used to assist decision makers in testing the effects of policy direction by testing different scenarios using the model. Examples of policies to be explored could be: assessing building earthquake resilience through the implementation of building codes; the effect of retrofitting old structures; launching information campaigns to raise awareness; building a smart city infrastructure, delineation of safe evacuation routes; installing clearer signage to safe areas. A game for example can consist of balancing the allocation of financial resources with respect to the cost of adopting earthquake preparedness strategies. A serious game for the public could be developed to both test and also raise the awareness of the public on earthquake preparedness (e.g. having a plan, securing indoor furniture, having an emergency kit, etc.), and adopting prescribed evacuation behaviour (e.g. drop/cover/ hold on, not running outside immediately, going to a meetup point, etc.)

Another possible area for future work is the integration of SOLACE with other models that are currently missing in the simulation. An example is the addition of a multi-modal transportation model with moving vehicles. This is missing in the current pedestrian evacuation model. Another improvement can be the integration of a model of rescue and emergency services (e.g. fire and medical teams). A model of fire can also be integrated into SOLACE. Fires also usually start after earthquakes due to exposed and leaking gas pipelines. Integrating more elements into the model needs to be studied. The added complexity into the model may require more computing resources.

Another area is testing the performance of the model in grid and in high performance computing (HPC) environments. The high complexity of the model results in very slow processing times. Adding more complexity to the model by involving larger populations of agents, larger spatial coverage, and more building elements, would require very powerful computing resources. Running the simulation using GPUs other than normal CPUs may also increase performance. The decrease in computational performance with increased model complexity also necessitates the search for and adoption of strategies that can enable running complex models with less powerful computing resources. This includes adoption of less demanding algorithms and cognitive architectures for the human agents. Computer code can also be streamlined and optimized. Having the ability to run the simulations will less computing resources may further promote the use of the model in disaster planning efforts by organisations and communities.

9.4 Concluding remarks

Earthquake crisis evacuations are social in nature. This character of evacuations requires that the behavioural and social nature of individuals be the centre of the research. Social attachment is an important framework in modelling human behaviour during evacuations. It's the provides a strong and logical explanation for the basis of human action during disasters. The SOLACE model developed in the research is built with social attachment as the basis for agent behaviour in the simulations. Results using SOLACE supports the argument that social aspects and human behaviour need to be considered in evacuation studies and in the development of evacuation models.

The role of the accurate geographic representation of the crisis environment has also been highlighted in the research. Distance is particularly important in the model since it limits perception. Longer distances mean longer time to reach safe areas. Shortest paths allow individuals to reach the nearest safe areas faster. Blocked pathways make the distance to safe areas longer, resulting in an increased time to reach safe areas. Social relationships are also defined by distance. In the model, familiar individuals (with whom one shares a very strong bond) are recognised much faster or easier than those with lesser bonds such as strangers. Distance is therefore is used as a preferential filter. With this core role of distance in the model, a less accurate representation of distance is not acceptable.

The role of cognitive and social agents has also been core to the research. The multiagent based modelling approach with BDI agents has been very useful in realising the crucial social interactions implemented in the model. The importance of the models and simulations are underscored by the ease with which different scenarios were designed, implemented, and used to generate the needed data for analysis and visualisations. The simulations generated a level of complexity in emergent social interactions and dynamics between spatial elements needed to simulate a believable crisis environment.

The contribution of the research as discussed in Section 9.2 points to its usefulness in earthquake evacuation research. More research in the future are admittedly needed to refine the model, and test its fit for use in applications in different domains.

Bibliography

Abdalla, R., & Li, J. (2010). Towards effective application of geospatial technologies for disaster management. International Journal of Applied Earth Observation and Geoinformation (Editorial), 405 - 407.

ACAPS. (2013). Call detail records: The use of mobile phone data to track and predict population displacement in disasters. Tratto da ACAPS, See the Crisis, Change the outcome: https://www.acaps.org/call-detail-records-use-mobile-phone-data-track-and-predict-population-displacement-disasters

ACAPS. (2013). Call detail records: The use of mobile phone data to track and predict population displacement in disasters. Tratto da ACAPS, See the Crisis, Change the outcome: https://www.acaps.org/call-detail-records-use-mobile-phone-data-track-and-predict-population-displacement-disasters

Adam, C., & Gaudou, B. (2016). BDI agents in social simulations: a survey. Knowledge Engineering Review, 31(3), 207 - 238.

Adam, C., Danet, G., Thanagarjah, J., & Dugdale, J. (2016b). BDI modelling and simulation of human behaviours in bushfires. Information systems for crisis response and management in mediterranean countries. Third International Conference. (p. 47-61). Madrid, Spain: ISCRAM-med.

Adam, C., Danet, G., Thangarajah, J., & Dugdale, J. (2016). BDI Modelling and Simulation of Human Behaviours in Bushfires. Information Systems for Crisis Response and Management in Mediterranean Countries: Third International Conference, ISCRAM-med 2016 (p. 47 - 61). Madrid, Spain: Springer International Publishing.

Adams, A. P., & R., G. E. (2011). An experimental evaluation of movement devices use to assist people with reduced mobility in high-rise building evacuations. In R. D. Peacock, E. D. Kuligowski, & J. D. Averill, Pedestrian Evacuation Dynamics (p. 129-138). Springer+Business Media.

Adilla, A. (1993). People Recognition: A historical /Anthropological Perspective. Behavioural Neurology, 6, 99 - 105.

AEPI. (2019, August 28). Key Economic Figures - Grenoble Isère, Franc Edition 2018. Tratto da http://www.grenoble-isere.com: http://www.grenoble-isere.com/media/upload/pdf_chiffrescles/AEPI-2018-Chiffres-Cles-GB-26-02-2018-2.pdf

AEPI_b. (2013). Leading companies and world-class production sites in Grenoble-Isère. Grenoble, France: Agence d'Etudes et de promotion de l'Isère.

Aguirre, B. (1983). Evacuation as population mobility. International Journal of Mass Emergencies and Disasters 1.3.

Aguirre, B. E., & Wenger, D. V. (1998). A test of the emergent norm theory of collective behaviour. Sociological Forum 13.2, 301-320.

Ainsworth, M. S. (1989). Attachments beyond infancy. American Psychologist, 44(4), 709 - 716.

Albuquerque, J. P., Eckle, M., Henfort, B., & Zipf, A. (2016). Crowdsourcing geographic information for disaster managemnt and improving urban resilience: an overview of recent developments and lessons learned. In C. Capinery, M. Haklay, H. Huang, V. Antoniou, J. Ketunen, F. Ostemann, & R. Purves, European Handbook of Crowdsourced Geographic Information (p. 309-321). London: Ubiquity Press.

Alexander, D. (1990). Behaviour during earthquakes: A Southern Italian Example. International Journal of Mass Emergencies and Disasters, 5 - 29.

Alexander, D., & Magni, M. (2013). Mortality in the L'Aquila (Central Italy) Earthquake of 6 April 2009: A Study in Victimisation. PLOS Currents, Disasters.

Alexander_2, D. (1985). Death and injury in earthquakes. Disasters.

Alexander_a, D. (2012). Models of Social Vulnerability to Disasters. RCCS Annual Review, 4, 22 - 40.

Amoroux, E., Chu, T.-Q., Boucher, A., & Drogoul, A. (2007). GAMA: an environment for implementing and running spatially explicit multi-agent simulations. Agent Computing and Multi-Agent Systems, 10th Pacific Rim International Conference on Multi-Agents. Bangkon, Thailand.

Anbazhagan, P. (2013). Method for seismic microzonation with geotechnical aspects. Disaster Advances, 6.

André-Poyaud, I., Chardonnel, S., Charleux, L., & Tabaka, K. (2016). Mobility activity patters of individuals and parenting couples in the metropolitan aera of Grenoble (France). Tratto da HAL : https://hal.archives-ouvertes.fr/halshs-01260244

Antolfe, T. E., Doherty, B., & Marin-Ferrer, M. (2018). Mapping of risk web-platforms and risk data: collecton of good practices. Improving the access and share of curated EU-wide risk data for fosterig DRM, JRC Technical Reports. Luxembourg: Europen Union, European Commission, JRC Technical Reports.

Ara, S. (2013). Analyzing population distribution and its effect on earthquake loss estimation in Sylhet, Bangladesh. MSc Thesis. Applied Earth Sciences.

Ara, S. (2014). Impact of Temporal Population Distribution on Earthquake Loss Estimation A Case Study on Sylhet, Bangladesh. International Journal of Disaster Risk Science, 5, 291-312.

Averill, J. D. (2011). Five Grand Challenges in Pedestrian and Evacuation Dynamics. In R. Peacock, E. Kuligowski, & J. Averill, Pedestrian and Evacuation Dynamics (p. 1 - 11). Boston, MA: Springer.

Averill, J. D., Mileti, D. S., Peacock, R. D., Kuligowski, E. D., Froner, N., Proulx, G., . . . Nelson, H. E. (2005). Occupant Behaviour, Egress, and Emergency Communications. Washington, D. C.: Federal Building and Fire Safety Investigation of the World Trade Center Disaster. Technical Report, NCSTAR 1-7, National Institute of Standards and Technology (NIST).

Bajracharya, R. (2018, November 26). Nepal Earthquake CCTV footage Kathmandu May 12, 2015 (Baisakh 29th 2072 B.S.). Tratto da YouTube: https://www.youtube.com/watch?v=tMMvsVHXy0I

Balas, B., Cox, D., & Conwell, E. (2007). The effect of real-world personal familiarity on the speed of face information processing. PLoS(11).

Balke, T., & Gilbert, N. (2014). How do agents make decisions? A survey. Journal of Artificial Societies and Social Simulation.

Bañgate, J. (2016, June 18). Building Indoor Evacuation (GAMA Simulation). Tratto da YouTube: https://www.youtube.com/watch?v=XiKERs_j6pI

Barbosa, H., Barthelemy, M., Ghoshal, G., James, C. R., Lenorland, M., Louail, T., . . . Tomasini, M. (2018). Human moblity: Models and Applications. Physics Reports, 1 - 74.
Barsics, C. (2014). Person recognition is easier from faces than from voices. Psycologica Belgica, 244 - 254.
Barton, J. J., & Corrow, S. L. (2016, Febuary). Recognizing and identifying people: a neuropsychological review. Cortex, 75, 132-150.
Barton, J., & Corrow, S. (2016). Recognizing and identifying people, A neuropsychological review. Cortex, 75, 132-150.
Batista e Silva, F., & Poelman, H. (2016). Mapping population density in Functional Urban Areas, A method to downscale population statistics to urban atlas polygons. JRC Technical Reports, Joint Research Center, European Comission.
Batty, M. (2003). Agent-based pedestrian modelling, CASA Working Papers, Paper 61. London, UK: Center for Advanced Spatial Analysis, UCL .
Bazzuro, P., Cornell, C. A., Menun, C., & Motahari, M. (2004). Guidelines for seismic assessment of damaged buildings. 13th World Conferenc on Earthquake Engineering. Vancouver, B. C. , Canada.
Beck, E., André-Poyaud, I., Chardonnel, S., Davoine, P. A., & Lutoff, C. (2010). MOVISS: Méthodes et Outils pour l'evaluation de la Vulnerabilité Sociale aux Séismes. Grenoble, France: Conseil Géneal Isère.
Beck, E., Dugdale, J., Truong, H. V., Adam, C., & Colbeau-Justin, L. (2014). Crisis mobility of pedestrians: from survey to modelling: lessons from Lebanon and Argentina. Information Systems for Crisis Response and Management in Mediterranean Countries, Lecture Notes in Business Information Processing, 196, 57-70.
Beckes, L., & Coan, J. A. (2011). Social Baseline Theory: The role of social proximity in emotion and economy of action. Social and Persolality Psychology Compass, 5.12 , 976-988.
Begault, D. (2008). Forensic analysis of the audibility of female screams. AES 33rd International Conference. Denver, CO, USA.
Benenson, I., & Torrens, P. M. (2004). Geosimulation: Object-based modelling of urban phenonomena. Computers Environment and Urban Systems, 28(1), 1 - 8.
Bengtsson, L., Lu, X., Thorson, A., Garfield, R., & Scheeb, J. v. (2011). Impoved response to disasters and outbreaks by tracking population movements with mobile phone network data: A post-earthquake geospatial study in Haiti. PLOS Medicine, 8(8).
Bengtsson_a, L., Lu, X., Thorson, A., Garfield, R., & Schreeb, J. v. (2011, July 21). Impoved response to disasters and outbreaks by tracking population movements with mobile phone network data: A post-earthquake geospatial study in Haiti. PLOS Medicine, 8(8).
Bernardini, A., Giovinazzi, S., Lagomarsino, S., & Parodi, S. (2007). The vulnerability assessment of current buildings by a macroseismic approah derived from the EMS-98 Scale. Congreso Nacional De Ingenieia Sismica. Girona.
Bernardini, G., D'Orazio, M., & Quagliarini, E. (2016). Towards a behavioural design appoach for seismic reduction strategies of buildings and their environment. Safety Science 86, 273-294.
Bevington, J., Eguchi, R., Huyck, C., Crowley, H., Dell'Acqua, F., Iannelli, G., . . . Wyss, M. (2012). Exposure data development for the Global Earthquake Model: Inventory data capture tools. 15 World Conference on Earthquake Engineering. Lisboa.
Bianchi, F., & Squazzoni, F. (2015, June 5). Agent-based models in sociology. Wiley Interdisciplinary Reviews: Computational Statistics, 7(4).
Bode, N. W., Holl, S., Mehner, W., & Seyfried, A. (2015). Disentangling the Impact of Social Groups on Response Times and Movement Dynamics in Evacutions. PLoS ONE.
Bode, N. W., Miller, J., O'Gorman, R., & Codling, E. A. (2015). Increase costs reduce reciprocal helping behaviour of humans in a virtual evacuation experiment. Scientific Reports (www.nature.com/scientificreports).
Bohannon, R. W. (1997, January). Comfortable and maximum walking speed of adults aged 20-79 years: reference values and determinants. Age and Ageing, 26, 15 - 19.
Boin, A. (2005). From Crisis to Disaster: Towards and Integrative Perspective. In R. W. Perry, & E. L. Quarantelli, What is a Disaster? New Ansers to Old Questions (p. 153 - 172). International research Committee on Disasters.
Bourgais, M., Taillandier, P., & Vercouter, L. (2018). Enhancing the behaviour of agents in social simulations with emotion and social relations. In G. P. Dimuro, & L. Antunes, Multi-agent based simulation XVIII (p. 89-104). Springer.
Bowlby, J. (1982). Attachment and Loss, Volume I. Basic Books.
Bowlby_a, J. (1982). Attachment and Loss, Volume I. Basic Books.
Boyce, K. E., Shields, T. J., & Silcock, G. W. (1999). Toward the characterisation of building occupancies for fire safety engineeing: capabilities of disabled people moving horizontally and on an Incline. Fire Technology 35.1, 51-67.
Bracha, H. S. (2004). Freeze, Flight, Fight, Fight, Faint: Adapatationist Perspectives on the Acute Response Spectrum. CNS Spectrums, 9(9), 679 - 685.
Brecht, H., Deichmann, U., & Wang, H. G. (2013). A Global Urban Risk Index, Policy Reseach Working Paper 6506. The World Bank.
BRGM. (2019, August 28). Zonage sismique de la France. Tratto da www.planseisme.fr: http://www.planseisme.fr/Zonage-sismique-de-la-France.html
Brown, D. G., Riolo, R., Robinson, D. T., North, M., & Rand, W. (2005). Spatial process and data models: Toward integration of agent-based models and GIS. Journal of Geographical Systems, 7, 25-47.
Brunyé, T. T., Gardony, A. L., Holmes, A., & Taylor, H. A. (2018, Dec.). Spatial decision dynamics during wayfinding: intersections prompt the decision-making process. Cognitive Research Pinciples and Implications, 13, 1 - 19.
Bulumulla, C., Padgham, L., Singh, D., & Chan, J. (2017). The importance of modelling realistic human behaviour when planning evacuation schedules. AAMAS '17 Proceedings of the 16th Conference on Autonomous Agents and MultiAgent Systems (p. 446-454). Sao Paulo, Brazil: International Foundation for Autonomous Agents and Multiagent Systems.

Burns, T. R., Roszkowska, E., Johansson, N. M., & Corte, U. (2018). Paradigm shift in Game Theory: Sociological Re-conceptualization of Human Agency, Social structure, and Agents' Cognitve-Normative Frameworks and Action Determination Modalities. Social Sciences, 7(40).

Cai, G., Sharma, R., MacEachren, A. M., & Brewer, I. (2006). Human-GIS Interaction Issues in Crisis Response. International Journal of Risk Assessment and Management, 6(4-6), 388-407.

Cardona, O.-D., Aalst, M. K., Birkmann, J., Fordham, M., McGregor, G., Perez, R., . . . Sinh, B. T. (2012). Determinants of Risk: Exposure and Vulnerablity. In C. Field, V. Barros, T. Stocker, D. Qin, D. Dokken, K. Ebi, . . . P. Midgle, Managing the Risks of Extreme Events and Disasters to Advance Climate Change Adaptation.]. A Special Report of Working Groups I and II of the Intergovernmental Panel on Climate Change (IPCC). (p. 65-108). Cambridge, UK and New York ,NY, USA: Cambridge University Press.

Cartier, S. (2007). Seismic micro-zoning in the alpine valleys and local application in urban planning regulations. Journal of Alpine Research, 95-2.

CEA. (2015). Risk Control Report 2014. Grenoble, France: Commisaiat à l'énergie atomique et auw énergies alternatives (CEA).

Chapleau, R., & Morency, C. (2005). Dynamic Spatial Analysis of Urban Travel Survey Data using GIS.

Chapuis, K., Taillandier, P., Renaud, M., & Drogoul, A. (2018). Gen*: a generic toolkit to generate spatially explicit synthetic populations. International Journal of Geographic Information Science, 32(6).

Chu, M. L. (2015). A Computational framework incorporating human and social behaviours for occupant centric egress simulation. Doctoral Dissertation. USA: Stanford University.

Chu, M. L., Pan, X., & Law, K. (2011). Incorporating social behaviours in egress simulation. Proceedings of 2011 Computing in Civil Engineering Workshop, (p. 19-22).

Chu, M. L., Parigi, P., Law, K., & Latombe, J. C. (2014). SAFEgress: A Flexible Platfom to Study the Effect of Human and Social Behaviours on Egress Performance. Proceedings of the Symposium on Simulation for Architecture and Urban Design, SimAUD '14. San Diego CA, USA.

Coan, J. A. (2008). Toward a Neuroscience of Attachment. In J. Cassidy, & P. R. Shaver, Handbook of attachment: theory, reseach, and clinical implications, 2nd Edition (p. 241-265). New York: The Builford Press.

Coburn, A. W., Spence, R. J., & Pomonis, A. (1992). Factors determining human casualty levels in earthquakes: Mortality prediction in building collapse. Earthquake engineering, Tenth World Conference. Balkema, Rotterdam.

Coburn, A., & Spence, R. (2002). Earthquake Protection, 2nd Edition. West Sussex, England: Joh Wiley & Sons, LTD.

Coburn_1, A. W., Spence, J. S., & Pomonis, A. (1992). Factors determining human casualty levels in earthquakes: Mortality predicion in building collapse. Earthquake Engineering: Tenth World Conference, (p. 5989 - 5994). Balkema, Rotterdam.

Cocking, C., Drury, J., & Reicher, S. (2007). The psychology of crowd behaviour in emergency evacuations: results from two intervies studies and implications for fire and rescue service. Psychology and thre fire and rescue service Irish Journal of Psychology.

Cocking, C., Drury, J., & Reicher, S. (2009). The psychology of crowd behaviour in emergency evacuations: Results from to interview studies and implications for the the fire and rescue services. The Irish Journal of Psychology, 30(1), 59 - 72.

Cohen, J. I., & Gordon-Salant, S. (2017). The effect of visual distraction on auditory-visual speech perception by younger and older listeners. Journal of the Accoutical Society of America, 141(5).

Comes, T. (2016). Cognitive biases in humans sensmaking and decision-makiing lessons from field research. 2016 IEEE International Multi-Disciplinary Conference on Cognitive Methods in Situation Awareness and Decision Support (CogSIMA), (p. 56-62).

Coppé, E., Enaudi, O., Menousse, C., & Munar, V. G. (2013). La Ville Prend La Hauteur. Grenoble, France: Architecture Ambiance Culture Numériqu, PFE-ENSAG.

Cornu, C., Bard, P.-Y., & Dietrich, M. (2003). Contribuion of Dense Array Analysis to the Identification and Quantification of Basin-Edge-Induced Waves, Part I: Methodology. Bulletin of the Seismological Society of America, 2604-2623.

Coutinho-Rodrigues, J., Natividade-Jesus, E., & Sousa, N. (2015). Design of evacuation plans for densely urbanized city centres. Municipal Engineer, Proceedings of the Institute of Civil Engineers, (p. 160-172).

CRED. (2016). Poverty & Death: Disaster Mortality, 1996 - 2015. Center for Research on the Epidemiology of Disasters (CRED), UNISDR.

Crooks, A. T. (2006). Exploring cities using agent-based models and GIS. UCL Working Papers Series, Paper 109 - Sept 06. London: UCL Centre for Advanced Spatial Analysis.

Crooks, A. T., & Castle, J. E. (2012). The Integration of Agent-based modelling and Geographic Information of Geospatial Simulation. In H. A, C. A, L. See, & M. Batty, Agent-based models of Geographical Systems. Springer, Dordrecht.

Crooks, A., Castle, C., & Batty, M. (2007). Key Challenges in Agent-Based Modelling for Geo-Spatial Simulation. Geocomputation 2007. Kildare, Ireland.

Daamen, W., Duives, D. C., Hoogendorn, S. P., Bernardini, G., D'Orazio, M., Quagliarini, E., & Spalazzi, L. (2014a). An agent based model or earthquake pedstians' evacuation simulation in urban scenarios. The Conference on Pedestrians and Evacuation Dynamics 2014 (PED 2014) (p. 255-263). Delft: Transportation Research Procedia 2.

Daamen, W., Duives, D. C., Hoogendorn, S. P., Siver, I. v., Templeton, A., Köster, G., . . . Philippides, A. (2014b). Humans do not always act selfishly, Social Identity and Helping in Emergency and Evacuation Simulation. The Conference on Pedestrian and Evacuation Dynamics, 2014 (PED 2014), 22-24 October 2014 (p. 585-593). Delft, The Netherlands: Transportation Research Procedia 2.

Dalton, R. C., Hölscher, C., & Montello, D. R. (2019). Wayfinding as a Social Activity. Frontiers in Psychology, 10.

Darvishi, M., & Ahmadi, G. (2014). Validation techniques of agent-based modelling for geospatial simulations. The 1st ISPRS International Conference on Geospatial Information Research, XL-2/W3 (p. 91-95). Tehran, Iran: The International Archives of the Photogrammetry, Remote Sensing and Spatial Information Sciences.

Daudé, E., Chapuis, K., Taillandier, P., Tranouez, P., Caron, C., Drogoul, A., . . . Zucker, J.-D. (2019). ESCAPE: Exploring by Simulation Cities Awareness on Population Evacuation. In Z. Franco, J. J. Gonzales, & J. H. Canos (A cura di), 16th International Conference on Information Systems for Crisis Response and Management (ISCRAM 2019. Valencia, Spain: ISCRAM.

Del Viva, M. M., & Agostini, R. (2007). Visual spatial integration in the elderly. Investigative Opthalmology and Visual Science, 48(6).

D'Orazio, M., Quagliarini, E., Bernardini, G., & Spalazzi, L. (2014b). EPES, Earthquake pedestrians' evacuation simulator: A tool for predicting earthquake pedestrians' evacuation in urban, outdoor scenarios. Journal of Disaster Risk Reduction 10, Part A, 153-177.

D'Orazio, M., Quagliarini, E., Bernardini, G., & Spallazi, L. (2014b). {EPES} Earthquake pedestrians' evacuation simulator: A tool for predicting earthquake pedestrians' evacuation in urban outdoor scenarios. International Journal of Disaster Risk Reduction, 10, 153-177.

D'Orazio, M., Spallazzi, L., Quagliarini, E., & Bernardini, G. (2014a). Agent-based model for earthquake pedestrians evacuation in urban outdoor scenarios: Behaviour patterns definition and evacuation paths choice. Safety Science 62, 450-465.

DREES. (2017). L'etat de santé de la population en France, Rapport 2017. Tratto da Santé Publique France: http://www.santepubliquefrance.fr/Actualites/Etat-de-sante-de-la-population-en-France-rapport-2017

Drogoul, A., Amoroux, E., Caillou, P., Gaudou, B., Grignard, A., Marilleau, N., . . . Zucker, J.-D. (2013). GAMA: a spatially explicit, multi-level, agent-based modelling and simulation platform. In D. Y., I. T., C. J.M., & B. J., Advances in Practical Applications of Agents and Multi-Agents Systems; PAAMS 2013, Lecture Notes in Computer Science (Vol. 7879).

Drury, J., Cocking, C., & Reicher, S. (2008). Everyone for themselves A comparative study of crowd solidarity among emergency survivors. British Journal of Social Psychology, 1 - 21.

Drury, J., Cocking, C., & Reicher, S. (2009). The nature of collective resilience, Survivor reactions to the 2005 London Bombings. International Journal of Mass Emergencies, 27, 66-95.

Drury, J., Cocking, C., Reicher, S., Burton, A., Schofield, D., Hardwick, A., . . . Langton, P. (2009). Cooperation versus competition in a mass emergency evacuation: A new laboratory simulation and a new theoretical model. Behaviour research methods, 41(3), 957-970.

Dunand, F., & Guéguen, P. (2012). Comparison between seismic and domestic risk in moderate seismic hazard prone regions: the Grenoble City (France) test site. Natural Hazards and Earth System Sciences, 511-526.

Dunbar, R. I. (2019, August 18). The Social Brain Hypothesis and Human Evolution. Tratto da Oxford Research Encyclopedia of Psychology: https://oxfordre.com/psychology/view/10.1093/acrefore/9780190236557.001.0001/acrefore-9780190236557-e-44

ECA. (2019, August 23). How to Protect Yourself During an Earthquake. Tratto da Earthquake Country Alliance, www.earthquakecountry.org: http://www.earthquakecountry.org/dropcoverholdon/

EC-JRC. (2018). Atlas of the Human Planet 2010, A World of Cities, JRC Science for Policy Report. Luxembourg: Europen Comission.

Ein-Dor, T., Mikulincer, M., Doron, G., & Shaver, P. R. (2010). The Attachment Paradox: How can so many of us (the insecure ones) have no adaptive advantages? Perspectives on Psychological Science, 5(2), 123-141.

Ein-Dor, T., Mikulincer, M., Doron, G., & Shaver, P. R. (2010). The Attachment Paradox: How Can so many of us (the insecure ones) have no adaptive advantages? Perspectives in Pyschological Sciences 5.2, 123-141.

Ein-Dor_a, T. (2014, December 10). Facing danger: how do people behave in times of need? The case of adult attachment styles. Fronteirs in Psychology, 5(1452).

Ein-Dor_b, T. (2014). Social defense theory: How a mixture of personality traits in group contexts may promote our survival. In M. Mikulincer, & P. R. Shaver, Mechanisms of social connection: From brain to group (p. 357-372). Washington, DC, US: Americal Psychological Association.

Engineering Toolbox. (2018, November 7). Inverse Square Law. Tratto da Engineering Toolbox: https://www.engineeringtoolbox.com/inverse-square-law-d_890.html

Fahy, R. F., & Proulx, G. (2001). Toward creating a database on delay times to start evacuations and walking speeds for use in evacuation modeling. 2nd International Symposium on Human Behaviour in Fire, (p. 175-183). Boston, MA. USA.

Farooq, B., Bierlaire, M., Hurbubia, R., & Flötteöd, G. (2013). Similation based population synthesis. Transportation resesarch part B/ Methodological, 58, 243-263.

Fekete, A., Tzavella, K., Armas, I., Binner, J., Garschagen, M., Gupponi, C., . . . Serre, D. (2015). Critical Data Source; Tool or Even Infrastructur? Challenges of Geographic Information Systems and Remote Sensing for Disaster Risk Governance. ISPRS International Journal of Geo-Information, 4, 1848-1869.

FEMA. (2019, January 14). Building Codes. Tratto da FEMA: https://www.fema.gov/building-codes

Ferber, J. (2007). Multi-agent concepts and methodologies. In D. Phan, & F. Amblard, Agent-based modelling and simulation in the social and human sciences (p. 7 - 33). Oxford, UK: The Bardwell Press.

FHWA. (2018, October 15). 5.1 No-notice urban evacuation In: Managing Pedestrians During Evacuation of Metropolitan Areas. Tratto da Federal Highway Admistration (FHWA), US Dept. of Tranportation: https://ops.fhwa.dot.gov/publications/pedevac/5_approaches.htm

Flight Safety Foundation. (2004). Attemps to retrieve carry-on baggage increase risks during evacuation. Cabin Crew Safety, Flight Safety Foundation 39.3.

Fontaine, M., Love, S. A., & Latinus, M. (2017). Familiarity and voice representation: from acoustic-based representation to voice averages. Frontiers in Psychology, 8.
Fotios, S., & Boyce, P. (2015). Understanding lighting for pedestrians, ILP discussion document. The Institure of Lighting Professionals.
Fotios, S., Yang, B., & Uttley, J. (2015). Observing other pedestrians: Investigating the typical distance and duration of fixation. Lighting Research and Technology Vol. 47, 548 - 564.
Franklin, J. (2015, September 25). How did Chile manage to survive its recent earthquake virtually unscathed? Tratto da The Guardian: https://www.theguardian.com/cities/2015/sep/25/how-chile-survive-earthquake-virtually-unscathed?CMP=share_btn_tw
Franz, G., Mallot, H. A., & Wiener, J. M. (2005). Graph-based models of spac in architecture and cognitive science - a comparative analysis. INTERSYMP - 2005, 17th International Conference on Systems Research, Informatics and Cybernetics, Special Focus Symposium on Systems Research in the Architecture, Engineering and Construction (AEC) of Built Environments. Baden-Baden, Germany.
Fraser, S. A., Wood, N. J., Johnston, D. M., Leonard, G. S., Greening, P. D., & Rosetto, T. (2014). Variable population exposure and distributed travel speeds in least-cost tsunami evacuation modelling. Natural Hazards and Earth System Sciences 14.11, 2975-2991.
Fraser_a, S., Leonard, G. S., Matsuo, I., & Murakami, H. (2012). Tsunami Evacuation: Lessons from the Great East Japan earthquake and tsunami of March 11th 2011. GNS Science Report.
Fraser_b, S., Leonard, G. S., Matsuo, I., & Murakami, H. (2012). Tsunami Evacuation: Lessons from the Great East Japan earthquake and tsunami of March 11th 2011. GNS Science Report.
Frey, B. S., Savage, D. A., & Torgler, B. (2011). Behaviour under extreme conditions: the titanic disaster. Journal of Economic Perspectives 25.1, 209-22.
Fritz, S., & Lusardi, M. (2009). White Paper: Walking Speed: the Sixth Vital Sign. Journal of Geriatric Physical Therapy, 32, 2 - 5.
Frydenlund, E., Elzie, T., Collins, A. J., & Robinson, R. M. (2014). A Hybridized approach to validation: The role of sociological research methods in pedestrian modelling. Transportation Research Procedia, 2, 697 - 705.
FSF. (2004). Attemps to retrieve carry-on baggage increase risks during evacuation. Cabin Crew Safety, Flight Safety Foundation (FSF) 39.3.
Gahegan, M. (2017). Our GIS is too small. The Canadian Geographer, 62(1).
Gaillard, J. (2019). Disaster studies inside out. Disasters, S7 - S17.
Gaire, N., Song, Z., Christensen, K. M., Sharifi, M. S., & Chen, A. (2018). Exit choice behaviour of pedestrians involving individuals with disabilities during building evacuations. Transportation Research Records.
GAMA Development Team. (2018, November 20). Operators. Tratto da GAMA Platform Documentation: https://gama-platform.github.io/wiki/OperatorsSplitted#flip
Gavrilets, S. (2015). Collective action and the collaborative brain. Journal of the Royal Society, Interface, 12(102).
Geller, R. J. (1997). Earthquake prediction: a critical review. Geophys. J. Int., 131, 425-450.
GEO-JRC. (2017). Global Exposure to Natural Hazards, Global Open Data for Monioring the Sendai Targets. Group on Earth Observations (GEO), EC-JRC.
Gilbert, N. (2007). Agent based models. London: Sage.
Gilbert, N., & Troitzsch, K. G. (2005). Simulation for the social scientist 2nd Edition. New York, NY, USA: Open University Press.
Giovinazzi, S., & Lagomarsino, S. (2004). A macroseismic method for the vulnerability assessment of buildings. 13th World Conference on Earthquake Engineering. Vancouver, B.C., Canada.
Glatron, S., & Beck, E. (2008). Evaluation of socio-spatial vulnerability of city dwellers and analysis of risk perception: industrial and seismic risks in Mulhouse. Natural Hasards and Earth System Sciences, 1029-1040.
Gobbini, M. I., Gors, J. D., Halchenko, Y. O., Rogers, C., Guntupalli, S., Hughes, H., & Cipolli, C. (2013). Prioritized Detection of Personally Familiar Faces. PLoS One, 8(6).
Goetz, M., & Zipf, A. (2012). Using crowdsourced geodata for agents-based indoor evacuation simulations. ISPRS International Journal of Geo-Information, 186-208.
Goltz, J. D. (2017). Tsunam Tendenko: A Sociological Critique. Natural Hazards Review, 18(4).
Goodchild, M. (2005). Chapter 1. GIS Modelling Overview. In D. J. Maguire, & M. Batty, GIS, Spatial Analysis, and Modeling. Redlands, California: ESRI Press.
Goodchild, M. F. (2011). Challenges in geographical information science. Proceedings of the Royas Society A, 467, 2431 - 2443.
Google. (2018). GoogleMaps.
Grünthal, G. (1998). European Macroseismic Scale 1998 (Vol. 15). Luxembourg: Cahiers du Centre Européen de Géodynamique et de Séismologie.
Grünthal, G. (1998). European Macroseismic Scale 1998. Luxmbourg: European Seismological Comission.
Granovetter, M. S. (1973, May). The Strength of Weak Ties. American Journal of Sociology, 78(6), 1360-1380.
Grignard, A., Taillandier, P., Gaudou, B., Vo, D. A., & Drogoul, N. Q. (2013). GAMA 1.6: Advacing the Art of Complex Agent-Based Modeling and Simulation. International Conference on Principles and Practice of Multi-Agent Systems, 117-131.
Guéguen, P., Lutoff, C., Davoine, P., Taliercio, G., Cotton, F., & Cartier, S. (2009). Analyse de la vulnerabilité sismique dans un pays à seismicité odérée: le cas de Grenoble. In S. Becerra, & A. Peltier, Risques et environnement: recherches interdisciplinaires su la vulnérabilité des sociétés (p. 285-302). L'harmattan.
Guettiche, A., Guéguen, P., & Mimoune, M. (2017). Seismic vulnerability assessment using association rule learning: application to the city of Constantine, Algeria. Natural Hazards.

Gupta, A., & Zafar, S. (2016, March). Seismic Microzonation - Principles and Methodology. International Journal of Engineering Research and Application, 6(3), 9 - 14.
Hall, E. T. (1990). The Hidden Dimension. USA: Anchor Books.
Harland, K., Birkin, M., & Martin, D. (2014). Simulating the pulse of the city: Using a combined approach for modelling commuter patterns. 22nd GIS Reseach UK (GISRUK). Glasgow, UK.
Heath, S. E., Kass, P. H., Beck, A. M., & Glickman, L. T. (2001). Human and pet-related factors for household evacuation failure during a natural disaster. American Journal of Epidemiology, 153(7), 659-665.
Heath, S. E., Kass, P. H., Beck, A. M., & Glickman, L. T. (2001). Human and Pet-related risk factors for household evacuation during natural disaster. American Journal of Epidemiology 153.7, 659-665.
Heide, E. A. (2004). Common misconceptions about Disasters: Panic, the "Disaster Syndrome," and Looting. In O. M, The First 72 Hours: A Community Approach to Disaster Preparedness (p. 340-380). Lincoln (Nebraska): iUniverse Publishing.
Helbing, D., & Johansson, A. (2013). Pedestrian, Crowd and Evacuation Dynamics. arXiv:1309.1609v1 [physics.soc-ph] 407.
Helbing, D., Farkas, I. J., Molnar, P., & Vicsek, T. (2002). Simulation of Pedestrian Cowds in Normal and Evacuation Situations. In M. Schreckenberg, & S. D. Sharma, Pedestrian and Evacuation Dynamics. Springer.
Helbing, D., Farkas, I., & Vicsek, T. (2000). Simulating Dynamical Features of Escape Panic. Nature 407.
Hollogram Studio Viral. (2018, November 26). Earthquake in Mexico 7.1, as it happened in Mexico City's Main Square (September 19, 2017). Tratto da YouTube: https://www.youtube.com/watch?v=-9Bsq5IcrFA&t=138s
Hori, M., Ichimura, T., Wijerathne, L., Ohtani, H., Chen, J., Fujita, K., & Motoyama, H. (2018). Application of High Performance Computing to Earthquake Hazard and Disaster Mitigation in Urban Area. Frontiers in Built Environment 4.1, 1 - 13.
Humes, L. (2007). The contributions of audibility and cognitive factors to the benefit provided by amplified speech to older adults. Journal of the American Acadely of Audiology, 590-603.
Hurst, D. (2019, June 12). This is not a"what if" story': Tokyo braces for the earthquake of a century. Tratto da The Guardian: https://www.theguardian.com/cities/2019/jun/12/this-is-not-a-what-if-story-tokyo-braces-for-the-earthquake-of-a-century
Hussein, M. (2016). Development of Agent Based Simulation Model for Pedestrian Interactions. PhD Thesis. Vancouver, Canada: University of British Columbia.
Ibrion_a, M., & Paltrinieri, N. (2018). The Earthquake Disaster Risk in Japan and Iran and the Necessity of Dynamic Learnng from Large Disaster Earthquake Disasters over Time. IntechOpen.
Ibrion_b, M., Mokhtari, M., & Nadim, F. (2015, December 18). Earthquake disaster risk reduction in Iran: Lessons and "Lessons Learned" from three large eathquake disasters - Tabas 1978, Rudbar 1990, and Bam 2003. Intenational Journal Disaster Risk Science, 6(4), 415 - 427.
Ibrion_c, M. (2017, December 20). Earthquake Culture: A Significant element in earthquake disaster risk assessment and earthquake disaster risk management. Intechopen.
IGN. (2017). BDTOPO Institut National de l'Information Geographique et Forestiere.
Iliyas, F. T., & Mani, S. L. (2018). Hazard-centric evacuation experiments - a study on occupant responses to earthquake alarm. Disaster Advances, 11(4), 18-27.
INSEE. (2019, August 28). Rensement de la population 2013 - Base infra-communales (IRIS). Tratto da Institut national de la statistique et des études économiques: https://www.insee.fr/fr/statistiques/2386737
INSEE_b. (2019, August 28). IRIS. Tratto da Institut national de la statistique et des études économiques (INSEE): https://www.insee.fr/fr/metadonnees/definition/c1523
IRIS_a. (2019, August 15). Buildings and earthquakes - Which stands? Which falls? Tratto da https://www.iris.edu/hq/files/programs/education_and_outreach/retm/tm_100112_haiti/BuildingsInEQs.pdf
IRIS_b. (2019, August 11). How Often Do Earthquakes Occur. Tratto da IRIS Integrated Researh Institutions for Seismology: https://www.iris.edu/hq/inclass/fact-sheet/how_often_do_earthquakes_occur
IS0. (2019, September 4). Evacuation Assembly point, ISO 7010 . Tratto da International Standards Organisation, Online Browsing Platform: https://www.iso.org/obp/ui#iso:grs:7010:E007
ISTerre. (2019, August 27). Near Grenoble: the Belledone Bordering Fault. Tratto da Institute des Scicnes de la Terre (ISTerre): https://www.isterre.fr/english/formation-1275/sciences-pour-tous-tes/seismes-failles-ondes/article/a-proximite-de-grenoble-la-faille-bordiere-de-belledonne.html
Iwanaga, S., & Matsuura, Y. (2014). Considering psychological conditions in a tsunami evacuation simulation. In A. Laurent, O. Strauss, B. Bouchon-Meunier, & Y. R. R, Information Processing and Management of Uncertainty in Knowledge-Based Systems. IPMU 2014. Communications in Computer and Information Science (Vol. 442, p. 437). Springer, Cham.
Jaiswal_1, K., & Wald, D. J. (2008). Creating a global building inventory for earthquake loss assessment and rsk management. US Geological Survey.
Jaiswal_2, K., Wald, D. J., & Hearne, M. (2009). Estimating Casualties for Large Earthquakes Worldwide Using an Empirical Approach (Open-File Report 2009 - 1136). US Geological Survey.
JICA. (2004). Chapter 2. Earthquake Damage Scenario, Earthquake Impact Reduction Study for Metropolitan Manila, Republic of the Philippines. Tratto da Open JICA Report: http://open_jicareport.jica.go.jp/pdf/11763737_02.pdf
JMA. (2018). Tables explaining the JMA intensity scale.
Johnson, C. W. (2006). What are Emergent Properties and HOw do they affect the engineering of complex systems. Reliability Engineering, System Safety, 91(12).
Johnson, P. F., Johnson, C. E., & Sutherland, C. (2011). Stay or GO? Human behaviour in major evacautions. In R. D. Peacock, E. D. Kuligowski, & J. D. Averill, Pedestrian Evacuation Dynamics (p. 675-684). Springer Science+Business Media.

Johnston, D., & S., L. (2009). The tragedy of cognition: psychological biases and environmental inaction. Current Science 97.11, 1593-1603.
Johnston, D., Standring, S., Ronan, K., Lindell, M., Wilson, T., Cousins, J., . . . Bissel, R. (2014). The 2010/2011 Canterbury Earthquakes: context and cause of injury. Natural Hazards, 73, 627-637.
Jon, I., Lindell, M. K., Prater, C. S., Huang, S.-K., Wu, H.-C., Johnston, D. M., . . . Potter, S. H. (2016). Behavioural response in the immediate aftermath and shaking: earthquakes in Christchuch and Wellington, New Zealand and Hitachi, Japan. International Journal of Environmental Research and Public Health 13.11, 1137.
JRC-EC. (2018, October 1). Eurocodes, Building the Future. Tratto da Joint Resesarch Center, Eurocodes: http://eurocodes.jrc.ec.europa.eu/showpage.php?id=138
Kady, R. A., & Davis, J. (2009). The effect of occupant characteristics on crawling speed in evacuation. Fire Safety Journal 44, 451-547.
Kawahata, Y., Mizuno, T., & Ishii, A. (2017). Measurement of human activity using velocity GPS data obtained from mobile phones. Physics and Society arXiv:1706.04301 [physics.soc-ph].
Kenny, C. (2009). Why do people die in earthquakes? The costs, benefits and Institutions of disaster risk reduction in developing countries. The World Bank.
Keyes, H., & Zalicks, C. (2016). Socially important faces are processed preferentially to other familiar and unfamiliar faces in a priming task across a range of viewpoints. PLoS ONE, 11(5), 1 - 12.
Khan, A. A., & Noji, E. K. (2016). Hajj stampede disaster, 2015: Reflections from the frontlines. American Journal of Disaster Medicine, 10(3).
Klepeis, N. E., Nelson, W. C., Ott, W. R., Robinson, J. P., Tsang, A. M., Switzer, P., . . . Engelmann, W. H. (2001). The national human activity pattern survey (NHAPS), A Resource for Assessing Exposure to Environment Pollutants. Journal of Exposure Analyis and Environmental Epidemiology, 11, 231 - 252.
Kneidl, A., Hartmann, D., & Borrman, A. (2012). Using multi-scale model fo simulating pedestrian behavior. PED 2012 - Pedestrian and Evacuation Dynamics. Zurich.
Kok, R., Taubert, J., Burg, E. v., Rhodes, G., & Alais, D. (2017). Face familiariy promotes stable identity recognition, exploring face perception using serial dependence. Royal Society Open Science 4:160685, 1-13.
Kolarik, A. J., Moore, B. C., Zahorik, P., Cirstea, S., & Pardhan, S. (2016). Auditory distance perception in humans: are review of cues, development, neuronal bases, and effects of sensory loss. Attention, Perception and Psychophysics, Springer, 78, 373 - 395.
Kormanova, A. (2013). A review on macroscopic pedestrian flow modelling. Acta Informatica Pragensia, 2(2), 30-59.
Krüchten, C. v., & Schadschneider, A. (2017). Empirical study on social groups in pedestrian evacuation dynamics. Physica A: Statistical Mechanics and its Applications, 475, 129 - 141.
Kravari, K., & Bassiliades, N. (2015, January 31). A Survey of Agent Platforms. Journal of Artificial Societies and Social Simulation , 18(1).
Kriegstein, K., & Giraud, A.-L. (2006). Implicit multisensory associations influence voice recognition. PLoS Biology, 4(10), 1809-1820.
Kuligowski, E. D., & Hoskings, B. L. (2010). Occupant Behaviour in a High-Rise Office Building Fire, NIST Technical Note 1664. Washington D.C.: National Institute of Standards and Technology (NIST).
Kuligowski, E. D., Peacock, R. D., Reneke, P. A., Weiss, E., Overholt, K. J., Elkin, R. P., & Spearpoint, M. (2015). Movement on Stairs During Building Evacuations, Technical Note 1839 NIST,. Washington, DC: National Institute of Standards and Technology.
Kunze, L., Doreswamy, K. K., & Hawes, N. (2014). Using Qualitative Spatial Relations for Indirect Object Search. IEEE International Conference on Robotics and Automation (ICRA). Hong Kong, China.
Kuwata, Y., & Tanaka, S. (2002). Instantaneous instrumental seismic intensity and evacuation. Journal of Natural Disaster Science, 35 - 42.
Lacasse, S. (2016). Hazard, Reliability and Risk Assessment - Research and Practice for Increased Safety. Proceedng of th 17th Nordic Geotechnical Meeting, Challenges in Nordic Geotechnic. Reykjavik: NGM 2016 .
Lacassin, R., Tapponnier, P., Meyer, B., & Armijo, R. (2001). Was the Tévarsse thrust the source of the 1909 Lamebesc (Provence, France) earthquake? Historical and geomorphic evidence. Earth and Planetary Sciences, 333, 571-581.
Larusdottir, A. R., & Diderichs, A. S. (2011). Evacuation Dynamics of Children - Walking Speeds, Flows, Through Doors in Daycare Centers. In R. D. Peacock, K. E. D, & J. D. Averill, Pedestrian Evacuation Dynamics (p. 139-147). Springer Science+Business Media.
Lavan, N., Scott, S. K., & McGettigan, C. (2016). Impaired generalization of speaker identity in the perception of familiar and unfamiliar voices. Journal of Experimental Psychology, 145(12), 1604-1614.
Legi il Firenzepost. (2016, September 1). Intervento dei vigili del fuoco di Firenze a Amatrice. Tratto da YouTube: https://www.youtube.com/watch?v=G1Q3HSJTay8
Liccione, D., Moruzzi, S., Rossi, F., Manganaro, A., Porta, M., Nugrahaningsih, N., . . . Allegri, N. (2014). Familiarity is not notoriety: phenoological accounts of face recognition. Fronteirs in Human Neuroscience 8.672, 1-10.
Liccione_a, D., Moruzzi, S., Rossi, F., Manganaro, A., Porta, M., Nugrahaningsih, N., . . . Allegri, N. (2014). Familiarity is not notoriety: phenomological accounts of face recognition. Fronteirs in Human Neuroscience 8.672, 1-10.
Liccione_b, D., Moruzzi, S., Rossi, F., Manganaro, A., Porta, M., Nugrahaningsih, N., . . . Allegri, N. (2014). Familiarity is not notoriety: phenomological accounts of face recognition. Fronteirs in Human Neuroscience 8.672, 1-10.
Lindell_a, M. K., Prater, C. S., Wu, H. C., Huang, S. -K., Becker, J. S., & Shirosita, H. (2016, January). Immediate behavioural responses to earthquakes in Christchurch, New Zealand, and Hitachi, Japan. T, 40(1), 85 - 111.
Lindell_b, M. K., Prater, C. S., Wu, H. C., Huang, S. -K., Becker, J. S., & Shirosita, H. (2016). Immediate behavioural responses to earthquakes in Christchurch, New Zealand, and Hitachi, Japan. Disasters 40.1, 85-11.

Liu, M., Zeng, W., Chen, P., & Wu, X. (2017). A microscopic simulation model for pedestrian-pedestrian and pedestrian-vehicle interactions at crosswalks. PLoS ONE.
Liu, Z., Jacques, C., Szyniszewsky, S., Guest, J. K., Schafer, B. W., Igusa, T., & Mirtani-Reiser, J. (2016). Agent-based simulation of building evacuation after an earthquake: coupling human behaviour with structural response. Natural Hazards Review, 17(1).
Loftus, G. R., & Harley, E. M. (2005). Why is it easier to identify someone close than far away? Psychonomic Bulletin & Review, 12(1), 43 - 65.
Lou, L., Zhou, S., Cai, W., Low, M. Y., Tian, F., Wang, Y., . . . Chen, D. (2008). Agent-based human behaviour modeling for crowd simulation. Computer Animation and Virtual Worlds, 19, 271-281.
Lu, X., Bengtsson, L., & Holme, P. (2012). Predicatability of population displacement after the 2010 Haiti earthquake. PNAS.
Lumbroso, D., Johnston, W., Bruijn, K., Di Mauro, M., Lence, B., & Tagg, A. (2010). Modelling Mass Evacuations to Improve the Emergency Planning For Floods In the UK, The Netherlands And North America.
M., L. J., Klatzky, R. L., Golledge, R. G., & Philbeck, J. W. (1999). Human Navigation by Path Integration. In Wayfinding Behaviour: Cognitive Mapping and other Spatial Processes (p. 125 - 151). Baltimore, MD: Johns Hpkins University Press.
Ma, H. K. (2017). The Development of Altruism with Special Reference to Human Relationships: A 10-Stage Theory. Frontiers in Public Health.
Ma, T., Wang, Q., & Larrañaga, M. D. (2011). The Utility of the Panic Model on Simulating Crowd Disasters. Proceedings, Fire and Evacuation Modelling Technical Confence 2011. Baltimore, Maryland.
Maertens, H. (1884). Der Optische Masstab in de Bildenden Kuenter 2nd edn. Wasmuth, Berlin.
Manley, M. (2012). EXITUS: An Agent-based Evacuation Simulation Model for Heterogenous Populations. Doctoral Disseratation. Logan, Utah, USA: Utah State University.
Marceau, D. J., & Beneson, I. (2011). Challenges and perspectives in Geosimulation. In A. G. Models.
Martinez-Gil, F., Lozano, M., Garcia-Fernandez, I., & Fernandez, F. (2017). Modelling, Evaluation and Scale on artificial Pedestrians: A literature review. ACM Computing Surveys, 50(5).
Mawson, A. R. (2005). Understanding mass panic and other collectiver responses to threat and disaster. Psychiatry 68.2.
Mawson_a, A. R. (2005). Understanding Mass Panic and Other Collective Responses to Threat and Disaster. Psychiatry, 68(2), 95 - 113.
Mawson_b, A. R. (2007). Chapter 10. Panic as Stimulation Seeking. In A. R. Mawson, Mass Panic and Social Attachment, The Dynamics of Human Behaviour (p. 113-119). Ashgate.
McBride, E., Davis, A. W., Lee, J. H., & Goulias, K. G. (2016). Spatial transferability using synthetic population generation methods UCTC-FR-2016-05. Santa Barbara, California: University of California Transportation Center.
McPartland, B. (2014, April 8). One day a deadly earthquake will hit France. The Local, FR.
Menin, A., Nedel, L., Davoine, P.-A., & Chardonnel, S. (2018). Exploring shfting densities hrough a movement-based cartographic interface. 10th International Conference on Geographic Information Science. Melbourne, Australia.
Mesa, S. d. (2016, October). The relevance of data integration during the August 24th 2016 earthquake in Central Apennines (Italy). Tratto da European Plate Observing System (EPOS), The EPOS Newsletter: https://www.epos-ip.org/relevance-data-integration-during-august-24th-2016-earthquake-central-apennines-italy
Mihalic, S., Ostric, M., & Krkac, M. (2011). Seismic microzonation: A review of principles and practice. Geofizika, 28.
Mikami_a, S., & Ikeda, K. (1985). Human response to disasters. International Journal of Mass Emergencies and Disasters, 107 - 132.
Mikami_b, S., & Ikeda, K. (1985). Human response to disasters. International Journal of Mass Emergencies and Disasters, 107-132.
Mikulincer, M., & Shaver, P. R. (2007). Attachment in Adulthood, Structure, Dynamics and Change. The Guilford Press.
Misyak, J. B., Melkonyan, T., Zeitoun, H., & Charter, N. (2014, October). Unwritten rules: virtual bargaining underpins social interaction, culture and society. Trends in Cognitive Sciences, 18(10), 512-519.
Mobbs, D., Hagan, C. C., Dalgleish, T., Silston, B., & Prévost, C. (2015). The ecology of human fear: survival optimization and the nervous system. Fronteirs in Neuroscience, 9(55).
Moughtin, C. (2003). Urban Design Street and Square 3rd Edition. Burlington, MA: Architectural Press.
Moussaid, M., Perozo, N., Garnier, S., Helbing, D., & Theraulaz. (2010). The walking behaviour of pedestrian social groups and its impact on crowd dynamics. PLoS ONE.
Moussaïd, M., & Trauernicht, M. (2016, September 15). Patters of cooperation during collectiv emegencies in the help-or-escape social dilemma. Scientific Reports, 6.
Murata, A., Nakamura, T., & Karwowski, W. (2015). Influence of Cognitive Biases in Distorting Decision Making and Leading to Critical Unfavorable Incidents. Safety 1.1, 44.
Musson, R. M. (2012). Intensity and Intensity Scales. In R. M. Musson, & I. Cecić, New Manual of Seismological Observatory Practice (p. 1 - 41). Potsdam : Deutsches GeoForschungsZentrum GFZ.
Musson, R., Grünthal, G., & Stucchi, M. (2009). The comparision of macroseismic intensity scales. Journal of Seismology, Springer Verlag, 413 - 428.
Nasi, M. (2013). Pedestrian Steering Behaviou Modelling within the build environment. Doctoral Dissertation. Australia: Deakin University.
Natapov, A., Czamanski, D., & Fisher-Gewirtzlan, D. (2016, January). Visiospatial search in urban environment simulated by random walks. International Journal of Design Creativity and Innovation.
Nath, S. K., & Thingbaijam, K. K. (2009). Seismic hazard assessment - a holistic microzonation approach. Natural Hazards Earth System Sciences, 9, 1445-1459.
Natu, V., & O'Toole, A. J. (2011). The neural processing of familiar and unfamiliar faces: a review and synopsis. British Journal of Psychology, 102, 726 - 747.

Ngai, K. M., Burkle, F. J., Hsu, A., & Hsu, E. B. (2009). Human Stampeds: A systematic Review of Historica and Peer-Reviewed Sourc. Disaster Medicine and Public Health Preparedness, 3(4), 191 - 195.
Nichols, T. F., & Powers, T. R. (1964). Moonlight and night visibility, Research memorandum, US Army training center human research unit. Presidio of Monterey, California.
Nienhuys, S. (2015). Seismic Building Cods, Global and Regional Overview. UK: Department of International Development.
No Comment TV. (2018, November 26). 8.8 Magnitude Earthquake hits Japan - no comment. Tratto da YouTube: https://www.youtube.com/watch?v=T-GpHf6fEmY
Norton, I., Schreet, J. V., Aitken, P., Herard, P., & Lajolo, C. (2013). Classification and minimum standads for foreign medical teams in sudden onset disasters. Technical Report. Health Cluster, World Health Organization.
Nwe, Z. Z., & Tun, K. T. (2016). Seismic Hazard Analysis using AHP-GIS. Internation Journal of Research in Chemical, Metallurgical and Civil Engineering (IJRCMCE), 184-189.
OECD. (2015). Ageing in Cities. Paris: OECD Publishing.
Ohta, Y., & Omote, S. (1977). An investigation into human psychology and behaviour during an earthquake. Proceedings of the Sixth World Conference on Earthquake Engineering v. 1, (p. 702-708). Meerut India.
Okaya, M., & Takahashi, T. (2011). Human relationship modelling in agent-based crowd evacuation simulation. In H. J. Kinny D., Agents in Principle, Agents in Practice. PRIMA 2011. Lecture Notes in Computer Science (Vol. 7047). Berlin, Heidelberg: Springer.
Open Data Grenoble-Alpes-Metropole. (2018). Voies et adresses. Tratto da http://data.metropolegrenoble.fr: http://data.metropolegrenoble.fr/ckan/dataset/voies-et-adresses
OpenStreetMap & Contributors. (2018, October 30). Planet dump retrieved from https://planet.osm.or url:https://openstreetmap.org, Shapefile. Tratto da OpenStreetMap: https://openstreetmap.org
OSHA. (2019, August 23). Earthquake Preparedness and Response. Tratto da US Department of Labor, Occupational Safety and Health Administration (OSHA): https://www.osha.gov/dts/earthquakes/preparedness.html
O'Toole, A. J., Philipq, J., Weimer, S., Roark, D. A., Ayyad, J., Barwick, R., & Dunlop, J. (2011). Recognizing people from dynamic and static faces and bodies. Disecting identity with a fusion approach. Vision Research 51, 74-83.
Pan, X. (2006). Computational modelling of human and social behaviours for emergency egress analysis. Doctoral Dissertation. USA: Stanford University.
Papelis, Y. E., Bair, L. J., Manepalli, S., Madhavan, P., Kady, .., & Weisel, E. (2011). Modelling of human behaviour in crowds using a cognitive feedback approach. In R. D. Peacock, E. D. Kuligowski, & J. D. Averill, Pedestrian Evacuation Dynamics (p. 265 - 273). Springer Science+Business Media.
Peacock, R. D., Hoskins, B. L., & Kuligowski, E. D. (2011). Overall and Local Movement Speeds During Fire Drill and Evacuations in Buildings up to 31 Stories. In .. D. Peacock, & E. D. Kuligowski, Pedestrian Evacuation Dynamics (p. 25 - 35). Springer Science+Business Media.
Peacock, R. D., Kuligowski, E. D., & Averill, J. D. (2011). Pedestrian Evacuation Dynamics. Springer.
Pearsons, K. S., Bennett, R. L., & Fidell, S. (1977). Speech levels in various noise environments, Environmental Health Effects Research Series. Washington DC: Office of Health and Ecological Effects, Environmental Protection Agency.
Pesaresi, M., Ehrlich, D., Kemper, T., Siragusa, A., Florczyk, A. J., Freire, S., & Corbane, C. (2017). Atlas of the Human Planet, 2017, Global Exposure to Natural Hazards, JRC Science for Policy Report. Luxembourg: U-JRC.
Philips, I., Clarke, G., & Watling, D. (2017). A fine grained hybrid spatial microsimulation technique for generating detailed synthetic individuals from multiple data sources: An application to walking and cycling. International Journal of Microsimulation, 10(1), 167-200.
Poal, P. (1990). Introduction to the theory and practice of crisis intervention. Quaderns de Psicologia, 10, 121 - 140.
Pokhrel, S. (2018, November 26). YouTube. Tratto da Nepal Earthquake 2015 CCTV Live Video of Asan 25/4/2015: https://www.youtube.com/watch?v=TqBEizoFUd4
Poorazizi, M. E., Hunter, A., & Steiniger, S. (2015). A volunteered geographic information frameworkd to enable bottom up disaster management platforms. ISPRS International Journal of Geo-Information, 1389-1422.
Prati, G., Catufi, V., & Pietrantoni, L. (2012). Emotional and behavioural reactions to tremors of the Umbria-Marche earthquake. Disasters 36.3, 439-451.
QGIS Development Team. (2018). QGIS Geographic Information System. Open Source Geospatial Foundation Project. . Tratto da https://qgis.org/en/site/: http://qgis.osgeo.org
Quest, W., Azzaro, R., Tertulliani, A., Bernardini, F., Camassi, R., & Del Mese, S. (2016). The 24 August 2016 Amatrice earthquake: macroseismic survey in the damage area and EMS intensity assessment. Annals of Geophysics, 59(Fastrack 5).
Rahm, J., & Johansson, M. (2018). Assessing the pedestrian response to urban outdoor lighting: A full-scale laboratory study. PLoS ONE, 13(10).
Rai, S., & Wong, K. (2009). Agent base simulation for infrastructure protection and emergency evacuation training. Computer Games and Applied Technology.
Ramirez, M., & Peek-Asa, C. (2005). Epidemiology of Traumatic Injuries from Earthquakes. Epidemiology of Traumatic Injuries from Earthquakes, 27.
Rezaie, F., & Panahi, M. (2015). GIS modelling of seismic vulnerability of residential fabrics considering geotechnical, structural, social and physical distance indicators in Tehran city using multi-criteria decision-making techniques. Natural Hazards and Earth System Sciences, 15(3), 461-474.
Riboldi, A. (2014). Pedestrian dynamics: modelling and calibration of a 2-dimensional cellular automata model. PhD Thesis. Milano, Italy: Poitecnico di Milano.
Riedel, I., Guéguen, P., & Dunand, F. C. (2014). Macroscale Vulnerability Assessment of Cities using Association Rule Learning. Seismological Research Letters, 295-305.

Riedel, I., Guéguen, P., Mura, M. D., Pathier, E., Leduc, T., & Chanussot. (2014). Seismic vulnerability assessment of urban environent in moderate-to-low seismic hazard regions using association rule learning and support vector machine methods. Nat Hazards.

Riedel_a, I., Guéguen, P., Mura, M. D., Pathier, E., Leduc, T., & Chanussot, J. (2015, March). Seismic vulnerability assessment of urban environments in moderate-to-los seismic hazard regions using association rule learning and support vector machine methods. Natural Hazards, 76(2), 1111-1141.

Rieldel, I., Gueguen, P., Mura, M. D., Pathier, E., Leduc, T., & Chanussot, J. (2014). Seismic vulnerability assessment or urban environments in moderate-to-low seismic hazad regions using association rule learning and support vector machine methods. Natural Hazards.

Roan, T. -R. (2013). Developing an agent based evacuation simulation model based on the study of human behaviour in fire investigation reports. Doctoral Dissertation. London, UK: University College London.

Robinson, T. R., Rosser, N. J., Densmore, A. L., Oven, K. J., Shrestha, S. N., & Guragain, R. (2018). Use of Scenario ensembles for deriving seismic risk. PNAS, 115(41).

Rojo, M. B., Beck, E., & Lutoff, C. (2017). The street as an area of human exposure in an earthquake aftemath: the case of Lorca, Spain, 2011. Natural Hazads and Earth System Sciences.

Ronchi, E., Kuligowski, E. D., Reneke, P. A., Peacock, R. D., & Nilsson, D. (2013). The process of verification and validataion of building fire evacuation models. National Institute of Standards and Technology (NIST), US Dept. of Commerce.

Rudnick, J., & Gaspari, G. (2004). Elements of the Random Walk, An Introduction for Advanced Students and Researchers. Cambridge University Press.

Sabillo, K. A. (2015, July 30). The Big One Could kill 34,000 in the Philippines. Tratto da gt government technology Emergency Management: https://www.govtech.com/em/disaster/The-Big-One-Could-Kill-34000-in-the-Philippines.html

Salameh, C., Bard, P.-Y., Builler, B., Harb, J., Cornou, C., Gérard, J., & Almakai, M. (2017). Using ambient vibration measurements for risk assessment at an urban scale: from numerical proof of concept to Beirut case study (Lebanon). Earth, Planets and Space 69:60.

Salameh, C., Guiller, B., Harb, J., Cornou, C., Bard, P.-Y., Voisin, C., & Mariscal, A. (2016). Seismic response of Beirut (Lebanon) buildings: instrumental results from ambient vibrations. Bullettin of Earthquake Engineering.

Salthouse, T. A., Hancock, H. E., Meinz, E. J., & Hambrick, D. Z. (1996). Interrelations of Age, Visual Acuity and Cognitive Functioning. Journal of Gerontology, 51B(6), 317 - 330.

Samuelson, D. A. (2011). Next steps for agent-based simulations of mass egress. In R. D. Peacock, E. D. Kuligowski, & J. D. Averill, Pedestrian Evacuation Dynamics (p. 871-874). Springer Science+Business Media.

Santarelli, S., Bernardini, G., & Quagliarini, E. (2018). Earthquake building debris estimation in historic city centres: From real world dat to experimental-based criteria. International Journal of Disaster Risk Reduction, 281-291.

Saputra, A., Rahardianto, T., Revindo, M. D., Delikostidis, I., Hadmoko, J. S., & Gomez, C. (2017). Seismic vulnerability assessment of residential buildings using logistic regression and geographic information syste (GIS) in Planet Sub District (Yogyakarta, Indonesia). Geoenvironmental Disasters 4:11, 1-33.

Sargent, R. G. (2000). Verification, validation and accreditation of simulation models. Proceedings of the 2000, 32nd Winter Simulation Conference (p. 50-59). Orlando, Florida: Society for Computer Simulation International.

Scannel, L., & Gifford, R. (2013). The Psychology of place attachment. In Environmental Psychology: Principles and Practice 5th Edition Ed. Gifford. Optimal Books.

Schlesinger, E. A. (1979). Terminology for model credibility. Simulation, 32(3), 103-104.

Schmidth, N. B., Richey, J. A., Zvolensky, M. J., & Maner, J. K. (2008). Exploring Human Freeze Responses to a Threat Stressor. Journal of behavior therapy and experimental psychiatry, 39(3), 292-304.

Seismology Research Centre. (2019, August 8). Earthquake Location. Tratto da Seismology Research Centre: https://www.src.com.au/earthquakes/seismology-101/earthquake-location/

Sekimoto, Y. (2013). Relationship of people and infrastructure during the 3.11 earthquake with information technology as mediating channel. Special . Journal of JSCE, 1, 276-285.

Senouci, A. B.-Y., Beck, E., Farsi, M. N., & Cartier, S. (2018). Mapping seismic vulnerability at urban scale: Discussion on relevant cartography representations and smoothing for urban planning purposes on the Oran case study. Soil Dynamics and earthquake Engineering 115, 545 - 563.

Senouci, A., Bard, P.-Y., Farsi, M. N., & Beck, E. (2013). Robustness and uncertainties of seismic damage estimates at urban scale: A methodological compaison on the example of the city of Oran (Algeria). Bullettin Earthquake Engineering, 1191-1215.

Shapira, S., Aharonson-Daniel, L., & Bar-Dayan, Y. (2018). Anticiapted behavioural response patterns to an earthquake: The role of personal household characteristics, risk perceptions, previous experience and preparedness. International Journal of Disaster Risk Reduction, 31, 1 - 8.

Shi, L., Xie, Q., Cheng, X., Zhou, Y., & Zhang, R. (2009). Developing a database for emergency evacuation model. Building and environment 44, 1724-1729.

Shimura, Y., & Yamamoto, K. (2014). Method of Seaching for earthquake disaster evacuation routes using multi-objective GA and GIS. Journal of Geographic Information System, 6, 492-525.

Sidtis, D., & Kreiman, J. (2011). In the beginning was the familiar voice: personally familiar voices in the evolutionary and contemporary biology of communication. Integrative Psychological and Behavioural Science, 42(1).

Sieben, A., Schumann, J., & Seyfried, A. (2017). Collective phenomena in crowds - where pedestrian dynamics need social psychology. PLoS ONE.

Singh, P. (2005). Population vulnerability for earthquake loss estimation using community base approach with GIS. Enchede, Netherlands: ITC.

Sivers, I. v., Templeton, A., Künzner, F., Köster, G., Druru, J., Philippindes, A., . . . Bungartz, H.-J. (2016). Modelling social identification and helping in evacuation simulation. arXiv:1602.00805 [physics.soc-ph].
Sivers, I. v., Templeton, A., Künzner, Köster, G., Drury, J., Philippides, A., . . . Bungartz, H.-J. (2016). Modelling social identification and helping evacuation simulation. Safety Science 89, 288-300.
Slovic, P., & Weber, E. U. (2002). Perception of Risk Posed by Extreme Events. Risk Management Strategies in an Uncetain World. Palisades, New York.
Smith, H. M. (2016). Matching novel face and voice identity using static and dynamic facial images. PhD Dissertation. Nottingham Trent University.
Smith, J. P. (2019, July 25). The world's most earthquake prone cities. Tratto da WorldAtlas.com: https://www.worldatlas.com/articles/cities-most-likely-to-be-hit-by-an-earthquake.html
So, E. K., & Pomonis, A. (2012). Derivation of Globally Applicable Casualty ates for use in Earthquake Loss Estimation Models. 15th World Conference on Earthquake Engineering.
Song, X., Zhang, Q., Sekimoto, Y., & Horanont, T. (2013). Modeling and Probabilistic Reasoning of Population Evacuation During Large-scale Disaster. KDD'13 Proceedings of the 19th ACM SIGKDD international conference on Knowledge Discovery and data mining, (p. 1231-1239). Chicago, Illinois, USA.
Sorensen, J. H. (1991). When shall we leave? Factors affecting timing of evacuation departures. International Jounal of Mass Emergencies and Disasters 9.2, 153-165.
Souza, P., Gehani, N., Wright, R., & McCloy, D. (2013). The advantage of knowing the talker. Journal of the American Academy of Audiology, 24(8), 689 - 700.
Spence, R., & So, E. (2011). Human Casualties in earthquakes: modeling and mitigation. Proceedings of the Ninth Pacific Conference on Earthquake Engineering Building an Earthquake-Resilient Society. Auckland, New Zealand.
Stern, E. K. (2003). Crisis Decisionmaking: A Cognitive Institutional Approach. Stockholm, Sweden: Swedish National Defence College.
Stevenage, S. V., Neil, G. J., Barlow, J., Dyson, A., Eaton-Brown, C., & Parsons, B. (2012). The effect of distraction on face and voice recognition. Psychological Research, 77(2), 167 - 175.
Stewart-Williams, S. (2007). Altruism among kin vs. nonkin: effects of cost of help and reciprocal exchange. Evolution and Human Behaviou 28 , 193-198.
Strauss, A. L. (1944). The literature on panic. Journal of Abnormal and Social Psychology 39, 317-328.
Suvilehto, J., Glerean, E., Dunba, R., Hari, R., & Nummenmaa, L. (2015). Typography of social touching depends on the bonds between humans. Proceedings of the National Academy of Sciences, USA, 112.45, 13811-13816.
Suvilehto, T., J., Glerean, E., Dunbar, R. R., Hari, R., & Nummenmaa, L. (2015). Topography of social touching depends on emotional bonds between humans. Proceedings National Academy of Scienes, 112 (45), 13811 - 13816.
Ta, X. H., Gaudou, B., Longin, D., Ho, T. V., & Nguyen, M. H. (2017). Modeling and Simulation of the Effects of Social Relation and Emotion on Decision Making in Emergency Evacuation. International Journal of Advanced Computer Science and Applications.
Tacikowski, P., & Ehrsson, H. H. (2016). Preferential processing of self-relevant stimuli occurs mainly at the perceptual and conscious stages of information processing. Consciousness and Cognition, 41, 139 - 149.
Taillandier, P. A., Amoroux, E., & Drogoul, A. (2010). GAMA: bringing GIS and multi-level capabilitie to multi-agent simulation. European Workshop on Multi-Agent Systems. Paris, France.
Tajfel, H., & Turner, J. C. (1986). The Social Identity Theory of Intergroup Behaviour In: Chapter 1. 7-24.
Teknomo, K., & Gerilla, G. (2008). Mesoscopic Multi-agent pedestrian simulation. In P. Inweldi, Transportation Research Trends. Nova Science Publishers Inc.
Teknomo, K., Takeyama, Y., & Inamura, H. (2010). Review on Microscopic Pedestrian Simulation Model. Proceedings Japan Society of Civil Engineering Conference . Morioka, Japan.
Thouvenot, F., Fréchet, J., Jenatton, L., & Gamond, J.-F. (2003). The Belledonne Border Fault: identification of an active seismic strike-slip fault in the western Alps. Geophysical Journal Interanational, 174-192.
Tokyo Metro. Govt. (2019). Tokyo Metropolitan Government Disaster Prevention Guide Book. Tokyo, Japan: Management section, Disaster Prevention Division, Tokyo Metropolitan Government.
Torrens, P. M. (2001). Can Geocomputation save urban simulation? Throw some agents into the mixture, simmer, and wait. Annual Association of American Geographers Meeting. New York.
Truong, H. V., Beck, E., Dugdale, J., & Adam, C. (2013). Developing a model of evacuation after an earthquake in Lebanon. Proceedings of the ISCRAM Vietnam 2013 Conference. Ha Noi, Vietnam.
Tsai, J., Fridman, N., Bowring, E., Brown, M., Epstein, S., Kaminka, G., . . . Tambe, M. (2011). ESCAPES - Evacuation Simulation with Children, Authorities, Parents, Emotions, and Social comparison. International Conference on Autonomous Agents and Multiagent Systems (AAMAS).
Turner, R. H., & Killian, L. M. (1987). Chapter 3. The Emergence of Collective Behaviour. In R. H. Turner, & L. M. Killian, Collective Behaviour (p. 35-51). Prentice Hall.
Turner, R. H., & M, K. L. (1987). Chapter 3. The Emergence of Collective Behaviour. In T. R. H, & L. M. Killian, Collective Behaviour (p. 35-51). Prentice Hall.
Twarogowska, M., Goatin, P., & Duvigneau, R. (2014). Comparative study of macroscopic pedestian models. Transportation Research Procedia, 2, 477 - 485.
UNCRD. (2008). From Code to Practice for Building Code Implementation and the Further Direction of Housing Earthquake Safety, Records and outcomes of International Symposium 2008 on Earthquake Safe Housing. Tokyo, Japan: United Nations Centre fo Regional Development (UNCRD), Disaster Management Planning Hyogo Office.
UNISDR_a. (2019, August 22). Terminology on Disaster Risk Reduction. Tratto da UNISDR: https://www.unisdr.org/we/inform/terminology
UNISDR_b. (2019, August 23). Exposure. Tratto da UNISDR, Prevention Web: https://www.preventionweb.net/risk/exposure

Urata, J., & Hato, E. (2012). Modelling the Cooperation Network Formation Process for Evacuation Systems Design in Areas with a Focus on Japanese Megadisasters. Leadership and Management in Engineering 12.4, 231-246.
USGS. (2018). The Modified Mercalli Intensity Scale. Tratto da USGS, Earthquake Hazards Program: https://earthquake.usgs.gov/learn/topics/mercalli.php
USGS_a. (2019, August 9). Magnitude/Intensity Comparison. Tratto da USGS Earthquake Hazards Program: https://earthquake.usgs.gov/learn/topics/mag_vs_int.php
USGS_b. (2019, August 16). What is and earthquake and what causes them to happen? Tratto da USGS: https://www.usgs.gov/faqs/what-earthquake-and-what-causes-them-happen?qt-news_science_products=0#qt-news_science_products
USGS_c. (2019, August 16). Magnitude, Earthquake Glossary. Tratto da USGS: https://earthquake.usgs.gov/learn/glossary/?term=magnitude
Vaez, S., Burke, M., & Alisadeh, T. (2016). Urban form and wayfinding: Review of Cognitive and Spatial Knowledge for Individuals' Navigation. Australasian Transport Research Forum.
van Westen, C. J., & Geordiadou. (2001). Spatial requireents and infrastructure for geological risk assessment. Proceedings workshop on natural disaster management, ISPRS Technical Committee VII, Ahmedabad, India. Ahmedabad, India: International Society for Photogrammetry and Remote Sensing (ISPRS).
Vaughan, E., & Turner, J. (2013, September 30). The Value and Impact of Building Codes. Tratto da Environmental and Energy sutyd Institute (EESI): https://www.eesi.org/papers/view/the-value-and-impact-of-building-codes
Ville de Grenoble. (2013). Ville de Grenoble, AVAP Aire de mse en Valeur de l'Architecture et du Patrimonie, Rapport de Presentation, Créée par délibération du conseil municipal du 18 novembre 2013. Grenoble, France.
Vistnes, J., Grubits, S. J., & He, Y. (2005). A stochastic approach to occupant pre-movement in fires. Fire Safety Science - Proceedings of the eight international symposium, 531 - 542.
Wang, P. (2016). Understanding social-force model in psychological principles of collective behaviour. arXiv:1605.05146 [physics.soc-ph]. Tratto da arXiv:1605.05146 [physics.soc-ph].
Wang, P., Luh, P. B., Chang, S. C., & Marsh, K. L. (2009). Efficient optimization of building emergency evacuation considering social bond or evacuees. IEEE International Conference on Automation Science and Engineering, (p. 250 - 255).
Waterson, N. P., & Pelliser, E. (2010). The STEPS Pedestrian Microsimulation Tool - A Technical Summary. Croyland, UK: Mott MacDonald Limited.
Weichsekgartner, J. (2016). Vulnerability as a concept in science and practice. Atlas of vulnerability and resilience, 20 - 21.
Weiss, K. M. (1978). A comparision of forward and backward procedures for the acquisition of response chains in humans. Journal of the Experimental Analyss of Behaviour, 29, 255 -259.
WHO-Europe. (2013). Combined or multiple exposure to health stressos in indoor built environments, An evidence-based review prepared fo the WHO training workshop "Multiple environmental exposures and risks". Bonn, Germany: World Health Organization, Regional Office for Europe.
Wilson, R., Erbach-Shoenber, E. z., Albert, M., Power, D., Tudge, S., Gonzalez, M., . . . Bengtsson, L. (2016). Rapid and near real-time assessment of population displacements using mobile phone data following disasters: The 2015 Nepar earthquake. PLoS Currents.
Wisner, B., Blaikie, P., Cannon, T., & Davis, I. (2003). At Risk, Second edition, Natural hazards, people's vulnerability and disasters.
Wood, M. M., & Glik, D. (2013). Engaging Californians in a Shared Vision for Resiliency, Practical Lessons Learned from Great California Shakeout, CSSC 12-02. California, USA: Alfed E. Alquist Seismic Safety Commission.
Wood, N. J., & C, S. M. (2012). Anisotropic path modelling to assess pedestian-evacuation potential from Cascadia-related tsunamis in the US Pacific Northwest. Natural Hazards 62.2, 275-300.
Wood, N., Ratliff, J., Schelling, J., & Weaver, C. (2014). Comparing population exposure to multiple Washington earthquake scenarios for prioritizing loss estimation studies. Applied Geography, 191 - 203.
Wooldridge, M., & Jennings, N. R. (1995, June). Intelligent Agents: Theory and Practice. The Knowledge Engineering Review, 10(2), 115-152.
Wright, G. A., & Rea, M. S. (1984). Age, a human factor in lighting. Proceedings of the 1984 conference on occupational ergonomics, (p. 508-512). Toronto, Ontario, Canada.
www.allaboutvision.com. (2018, November 13). Is 20/20 Vision "Perfect Vision". Tratto da allaboutvision.com: https://www.allaboutvision.com/eye-exam/2020-vision.htm
www.EngineeringToolBox.com. (2018, November 7). Voice level at distance. Tratto da The Engineering ToolBox: https://www.engineeringtoolbox.com/voice-level-d_938.html
www.sisfrance.net. (2018, August 30). Retrieved from Sismicité historique de la France Métropolse. Tratto da www.sisfrance.net: http://www.sisfrance.net/donnees_resultat.asp?LST=true&AN0=&AN9=&NV0=&NV9=&DPT=38&COM=38185
Yoti. (2018, November 26). Dramatic Mexico City Earthquake footage (Prt 3). Tratto da YouTube: https://www.youtube.com/watch?v=pcjUK7xYzWs
Young, K. S., Parsons, C. E., Elmholdt, E.-M. J., Woolich, M. W., Hartevelt, T. J., Stevner, A. B., . . . Kringelbach, M. L. (2016). Evidence for a caregiving instinct: rapid differentiation of infant from adult volcalizations using magnetoencephalography. Cerebral Cortex, 26, 1309 - 1321.
Yovel, G., & Belin, P. (2013). A unified coding strategy for processing faces and voices. Trends in Cognitive Sciences, 17(6), 263-271.
Zhao, X., Coates, G., & Xu, X. (2017). Solving the earthquake disaster shelter location-allocation problem using optimization heuristics. Proceedings of the 4th ISCRAM Conference. ISCRAM.
Zhao, X., Xu, W., Ma, Y., Qin, L., Zhang, J., & Wang, Y. (2017). Relationship between evacuation population size, earthquake emergency shelter capacity, and evacuation time. International Journal of Disaster Risk Science, 8, 457-470.

Zhou, S., Chen, D., Cai, W., Lou, L., Yok, M., Low, H., & Tian, F. (2010, October). Crowd Modeling and Simulation Technologies. ACM Tranactions on Modeling and Computer Simulation, 20(4).
Zhou_a, J., Li, S., Nie, G., Fan, X., Tan, J., Li, H., & Pang, X. (2018). Developing a database for pesestrians' earthquake emergency evacuation in indoor scenarios. PLoS ONE, 13.
Zhou_b, J., Li, S., Nie, G., Fan, X., Tan, J., Li, H., & Pang, X. (2018). Developing a database for pedestrians' earthquake emergency evacuation in indoor scenarios. PLoS ONE.
Zia, K., Farrahi, K., Riener, A., & Ferscha, A. (2013). An agent-based parallel geo-simulation of urban mobility during city-scale evacuation. Simulation: Transactions of the Society for Modelling and Simulation International, 89(10), 1184-1214.

APPENDIX

Appendix 1.0 GAMA Code

Code 30 Getting the shapefile with damage and vulnerability data. (Equivalent to Code 1)

```
buildingIntensityVShapefile <-
     file('../includes/GrenobleCore_BuildingsDamageAug202k18_GTEST_PROB_run.shp');
```

Code 31 Getting the values from fields of type float. (Equivalent to Code 2)

```
float D_pa; float D_pb; float D_pc; float D_pd; float D_pe;
float D_d0V_P; floatD_d1V_P; float D_d2V_P; float D_d3V_P; float D_d4V_P;
float D_d5V_P;
float D_d0VI_P; float D_d1VI_P; float D_d2VI_P; float D_d3VI_P; float D_d4VI_P;
float D_d5VI_P;
```

Code 32 Assigning building typology (vulnerability class) using the flip() function. (Equivalent to Code 3)

```
string typeVC <- flip(D_pa) ? "a" :( flip(D_pb) ? "b": (flip(D_pc) ? "c":
(flip(D_pd) ? "d": (flip(D_pd)?"e":"e"))));
```

Code 33 Assigning building damage for intensity scenarios using the flip() function. (Equivalent to Code 4)

```
int typeDCV <- flip(D_d0V_P) ? 0 : (flip(D_d1V_P) ? 1: (flip(D_d2V_P) ? 2:
     (flip(D_d3V_P) ? 3:(flip(D_d4V_P) ? 4 : (flip(D_d5V_P) ?5:1)))));
int typeDCVI <-flip(D_d0VI_P) ? 0 : (flip(D_d1VI_P) ? 1: (flip(D_d2VI_P) ? 2:
     (flip(D_d3VI_P) ? 3:(flip(D_d4VI_P) ? 4 : (flip(D_d5VI_P) ?5:2)))));
```

Code 34 Saving building data to shapefile (Equivalent to Code 5)

```
save buildings to:"../shapefiles/buildingsDamageRun_Scenario5.shp" type:"shp"
     with:[ID::"ID",HAUTEUR::"HAUTEUR",IRIS::"IRIS",IRIS_NAME::"IRIS_NAME",
     typeVC::"ScBH1_VC",typeDCV::"ScBH1DV",typeDCVI::"ScBH1DVI",
     typeDCVII::"ScBH1DVII",typeDCVIII::"ScBH1DVIII",
     typeDCIX::"ScBH1DIX",typeDCX::"ScBH1DX",
     typeDCXI::"ScBH1DXI",typeDCXII::"ScBH1DXII"];
```

Code 35 Load the building shapefile for intensity VI scenario (Equivalent to Code 6)

```
file buildingIntensityVIShapefile <- file('../includes/
     GrenobleCore_BuildingsDamageAug202k18_CLIP_IntV_Sc5_Outer_IntVI.shp');
```

Code 36 Initialise building agent from building shapefile (Equivalet to Code 7)

```
init {
     create buildingsIntVI from: buildingIntensityVIShapefile;
}
```

Code 37 Building species (Equivalent to Code 8)

```
species buildingsIntV {
     int HAUTEUR; /*building height from BDTOPO */
     string ScBH1_VC; //EMS-98 Vulnerabilty Class ( a,b,c,d,e)
     int ScBH1DVI; //Scenario: Damage at Intensity VI (0, 1, 2,3,4,5)

     aspect default{
          //VULNERABILITY TYPOLOGY
          if (eqMagnitude <= 3){
               draw shape colour: (ScBH1_VC = "a") ? # red : ((ScBH1_VC = "b") ? #
green
               : ((ScBH1_VC = "c") ? # blue : ((ScBH1_VC = "d") ? # yellow :
((ScBH1_VC
               = "e") ? # violet : #black)))) border: # grey depth: HAUTEUR *
               height_multiplier;
          }
          //DAMAGE
          elseif (eqIntensity = 6){
               draw shape colour: (ScBH1DVI = 0) ? # white : ((ScBH1DVI = 1) ? #
yellow
               : ((ScBH1DVI = 2) ? # orange : ((ScBH1DVI = 3) ? # red : ((ScBH1DVI =
4)
               ? # maroon : ((ScBH1DVI = 5) ?# black : # lightblue))))) border: #
               Grey depth: HAUTEUR * height_multiplier;
          }
     }
}
```

Code 38 Creating debris at every timestep within the duration of the simulated earthquake. Equivalent to Code 9

```
reflex createDebris when: (time >= eqtime) and (time <= (eqtime + eqDuration)){ }
```

Code 39 Amount of debris created based on typology (Equivalent to Code 10)

```
int k_debris;
int DLAYER;
//added random probabilities with max range for creation of debris wrt typology
if (ScBH1_VC = 'a'){
     k_debris <- rnd(1, 10);
} else if (ScBH1_VC = 'b'){
     k_debris <- rnd(1, 7);
} else if (ScBH1_VC = 'c'){
     k_debris <- rnd(1, 5);
} else if (ScBH1_VC = 'd'){
     k_debris <- rnd(0, 3);
} else if (ScBH1_VC = 'e'){
     k_debris <- rnd(0, 1);
}
```

Code 40 Debris created at each time step (Equivalent to Code 11)

```
int n_debris;
if eqIntensity = 5{
     n_debris <- int(ScBH1DV * k_debris * eqIntensity * HAUTEUR / 650);
     create smallDebris number: n_debris{
          shape <- square(1.0) rotated_by rotation;
          location <- any_point_in((dangerZoneV_VIII where (each.DLAYER = 5)
               closest_to (myself))intersection
                    geometry(freeSpaceLayer));
}
```

Code 41 Building collapse (Equivalent to Code 12)

```
if (eqIntensity = 6 and ScBH1DVI = 5){
     create hugeDebris number: 1{
          BSource <-myself.ID;
          shape <- square(4.0) rotated_by rotation;
          list<doors> nearby_doors <- doors overlapping (2 around myself);
          location <- (doors where (each.ID = myself.ID));
     }
}
```

Code 42 General parameters. Equivalent to Code 13.

```
list<string> use <- ["Home", "Work", "School", "Public", "Outdoor"];
list<string> agegroup <- ["adult", "elderly", "child"];
list<float> evacSpeedsMax <- [3.8, 0.0, 2.23, 1.11, 1.77];
//Format for SPEEDS: adult, child_0_2,child3_14, elderly, disabled
list<float> probDisability <- [0.012, 0.024, 0.013, 0.028, 0.039, 0.035, 0.090, 0.067,
0.123,
     0.102, 0.125, 0.124, 0.217,0.229, 0.423, 0.361];
bool disabilityON <- false; //true if disability ON, and false if not included
```

Code 43 List of IRIS units. Equivalent to Code 14

```
list<string> iris <- ["Crequi_VHugo", "Grenette", "AIGLE","CHAMPIONNET","GENISSIEU",
     "HOCHE","JEAN JAURES","PREFECTURE,…,"WALDEC ROUSSEAU"
];
```

Code 44.Generating night time population. Equivalent to Code 15

```
//NIGHT TIME SCENARIO
float pctPop<-0.002;//percentage of population, to limit agent creation

//1. Crequi-VictorHugo format: [home, work, school, public, outdoors]
list<int> VHpopChild0_2 <-[pctPop*45,pctPop*0,pctPop*0,pctPop*0,pctPop*0];
list<int> VHpopChild3_14 <-[pctPop*199,pctPop*0,pctPop*0,pctPop*0,pctPop*0];
list<int> VHpopAdultY15_29 <-[pctPop*739,pctPop*0,pctPop*0,pctPop*0,pctPop*0];
list<int> VHpopAdultM30_59 <-[pctPop*660,pctPop*0,pctPop*0,pctPop*0,pctPop*0];
list<int> VHpopElderlyG60 <-[pctPop*535,pctPop*0,pctPop*0,pctPop*0,pctPop*0];
```

Code 45 Generating day time population. Equivalent to Code 16.

```
//DAYTIME SCENARIO
float pctPop<-1.00;//percentage of population, to limit agent creation

//1. Crequi-VictorHugo format: [home, work, school, public, outdoors]
list<int> VHpopChild0_2 <-[pctPop*41,pctPop*0,pctPop*0,pctPop*0,pctPop*4];
list<int> VHpopChild3_14 <-[pctPop*0,pctPop*0,pctPop*179,pctPop*0,pctPop*20];
list<int> VHpopAdultY15_29 <-[pctPop*38,pctPop*246,pctPop*381,pctPop*0,pctPop*74];
list<int> VHpopAdultM30_59 <-[pctPop*0,pctPop*594,pctPop*0,pctPop*0,pctPop*66];
list<int> VHpopElderlyG60 <-[pctPop*354,pctPop*128,pctPop*0,pctPop*0,pctPop*54];
```

Code 46 List of the population of Adults (30 -59 y.o.) for each IRIS. Equivalent to Code 17.

```
list<list> I30_59 <-[VHpopAdultM30_59,GRpopAdultM30_59,I214AdultM30_59,I215AdultM30_59,
     I211AdultM30_59,I216AdultM30_59,I203AdultM30_59,I212AdultM30_59,I206AdultM30_59,
     ….,I610AdultM30_59,I110AdultM30_59
];
```

Code 47 Generating human agent population. Equivalent to Code 18.

```
loop i from: 0 to: 3 step:1{
     int k<-0;
     loop j over:I30_59 {
          create adult number:j[i]{
               location <- one_of(doors where ((each.Activity = use[i]) and
               (each.IRISName = iris[k]))).location;
            a_ageGroupsChoice<-agegroup[0];a_subGroup <- subgroup[0];a_use <- use[i];
            a_role <- role[0];a_age <- rnd(30, 59);a_speed <- rnd(evacSpeedsMax[0]);
            a_indoor <- true;a_outdoor <- false;a_IRIS <- iris[k];

            if (disabilityON = true){
                 if ((a_age >= 25) and (a_age <= 34)){
                      a_disabled <- flip(rnd(probDisability[2], probDisability[3]));
                 } else if ((a_age >= 35) and (a_age <= 44)){
                   a_disabled <- flip(rnd(probDisability[4], probDisability[5]));
                 } else if ((a_age >= 45) and (a_age <= 54)){
                   a_disabled <- flip(rnd(probDisability[6], probDisability[7]));
                 } else{
                   a_disabled <- flip(rnd(probDisability[8], probDisability[9]));
                 }
                 if (a_disabled = true){
                   a_speed <- rnd(0, evacSpeedsMax[3]);
                 }
            }
        }
     k <- k+1;
     }
}
```

Code 48 Agent avoiding buildings. Equivalent to Code 19.

```
reflex adult_avoidBuildings when: (self.location distance_to
     any_point_in(buildings closest_to (self)) < 5.0){
     point acc <- { 0, 0 };
     list<buildings> nearby_Buildings <- (buildings at_distance 2.0);
     loop obs over: nearby_Buildings{
          acc <- acc - (obs.location - location);
     }
     heading <- heading + rnd(-30, 30);
     speed <- a_speed;
     velocity <- velocity + acc;
}
```

Code 49 Generating casualties. Equivalent to Code 20.

```
reflex adult_hurtBy_smallDebris when: a_outdoor = true and (eqIntensity = 5) and
      is_active = true and (time >= eqtime) and (time <= (eqtime + eqDuration)) and
      self.location distance_to centroid(smallDebris closest_to (self)) <= 1{
      if length(smallDebris overlapping (self))>0{
           speed <- 0.00001;
           if flip(0.5) = true{
                is_deceased <- true;
                is_active <- false;
           } else{
                is_injured <- true;
           }
      }
}
```

Code 50 Agents avoiding debris. Equivalent to Code 21.

```
reflex adult_avoid_smallDebris when: is_active = true and (eqIntensity = 5){
     point acc <- { 0, 0 };
     list<smallDebris> nearby_smallDebris <- (smallDebris at_distance separationDebris);
     loop obs over: nearby_smallDebris{
          acc <- acc - (obs.location - location);
     }
     velocity <- velocity + acc;
}
```

Code 51 Defining social relationships. Equivalent to Code 22.

```
string idColleague;
string idFamily;

reflex initialize when: time = 0{
     bldgfloor <- int(((doors closest_to (self)).HAUTEUR) / floorHt);
     b_floor <- rnd(0, (bldgfloor - 1));

     if (doors closest_to (self)).Activity="Home"{
          idFamily <- string((doors closest_to (self)).ID)+string(b_floor);
     } else if (doors closest_to (self)).Activity="Work"{
          idColleague <- string((doors closest_to (self)).ID)+string(b_floor);
     } else if (doors closest_to (self)).Activity="School"{
          idColleague <- string((doors closest_to (self)).ID)+string(b_floor);
     }
     do add_desire(normal);do add_belief(normal);
}
```

Code 52 Assigning kin and friend IDs. Equivalent to Code 23.

```
int idKinMax;
int idFriendMax;

int idKin <- rnd(0, idKinMax);
int idFriend <- rnd(0, idFriendMax);
```

Code 53 Predicates for adult agents. Equivalent to Code 24

```
predicate normal <- new_predicate("normal_stay");
predicate adult_move_to_Door <- new_predicate("adult_move_to_Door");
predicate stay_feelsafe <- new_predicate("stay_feelsafe");
predicate moveout <- new_predicate("adult_moveout");
predicate adult_move_to_road <- new_predicate("adult_move_to_road");
predicate adult_move_to_safearea <- new_predicate("adult_move_to_safearea");
predicate adult_move_to_safeareaSPOTS <- new_predicate("adult_move_to_safeareaSPOTS");
predicate adult_move_to_safearea0p5SPOTS <- new_predicate("adult_move_to_safeareaSPOTS");
predicate adult_helpInjuredAdult <- new_predicate("adult_helpInjuredAdult");
```

Code 54 Predicates for child agents. Equivalent to Code 25

```
predicate child_move_to_safearea <- new_predicate("child_move_to_safearea");
predicate child_move_to_road <- new_predicate("child_move_to_road");
predicate child_move_to_adultTeacher <- new_predicate("child_move_to_adultTeacher");
predicate child_move_to_adultFamily <- new_predicate("child_move_to_adultFamily");
predicate child_move_to_adultFamilyParent <- new_predicate("child_move_to_adultFamilyParent");
predicate child_move_to_adultKin <- new_predicate("child_move_to_adultKin");
predicate child_move_to_adultFriend <- new_predicate("child_move_to_adultFriend");
predicate child_move_to_adultColleague <- new_predicate("child_move_to_adultColleague");
predicate child_move_to_adultStranger <- new_predicate("child_move_to_adultStranger");
predicate child_move_to_childFamily <- new_predicate("child_move_to_childFamily");
predicate child_move_to_childKin <- new_predicate("child_move_to_childKin");
predicate child_move_to_childFriend <- new_predicate("child_move_to_adultFriend");
predicate child_move_to_childColleague <- new_predicate("child_move_to_childColleague");
predicate child_move_to_childStranger <- new_predicate("child_move_to_childStranger");
```

Code 55 Reflex when detecting earthquakes. Equivalent to Code 26..

```
reflex detectEarthquake when: (time = eqtime){
     //PRE-EVACUTION ACTIONS SECTION

     //WHEN THE DECISION IS TO MOVE OUT TO EVACUAT
     //BDI SECTION
     do remove_desire(normal);do remove_belief(normal);
     do add_desire(adult_move_to_road);do add_desire(adult_move_to_safearea);
     do add_desire(adult_move_to_adultFamily);do add_desire(adult_move_to_childFamily);
     do add_desire(adult_move_to_childFamily_Parent);
     do add_desire(adult_move_to_adultKin);do add_desire(adult_move_to_childKin);
     do add_desire(adult_move_to_adultFriend);do add_desire(adult_move_to_childFriend);
     do add_desire(adult_move_to_adultColleague);do add_desire(adult_move_to_childColleague);
     do add_desire(adult_move_to_adultStranger);do add_desire(adult_move_to_childStranger);
     do add_desire(adult_Teacher_move_to_child); do add_desire(adult_helpInjuredAdult);
```

Code 56 Perception distances. Equivalent to Code 27.

```
global {
     /** Insert the global definitions, variables and actions here */
     //for social ties, this are set here from pre-calculated values in the formula, but
     can be dynamically set,

     //perception distance (format: DAY, NIGHT, SNOW)
     //list<string> Context <-["day","night","snow"];
     list<float> PD_Child <- [100.0, 100.0, 100.0];
     list<float> PD_Partner <- [94.10, 4.11, 43.03];
     list<float> PD_Parent <- [88.85, 3.89, 40.63];
     list<float> PD_Kin <- [76.45, 3.34, 34.96];
     list<float> PD_Friends <- [87.85, 3.84, 40.17];
     list<float> PD_Acquintance <- [69.20, 3.03, 31.65];
     list<float> PD_Stranger <- [60.85, 2.66, 27.83];
     list<float> PD_Family <- [100.0, 100.0, 100.0];
}
```

Code 57. Perceiving other agents. Equivalent to Code 28

```
plan adult_move_to_adultFamily intention: adult_move_to_adultFamily when: is_active = true
and (atEvacZone = false) and (self.location distance_to (adult closest_to (self)) <
PD_family) and (self.idFamily = (adult closest_to (self)).idFamily){
     point pointAdultFamily <- (adult closest_to (self)).location;
     perceived_areaAdultFamily <- (cone(heading - 10, heading + 10) intersection
     world.shape) intersection polygon([self.location, pointAdultFamily.location]);

     if (perceived_areaAdultFamily != nil){
        perceived_areaAdultFamily <- perceived_areaAdultFamily masked_by (buildings,
        precision);
        perceiveChildDeceased_Child <- false;perceiveAdultDeceased_Child <- false;
        perceiveChildDeceased_Adult <- false;perceiveAdultDeceased_Adult <- false;
        perceiveChildTeacher <- false;perceiveAdultTeacher <- false;
        perceiveFamilyAdult <- true;perceiveFamilyChild <- false;
        perceiveKinAdult <- false;perceiveKinChild <- false;
        perceiveFriendAdult <- false;perceiveFriendChild <- false;
        perceiveColleagueAdult <- false;perceiveColleagueChild <- false;
        perceiveStrangerAdult <- false;perceiveStrangerChild <- false;
        perceiveSMALLDebris <- false;perceiveMEDIUMDebris <- false;
        perceiveBIGDebris <- false;perceiveHUGEDebris <- false;
        perceiveAreaInFront <- false;perceiveRoad <- false;
        perceiveSafeArea <- false;
        a_following <- true;
     } else{
        perceiveFamilyAdult <- false;
        a_following <- false;
     }
}
```

Code 58 End simulation. Equivalent to Code 29.

```
int endCyle <- eqtime+900;
```